20030305218

AD-A282 306

REPORT DOCUMENTATION PAGE

Form Approved
OMB No 0704-0188

1. AGENCY USE ONLY (Leave blank)

2. REPORT DATE

3. REPORT ~~TYPE AND DATES~~ COVERED
~~THESIS/~~DISSERTATION

4. TITLE AND SUBTITLE
Fibre Optic Sensors using Adiabatically Tapered Single Mode Fibres

5. FUNDING NUMBERS

6. AUTHOR(S)
Zoe Miranda Hale

7. PERFORMING ORGANIZATION NAME(S) AND ADDRESS(ES)
AFIT Student Attending:
University of Cambridge

8. PERFORMING ORGANIZATION REPORT NUMBER
AFIT/CI/CIA-94-011D

9. SPONSORING/MONITORING AGENCY NAME(S) AND ADDRESS(ES)
DEPARTMENT OF THE AIR FORCE
AFIT/CI
2950 P STREET
WRIGHT-PATTERSON AFB OH 45433-7765

10. SPONSORING/MONITORING AGENCY REPORT NUMBER

11. SUPPLEMENTARY NOTES

12a. DISTRIBUTION/AVAILABILITY STATEMENT
Approved for Public Release IAW 190-1
Distribution Unlimited
MICHAEL M. BRICKER, SMSgt, USAF
Chief Administration

12b. DISTRIBUTION CODE

94-22879

13. ABSTRACT (Maximum 200 words)

14. SUBJECT TERMS

94 7 20 125

15. NUMBER OF PAGES
191

16. PRICE CODE

17. SECURITY CLASSIFICATION OF REPORT

18. SECURITY CLASSIFICATION OF THIS PAGE

19. SECURITY CLASSIFICATION OF ABSTRACT

20. LIMITATION OF ABSTRACT

NSN 7540-01-280-5500

Standard Form 298

SUMMARY

The ultimate goal of the research presented in this dissertation was to determine if an adiabatically tapered single mode fibre could be used as an effective basis for a chemical or biological sensor. This required a phased investigation examining:

- The evanescent absorption behaviour of the tapered fibre
- The fluorescent capture efficiency of the tapered fibre
- The effect of immobilising an indicator to the surface of the tapered fibre
- A suitable configuration for the tapered fibre to allow simple application of selective elements as well as interaction with the sample solution
- The new configuration in conjunction with a simple immobilisation method and model analytes
- The new configuration in a realistic chemical or biological assay

It was shown both theoretically and experimentally that the adiabatically tapered single mode fibre could capture enough fluorescent energy, or be absorbed sufficiently, to make determinations of the concentration of analytes in solution. Immobilisation of suitable recognition elements to the surface of the fibre did not degrade the performance of the sensor; in fact, it was found this could enhance dramatically the fluorescent capture efficiency. Using a silanisation process to attach proteins to the surface of the tapered fibre served to form a novel waveguide system, which displayed high sensitivity levels to the analyte.

Chapter 1 introduces chemical and biological sensing systems, as well as defining their components.

94-C-11D

Fibre Optic Sensors using Adiabatically Tapered Single Mode Fibres

Zoë Miranda Hale

A dissertation submitted to the University of Cambridge for the degree of Doctor of Philosophy

King's

February 1994

Chapter 2 reviews optical techniques that have evolved to analyse chemical and biological samples. The use of optical fibres as a basis for chemical and biological sensing is introduced.

Chapter 3 describes the major components of the expeimental systems used throughout the research presented in this dissertation. The computer program used as a basis for theoretical modelling of the different experiments is discussed as well.

Chapter 4 discusses the theoretical background for the behaviour of the tapered single mode fibre. It reviews the existence of the evanescent field, and methods of gaining access to it, in optical fibres. The criteria for constructing adiabatically tapered fibres is defined.

Chapter 5 reviews efforts in evanescent absorption optical sensors. Limitations of this application reported in the literature is examined theoretically, and evanescent absorption experiment based on tapered fibres is performed.

Chapter 6 discusses the use of fluorophores in optical fibre sensing, and a theoretical model for fluorescent capture in tapered fibres is developed. Fluorescence capture in a taper is demonstrated experimentaly using the titration of a pH-sensitive fluorescent indicator in solution.

Chapter 7 looks at the development of a "true sensor": the actual immobilisation of the selective element of the sensor to the fibre. Various immobilisation schemes that have been applied to optical fibres are reviewed. An experiment immobilising penicillinase to the tapered fibre is performed, and the ability of the device to still capture sufficient fluorescent energy to make concentration determinations of the analyte is confirmed.

Chapter 8 describes the development of a more convenient geometry for the taper, where a lossless macrobend (180°) is introduced to the fibre. This results in a fibre loop, which can easily be chemically modified through silanisation process to include a recognition element. A sample assay using model analytes is performed, and an examination of the fluorescent capture ability is carried out. It is determined that the applied selective coating serves to act

as an effective waveguide for the fluorescent energy, which may couple significantly into the standard fibre mode.

Chapter 9 presents the development of a suitable chemical scheme to use the tapered fibre loop in an immunoassay. Methods of making the fibre sensor reusable are discussed, and performed experimentally. An immunoassay based on material provided by the Center for Vaccine Development, University of Maryland and the Institute of Biotechnology, University of Cambridge, was performed. This immunoassay, based on the detection of cholera toxin antibodies in blood samples, not only demonstrated the ability of the tapered fibre loop sensor to be reused, but also the high fluorescent capture levels seen in the model analyte systems.

Chapter 10 discusses follow-on work that should be performed to better characterise the "novel" waveguide. Other experimental work to combine interesting optical elements to the fibre loop (semiconductor laser or luminescent sources, and surface plasma interaction) is proposed.

PUBLISHED WORK

Research presented in this dissertation has been published in the following refereed journal articles and conference proceedings.

1. Z. M. Hale, R.S. Marks, "Tapered Fibre Biosensor," British Patent Application 9401170.7, 21 January 1994.

2. Z.M. Hale, R.S. Marks, C.R. Lowe, and F.P. Payne, "The single mode tapered optical fibre loop immunosensor: I. Characterisation with model analytes," **Proceedings of Biomedical Optics**, Los Angeles, California, 22-29 January 1994.

3. R.S. Marks, Z.M. Hale, M.M. Levine, C.R. Lowe, and F.P. Payne, "The single mode tapered optical fibre loop immunosensor: II. Assay of anti-cholera toxin immunoglobulins," **Proceedings of Biomedical Optics**, Los Angeles, California, 22-29 January 1994.

4. Z.M. Hale and F. P. Payne, "Fluorescent sensors based on tapered single mode optical fibres," Sensors and Actuators B, 17 No 3 (February 1994), 233-40.

5. F.P. Payne and Z.M. Hale, "Deviation from Beer's Law in multimode optical fibre evanescent field sensors," International Journal of Optoelectronics, 8, (1994).

6. Z. M. Hale, F.P. Payne, "Demonstration of an optimised evanescent field optical fibre sensor," Analytica Chimica Acta, 1994 (to be published).

7. Z.M. Hale, R.S. Marks, C.R. Lowe, F.P. Payne, "A tapered single mode fibre as a penicillin sensor," In Proceedings of Conference on Lasers and Electro-optics, Anaheim, California, 8-13 May, 1994.

ACKNOWLEDGEMENTS

Colonel Radcliff deserves first mention, as his support for this assignment made attendance of the Cambridge PhD program possible. I am most grateful to Colonel Klayton at USAFA/DFEE for accepting me "sight unseen," and to Lt Col Maher for making it all happen.

My supervisor, Dr. Payne, gets mention for his support in letting me design my own experiments. Further, he has saved me endless hours of work by running many iterations of Harry MacKenzie's computer model on his multiple and fast computers.

I extend thanks to the many members of the Optoelectronics Group who have patiently reviewed, edited and commented on both experimental set-ups and this dissertation. Graeme Pendock, Jon Lacey, and Harry MacKenzie deserve special additional praise for their combined efforts to introduce me to single mode fibre, and tapers. Melanie Holmes and Mark Bray have given me huge supprt in ways too numerous to mention. Tim Wilkinson and his unfailing computer support, even when we re-built from bit parts the 286 that was **the** data collector for all my experiments, were saving graces.

None of the experiments performed here would have been possible without the talents of Russell Crane, Steve Drewitt, Andy Denson, Adrian Ginn, Mick Stone and Jose Montero. Their dedicated assistance, from creating Perspex for aged PCs to infinite components for taper loops, has been superb, and well beyond the call of duty.

Chris Lowe deserves a special mention for allowing me to use the resources of the Institute of Biotechnology - not only many pieces of equipment but also countless hours of the expertise of Robert Marks, Roger Millington and Dave Cullen. Dr Levine's kindness in providing "real world" samples made the portion of the experimentation much more interesting. The technical help lines of Sigma and Pierce & Warriner have been a boon, as was the succinct and accurate chemistry advice of Dr Meir Wilchek.

The absolutely splendid scanning electron microscope photographs are the result of the extensive talent and perseverance of Alan Heaver.

Lastly, on the home front: to my husband Dave, for support of long and peculiar hours and diagnosis and cure of disruptive computer problems; to Miranda and Katrina, for proving unequivocally that sleep is unnecessary (as well as some much needed comic relief); to Junior 3, for waiting until after this was complete to arrive; many, many, many thanks......

DECLARATION

This dissertation is the result of my own work and, except where acknowledged, includes nothing which is the outcome of work done in collaboration. The contents of this dissertation have not been submitted, in whole or in part, for any other degree or diploma.

Zoë M. Hale

Table of Contents

Chapter 6

Chapter 7

List of Figures

Chapter 1

An Introduction to Chemical and Biological Sensing

Summary

The ability of sensing for particular analytes depends critically on combining sensitivity and selectivity. Many portions of the sensing problem as a whole constrain the ultimate sensor design. A generic sensor system can be described in functional terms. All of these functions, as discussed in this chapter, must be suitably addressed in order to develop a completely satisfactory product for the end user. It is not enough to choose a very sensitive technology. A sensor and and the elements of the sensing system are defined in this chapter, and typical analytes and technologies are generally reviewed. Optical sensing techniques are chosen as the basis for a chemical or biological sensor.

1.0 A general sensing system

In many areas, interest in chemical analysis is vital. Until the last three decades, the chemical composition of materials, especially those materials specific to a biological system, was determined only through laboratory testing. This process was frequently time-consuming, and often depended on the preparation of individual background samples. Much effort has been devoted to making these measurements automatic (rapid) as well as minimising the total amount of human involvement. Further, in some industrial applications on-line sampling is highly desirable or even critical. The enormous variety in sensor requirements has led in turn to the development of an enormous number of devices. Many different types of sensitive elements, such as electro-chemical, pressure-sensitive, pyrometric, or optical devices, have been made specific through the application of selective chemical elements (variable conversion element). A generalised diagram for a sensor system is illustrated in Figure 1.

The selectivity (variable conversion and manipulation element) of a device may depend on a semi-permeable membrane, an adsorbed or covalently (or non-covalently) bound indicator

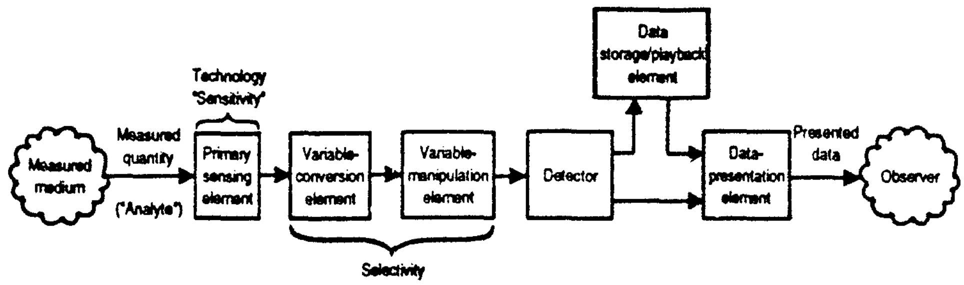

Figure 1.1 *Functional elements of a sensing system (not in time sequence).*

layer, or direct contact with a sample to alter the monitored variable. The development of a complete sensor system depends upon the analyte and its state (gaseous, liquid or soiid), the technologies available, and the sensitivity required (how much concentration across what time period). The sensitivity may be defined as a minimum concentration level (presence of an analyte), a dosage level (concentration over time), or a maximum level (yield of a reaction). The methods of storage, playback and presentation are usually independent of these inputs. This means that the critical elements of the sensor system are the sensitivity element and the analyte. No idealised or generic sensor system exists that performs well for every sensing requirement: each of the functional variables can fundamentally alter the design. To begin the discussion of sensing, a defininition of a sensor is required, as well as an overview of some of the determinant portions of sensor design.

1.1 Sensor definition

A sensor or transducer has been given many definitions; for the purpose of this discussion, it can be defined as a device with a portion that allows it to be sensitive to the analyte of interest, a method of carrying its response (with whatever conversion and manipulation necessary) to a detector, and a final portion that allows the measurement to be converted into an understandable value. A *chemical* sensor has been defined as "a small-sized device ... with the three elements ... capable of continuously and reversibly reporting concentration" [47]. Similarly, a *biosensor* is "a device which converts biological activity into a quantifiable signal"[342]. In general, sensors have been investigated for decades to develop methods of carrying out the traditional laboratory testing in non-laboratory environments, whether it be

for industrial, medical, environmental, or defence purposes. The underlying problem of sensor development is to retain sensitivity while at the same time becoming selective.

1.2 Sensing system determinants: some specific analytes

1.2.1 Biological sensing

Biological sensing is the detection of chemical species within the biological framework†. The biosensing field has been growing rapidly over the past few decades, as well as diversifying at the same time. Considerable interest has focused on monitoring of blood gases, pH, glucose and other chemicals with physiological or clinical importance[90]. The selective portion of the sensor could be enzymes, DNA components, hormone and neurotransmitter receptors or antibody/antigens. Biosensors have further subdivided into biological sensors, where the analyte is perhaps of environmental concern or is assayed clinically; and immunosensors[58], where an immediate patient diagnosis is often the result of the information.

Biosensors have been developed for a variety of applications. Enzymes and their substrates are a selective pair that can form a basis for sensing†† . A specific enzyme, penicillin, is of interest due to its widespread use: its presence is monitored as a contaminant in milk, and the level of completion of the fermentation process is also monitored†††. NADH determination is vital in many enzymatic reactions[127]. Ethanol as well is sensed based on an enzymatic scheme[423,406]. Narcotics as well as other drugs are a natural target for immunoassays††††. Toxins have also been monitored[133,352,412], and remote sampling (i.e., far from the human observer examining the concentration display) is highly desirable. Pesticides are also another hazard that require environmental monitoring[318], and may require either that their presence be detected or a dosage level calculated.

---

† [151,197,230,340,384]
†† [17,121,126,404,405,418]
††† [76,132,161,193,194,434]
†††† [44,196,283,218,365,410]

Immunosensing techniques may rely upon antibody or enzyme-based detection in order to provide their vital medical information. Antibodies and antigens are nearly perfect pairs for sensing applications due to their specificity. Detectors based on these sets can achieve great sensitivity and selectivity. Generic antibody/antigen systems have been utilised to test basic sensor concepts (similar to the role of pH for chemical sensors)†. Some specific biochemicals are detected, such as bilirubin, which is an indicator of bile reflux from the duodenum into the stomach to detect biliary diseases[84,92,117,184]. Carcinogens are detected through an antibody-based assay[402]. Urea is also of interest for immunoassays[314]. Although enzyme-based, glucose concentration is monitored in the blood as an indicator for a variety of diseases††, as is determination of lactate[16,392,407].

1.2.2 Chemical sensing

The approaches to enabling a sensing element to detect a chemical species fall into two categories: either an intrinsic property of the analyte is utilised, that is, some reaction unique to the chemical; or an extrinsic recognition element is added to the system so that a modification of that element represents the concentration of the chemical. Some analytes are intrinsically fluorescent or have a colour change, as in urease. An example of the extrinsic type of detection is the traditional pH indicator: many chemical reactions result in a modification of the local pH level, such as those involving glucose, CO_2, and penicillin. The indicator is then used in an environment where the most likely source of pH change is an alteration in the concentration of the analyte. This is usually done through the immobilisation of one half of a reaction pair, for example, penicillinase, onto the sensor.

The type of chemical (including biological molecules) to be detected often determines the technical approach taken. Unique characteristics of the analyte, such as mass, size, hydrophobic or hydrophilic nature and electrostatic behaviour tend to determine the selective portion of the sensor. There are many classes of molecules (compounds) that require

---

† [9,10,12,21,41,67,78,85,111,286,351,353,354,372,373,394,446,91,301]
†† [1,241,245,320,390,391,247]

detection by chemical sensors. Some of the chemical systems currently under investigation are reviewed briefly below, including cations, anions, water content, oils, and gases. Many other specialised sensors[220] for specific reactions have been developed, but these areas cover the bulk of investigated reactions.

1.2.2.1 Cations

Cation measurement can include measurement of trace species in the environment, blood cations such as potassium or sodium, water contaminants, cell membrane cations, as well as many of the metal ions. A cation is a positively charged chemical species, and often a specific membrane for selective diffusion is used in conjunction with the transducer. A special case for sensor work in cations is the detection of pH change, sometimes for industrial applications. Further, since pH can be used to diagnose changes in health (a small change in blood or gastric pH can signal the onset of large-scale physiological problems), it has been studied extensively, with many sensor configurations reported. In addition, since various clinical methods of determining pH exist, establishing a comparative baseline is simple. This allows a methodology of testing new immobilisation or technological methods. Optical fibre sensor development alone, which is still a relatively new field, has had scores of researchers examining pH sensors†.

Many of the indicators for a given cation can be used for other ones by merely changing the pH environment (for example, the buffer solution) of the sensor. Sensors examining Li^{+}, Na^{+}, K^{+}, Ag^{2+}, Mg^{3+}, Ca^{2+}, Sr^{2+}, Ba^{2+}, Cu^{2+}, Cd^{2+}, Hg^{2+}, Sn^{2+}, Zn^{2+}, Pb^{2+}, Tl^{2+}, Fe^{3+}, Al^{3+}, and Tl^{3+} have been developed [298,68] using this principle. Other cations detected include aluminium Al^{3+} [328] and ammonium, NH_4^{+}, for monitoring of ground water streams and drinking supplies[311], and beryllium[326]. Calcium, Ca^{2+}, which can be considered a contaminant to water supplies or a very useful biological indicator (i.e., muscle contraction, synaptic transmission, hormonal actions), has also been studied††. Potassium, K^{+}, another physiologically-important cation, has also been examined[8,154,335]; some of the recognition elements for K^{+} can be used

† [3,5,27,32,106,123,172,173,183,225,234,236,257,279,281,299,305,310,327,361,387,417,418,421,432,110]
†† [20,56,201,329,334]

for sodium, Na^+, which is of similar physiological interest [336]; discrimination between the two ions may pose difficulties.

A unique environment, such as seawater, can have further requirements for detection of cations. Marine optical fibre sensors have been applied to reduce potential interference effects from the high concentrations of electrical equipment (off-shore rigs, submarines); pollutant monitoring within the sea from a variety of sources, including thermal effects, is in its infancy, and is based on cation increases. Lastly, those cations of plutonium and uranium useful to chemical process control in irradiated nuclear fuel reprocessing installations have been detected with sensors[61].

1.2.2.2 Anions

Anions are negatively charged chemical species, and include the halides, i.e., Cl^-, I^-, and Br^-. Some anions are destructive to the system in which they are being measured, and in the gaseous forms can be toxic. The halides traditionally are detected as contaminants in water systems. Bromine ions can best be detected through a fluorescent quenching process[427]; chlorine ions are monitored in water purification applications† ; and the concentration of fluoride ions in aqueous solutions are also examined[270]. Iodine, in aqueous solutions as well as in vapour form, has been detected[397,428]. The gaseous form of CN^-, a toxic gas, is monitored to give warning of a minimum dosage level (concentration-time product) that is hazardous [33]. Sulphide ions too can be toxic, as well as having undesirable corrosive effects[243,271].

1.2.2.3 Water and water content

Moisture is of great importance to food industries and in telecommunication systems (especially at splicing points), as well as for airports (prediction of fog and ice). The relative humidity of the environment may be measured, or specific humidity or a volume ratio (parts of water vapour per million parts of air). A classic method for determining the humidity (in

† [35,302,303,419,428,284]

a laboratory-based system only) is the gravimetric hygrometer. In this case, chemicals that are known to absorb water are weighed while dry, exposed to the sample, and then re-weighed. For relative humidity, electrical transducers which are based on a resistance element that changes resistance with respect to water content are used, though an independent temperature measurement must also be made. A number of schemes for detecting water vapour for specific humidity measurements have been developed, either looking at added mass (absorption) characteristics (for example platinum oxide) or a colourimetric chemical change (based on cobalt chloride, for instance)[62,158,330,389]. Methods of performing the traditional laboratory (and reliable) system in field environments are still in demand.

1.2.2.4 Oils

Oily substances can be detected in soils or in liquid colloids. The nature of the analyte (viscosity, speed of interaction) determines the sampling means. In soil, the oils being detected are likely to be contaminants, gasoline or organic solvents. This type of detection is a low-endpoint one (i.e., presence versus absence of the contaminant is necessary), as these are often considered hazardous contaminants, so sensitivity requirements are quite strict[71,136]. If the transducer is based on an optical fibre, a simple bare fibre sensor system for colloids can be used: when the core is dipped into water, with a relatively low index of refraction, the optical field remains bound; if the core is in contact with an oil, with a refractive index typically higher than that of the fibre, the optical field is attenuated. Coatings can be applied to limit the classes of oil that the system reacts with. Because of the small amount of material to be detected relative to the interferents in the detection environment, the sensor in this situation must be very sensitive and very specific.

1.2.2.5 Gases

Gaseous sensing as opposed to sensing in the liquid phase has specific requirements. Sample handling is typically more difficult, and the substances monitored are often dangerous (as in the case of HCN). Ammonia gas is detected as an environmental hazard† and thereby requires a dosage level to be detected (either a low concentration over a long period of time,

or a high concentration over a short period of time, or some combination leading to a dangerous accumulation). Carbon dioxide can be studied when dissolved either in blood or in sea water[103,264,443]; the two different environments require almost totally different approaches. Carbon monoxide is a familiar hazard and is monitored as a health and an explosive danger[444,446]; here, although the environment for the analyte is the same in either case, the 'alarm states' (concentration levels that require explicit declaration in the data presentation element) are quite different.

Volatile organochlorides are contaminants in ground water and soil [13,254]. Hydrocarbons, such as xylene, propane and toluene, as well as the potentially carcinogenic polynuclear aromatic hydrocarbons, are monitored as environmental hazards whether in soils, dissolved in water, or in the atmosphere†, which will require different sampling techniques. Hydrogen sulphide is another environmental hazard that is monitored, frequently as an industrial by-product [270]. Methane gas, with its widespread domestic use, and its potential as an explosive hazard when mixed with air (in the v/v ratio 5 to 15%), which may come from industrial or natural (farm-based) sources [98,263,264,377]. Sample handling is extremely important in all these examples, and may completely drive the design of the sensor. For example, a simple flow-through column may be used which flushes the sample past the sensing elements at a certain rate, allows a determination of concentration but reduces the likelihood of contamination of the sensing region: a sample cell for fluids may instead allow a static environment for sensing.

The medical environment (i.e., in hospital or at the laboratory) has very stringent requirements: minimum detectable concentrations or rigid concentration regimes are demanded. Oxygen gas sensing (particularly as a blood gas) has been extensively studied for its applications in biomedical applications as well as environmental and industrial areas††. Oxygen detected *in vivo* constrains size, materials chosen, and the response time of the sensor. Narcotics, such as the anaesthetic halothane, are detected in combination with oxygen [424,427]. Nitrogen oxides

‡ [18,73,129,268,314,344]

† [78,87,176,287,322]

†† [30,122,162,178,211,214,215,223,300,346,347,418,422,424,429,430,431,447]

are monitored, frequently with the use of a gas-permeable membrane[120].

In various industrial applications, gases which are not otherwise hazards also require detection. Sulphur fluoride is used to insulate switches in electrical substations and its discharge is closely monitored to prevent explosions[199]. Various solvents, both polar and non-polar, have been investigated for process control monitoring[165,182,306], and the concentration levels can relate to a degree of completeness (of a fermentation, for example) or the need to change chemical components.

1.3 Sensing system determinants: technologies

1.3.1 Non-optical sensing technologies

The many chemical analytes that are of medical, industrial, environmental or military interest have been examined by a variety of technologies. All the sensors developed are changed by the environment in some measurable manner. Although there are some exceptions, most of the techniques[145] used up to the present time fall into the categories of electrochemical, pressure-sensitive (acoustic), or pyrometric. These are briefly reviewed below: an excellent coverage of these technologies (and others) is available in the series entitled **Sensors: A Comprehensive Survey**, edited by W. Gopel, J. Hesse, and J. N. Zemel. The technological choice for the sensor system can dictate sample handling, response time, as well as other portions of ultimate system design.

1.3.1.1 Electrochemical

1.3.1.1.1 Amperometric

One of the first types of chemical sensors to be considered was based on amperometry[7,41,51], which depend on the maintenance of a fixed potential between two electrodes. The current flow in the cell is measured at the single applied potential[38]; optimally, the target chemical species will undergo chemical transfer with the electrode, so the change in current is directly related to concentration[63]. Alternatively, an intermediary can be used, which interacts with

the analyte, and then undergoes electron transfer with the electrode. Problems of flexibility in sample handling, and 'electrode poisoning' must be addressed during the design and manufacture of sensing systems based on such devices.

1.3.1.1.2 Potentiometric

Potentiometric-based sensors operate on the principle of the accumulation of charge density at an electrode surface, which in turn develops a measurable potential at that electrode. Many sensors using this principle are based on field effect transistors (FETs)†. The potential detected is related to the analyte activity present in the sample and is measured relative to an inert reference electrode also in contact with the sample[43]. Chemical sensors of this type are insulated gate FETs in which the gate metal electrode is replaced by a suitable membrane and a reference electrode. For biosensors, this suitable membrane may include structures from various plant and animal sources[43]. Difficulties in devising membranes without ionic leakage had hindered the manufacturability of these otherwise simple devices, though recent efforts have improved matters, leaving the sensitivity to ionic differences in samples (i.e., 0.1M versus 0.05 M) a potential difficulty.

1.3.1.1.3 Conductimetric

As chemical reactions produce or consume ionic species, the overall conductivity of the solution changes, usually monitored by the application of an alternating current between the two electrodes[146]. These changes will be nonspecific unless monitored on, or in close proximity to, immobilised 'indicators'. These indicators may be pH-sensitive, enzymes and their substrates, or anything else specific to the desired interaction. In this case, the changes in solution conductivity can be attributed to changes in concentration of these indicators.

One example of a conductimetric sensor is a biosensor based on a pair of microelectrodes with an applied electric field. The electrodes are surrounded by an electrolyte or buffered

† [55,179,191,255,414]

solution containing an enzyme and the species to be detected. The circuit's temperature must be closely controlled to prevent thermal effects from dominating, but once done, the instrument may be calibrated against a standard resistor across the sample cell electrodes to allow the output voltage change of the conductimetric sensor to be related to the reaction change in conductance. A type of chemical reaction that would produce such changes is the

$$\underset{\text{urea}}{NH_2 \cdot CO \cdot NH_2} + 3H_2O \xrightarrow[\text{enzyme}]{\text{urease}} 2NH_4^+ + HCO_3^- + OH^-$$

decomposition of urea to produce ammonium (NH_4^+) and bicarbonate (HCO_3^-) ions, which both serve to increase the conductivity of the test solution.

1.3.1.2 Pressure-sensitive

Piezoelectric sensors measure mass change as species are adsorbed on the sensors' surface, changing the resonant frequency of a crystal. These mass changes are made specific through the immobilisation of an indicator onto the crystal surface[343]. Some form of acoustic electrical wave propagates through the crystal either as a surface wave, bulk wave, or a combination of both types of waves[145]. An example of the piezoelectric sensor is that based on surface acoustic waves (SAW) with two sets of interdigitated metal electrodes on a piezoelectric thin planar substrate. An AC electrical signal is applied to one set of electrodes, an acoustic wave is generated and the other set of electrodes receives this wave and converts it back into an electrical signal. A sensitive coating is immobilised in the propagation path of one of the oscillators; if an analyte binds to the coating, the mass of the crystal increases, the delay time changes (as the resonant frequency of the crystal changes), and the frequency shift of the change can be related to the mass change. SAW devices have been used extensively for gaseous measurements[129] and more recently for biosensors. The investigations continue for suitable chemical coatings which display insensitivity to high-frequency oscillation while retaining selective behaviour for the analyte.

1.3.1.3 Pyrometric (calorimetric)

These sensors are based on a response, electrical or otherwise, to a change in the heat environment of the sensor. An example is the heat wire sensor, which is used in the automotive industry to measure intake air for fuel injection control, based on thin platinum wires and their heat capacity (known expansion rate as a function of temperature change)[256]. In addition, certain chemical reactions, especially biological ones, can be monitored by the heat evolved in the catalytic process. Such a device is the enzyme thermistor, which measures heat output when a sample solution is passed through an 'enzyme reactor'[262] surrounding a thermistor. The changes in resistance recorded electrically can then be correlated to a change in enzyme action.

1.3.2 Optical techniques

1.3.2.1 Bulk optics

Optical techniques are among the oldest and best established methods for sensing chemical and biochemical analytes[249]. Since the optical sensor has no metal components, it will not present a risk of generating sparks, nor will it contribute to electromagnetic interference. Although many optical geometries exist to direct light, prisms, slab waveguides and gratings are typical structures used for sensing†. All of these waveguides function to conduct light (optical energy) in a known manner, and the selective interaction of light at the interface between the sample and waveguide provides information about the sample. One of the most successful and powerful techniques[153] for chemical sensing utilises evanescent field penetration[338], in any of number of methods. These optical evanescent techniques will be discussed in Chapter 2.

---

† [23,29,39,129,132,203,204,232,253,302,303,316,353,354,367,373,381,410,356,159,164]

1.3.1.2 Optical fibre sensing

In some applications, the use of optical fibres would present significant advantages[34,341,384,388]. Their small size and weight make it a useful component for aerospace or offshore applications, or remote applications where heavy electrical cabling is excessively expensive. Most optical fibre is very flexible and can be readily inserted into small volumes or wound into various shapes (i.e., coils or loops) for particular sensing requirements[350]. It is relatively simple to multiplex (in time, or wavelength, with various wavelengths transmitted simultaneously) and have multiple endpoints[97,384,388]. Optical fibres may be used as temperature sensors†; for example, as neodymium ions in the core region of a fibre change temperature, their absorption spectrum changes; the ratio of transmitted intensity of two wavelengths is an indication of temperature[15].

1.4 Conclusions

Two main determinants for a sensor system are the analyte of interest and the technology chosen to perform the detection. The application for which the analyte must be analysed can also alter system requirements. No single technology or design is suitable for all sensor systems. In order to be successful in developing a useful sensor system, the end user or market for the system must be understood. Market studies[146,316] have examined the focus for sensors in the (near) future, and most have concluded the medical diagnostics market is the dominant area for future sales[415,416]: this includes "clinical" testing, consumer (take-home) testing, and immediate patient diagnostics (*in vivo*)[240]. The chemical sensor development lab at the Instituto di Ricerca sulle Onde Elletromagnetiche, Italy has been developing a commercialised bile monitor[45,84]. Scientists there claim that optical fibre chemical sensors are advancing faster in biomedicine than any other technology. Other areas of development include the food industry, and environmental monitoring (both for the factory and public areas). Optical sensing techniques adapted for use in these areas will be reviewed in Chapter 2.

† [3,36,40,93,118,139,269,308,359,436]

Chapter 2

Optical Sensing Techniques

Summary

The approaches to chemical and biological sensing can vary widely, but some that have met with much success use an optical technique. A number of optical approaches to gathering information about a chemical or biological sample have developed. Most are evanescent field interactions, but ellipsometry, which depends upon the polarisability of light, is also a powerful technique. In this chapter, the techniques for using optical interaction with an analyte are generally reviewed, and the applicability of such techniques to optical fibres are discussed.

2.0 Optical sensing

Of the vast number of transduction mechanisms that have been developed for use with chemical sensing, the optical property changes often provide the most readily detectable system[155,304]. Part of this stems from the fact that much of the chemical sensing currently performed relies upon the interaction of the analyte with the sensitive element of the device at a surface. The analyte typically is a relatively small molecule and the sensing problem has been interpreted to be reduced to only two dimensions[304,233]. For biosensors in particular, this would be considered an advantage as the level of interference from the bulk solution is drastically reduced. If such a surface reaction was taking place, then the chemical system being examined is not allowed to come to a true equilibrium, and an arbitrary (sensor-dependent) time frame can be chosen to suit the dynamics of interaction, thus speeding up the detection time. Some of the typically used optical sensing techniques are ellipsometry, internal reflection spectroscopy, and surface plasmon resonance.

Many efforts have been pursued in adapting optical techniques, especially optical fibres, to chemical sensing, as summarised in Appendix I. The type of waveguide used is all but irrelevant to the technique chosen, as long as it meets the assumptions of the methodology

employed (i.e., a suitable number of interactions per unit length). The abilities of the most typically used techniques are reviewed, as well as the unique features of the optical fibre that make it a most useful basis for portable and "in the field" sensor systems.

2.1 Ellipsometry

Ellipsometry is a measurement technique for thicknesses and refractive indices of thin films (up to tens of nanometers) on solid surfaces and for the measurement of optical constants (index of refraction and film thickness) of reflecting surfaces. A thin transparent film on a reflecting surface causes changes in polarisation state from which the thickness and refractive index of the film may be determined. The initially linearly polarised collimated light beam (monochromatic) upon reflection becomes elliptically polarised. The degree of ellipticity (ratio of minor to major axis) and azimuth (orientation of ellipse) provides information on changes in film thickness and refractive index[233,304]. A typical set-up for ellipsometry measurements is shown in Figure 1.

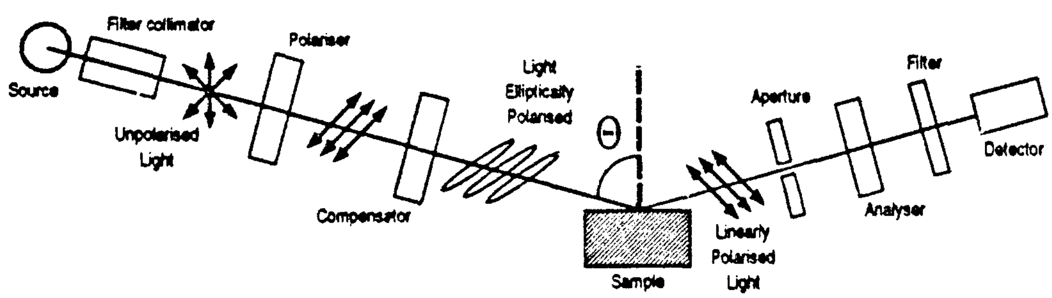

Figure 2.1 *General ellipsometric set-up .*

In general, an optical model is used[101,19] to represent the surface (substrate)-organic layer (i.e., protein)-buffer solution. This is known as the three-layer or three-phase model, and the film is assumed to be uniform (homogeneous) and non-absorbing. The thickness (d) and refractive index (n) may then be calculated. It is obvious that these are average values, as protein films are not uniform (particularly in solution), and often dynamic. Arwin[19] has examined this problem extensively, but this essential difficulty remains. Nonetheless, even these average

values provide a reference, and changes on the surface can be related to analyte concentration changes.

2.2 Internal reflection techniques

Either the characteristic absorption or fluorescence of molecular layers may be determined, based on the same principles. The optical spectrum of a sample material that is in contact with an optically denser but transparent medium is recorded. Light is then introduced into the denser medium and the wavelength dependence of the reflectivity at the interface is measured in any one of a number of ways (Figure 2).

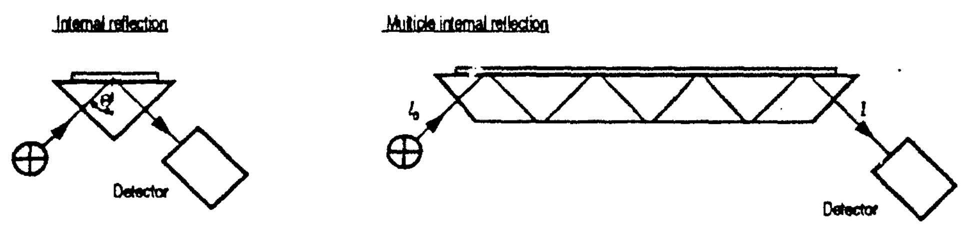

Figure 2.2 *Internal reflection techniques. The layer thickness is shaded, Θ is the internal reflection angle, I_0 the incident light intensity and I the reflected light intensity.*

When the light beam strikes the interface between the two transparent media from the optically denser side ($n_1 > n_2$), total internal reflection occurs when the angle of reflectance $\theta > \sin^{-1}\left(\frac{n_2}{n_1}\right)$. In this case an electromagnetic component of the light, termed the evanescent wave, penetrates a characteristic distance beyond the reflecting surface into the optically rarer medium. A depth of penetration is typically defined (when the electric field amplitude has decayed to a fraction of its value at the surface), which is usually of the order of several hundred nanometers. Because of this small distance, the evanescent field is absorbed by compounds on or close to the reflecting surface.

The chemical species on or near to the reflecting surface may simply absorb the evanescent field, resulting in attenuation, or may chemically convert it into fluorescent light (of a longer wavelength) that can be detected separately from the incident light.

2.2.1 Attenuated Total Reflection (ATR) spectroscopy

If the analyte has a characteristic absorption maximum or spectrum, it should be possible to monitor interface binding reactions optically. A great mass of data is readily available on many chemical compounds (and elements) in the UV and IR portions of the electromagnetic spectrum[384]. Data are not so readily available in the visible portion, and thus must be determined prior to system development. Virtually any type of waveguide may be used to assess the absorption spectra; the most successful systems rely upon the use of the evanescent field to interact with the surface†. Many techniques rely upon a planar waveguide[371,382], with many points at which the optical energy interacts with the analyte. For similar reasons, optical fibres could be used, since with a suitably long interaction length, many sampling points could be obtained.

2.2.2 Totally-Internally-Reflected Fluorescence (TIRF) spectroscopy

Internal reflection fluorescence is a subset of internal reflection techniques[153,304,371]. Detecting fluorescent light, as used in TIRF spectrometry, typically reduces interferent affects that would result in attenuation of the original light beam from factors unrelated to the analyte [24]. The set-up for TIRF, shown in Figure 3, is very similar to that of internal reflection techniques for absorption, but incorporates a filter to eliminate the input (pump) light. The waveguide in this case may be planar, a prism, or even an optical fibre.

† [338,353,354,355,384]

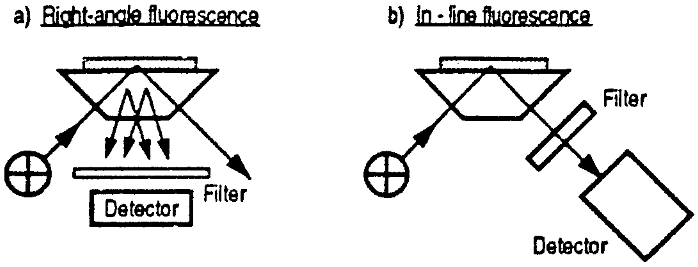

Figure 2.3 *Internal reflection fluorescence: right-angle (a) and in-line (b) detection.*

2.3 Surface Plasmon Resonance (SPR)

A surface plasmon wave is an electromagnetic wave which propagates along the surface of a metal. In general, this wave is a guided wave formed at the interface of a metal and a dielectric when TM polarised light is incident at a suitable angle on the interface from the dielectric side. A surface plasmon can be optically excited by evanescent waves if, for example, an incident light beam is reflected at the surface of a glass substrate coated with a thin metal film (often gold or silver). If surface plasmon resonance is induced, light will be readily absorbed at a certain angle of incidence of the light beam. This effect can then be observed as a sharp minimum in the intensity of reflected light[34]. The resonance angle is extremely sensitive to variations in the refractive index of the medium bonding on top of the metallised surface (illustrated in Figure 4).

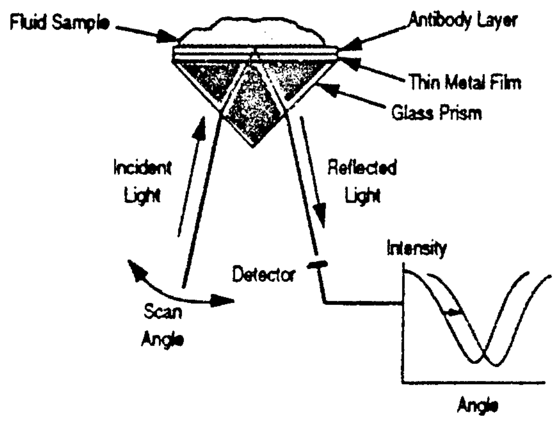

Figure 2.4 *Surface plasmon resonance and optical biosensing.*

If the metal surface had one half of an antigen-antibody pair attached to it, the binding of the second half will change the resonance angle. A limitation of this technique is that the sensitivity depends upon the molecular weight of the absorbed layer which controls its optical thickness, so low concentrations of small molecules (with a molecular weight of less than 250) are not measurable. In biological systems, however, and proteins in particular, the analytes are frequently many times larger than this limit, and SPR has had much success (including commercialised systems).

2.4 Optical fibres

For many of the techniques described above, virtually any type of waveguide can be used. The essential portion of the information is simply optical: i.e., reflectance, absorption or received fluorescence information rather than geometric, so any configuration can be used. The overall goal of most sensor research is to develop a field-deployable system (whether the 'field' is medical, environmental or industrial). Because of the growing interest in performing analysis from a remote location, optical fibres have begun to receive a great deal of attention[84].

Optical fibres can be used as a sensing element in a number of the optical techniques so far discussed (for example, SPR, TIRF and ATR spectrometry). In general, optical fibres are waveguides made of transparent dielectrics whose function is to guide visible and infrared light over long distances. A typical optical fibre consists of an inner cylinder of glass, called

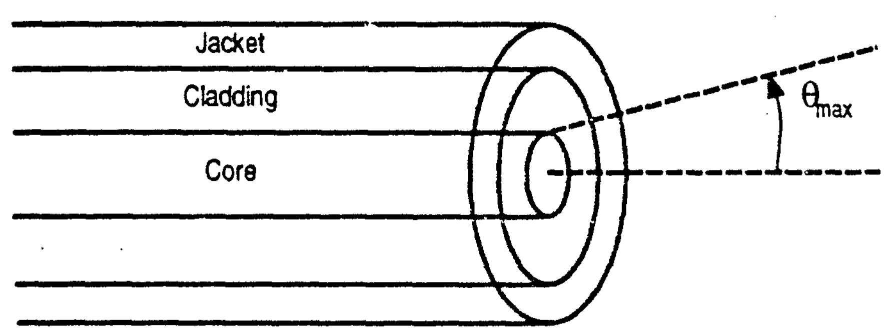

Figure 2.5 *Optical fibre: core, cladding, jacket (protective rather than waveguiding, for the most part), and angle of acceptance,* θ_{max}

the core, surrounded by a concentric shell of glass (or other material) of lower refractive index, termed the cladding, as illustrated in Figure 5.

Optical fibres may be classified in terms of the refractive index profile of the core and whether one electromagnetic mode (single mode, where a mode is the method of field propagation) or many modes (multimode) can propagate through the waveguide. Each of these configurations can have specific advantages or disadvantages, depending on the requirements of the analyte. The inherent design of fibre devices lends further advantages to the optical chemical sensing technique. Optical fibre probes are mechanically flexible, (typically) small, (potentially) inexpensive and disposable[343].

The other advantages of optical fibres cited tend to be their lack of electrical components, and continuous operation with the possibility of real-time remote output[36,330,384]. The sensing portion of the optical fibre may be remote from the optical instrumentation meaning that the probe itself can be made inexpensively (and possibly disposable), and the source can be more sophisticated. The ease of constructing arrays or networks of fibres† suggests that multiple measurements (either for different analytes or from different locales) could be performed simultaneously. Various techniques have evolved for the use of the evanescent field of the fibres, with the same advantages expected as seen for other optical detectors††. Optical fibre biosensors, especially for biomedical applications, are generating great commercial interest.

2.5 Conclusions

Optical techniques in general have had success in measuring chemical concentration as well as other parameters of samples. Most of the techniques available for other optical waveguides and configurations are adaptable to optical fibres, and their mechanical flexibility and ability to be multiplexed are further benefits. The largest future market for sensors is expected to biomedical, where optical fibres are considered to be an attractive option. The use of optical fibres in conjunction with the evanescent field should provide a reliable and sensitive sensing

† [97,99,136,317,381,448,356,331,349]
†† [167,203,208,212,235,218]

system. The method used for gaining access to the evanescent field in this research is based on adiabatically tapered fibres. The fabrication of the tapered fibre, as well as other important experimental components, is discussed in Chapter 3. The origin of the evanescent field, and methods to take advantage of it, is discussed in Chapter 4.

Chapter 3

Details of taper, coupler and taper loop fabrication and packaging

Summary

A suitable method for gaining access to the evanescent field in optical fibres was established using adiabatic tapering. The details of fabricating the basic tapered fibre, as well as fused fibre couplers are described in this chapter. A method of allow the sensitive portion of the tapered fibre to become selective as well as readily exposed to the sample was chosen, and an appropriate mount designed and described. Lastly, the computer program used to develop a theoretical understanding of the evolution of the modal fields is reviewed.

3.0 Tapering rig

The basic adiabatic taper, at the Engineering Department of Cambridge University, was made on the tapering rig originally designed by H.S. MacKenzie[237] and subsequently upgraded for better fibre alignment and gas control by G.J. Pendock[295]. The rig is similar in concept to those used for making fused fibre couplers and other tapered fibre components[64, 46]. It consists of two motor driven stages (Oriel) incorporating a micrometer and a gas burner flame to soften the fibre. The stages moved apart in opposite directions at the same speed (2 to 100 μm/second) to ensure symmetric tapering. The gas flame was a mixture of oxygen and methane (town gas; or butane or propane). The length of the flame was adjustable, as was the ratio of gases used (with a flow rate of approximately 25 cm^3/minute), which was accomplished through the use of needle-valves and flow meters in the gas supply lines. The burner heads were custom made within the workshop, and were mounted on a sliding stage that could easily remove the heat from underneath the taper once the process was complete. Jigs in conjunction with magnets held the fibre in place during the tapering.

3.0.1 Fibre preparation

The fibre used in all cases was SM450 fibre from York Technology (preform YD580) with a numerical aperture of 0.18, an outer cladding diameter of 80 microns, and a nominally circular core of diameter 1.7 microns. A central portion of the fibre's protective coating was removed by dipping it in NitroMors (a commercially available paint stripper), waiting a short period of time (two minutes), and stripping off the affected portion. This portion was then thoroughly cleaned with acetone, and placed in the grooves of the supporting jigs (fixed in place with small magnets). The jigs holding the fibre were carefully aligned to prevent the taper from bending during the heating process. One end of the fibre was then illuminated with a monochromator-selected white light source (tungsten); the other end illuminated a large area photo diode (RS Components). The transmission through the fibre was monitored during the tapering process (an acceptable loss was 0.1 dB or less). The general set-up for the tapering rig (without light source, monochromator, or photodiode) is shown in Figure 1.

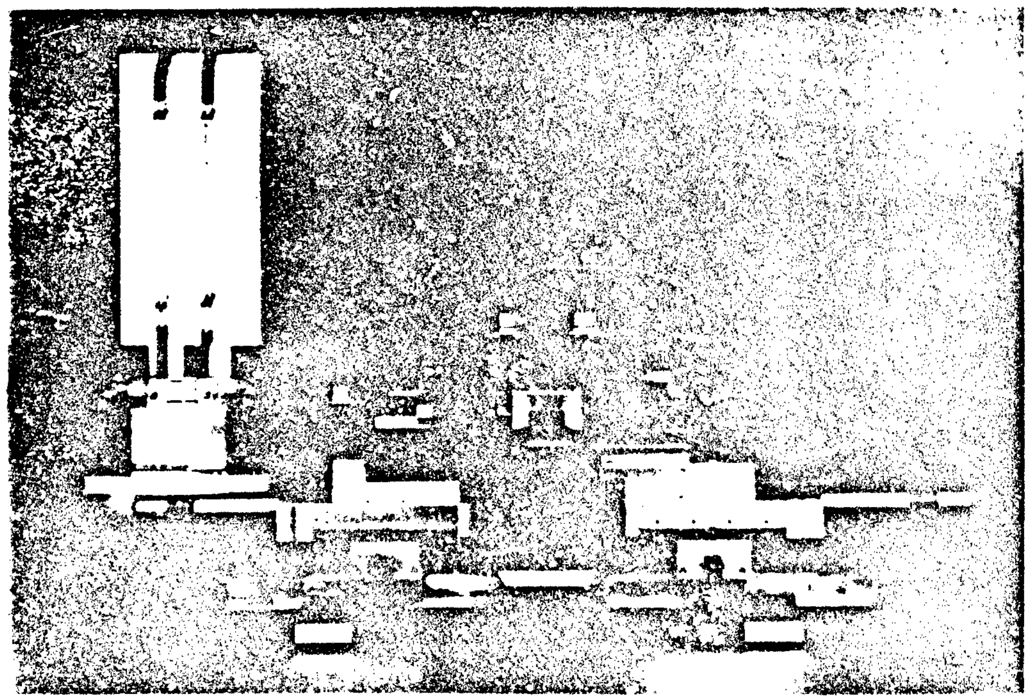

Figure 3.1 *The tapering rig: motor-driven mounts with supporting jigs for fibre, burner head on sliding stage, gas supply lines.*

3.0.2 Tapering process

The tapering was started by placing the flame underneath the prepared fibre and engaging the motor driven stages. The speed of the motors had to be slow enough to ensure a smooth profile (6 to 10 μm/second) though rapid enough to prevent taper sagging. When the taper waist reached the desired diameter, the process was stopped, the tapered fibre mounted suitably, and the actual diameter measured by microscope. The waist diameter was gauged largely by eye during the process, and by noting the distance traveled by the stages, which was at least 10 mm (from the centre point, or a total of 20 mm, and up to 40 mm). The profile of the tapered fibre could be approximated conveniently by an exponential function[186]. Taper waists of the order of one micron were used routinely for most experiments, especially those involving tapered loops (section 1.2).

3.0.3 Initial dye cell mounts

For several of the initial experiments, the finished tapered fibres were mounted in aluminium dye cells, as illustrated in Figure 2. The fibre and dye cell were covered with a small, thin slab of Perspex to prevent dust and other foreign objects from landing on the fibre surface, as well as to provide a fixed volume for interaction inside the dye cell. The fibre was bonded to the mount using a reagent-resistant glue (Plastic Padding Chemi-Dry, with additional resin to achieve a proper viscosity), and the Perspex slab to the mount with a silicone adhesive (commercially available bath sealant). A peristaltic pump, shown in Figure 3, with a magnetic stirrer, was used in the experiments using the dye cell, which served to circulate the solution along the taper at speeds from 2 to 7 cm/s. This speed did not break the taper nor did it cause quenching of fluorescent solutions (when used).

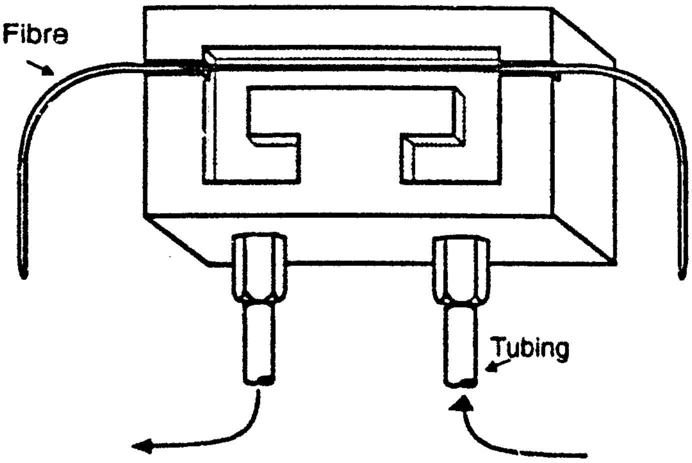

Figure 3.2 *Custom made dye cell mount (45 by 20 mm) for tapered fibre: aluminium with plastic (Tygon or other suitably flexible material) tubing to allow solutions to flow.*

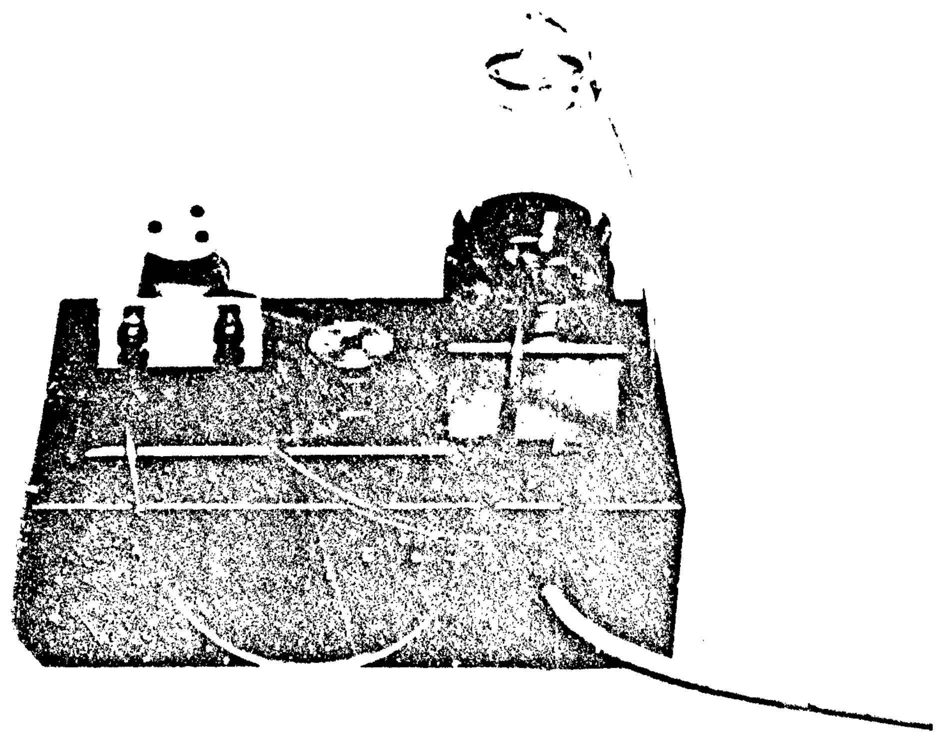

Figure 3.3 *Peristaltic pump used to circulate solutions through the dye cell, along the taper interaction length: magnetic stirrer in reservoir to mix solutions.*

3.1 Couplers

Couplers were used throughout these experiments to monitor input power to the tapered fibre or tapered fibre loop. These were constructed using the same tapering rig with a minor adaptation to the methodology. The fused fibre couplers are cladding mode devices which, during the tapering process, allow the fields in the fibres to become cladding guided. When the fields enter the fused region, the zeroth and first order cladding modes of the effective waveguide system (two cores, partially fused cladding region, outer cladding region) are excited[292], and coupling between the two branches arises from the interference between these two modes as they propagate across the fused, tapered region. The splitting ratio between the two branches depends on the phase difference between the two modes as they leave the fused region and are recaptured back into their respective cores. In practise, it is difficult to 'design' the actual ratio required (i.e., a desired ratio of 95:5 may turn out to be 97:3 and so forth).

Fabrication of a coupler required two lengths of fibre to positioned side by side on the tapering rig with contact between the exposed cladding but no twist. This was critical to minimising loss, and was examined carefully with a microscope prior to initiating the taper process. The transmission loss and power transfers during the tapering process were monitored as before, and the process was stopped when the desired output ratio was achieved. Removing the flame always resulted in a slight increase in the coupling coefficient as cooling took place[58], but this was not critical for any of the experiments as long as the ratio between the two branches was known. Couplers were packaged in grooved silica rods (with the tapered portion in air)[66], and subsequently in Perspex containers, as pictured in Figure 4. When needed in the optical circuit, a coupler was spliced in front of the taper to monitor the input power. The splicer used was a B.I.C.C. (British Insulated Calendar Cable) Test Instruments AFS 3100 fibre splicer, and the insertion loss of adding a splice coupler was no more than 0.3 dB.

3.2 Taper loop

As will be discussed in Chapter 8, a 180° macroloop could be losslessly introduced into the tapered region of the fibre after it had been made. Loops were made using a custom-made

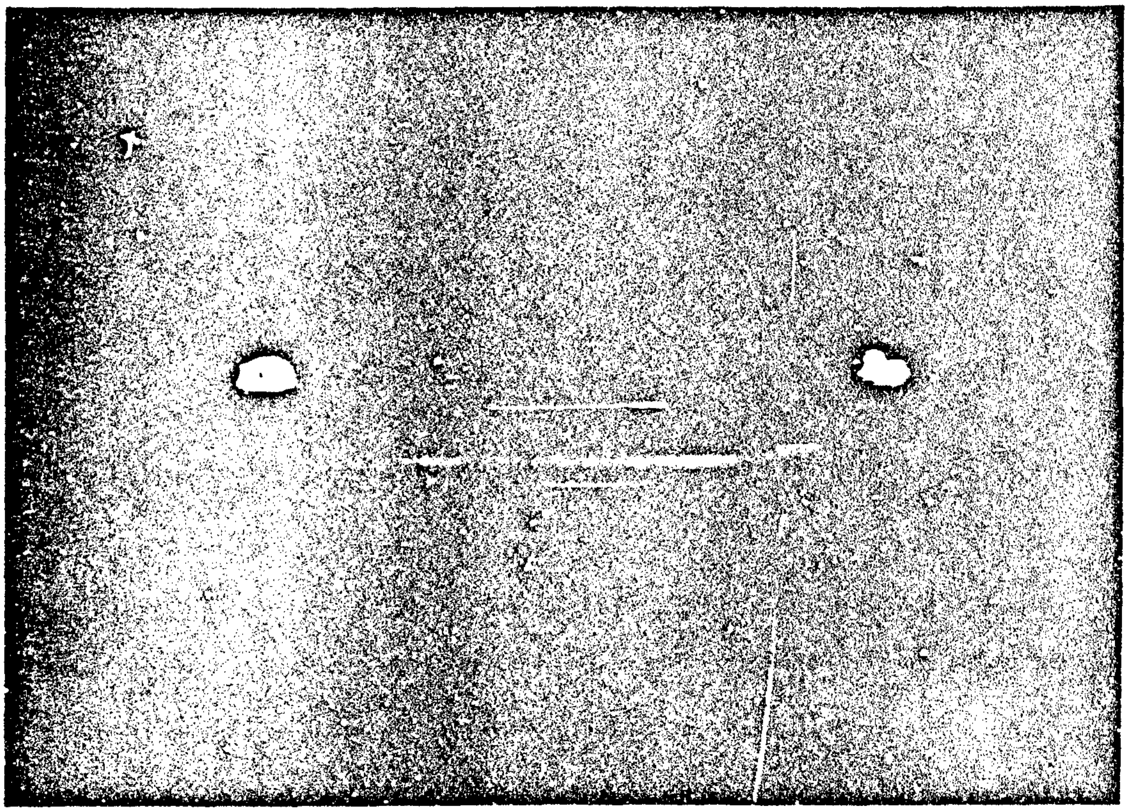

Figure 3.4 *Packaged coupler: a Perspex container was used to store the couplers for use in experiments (cover removed here for clarity). Some of the chemical processes required that the coupler be respliced onto the fibre leading to the mounted taper at the beginning of every sample run.*

jig, as shown in Figure 5. After the tapering process was complete, one side of the tapered fibre (near the original diameter portion) was bonded to a new (from the dye cell) mount (shown in Figure 6). Once the glue had set, the end of the tapered fibre farthest from the mount was slipped out of the jig and rotated 180° and slipped into the groove of the mount. The length of the looped portion could be adjusted with the use of a metal guide rod (shown in Figure 5). The transmission was monitored throughout the process to ensure a return to the original transmission. The fibre could be slid along the groove to recover the initial signal, if necessary. The second end of the fibre was then bonded to the mount (made of brass to be chemically inert, as made necessary during some of the heating steps in the cholera immunoassay). The upper portion of the mount was then joined to the base forming a

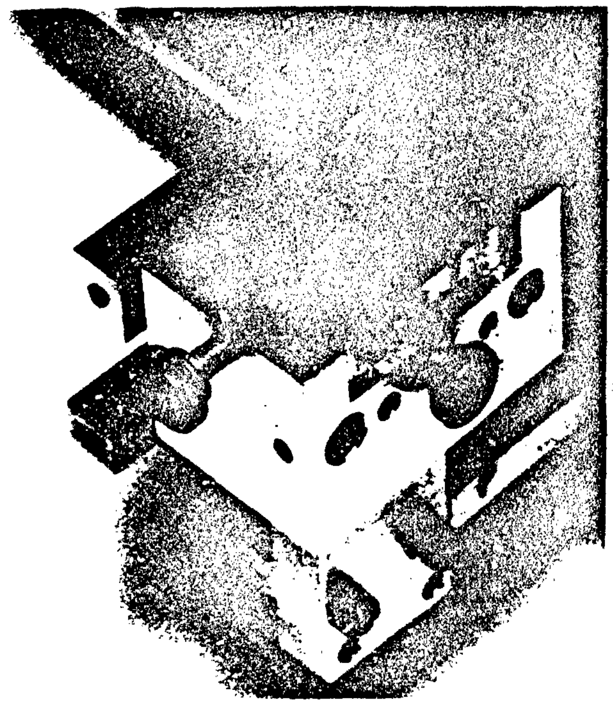

Figure 3.5 *Jig for making tapered loops with centre post to guide length of loop.*

complete unit, and a protective cap (made of Perspex, lead, glass, or any other material as required) slipped over the looped portion to protect it (or to allow chemical interaction with the waveguide).

These mounts were found to be very robust, and could easily withstand any number of knocks (barring head-on drops onto the loop) without breakage or transmission loss. The length of the tapered loop available for interaction with solutions in its cap ranged from 10 to 40 millimeters (though the amount of evanescent interaction possible at thicker portions of the fibre is small), with an average of 20 millimeters being standard.

3.3 Computer model for field description

A computer model (developed by Dr H.S. MacKenzie in the process of his PhD[245]) was used in this research to determine the necessary transverse modal field profiles and propagations

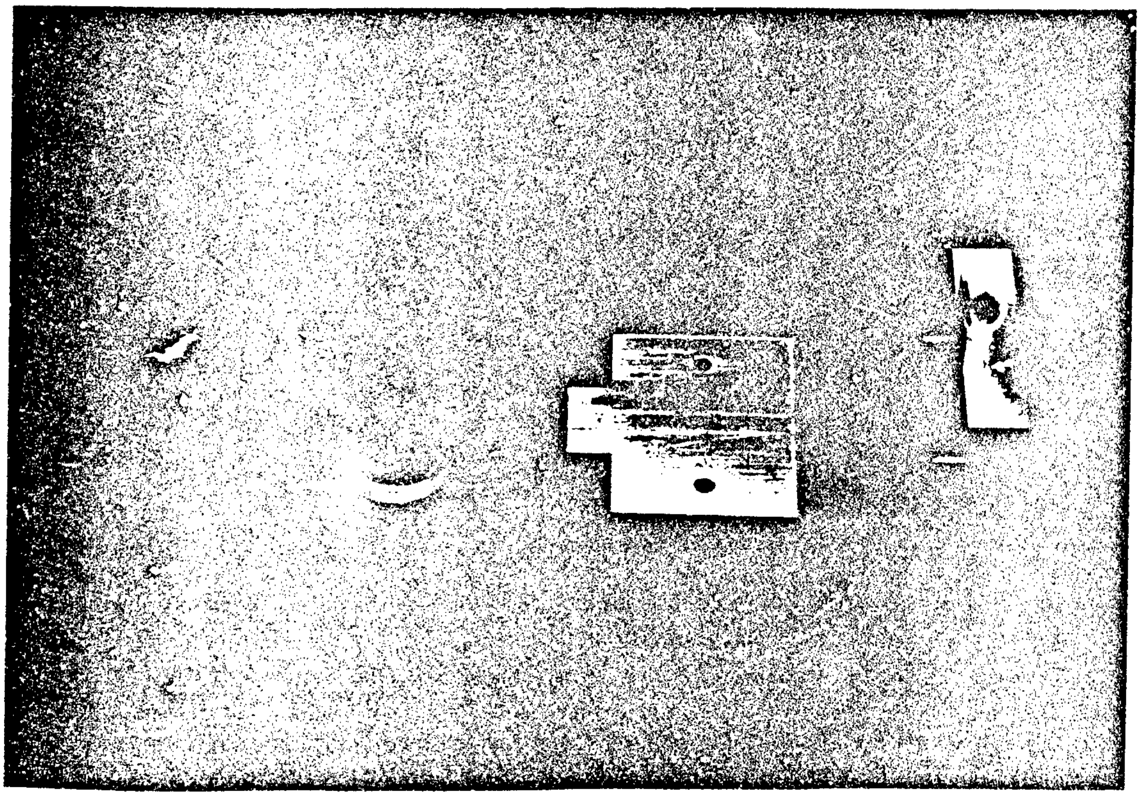

Figure 3.6 *Mount for supporting taper loops; the two sections snap into place via pins, shown on top section, which is face up, and a suitable cap (depending on type of chemical interaction required) was placed over the finished loop. Caps pictured here are Perspex and lead. The lower section of the mount is held in the jig of Figure 5. The mount is approximately 15 by 20 mm.*

in each waveguide system considered. This computer model produced the optical fields depicted throughout Chapter 8. It is a numerical algorithm based on the Strum sequence[2]: the sequence determines the minor determinants of the eigenvalue matrix, and then converges on the modal propagation constants of the pre-specified modes of the fibre. The propagation constants then determined the modal field profiles of the waveguide.

3.4 Conclusions

The components described in this chapter are the foundations of all experimentation described in Chapters 5 through 9. Although all the equipment was 'hand made', the criteria for selecting suitable optical components (i.e., low loss and acceptable configuration) allowed a known

baseline of performance to be established from which experimental success (or failure) could be judged. The characteristics of the optical field, especially the evanescent field, are discussed in Chapter 4, as this is another fundamental component of the experimental work.

Chapter 4

Applications of the Evanescent Field in Optical Fibre Sensing

Summary

This chapter contains the theoretical building blocks for the description of light propagation in fibres, as used for this research. The single mode fibres, used in all the experimental work, are treated by solving a boundary value problem while multimode fibres (frequently used in sensors decribed in the literature) apply ray optics approximations. The evanescent field, which arises in both treatments, is defined, and methods of gaining access to it are described. Details of adiabatic construction of the tapered single mode fibres are also presented. The principles presented in this chapter are applied to all the theoretical treatments of experiments presented in later chapters.

4.0 Optical fibres

Optical fibres are made of transparent dielectric material which can guide visible light (for the purpose of this dissertation) over long distances. The refractive index profile for the fibres used in this research was that of a step index fibre, with a core of higher refractive index than the cladding, as depicted in Figure 1. Most of the optical power is confined to the core, but the evanescent field, described by modified Hankel functions (K_ν), extends into the cladding. The derivation of this field is discussed in the next section.

4.1 Description of the fibre

The optical power in a fibre is described in terms of the fields of the electromagnetic energy. These are expressed as superpositions of simpler field configurations, and for guided modes, the values of the propagation constants (β) must be solutions of the eigenvalue equation satisfying the requirements of Maxwell's equations and certain boundary conditions. For

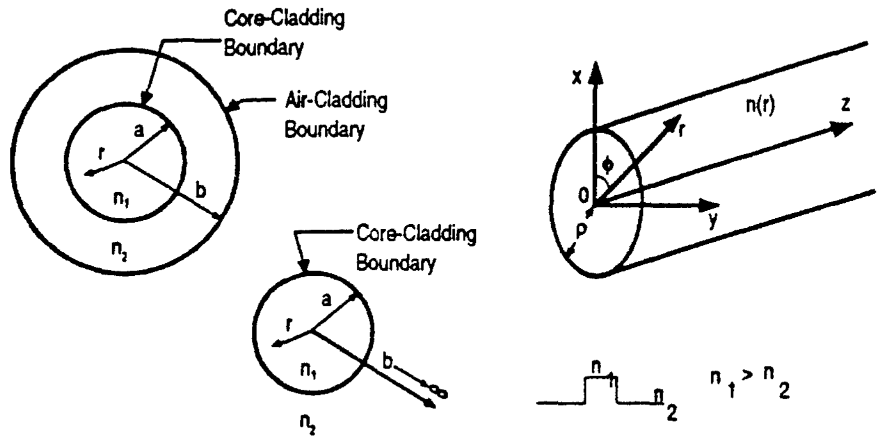

Figure 4.1 *Step-index optical fibre: r is the radial coordinate, n(r) is the index of refractive distribution,* ρ *is the radius of the fibre, a is the core radius, b is the cladding plus core radius,* n_1 *and* n_2 *are the refractive indices of the core and cladding respectively.*

monochromatic light fields, the time dependence of the electric field is $e^{i\omega t}$; the symmetry allows for a simple dependence on the longitudinal z-coordinate $e^{-i\beta z}$.

$$\beta = \text{propagation constant} = nk;\ k = \text{wave number} = \frac{2\pi}{\lambda}$$

$$\omega = \text{radian frequency};\ \lambda = \text{wavelength}$$

4.1.1 Weakly guiding fibres

In most cases, the difference between the cladding and core refractive indices is small. This is expressed by Δ, the fractional refractive index difference or the profile height parameter:

$$\Delta = \frac{1}{2}\left[1 - \frac{n_{cl}^2}{n_{co}^2}\right] \approx \frac{n_{co} - n_{cl}}{n_{co}} \tag{1}$$

Defining a modal cutoff parameter V (also termed waveguide parameter or frequency):

$$V = \kappa_c a = \frac{2\pi a}{\lambda_o}\sqrt{n_{co}^2 - n_{cl}^2} = \frac{2\pi a}{\lambda_o} n_{co}\sqrt{2\Delta} \tag{2}$$

n_{co} = core refractive index

n_{cl} = cladding refractive index

a = core radius

λ_0 = source wavelength

If the approximation $n_{co} \approx n_{cl}$ is used, then Δ is small, and $\Delta^2 << 2\Delta$

$$\kappa_a = \frac{2\pi\,NA}{\lambda_o}\,;\ NA = \sqrt{n_{co}^2 - n_{cl}^2} \approx n_{co}\sqrt{2\Delta}$$

Usually, $\Delta < 1$. The propagation constants for the guided modes may be approximated by [358].

$$\beta \approx n_o k \qquad (3)$$

It can be shown that the fields of the guided modes of weakly guiding fibres are very nearly linearily polarised and are termed LP modes[131]. All the field components can be obtained as derivatives of one dominant transverse component of the electric field vector.

4.1.2 LP modes

LP modes are the approximate mode solutions when the approximation for the propagation constant is used. LP modes are valid locally, and are actually superpositions of exact solutions[131]. These LP modes are useful because they allow simple approximate eigenvalue equations for the guided modes. Inside the core ($r \leq a$), J_ν is the solution for the electric field:

where $J_\nu \equiv$ Bessel function of the first kind of order ν ; finite at the origin .

Outside the core ($r \geq a$), "modified" Hankel functions, K_ν, are used[14,357]. The cladding field must satisfy the condition that field amplitudes tend to zero as they extend to infinity and for large values of γ the modified Hankel function behaves asymptotically like an exponentially decaying function.

$K_{\nu}^{(1)} \equiv$ modified Hankel function of the first kind of order ν.

For large values of γ, where γ is defined by $\gamma^2 = \beta^2 - n_2^2 k_o^2$,

$$K_{\nu}^{(1)}(j\gamma) \approx A\sqrt{\frac{2}{\pi\gamma}}\, e^{-\gamma}. \qquad (4)$$

The exact mode solutions, even in step index fibres, would have very complicated equations: using the weakly guiding LP approximation the solutions are obtained from matching boundary conditions that require continuity of the transverse and longitudinal electric field components at the core boundary.

4.1.3 Power outside the core: the evanescent field

The power contained outside the core decays exponentially at large distances from the core-cladding interface. Gloge [131] has calculated the power in the cladding as a function of V, using the ratio:

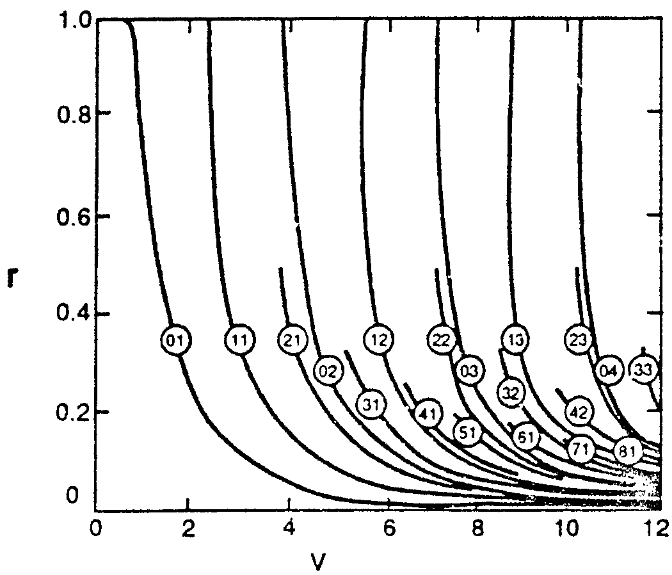

Figure 4.2 *Fraction of total available evanescent field power versus V number (note that the mode number appears in circles on the curves)*

$$r = \frac{P_{clad}}{P_{tot}} \tag{5}$$

For sensor systems using the evanescent field as the method of interaction with the sample solution, modes with almost all of their power in the cladding would be preferred, and selective excitation of these modes is through the use of masks and mode strippers is often attempted in multimode fibre sensors.

Fibres may be constructed to have either one or many modes at a given wavelength (multimode fibres referred to earlier). If only the LP_{01} mode (fundamental mode obtained from the exact analysis of the fibre) will propagate, then the fibre is termed single moded. The cutoff conditions for these modes are shown in Figure 3. For multimoded fibres, the number of modes is large, but finite, and approximated by [131]:

$$N = \frac{V^2}{2} \tag{6}$$

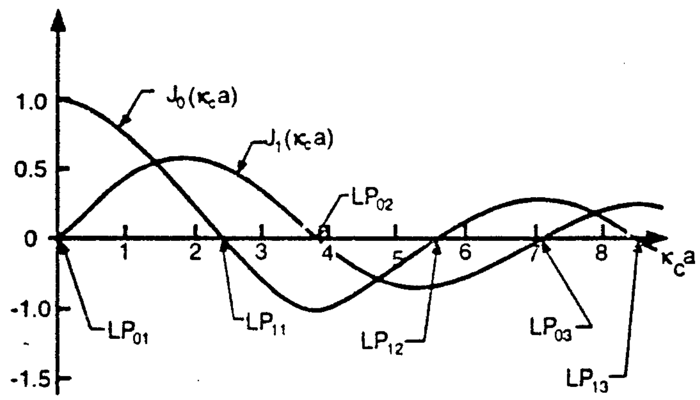

Figure 4.3 *Plot of Bessel functions used for calculating cutoff conditions of LP_{0m} and LP_{1m} modes.*

4.2 Multimode fibres and ray optics

An alternative method for analysing optical fibres, particularly multimode fibres, is that of ray optics (Figure 4)[125]. The ray picture is valid when the number of modes in a fibre is large (compared to one). The guided mode is described as a guided ray, which is totally internally reflected at the core-cladding interface.

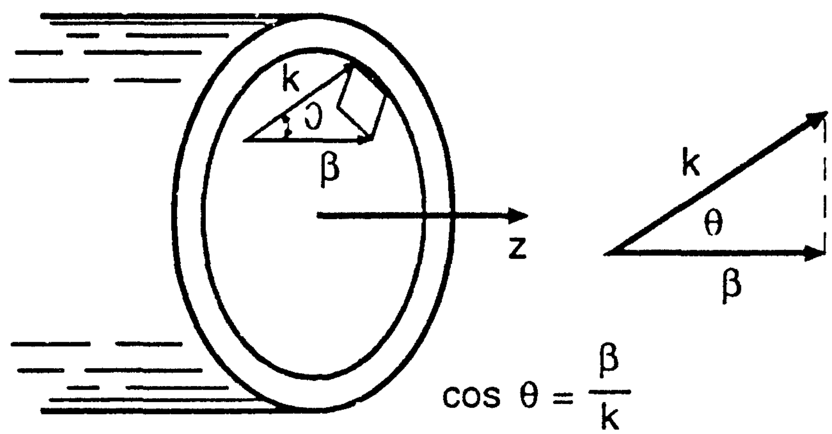

Figure 4.4 *Geometric (ray) description of optical fibre*

4.2.1 Total internal reflection

Snell's law states:

$$\frac{\sin \theta_1}{\sin \theta_2} = \frac{k_2}{k_1} = \frac{n_2}{n_1} \tag{7}$$

for an obliquely incident wave upon a boundary going from a denser medium of refractive index n_1, to an optically rarer medium of refractive index n_2 (*i.e.*, $n_1 > n_2$).

For $n_1 > n_2$, as θ_1 increases, an angle of θ_c is reached where $\theta_2 = \frac{\pi}{2}$, or

$$\sin\theta_2 = 1 = \frac{n_1}{n_2}\sin\theta_c \qquad (8)$$

When $\theta_2 = \frac{\pi}{2}$, there is no propagating wave in medium 2 and the wave will be "totally internally reflected" in medium 1.

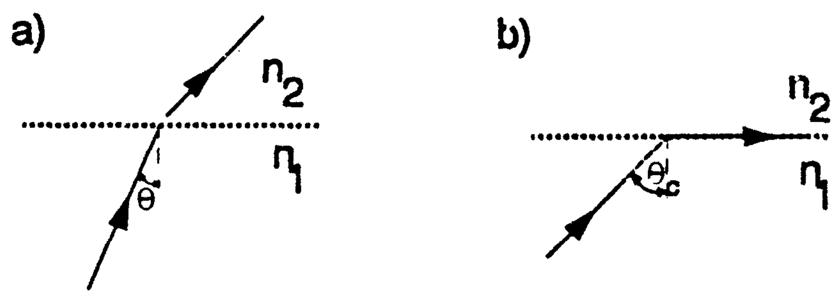

Figure 4.5 *Total internal reflection: a) oblique incidence; b) at the critical angle, where the light is totally internally reflected*

$$\vec{E}_T = \vec{E}_2 e^{-\alpha z} e^{j\beta y} \qquad (9)$$

Defining α and β:

$$\alpha = k_2\sqrt{\frac{n_1^2}{n_2^2}\sin^2\theta_1 - 1} = \omega\sqrt{\mu_o\varepsilon_2}\sqrt{\frac{n_1^2}{n_2^2}\sin^2\theta_1 - 1} \qquad (10)$$

$$\text{and } \beta = k_2\frac{n_1}{n_2}\sin\theta_1 = \omega\sqrt{\mu_o\varepsilon_2}\left(\frac{n_1}{n_2}\right)\sin\theta_1 \qquad (11)$$

The "evanescent" wave has an attenuation constant α in medium 2. β is a phase propagation constant. A "penetration depth" is often defined which describes the distance travelled for a given reduction in E (sometimes taken to be 90%, or e^{-1} - 63%). As an example, for the electric field amplitude to fall to $\frac{1}{e}$ of its initial value, E_o (at the interface),

$$E = E_o \exp\left(\frac{-z}{d_p}\right). \tag{12}$$

The magnitude d_p is given by

$$d_p = \frac{\lambda}{2\pi n_1 \sqrt{\sin^2\theta_i - \left(\frac{n_2}{n_1}\right)^2}} \tag{13}$$

Further, the quantity of evanescent power which is available within this depth is important. Various techniques have evolved to gain access to the evanescent field power in an optical fibre.

4.3 Access to the evanescent field

In general, exposure of the evanescent field involves removal of the cladding of the fibre. Three methods of doing this are etching, polishing or tapering the optical fibre, as depicted schematically in Figure 6.

Etching relies on a glass solvent, such as hydrofluoric acid, to dissolve or etch away the cladding[illegible]. As the cladding is removed concentrically from the fibre, an increasing fraction of the modal evanescent field will be exposed. These devices are typically delicate, non-ruggedised components[276-311]. Etching causes an abrupt profile to be presented to the modal fields, and will not maintain the distribution of power amongst the fibre guided fibre modes. Some of the power will be coupled into radiative modes, and thus represent an overall

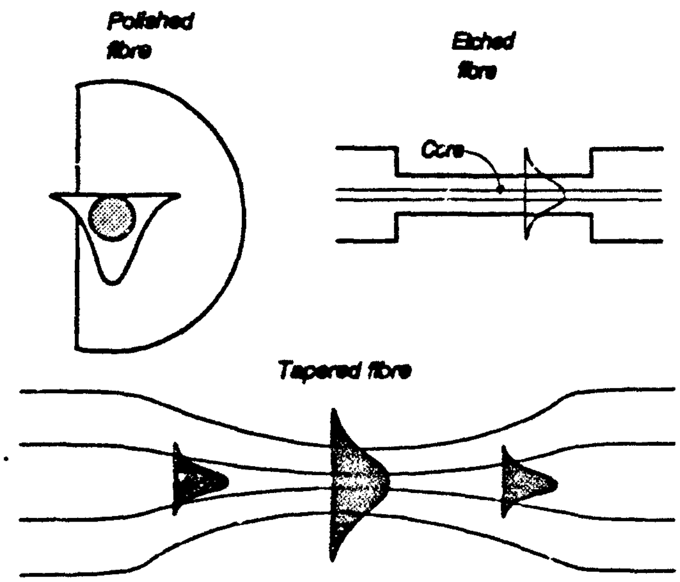

Figure 4.6 *Depictions of methods of gaining access to the evanescent field*

loss to the power within the fibre. Even with the most careful etching, at most 60-80% of the evanescent field can be exposed to the external solution.

Polishing is similar in a number of respects to etching, but removes only (up to) one half of the cladding, forming a D-profile, until the core is almost exposed[163,396,362]. These devices can be made adiabatically (without power loss) as long as longitudinal changes are made gradually, and the optical surfaces are made optically smooth[96]. A maximum of about 20% (due to asymmetry and refractive index sensitivity) of the modal evanescent field can be exposed to the surrounding media.

The third and most important technique for exposing the evanescent field involves tapering the fibre over an arc or flame†. The tapering makes the core diameter and the localised V value so small that the field(s) extend greatly into the taper region, to the point that potentially all the evanescent field can interact with the outside material. These devices can be readily manufactured with low loss (0.1 dB)††.

† [31,49,51,72,379,64,81,70]
†† [181,238,239,293,296,276]

4.4 The adiabatic taper

In the course of tapering, the field within the fibre becomes less confined to the core and gradually spreads out into the cladding. The field is guided by a combination of core-cladding-external refractive index and, at the taper waist, finally only by the cladding and the external medium. As the radius of the fibre changes, coupling of the energy in the LP_{01} mode may occur to the higher order LP_{0m} modes. These are lossy modes for the taper. In an adiabatic tapered fibre, negligible transmission losses (0.1 dB or less) occur during the tapering process. For tapered fibres to be suitably adiabatic, their longitudinal refractive index profiles must change with sufficiently small taper angle $\Omega(z)$ (between the tangent to the core-cladding interface and the fibre axis and the local core radius $\rho(z)$)[228] to prevent lossy coupling into radiative modes[53,204,229,54]. This is shown in Figure 7.

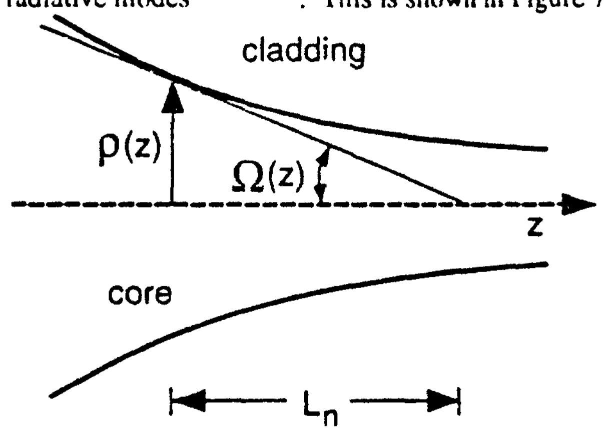

Figure 4.7 *Length scale for adiabatic taper*

L_n = distance from the origin of ρ to origin of cone with half-angle Ω.

$\Omega < 1$, in practice, and thus $L \approx \frac{\rho}{\Omega}$.

The radius along a taper changes as

$$\rho(z) = R_o \exp\left(\frac{-z}{L}\right) \qquad (14)$$

R_o = untapered fibre radius

Low losses result when the taper profile does not change abruptly and the slope of the taper is far smaller than the normalised beat length, $\frac{\rho}{z_\beta}$, no coupling will occur. The smallest inverse beat length will be above the slope of the taper (this will be seen again in Chapter 8).

4.5 Applications of tapered single mode fibres as evanescent sensors

Having now selected an optimal method of obtaining access to an optical fibre's evanescent field power, it is necessary to develop several sensor configurations to compare the actual performance of our devices with that reported in the literature using different techniques. For chemical sensing, the light in the evanescent field may be attenuated by the external media (absorption-based sensing) or light generated external to the fibre (near the surface) may be captured by the evanescent field and transferred to the fibre's guided mode (fluorescent or luminescent based sensing). As with most systems, problems are often found putting into practise what seems an improvement in theory. Many of the optical fibre sensors reported by other researchers have had their share of both successes and failures. The tapered single mode fibre was examined for its potential as an evanescent field chemical sensor by measuring its performance in detecting absorption changes and capturing induced fluorescence. The behaviour of the waveguide was assessed in each case by resorting back to LP mode theory. Once this baseline had been accomplished, more complicated systems were assayed. Before describing this, however, it is necessary to review some of the earliest efforts to use optical fibres as sensors to compare the tapered single mode fibre's effectiveness as a new and improved platform for a sensor system. This will be accomplished by examining absorption-based sensing with optical fibres in some detail in Chapter 5.

Chapter 5

Absorption-based evanescent field optical fibre sensors

Summary

A potentially elegant method of applying internal reflection techniques to optical fibres would make use of the evanescent fields of the guided modes. Difficulties in implementing this in a satisfactory manner has led investigators to use optical fibres primarily for their light carrying capability, and have merely substituted photons for electrons in analysis of the analyte. The initial absorption-based optical fibre sensors, and the subsequent efforts to apply evanescent absorption to optical fibres are discussed. Lastly, the promise of the tapered mode single mode fibre as an evanescent absorption sensor is explored, experimentally and theoretically.

5.0 Absorption-based fibre sensors: initial efforts

The earliest efforts to exploit the potential of optical fibres for optical chemical sensing relied on the absorbance characteristics of a chemical system and the capability of optical fibres to carry light to and from the sensing region†. Absorption coefficients, based on Beer's Law, were well-known for many compounds (and elements) of interest.

Beer's law describes the attenuation of a beam of light as it passes through a solution of an absorbing chemical species. For many species it is found that the optical power P_{out} after passing through a length l of solution (of uniform concentration) is given by

$$P_{out} = P_{in}\,10^{-\varepsilon c l}, \tag{1}$$

† [16,17,18,22,26,32,33,35,60,73,92,103,120,147,148,169,172,173,183,243,270,272,299,306,311,313,403,430, 431,432,444, 445]

where c is the molar concentration of the solution and ε is the molar absorption coefficient. Equation 1 may be rewritten as the more familiar

$$P_{out} = P_{in} \exp(-\alpha l), \tag{2}$$

where the absorption coefficient α is given by

$$\alpha = \frac{\varepsilon c}{\log_{10} e} \tag{2a}$$

Equation 2 is the exponential absorption law for a bulk material, with α proportional to the concentration of the absorbing compound. For those materials not obeying Beer's law, a more complex absorption/concentration calibration curve must be derived.

An absorption-based optical fibre system was devised in the 1960's for detection of oxygen in the blood[178]. This required the development of an absorbance spectrum based on concentration because Beer's law does not apply to blood. Although many other fibre sensors have been developed since then, many suffer from the same problems of this first attempt: low sensitivity when compared to other technological methods and insufficient specificity. Most work has focussed on the use of multimode fibres as a type of light pipe - that is, a means of transmitting light from one point to another (shown in Figure 1), rather than utilising the convenient properties of the evanescent wave.

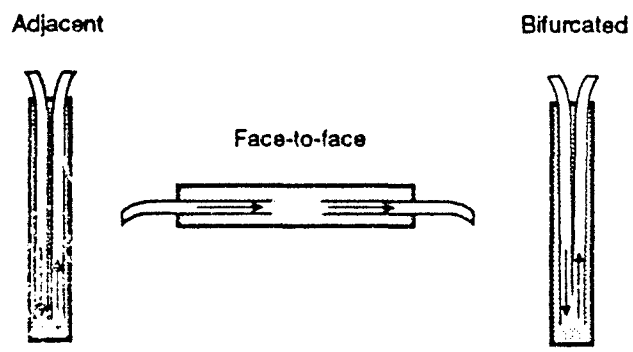

Figure 5.1 *Extrinsic "light pipe" sensor arrangements (abridged from Appendix I)*

Kapany's work in 1964[178] used an optical fibre device as an *in vivo* oximeter. It was designed to measure the oxygen saturation in the blood, to replace an off-line sampling system. The system was based on the detection at two wavelengths of back-scattered light from the blood cells: one fibre conducted light to the sample, and another collected it and guided it through a filter to a photo detector. The investigators found some difficulties in interpreting their results, as blood is a complex medium to analyse optically because it does not adhere to Beer's Law, the flow velocity alters some of the detected optical properties, and so forth. The conclusions of this study were simply that optical fibres can be a useful research and clinical tool as they permit sampling of specimens in remote locations and in the dynamic state.

Nearly thirty years later, advances have been made, with the development of smaller optical fibres, and more sophisticated techniques to interpret absorptive data. A commercialised bile monitor[45,84] system is being developed and placed on the market. The bile sensor can monitor the level of bilirubin (a major disease causing compound in the stomach) in bile which has an absorption peak at 452 nm[117,184,45,84]. There is no absorption above 750 nm, allowing for a simple differential absorption scheme to be carried out. This device, though marketed, is optically clumsy, as a bundle of fibres brings the light to the sample, and another bundle brings the light to the detector. The biggest stumbling block to overcome with this type of set-up is the typically low signal losses received in such a scheme. A more elegant technique would involve evanescent absorption detection, and would enhance the sensitivity of such a device, since the portion of light from the optical fibre interacting with the sample remains guided by the waveguide.

Researchers have been actively pursuing development of an all-fibre evanescent spectroscopic probe†. Approaches which remove the cladding through etching or polishing typically result in a fragile optical element that is susceptible to chemical attack and fouling. For analytes that are solvents, a polymer clad fibre can be used, as the polymer acts as a diffusion membrane. In one such system[104] a dye had to be added to the sample, and the multimode fibre was tightly coiled about a mandrel before insertion into the sample solution. Beer's Law

† [104,198,268,291,251,323,16,29,324,338,370,375,377,401]

was not completely obeyed for the chemical system, despite the fact that bulk spectrophotometric tests showed that the dye itself obeyed Beer's law. DeGrandpre et al[105] pointed out that the assumption of equal power distribution amongst fibre modes made for analysing the absorption of the evanescent fields of all the fibre modes could not be valid.

Further work involved examining the evanescent absorption behaviour for unclad fibres[321,322,323,324]. Simple straight line adherence to Beer's Law was not found. The analysis of these results caused the researchers to conclude that surface adsorption effects existed due to the electrostatic interactions between the polar silica surface and the ionic solution (DeBye-Huckel interactions[323,324]), and interfere with evanescent absorption. This phenomenon was considered to be irreversible and a fundamental fibre limitation for evanescent absorption devices.

5.1 Absorption-based evanescent field fibre sensor modal behaviour

Some researchers[93,291,401] examining the interaction between the evanescent field of the fibre modes and the surrounding medium (usually a solution) have reported successful use of Beer's Law to interpret their absorbance data. In this case, the concentration of the analyte is then simply related to the measured optical attenuation along the fibre's sensing region. Polished multimode fibres were often used: the distribution of optical power amongst these modes is critical to overall sensitivity. It is not trivial to launch light into a given distribution of modes or a specific, higher order mode. Various configurations have been tried, as depicted in Figure 2. Although the initial distribution launched into the multimode fibre is not maintained along

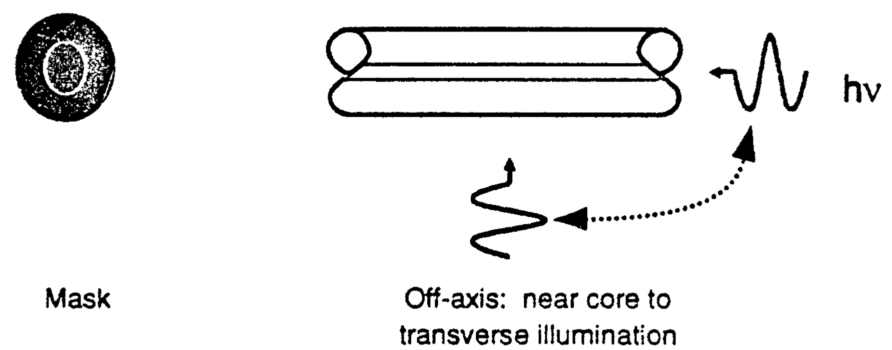

Figure 5.2 *Selective launch methods in multimode fibre to access higher order modes*

the length of the fibre, selectively exciting higher order modes with a higher proportion of energy in the evanescent field could improve sensitivity. Another option is to uniformally excite all possible modes in the fibre at once and have a uniform distribution of optical power throughout the whole of the fibre, including the sensing region. Knowing the power distribution amongst the modes of the fibre at the point of sensing allows Beer's Law to be applied.

For fibres interacting with the evanescent field, a slight modification of Equation 2 is necessary to account for all the modes absorbed by the medium. For a single mode fibre with just one mode to be absorbed, Beer's law still holds, and no modification beyond accounting for the fraction of power of the fibre contained within the evanescent wave need be made[358], as expressed in Equation 3. However, in the case of a multimode fibre, it has been argued that this will also be the case if a uniform distribution of modes is present, and that η will account for the total fraction of power in the evanescent fields of all the fibre modes launched.

$$P_{out} = P_{in} \exp(-\alpha \eta l) \tag{3}$$

where η is the fraction of power in the evanescent field(s)

For a uniform distribution of power among the fibre modes, an expression for η has been derived by Gloge[131]:

$$\eta = \frac{4}{3V} \tag{4}$$

where V is the waveguide parameter, $V = \frac{2\pi a}{\lambda_o} NA$

5.2 Apparent limitations of fibres as evanescent absorption sensors

There have been significant deviations from measured absorbance ($\log_{10} \frac{P_{out}}{P_{in}}$) using multimode fibres and the predictions of Equations 3 and 4. The actual absorbance was

consistently less than that predicted and seemed often to have a nonlinear variation with concentration (unlike what Beer's law would predict)[104,322,323,324]. The fundamental utility of fibres as evanescent absorption sensors was called into question. This limitation was seen as a fundamental basis for discontinuing efforts in this area beyond very specialised applications.

The inherent question of determining whether this non-Beer's Law-type behaviour was caused by fibre characteristics or modal characteristics had to be resolved. The validity of Equations 3 and 4 can be questioned if it is seen as the consequence of the assumptions of equal distribution of power amongst the different modes of the waveguide[131]. This is not the case when the cladding has been removed and a solution with a refractive index quite different from that of the core placed in contact with the fibre. Modes that were weakly guided enter a region where they are now much more strongly guided by the core. Only a few possible bound modes are now propagating in the sensing region, and the overall distribution of modes is not uniform. An effective attenuation coefficient for a polished multimode evanescent absorption sensor has been derived[321], though this seems again to be an upper limit (rather than a specific dependence on concentration) for possible absorption. Equation 4 may be valid (with $V > \frac{3}{4}$) in a fibre propagating only one mode or by continuous coupling between all the modes of a multimode fibre. In general, however, each mode of the initially uniform distribution has a different profile and extent of penetration for its own evanescent field and so experiences a different attenuation throughout the sensing region, thus causing the distribution of modes to become non-uniform. The true response of such a sensor will deviate from that predicted from Equation 4, which now can be seen as an upper limit or (realistically) an overestimate. A careful examination of the total absorption experienced by the fibre modes will help determine if modal characteristics limit the use of multimode fibres as evanescent absorption sensors, or if fibres themselves have inherent limitations.

5.3 Analysis of absorption of fibre modes in the sensing region

Using an unclad multimode fibre of refractive index n_1 and core radius ρ immersed in an absorbing medium of lower refractive index n_2 and absorption coefficient α, the total number of modes present can be derived by starting from the following equation:

$$N \approx \frac{V^2}{2} \tag{5}$$

This expression for N is valid for large V and counts all possible polarisation states of the optical field[131].

$$\text{Defining } \gamma = \left(\sqrt{\frac{2}{N}}\right) \alpha l = \frac{2 \alpha l}{V}$$

For the large V values of multimode fibres, a function of one variable, γ, representing absorbance, can be asymptotically simplified to[294]:

$$f(\gamma) \approx \frac{2}{\gamma} \tag{6}$$

Plotting the fibre absorbance as a function of γ from Equation 6 and comparing it to Beer's Law, as shown in Figure 3, and data extracted from a multimode fibre-based evanescent absorption sensor reported by DeGrandpre and Burgess[104], it can be seen that Beer's Law will over-estimate the absorbency considerably. Further, the experimental data deviating from the prediction of Equation 6 makes clear the difficulty of using multimode fibres as evanescent absorption sensors, as it would seem that not all modes had been completely excited. This is to be expected practically.

If a restricted range of modes is launched into a fibre[321], as depicted in Figure 4, then the number of modes excited within the fibre is

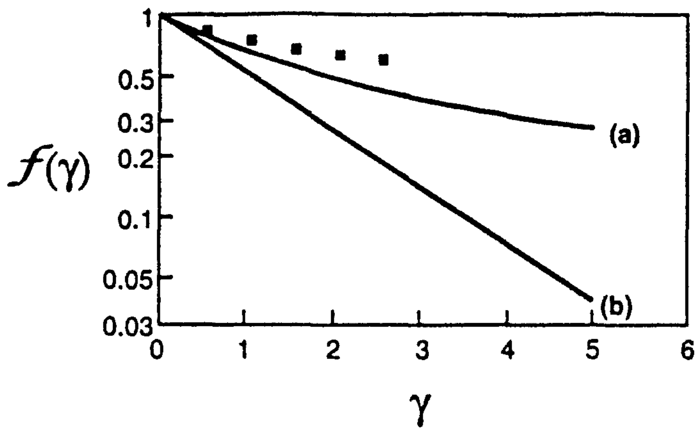

Figure 5.3 *Fibre absorbance as a function of γ (a); Beer's law (b); and data from an evanescent absorption sensor*

$$N_\theta = \frac{V^2}{2} \frac{\theta^2}{n_1^2 - n_2^2} \tag{7}$$

and this N_θ can be used to calculate the expected attenuation.

The modified Beer's Law will be valid if the fibre is forced to maintain a uniform modal distribution along the interaction length, along a relatively long interaction length. In the case of a single mode fibre, this modified Beer's Law should always be obeyed. An experiment was designed to verify that this is the case.

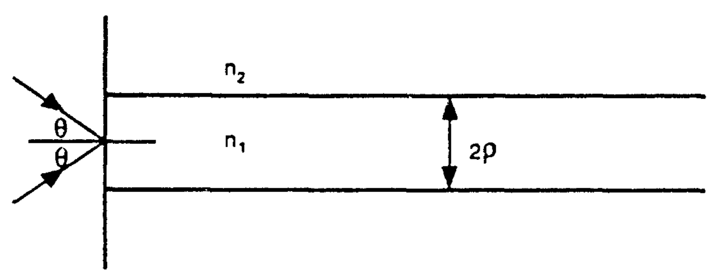

Figure 5.4 *Restricted range of modes*

5.4 Demonstration of an optimised evanescent field optical fibre absorption sensor

An adiabatically tapered single-mode fibre was exposed to solutions of a dye known to conform to Beer's Law. It was expected that the absorption through the tapered region will be described by the modified Beer's Law of Equation 3, as there is just one mode in the sensing region. Further, an absorption based assay for calcium ions in solution was performed as a demonstration of the tapered fibre as a practical sensor.

The tapers were fabricated by placing a section of the single mode fibre over a stationary flame and melted whilst being gradually stretched. The speed of the process is chosen to be slow enough to obey the slowness criteria established in Chapter 4. The fundamental fibre mode that entered the tapered region does not couple to either cladding or radiation modes. The overall transmission loss across the taper was of the order 0.1 dB or less for all tapers used in this demonstration. Very small diameter tapers were constructed, with a waist diameter of approximately one micron. This ensured that the core played no significant contribution to the waveguiding in the tapered (interaction) region. The evanescent field extends into the medium surrounding the cladding at the taper waist, where a new effective waveguide is formed consisting predominantly of the fibre cladding and the external solution.

5.4.1 Materials for initial absorption scheme and calcium ion assay

Methylene Blue (Aldrich) was used in the initial absorption scheme to confirm Beer's Law. The calcium assay used calcium acetate (Sigma) and Calmagite (1-(1-hydroxyl-4-methyl-2-phenylazo)-2-naphthol-4 sulphonic acid) (Sigma), and a 0.1 M borate buffer pH=10 (Fisons).

The single mode silica optical fibre used for the basis of the sensor, SM-450, was supplied by York Technology and had a numerical aperture of 0.18. A tungsten white light source was used for the bulk absorption measurements with Methylene Blue, and a red HeNe laser (wavelength 632.8 nm) for comparable taper absorption measurements. The Calmagite

solutions were illuminated with the 514.5 nm line of an air-cooled argon-ion laser (Omnichrome). The optical detection system used in all the measurements consisted of a large area photo diode (RS Components, data sheet 12508) and a lock-in amplifier (Stanford Research Systems, model SR510) linked to a personal computer via an analogue to digital acquisition card (PC LabCard).

5.4.2 Evanescent absorption experiment and results

The absorption characteristics of the tapered single mode fibre were first measured using aqueous solutions of Methylene Blue, concentrations ranging from 5×10^{-6} M to 2×10^{-3} M. Comparative spectrophotometric data were taken with solutions in a dye cell one millimeter thick. The experimental setups for these measurements are shown in Figure 5.

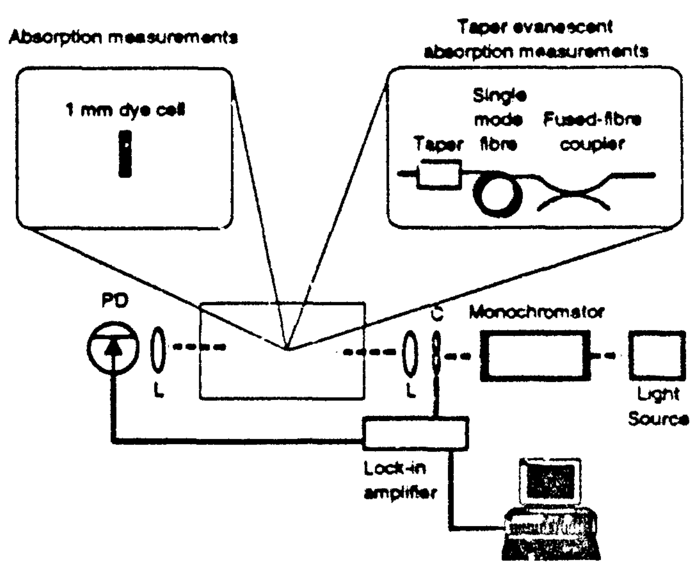

Figure 5.5 *Apparatus used for absorption measurements. The absorption spectra of the Methylene Blue through the dye cell and across the mounted taper were made with a white light source and a monochromator. The variation of absorption with dye concentration for the taper was made a fixed wavelength using a HeNe laser (632.8 nm) and with the monochromator removed. PD = photo diode, L = lens, C = optical chopper.*

The absorbance levels for the visible spectrum were taken, with an absorption peak found at 664 nm for both the tapered fibre and the dye cell. Figure 6 shows absorption levels, with the reduced absorption for the tapered fibre due to the relatively low refractive index of the solution (n=1.33); which caused little of the evanescent field to be available for interaction with the external solution. After exposure of the tapered fibre to each concentration level, the taper was cleaned with deionised water until the baseline spectrum of water was once again obtained. This ensured that no dye was adsorbed to the surface of the taper.

A better light source for the fibre, a He-Ne laser, with transmission at 632.8 nm, was used to measure evanescent absorption levels more accurately through the concentration range. The data were analysed with a least-squares regression fit for a linear and a square root dependence[41,3] on concentration. The chi-squares of the two hypotheses made the choice between the two alternatives quite clear, as seen in Table 1.

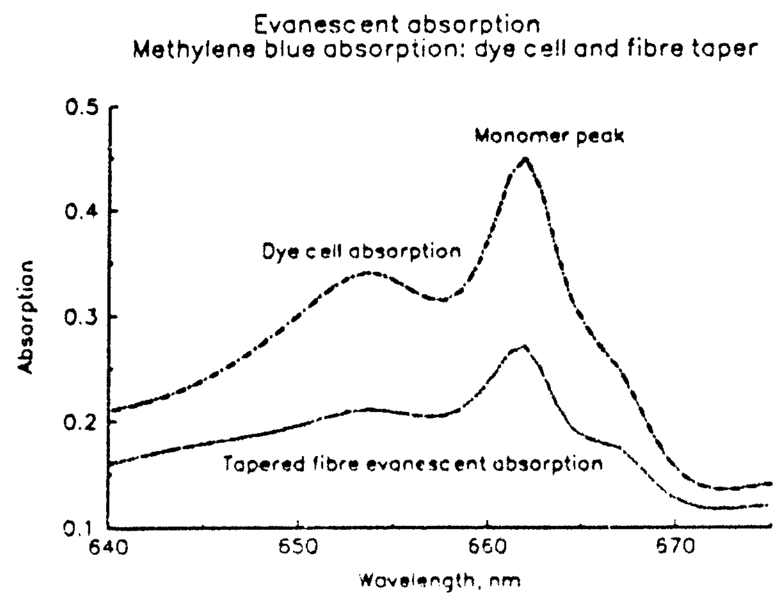

Figure 5.6 *Methylene blue absorption spectra: dye cell and fibre taper evanescent measurements (note that the index of refraction is approximately 1.32)*

Test	χ^2
Linear	0.32
Square root	4

Table 5.1 *Comparison of likelihood of distribution for evanescent absorption methods.*

A linear fit, shown in Figure 7, was confirmed as most appropriate for the data, indicating that the evanescent absorption of the taper followed Beer's Law with little measurable deviation. Adsorption effects can also be seen at low concentrations.

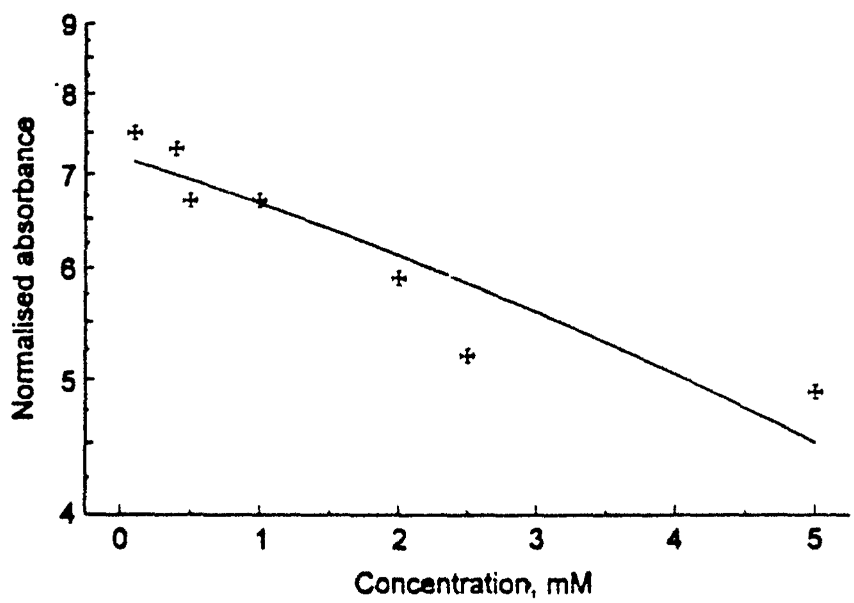

Figure 5.7 *Methylene blue evanescent absorption as a function of concentration. The* r^2 *value is 0.83 with* $n = 105$ *(15 repetitions across 7 concentrations).*

5.4.3 Calcium ion assay based on evanescent absorption

The detection of calcium, as well as magnesium, ions is currently performed in clinical assays†, which typically require the preparation of standards and numerous dilutions. The use of

† [102,192,217,258,259]

fluorescent or absorption based optical sensors for analysis of such ions is of interest due to the potential for real-time results[20,146,177,201]. Calcium ions levels were determined optically in this experiment through the use of an indicator, Calmagite[216,333]. Calmagite functions as a typical acid-base indicator, with different colours corresponding to different levels of pH. This indicator conforms to Beer's Law[222]. If Calmagite is placed in an alkaline (in this case pH of 10) buffer, the typically blue colour is changed gradually to red by the addition of either magnesium or calcium[222]. The absorption maximum of Calmagite solutions in a 0.1 M borate buffer pH=10 was found to be 523 nm. The 514.5 nm line of an argon-ion laser was used as the source for the tapered fibre dye cell containing Calmagite solutions throughout the calcium assay. All calcium detection with the tapered fibre was performed without altering the refractive index of the sample solution. Initial efforts to index match the solution to the cladding refractive index were hampered by poor miscibility of high refractive index solutions such as benzyl alcohol. A concentration range, derived from calcium acetate, from 40 µm to 5 mM was tested. As with the Methylene Blue measurements, after each sample exposure the tapered fibre was rinsed with deionised water to ensure no adsorption had occurred. The optimised experimental configuration for evanescent absorption-based tapered fibre measurements is shown in Figure 8. A fused fibre coupler, with the power split between the

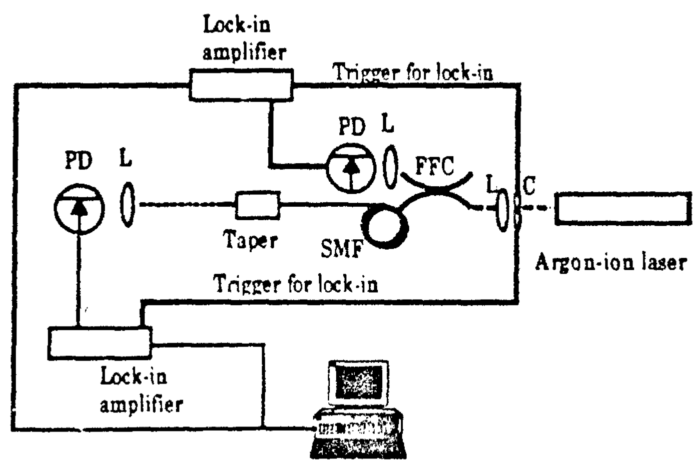

Figure 5.8 *Optimised set-up for evanescent absorption Ca^{++} detection based on Calmagite. Both lock-in amplifiers were triggered from the optical chopper. FFC = fused fibre coupler, SMF = single mode fibre, PD = photo diode, L = lens, C = optical chopper.*

two output arms in the ratio 55/45 (the value of the ratio was experimentally arbitrary), was constructed to monitor input power from the laser simultaneously with output power. This allowed the laser power fluctuations to be extracted from the received attenuation data at the far end of the optical fibre. Once again, a linear least-squares analysis was performed on the absorption data to confirm that the sensor system had the expected linear (rather than square root dependence) response, Figure 9, predicted by Beer's Law (with an r^2 of 0.98). Note adsorption may still dominate at lower concentrations.

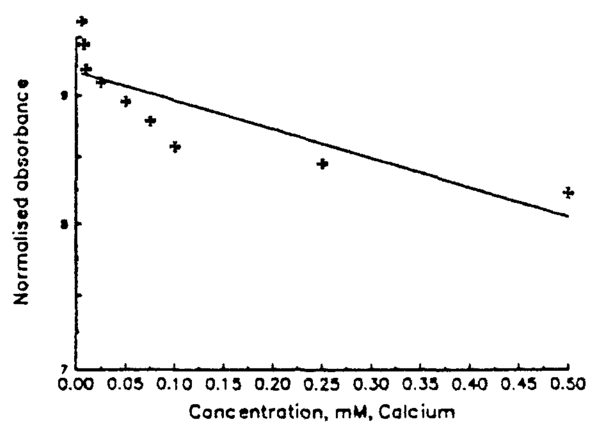

Figure 5.9 *Evanescent absorption of Calmagite with increasing concentration of Ca^{++} ions in solution; index of refraction of 1.32.*

5.5 Conclusions

The single-mode fibre evanescent absorption sensor is free from some of the difficulties facing multimode systems[37]. A Beer's law-type response is found (e.g., linear concentration variation with absorbance) in single mode adiabatically tapered fibres but not generally in multimode fibre systems. However, although the tapered single mode fibre system did measure calcium ion concentrations, the samples had to be pre-treated before analysis could take place, and treatment to minimise adsorption effects would have to be considered. Further, a specific absorption indicator for the analyte in question had to be selected, which may not be readily available for every chemical detection scheme desired.

A potentially more useful design would use fluorescent light, which would allow the separation of the source light in a simplistic manner. Fluorophore-based systems can use a secondary reaction to detect a range of analytes in a manner that is not specific to the analyte (e.g., the chemical reaction of the analyte with a compound labelled with a fluorophore releases an acid, thereby quenching the fluorescence). Fluorescent systems are examined in Chapter 6. Further, it is highly desirable that the indicator portion of the detection system be an inherent portion of the optical fibre. Immobilisation schemes have been well documented[25,28] and are explored in Chapter 7.

Chapter 6

Chemical sensing with fluorophores and tapered single mode fibres

Summary

This chapter discusses the capture of light generated by fluorophores by optical fibres. The general properties of fluorophores are reviewed. A method for assessing the expected amount of fluorescent energy by optical fibres is derived. A simple fluorescent capture experiment, based on a pH indicator dye, fluorescein, in solution about a tapered optical fibre is performed. The level of fluorescent energy captured experimentally is compared to that predicted by theory, and the performance of the tapered single mode fibre is assessed.

6.0 Fluorescent evanescent wave sensors

Many researchers† have developed chemical sensors based on capture of a fluorescent signal into an optical fibre. A change in the light signal output at a longer wavelength than the source wavelength is captured back into the fibre core and detected, usually at the far end of the fibre, though some sensors rely on the detection of backscattered fluorescence (i.e., fluorescence returned to the pump end of the fibre)[301]. In some devices, the dye is bound in the cladding surrounding the fibre and is excited optically††.

In order to develop an optical fluorescent sensor, the fluorescent indicator and the solution of interest are exposed to the evanescent field. This external optical power can excite molecules of the fluorescent indicator sufficiently near enough to the waveguide. Their

† [3,9,11,10,12,21,29,40,44,67,74,85,87,106,111,121,123,130,133,134,154,174,192,190,195 201,202,211,214,215,223,227,234,241,266,281,282,285,287,300,305,307,314,318,326,327,328,329,334,335,336,339,346,347,351,357,366,368,385,386,387,390,391,392,393,394,402,404,407,117,418,419,420,421,422,423,424,425,426,427,428,429,438,439,267,68,86,284,189,301,247,406]

†† [106,123,214,215,236,266,281,282,285,305,314,326,327,328,329,392,402,446,294]

emitted light can then be coupled back into guided modes which propagate along the fibre. The overall sensitivity of this process depends on the modes chosen and the thickness of the cladding [368].

6.1 Fluorophores and optical fibres

A fluorophore is a chemical that absorbs light of a particular range of wavelengths, which in turn excites some of the fluorophore's electrons to higher energy levels (excited state). When the electrons return to their previous energy state (relaxed state), light is emitted. The light emitted is always of a longer wavelength than the incident light due to energy conservation. In general, fluorophores or fluorescent markers, are chosen for good absorption, stability of excitation and efficiency of fluorescence. Fluorescent markers can be added to another chemical, thereby labelling it. A reaction of the fluorescently-labelled chemical(s) with some other substance can alter the fluorescent characteristics of the marker, sometimes quenching it † (for example, as acid by-products are produced during the reaction) or shifting its wavelength response [48,74,86,123,182,223]. There is a limitation in the number of markers that can be placed on one chemical (i.e., protein), as too many fluorescent molecules too close to one another can transfer electrons among themselves rather than routing the transferred energy from the pump source through the fluorescent energy release route. Most applications require a large Stokes shift (distance between the excitation maximum and fluorescent maximum, in nm) to allow easy discrimination of the label after excitation [158,177,383]. Some reaction products are naturally fluorescent, but this is not generally the case (unfortunately!).

6.2 Fluorescence capture at interfaces

The fluorescence generated by fluorophores has been modelled as radiating dipoles †† near an interface to study the potential collection efficiency of such systems. Once the factors contributing to the fluorescent capture levels have been derived, efforts have been made to optimise systems to take advantage of these parameters. It has been claimed that in general,

† [44,68,121,174,211,290,300,346,347,428,438,446]
†† [156,205,227,231,368,369]

when a radiating dipole (the fluorophore) is located in the optically rarer medium (cladding or external solution to a waveguide with an index of refraction less than that of the core) very close to the interface, the emission by the evanescent waves into the optically denser medium (core or waveguide material) is the dominant contribution to the power collected.

Other researchers take into account the thickness of the layer, but in all cases this description assumes an orientation for the light striking the interface, as might be the case for a prism, diffraction grating, or planar surface acting as a waveguide where the ray theory can be applied. Further, the films are expected to be very thin and uniform, $n_o d_o < \frac{\lambda}{8}$, where n_o is refractive index of the layer, and d_o is the depth of the layer. This is not always the case for typical deposition methods, especially those involving proteins. The results in this chapter are based on systems involving fluorophores in a bulk solution surrounding the waveguide. Chapter 7 will focus on methods to immobilise indicators in thin layers about the waveguide.

6.2.1 Multimode fibre fluorescence capture

Many devices studied so far are based on unclad multimode fibres, particularly those with plastic clad fibres (with a large core radius, such as 50 µm). Higher order modes in these fibres have the advantage of a large number of reflections per unit length, and consequently a long effective interaction length with the external material [323]. The use of multimode fibres, however, does entail a number of disadvantages. Theoretical calculations [112,113,114,115,242] show the efficiency of the coupling of cladding fluorescence to the guided modes of a multimode fibre depends strongly on the dimensionless waveguide frequency, V number, of the fibre:

$$V = \frac{2\pi\rho}{\lambda}\sqrt{n_1^2 - n_2^2} \tag{1}$$

where ρ is the core radius, n_1 is the refractive index of the core, n_2 is the refractive index of the cladding, and λ is the free space wavelength of light propagating in the fibre. The evanescent field of a multimode fibre is extremely weak, of the order of 2% of the total power in the fibre for a V of 100 [291]. Fibres with higher V numbers have higher coupling coefficients.

This is because they have many modes near cutoff and the evanescent fields of such modes penetrate more deeply into the surrounding cladding [214]. Fluorescence from a dye may be excited by the evanescent field of the guided radiation if the dye is close to the fibre core. The fluorescent light generated must be re-radiated in a manner that allows it to be coupled (or captured) into a guided mode, as portrayed in Figure 1.

As a result, most multimode fibre devices rely on preferential excitation of higher order modes, either by launching the light off axis, or by means of suitable masks. This in itself can cause problems in maintaining repeatable launch conditions. Lastly, multimode fibres themselves are incompatible with single mode fibres, and thereby unable to take advantage of the very high quality single mode fibre couplers and power splitters now commonly available.

6.2.2 Single mode fibre fluorescence capture

As an alternative to unclad multimode fibres, a number of devices have been reported based on polished fibres. In these devices, part of the fibre cladding is removed mechanically to

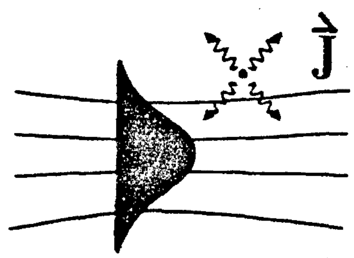

Figure 6.1 *Fluorescent light coupled into a guided mode at the waist of the tapered fibre; $\vec{J}$ current element generated by fluorophore.*

within several microns of the core, resulting in a D-shaped cross section. This exposes the evanescent field to the surrounding medium, as discussed in Chapter 4. The evanescent field of the fibre mode or modes can then interact with a dye solution with spectrochemical properties of interest to the sensor type desired. However, the evanescent field of polished fibres is extremely weak unless the refractive index of the external dye solution is very close to that of the fibre (typically to within a few parts per thousand). As a result, polished devices

exhibit extreme sensitivity to changes in external refractive index which is useful in a refractometric system, but troublesome for other applications.

The use of single mode fibre tapers can avoid the negative aspects of multimode fibres while still retaining the advantages. A single mode fibre is used because modal coupling amongst the higher-order modes of a multimode fibre along a taper would result in high losses. Further, the modal field in a single mode fibre is well defined. Power guided by the fundamental mode is concentrated in a very small circular cross-section at the taper waist. If such tapers were made with a diameter of about 5 microns, a very small optical power, of the order of a milliwatt, can cause a high power density of kW/cm^2 at the waist [276].

At the taper waist the fibre core is so small that it plays no role in guiding the light. Guiding is achieved by a new effective waveguide consisting of the fibre cladding and the surrounding medium. The local value of V is reduced in proportion to the fibre diameter and in very small diameter tapers (of the order of microns), the fundamental mode field extends into the medium surrounding the cladding. This has been shown experimentally [293], as well as predicted theoretically. The level of interaction with the field, as well as the fluorescent indicator used, determines the efficiency with which the fluorescence can be re-captured into the fibre.

6.2.2.1 Theoretical fluorescence capture for tapered single mode fibres

A theoretical description of the efficiency with which the external fluorescence in the dye solution surrounding the tapered fibre is coupled into the fundamental mode of the taper has been developed [149], based on Snyder and Love [358], who have given a general account of radiative capture into the core of an optical fibre. A corresponding analysis for the case of highly multimoded fibres has been given by Marcuse [242]. This analysis assumes a taper waist is of constant radius ρ and length L. At the taper waist, the original core of the fibre is so small that it can be neglected, so that the light is guided by a new effective waveguide consisting of the fibre cladding and external medium, as illustrated in Figure 2.

At the taper waist, the pump light excites the dye molecules into the first excited state, from which they fluoresce as an incoherent mixture of radiative dipoles. A dipole at position $\vec{r_d}$

can be represented by a current density $\vec{J}$. The current density from the excited fluorophores will in turn excite a fibre mode to a certain amplitude, and thereby transfer a certain level of power [358]. The total power from all the radiating dipoles is summed, and the efficiency of fluorescent capture can be defined as the total fluorescent power captured into the tapered fibre divided by all the fluorescent energy generated. This can be written as:

$$\eta = \frac{P_{cap}}{P_{tot}} = \frac{\log_e V (NA)^2}{V^4 \quad n_1^2} \qquad (2)$$

NA, the numerical aperture of the taper, is given by $(n_1^2 - n_2^2)^{1/2}$. V is the normalised waveguide parameter, $\frac{2\pi a}{\lambda_o}$ NA, and n_1, n_2 are the refractive indices of the core and cladding, respectively. In this form, η can be seen to be always less than one.

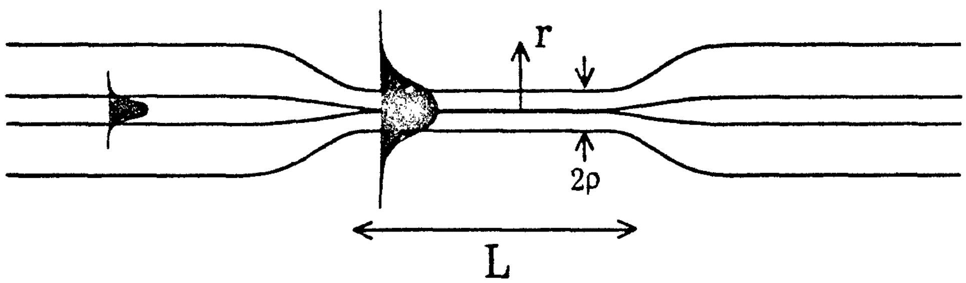

Figure 6.2 *Light guided by a new effective waveguide consisting of the fibre cladding and external medium.*

Equation (2) is plotted in Figure 3 as a function of V for different values of NA. From these curves, the efficiencies of fluorescent capture can be estimated for various taper diameters and external dye refractive indices.

The smallest tapers used in these pH experiments had diameters of approximately 0.5 microns. The external dye index was always adjusted to (at least) 1.44, which, combined with the index of refraction for the cladding of 1.458, corresponded to an NA of 0.23. The fluorescent wavelength was 0.526 microns, yielding an estimated efficiency of 0.2%. For tapers with a 2 micron diameter the corresponding efficiency would be just 0.04%. Results using multimode polished fibres give efficiencies of approximately 10^{-4}, i.e., 0.01% [214]. Similarly,

given that the fluorescein dye exhibits a very high quantum yield of 90 ± 5% [†], a taper diameter ranging from 1.5 to 2 microns, a typical experimentally derived fluorescent energy taper capture rate was of the order of 10^{-3}, i.e., 0.1%, of the input light energy to the dye molecule. It is important to note that theoretical fluorescent capture and experimentally measured fluorescent capture are not the same; experimentally, the ratio of fluorescent power capture to pump power is used, as the absorption cross section and quantum efficiency of the fluorophore is not known.

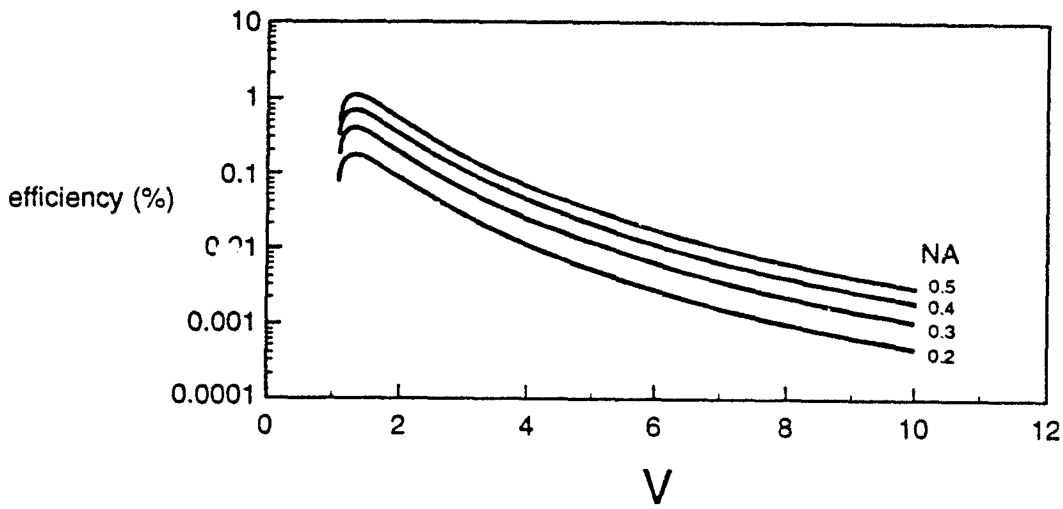

Figure 6.3 *Fluorescent capture efficiency as a function of the dimensionless waveguide frequency at different levels of numerical aperture*

There is a further, more important distinction between the tapered and multimode fibre cases: the much higher optical intensities achievable with a tapered fibre translated into higher absolute levels of captured fluorescence. The total fluorescence is proportional to the fraction of pump power in the external dye solution. For a multimode fibre with equal excitation of modes, this is $\frac{4}{3V}$ [131]. For a tapered fibre propagating the fundamental mode, the fraction is $\frac{1}{V^2}$. A typical value for a 200 micron diameter multimode fibre is V = 300, whereas for a 2 micron waist diameter of a single mode fibre taper V is about 2.7; in each case assuming a

† [47,107,108,135,312,363,364,442]

wavelength of 0.5 microns and an external dye index of 1.44. From this the level of fluorescence should be 30 times higher in a taper than in a multimode polished fibre of the same length. Furthermore, most of the pump power is absorbed in a taper. Consequently, for small diameter tapers (2 microns or less), much higher absolute efficiencies are possible compared to multimode fibres. Tapered fibres are also less sensitive to variations in the external refractive index than unclad multimode fibres, as shown in Figure 4. Here the efficiency of a two micron taper is plotted as a function of dye index over the range of n = 1.33 (water) to 1.44. As can be seen, the efficiency does not vary by more than a factor of three over the whole index range.

6.3 A practical demonstration of a fluorescent sensor based on tapered single mode optical fibres

6.3.1 Materials and apparatus

The indicator, disodium fluorescein, and methanol, the solvent chosen for this experiment, as well as pH buffer solutions, were purchased from Fisons Scientific Equipment. For the titration process, glacial acetic acid (17.4 M) and concentrated aqueous potassium hydroxide (100 M) were respectively obtained from Aldrich Chemical Company and Fisons. The pH levels of the buffers and titration products were verified using a hand-held pH electrode

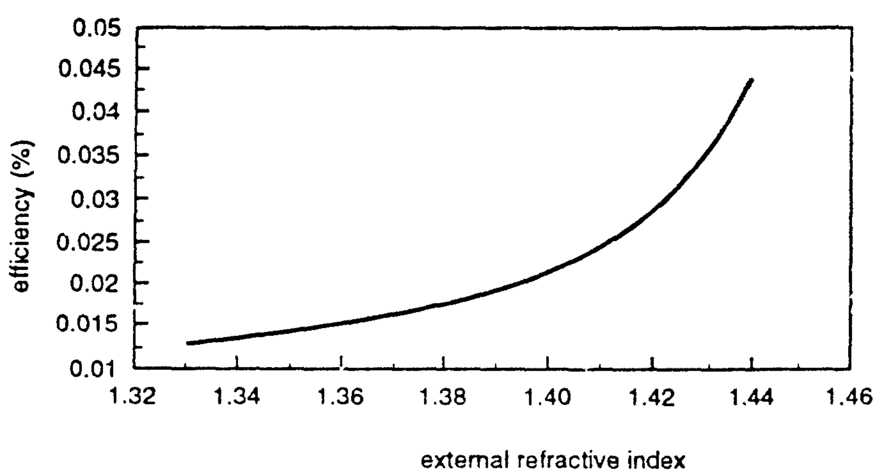

Figure 6.4 *Sensitivity to variations in the external refractive index for a 2 micron taper*

supplied by RS Components with an overall stated accuracy of ± 0.03 pH units. To ensure a constant external refractive index, appropriate amounts of dimethyl sulphoxide, supplied by BDH Laboratory Supplies, were added and regularly confirmed using a Bellingham and Stanley sugar refractometer.

The single-mode optical fibre used for the sensor was the silica York Technology SM450 with a numerical aperture of 0.18. Tapers were made in a manner reported earlier [239] and shown in Figure 5. The tapers used in this study had waist diameters from 0.5 to 2.5 microns (transmission losses of 0.1 dB), which represented a compromise between a sensitive system and a durable one. Narrow tapers tended to break, and wide tapers were not sufficiently sensitive. The tapers were then mounted in the custom built linear dye cell, as shown in Figure 6, to provide a means of circulating solutions about the taper. The refractive index of the solutions ranged from 1.32 to 1.453. Once mounted, the tapers could be easily handled and have been in use for several months.

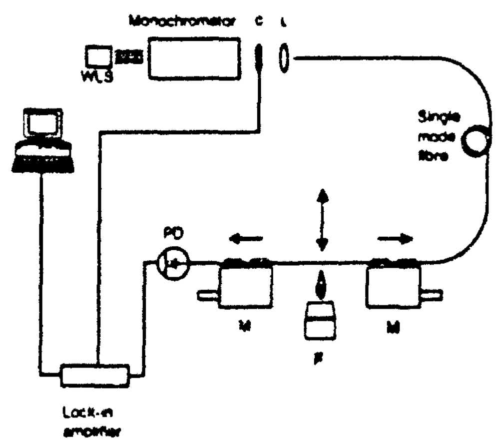

Figure 6.5 *Set-up for taper fabrication: WLS = white light source (tungsten), C = optical chopper; L = lens; M = motor-driven stage; F = flame*

The experimental configuration, shown in Figure 7, measured output fluorescence level as a function of pH. An Argon-ion laser, tuned to the 488 nm line, was used to excite the fluorescent dye around the taper. The indicator in solution released fluorescent energy when excited by the evanescent field of the fibre. The fluorescent emissions from the excited dye molecules were then coupled back into the fundamental guided mode of the taper. The level of these emissions was characterised by using a monochromator. This light was then detected

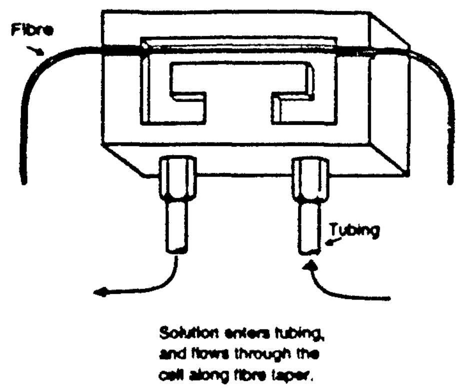

Figure 6.6 *Dye-cell apparatus for exposing the taper to different pH levels with a constant concentration of indicator dye, at a constant index of refraction.*

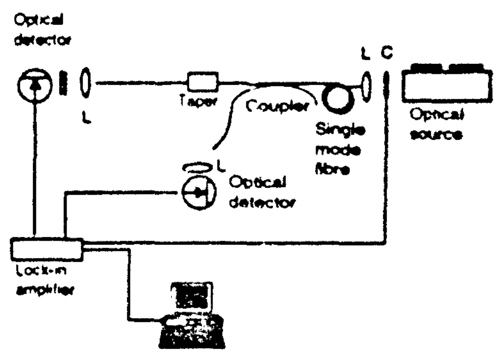

Figure 6.7 *Fluorescent measurement system using tapered single mode optical fibre: L= lens, C = optical chopper. Taper is mounted in a dye cell support and solution is pumped through the cell by a peristaltic pump.*

by a large-area photo diode (RS Components, data sheet 12508). Due to the signal levels, intensity measurements were made using lock-in detection (Stanford Research Systems). The lock-in amplifier was linked to a personal computer via an analogue to digital data acquisition card. The fluorescence spectrum found was typical for that of bulk absorption [34], as seen in Figure 8. Subsequent measurements were then made with the monochromator set at 526 nm, the wavelength of maximum fluorescence.

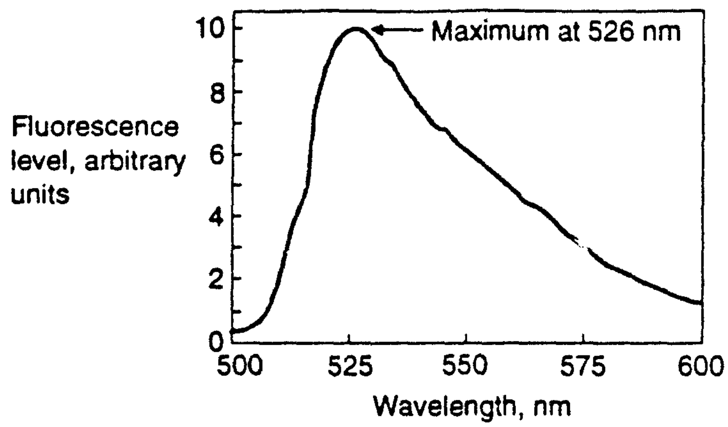

Figure 6.8 *Spectrum of disodium fluorescein (Uranin) in methanol.*

6.3.2 Measurements and results

A volumetric titration of 100 M potassium hydroxide and 17.4 M acetic acid was carried out to establish a baseline for pH level as a function of volume of added base. The amount of acetic acid used was then fixed for all subsequent experiment trials, and the pH levels obtained were verified by the pH meter. This baseline curve, as shown in the solid line of Figure 9, exhibited the typical sigmoid shape of pH as a function of added H^+ ions (represented by volume added). The data represented by squares in Figure 9 describes the same titration performed using a tapered fibre with the fluorescein indicator in solution: the right-hand y-axis applies. Approximately fifty sets of data were taken on the described experimental apparatus, and they clearly demonstrated the expected titration curve.

6.3.3 Limitations of current system

All optical fibre sensors for pH share some fundamental difficulties in assessing pH precisely. The relationship between the surface-measured pH and the actual pH of bulk solution differs due to the effect of electrostatic repulsion. The surface of the optical waveguide possesses acid-base properties that are reflected in the surface pH. In the case of this sensor, and many

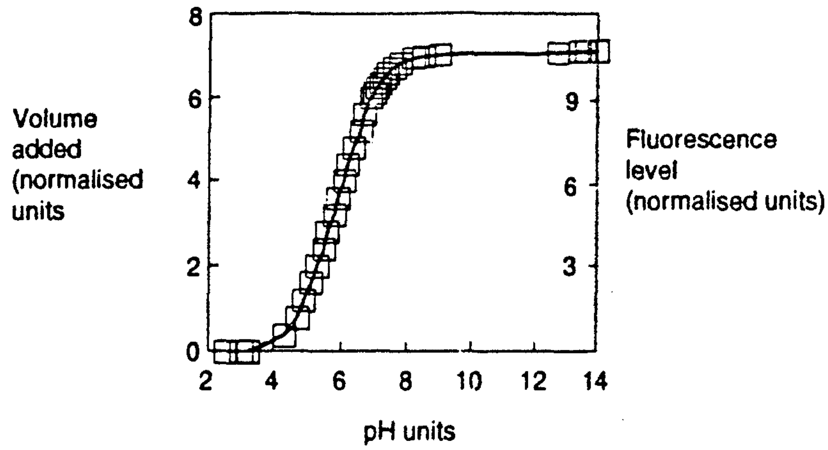

Figure 6.9 *pH titration curve: solid line from pH meter, □ for tapered fibre. Note that in both cases the external refractive index is adjusted to 1.44.*

others reported in the literature, the sample solution (and thereby all the other ionic components of the solution), has been kept constant. In this case, the errors tend to cancel [168]. For application in biochemical assays (particularly biomedical), this condition is likely to always be met.

6.4 Conclusions

Tne tapered optical fibre sensor as discussed here was found to be very responsive to pH changes. A calibration curve between level of fluorescent light and pH could be readily determined. However, because the indicator was not a fundamental portion of the sensor, the solutions used had to be pre-conditioned - both for refractive index and indicator dye content. A possible cure for this limitation would be to immobilise [106,138,185] the indicator in the cladding (or as the cladding) along the taper. Such "active coating" sensors often provide much higher sensitivity [213,214,215]. Many immobilisation methods are described in the literature, and will be discussed in Chapter 7. Immobilisation of a thin layer with indicator molecules in it would both fix the refractive index and the concentration of the indicator. Nonetheless, the use of single mode rather than multimode fibres results in a more stable and repeatable optical launch as well as higher achievable levels of fluorescent capture.

Chapter 7

Immobilisation

Summary

This chapter reviews some of the techniques available to combine a selective or recognition element in conjunction with a sensitive one (here, an optical fibre). The expected fluorescence capture performance of an optical fibre with an immobilised fluorescent indicator is presented. A simple experiment is described to determine if the tapered single mode fibre would be able to respond to an external sample solution with a fluorescent indicator immobilised to its surface. The sensitivity of this assay is assessed, and the groundwork is laid for the development of the tapered single mode fibre as a 'true' sensor.

7.0 A true sensor: sensitive and selective

The optical fibre sensor in general must be developed to take advantage of the benefits of its configuration, especially its ability to perform remote operation. This usually dictates that a chemical that is selectively sensitive to the analyte be immobilised in some manner to the waveguide. As many chemical fibre sensors depend upon the evanescent field for interaction, the process of immobilisation chosen must not restrict the access of the sample to the waveguide. Notwithstanding these constraints, many of the types of immobilisation techniques used for other optical detection systems have been successfully applied to optical fibres.

7.1 Immobilisation techniques for optical waveguides

Many techniques have evolved to attempt to bring together the chemically-selective elements of an immobilised-indicator sensor to waveguides†. At least some of these techniques must

† [28,42,59,80,193,221,245,248,310,342,365,372,390,397,408,412,433,446,447]

be attempted in order for the tapered optical fibre loop to demonstrate adequately that it can perform as a biochemicai sensor. Some methods typically used to attach selective chemistries to waveguides are silylation (or silanisation), Langmuir-Blodgett films and the sol-gel process. These techniques are generally reviewed in the next sections.

7.1.1 Silanisation

Silylation is defined as the substitution of a hydrogen atom, bound to the hetero atom of an inorganic (i.e., without carbon) substrate, with a silyl group (depicted in Figure 1), forming a hetero-silicon atom bond without further alteration of the molecule. Silanisation involves converting a silanol group to a less polar group, which converts a terminal hydrogen to some other group, frequently an organic compound (for chemical and biological sensors). Silylation (and silanisation) can be applied to many biochemical systems with the use of organofunctional silanes. These silanes (and others) have reactive groups at one end for covalent attachment to supports such as quartz, glasses of a variety of configurations, as well as optical fibres themselves†.

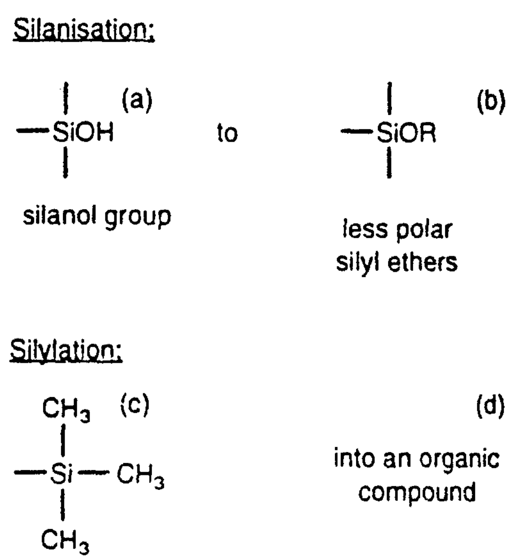

Figure 7.1 *Silanisation (a and b) and silylation (c and d).*

---

† [25,41,77,219,408,91]

Depending on the chemical attached to the arm of the silane linker not bound to the optical fibre, sufficient optical signal may be generated by silanising directly onto the fibre itself without introducing any support structure. Some of the optical systems reviewed in Appendix I did include an additional layer or polymer to increase the optical path, but frequently these systems already suffered from inefficiencies in capturing the available optical information (attenuation or received fluorescence): the additional complexity of another substrate usually made matters worse, rather than correcting the initial deficiencies of the system being employed. The combination of the amount of responding material (absorbed by or fluorescent to the analyte) and the length of silanisation of the fibre, together with the intensity of the evanescent field at the silanised layer determine the overall sensitivity of such devices. The ease of configuring the chemically-reactive end of the silane to any desired functional group for many applications make this technique very attractive. Further, the potential for monolayers or thin layers on the fibre surface allow a high proportion of the evanescent field to interact with the analyte (directly or indirectly) reacting with the silanised layer. Silylation (or silanisation) can be applied to silica-based optical fibres (or any other waveguide) for chemical sensing.

7.1.2 Langmuir-Blodgett films

Langmuir and Blodgett pioneered a technique sixty years ago to place monolayers of chemical films on surfaces. An organised assembly of molecules can be transferred to a solid substrate by dipping the substrate through the film to produce a monolayer, or by repeated dippings, multilayers. These films are generally characterised as well-ordered and mono-molecularly layered[57,398,119]. These characteristics of Langmuir-Blodgett films allow for rapid and sensitive interaction with the external environment if these molecular layers are reactive biomolecules (or other suitable recognition entity). Troughs for depositing Langmuir-Blodgett films in a repeatable manner are commercially available, though typically more suitable to a planar surface rather than a cylindrical one. Attempts to apply these films to optical fibres have met with mixed success[39,440,441]. Some of these problems relate to the unknown configuration of the molecules in the layer, but others relate to the geometry of the fibre. Since many optical fibre sensing systems use only the tip of the fibre for sample

interactions, this portion may be made planar. Similarly, the polished fibre sensors (the flat portion of the D profile) could be used in conjunction with Langmuir-Blodgett films. The limitation in these cases may be the amount of material available for interaction (particularly with a monolayer of selective molecules), but this may be sufficient for many biochemical sensor applications.

7.1.3 Sol-gel

The sol-gel technique is a method (for which there are at least three approaches) of deposition of thin coatings onto glass and other substrates. It has been used to place specific coatings (i.e., antireflective) onto optical components†. Its greatest benefit is that it can produce optically smooth surfaces. These coatings can be used in many different applications, including those involving chemical sensors. The chemistry behind this process is complex, and must be carefully controlled at every stage in order to avoid fracture during the drying of such films. The basic sol-gel process is approached from any one of three methods[396]:

- gelation of a solution of colloidal powders
- hydrolysis and polycondensation of alkoxide or nitrate precursors followed by a hypercritical drying of gels
- and hydrolysis and polycondensation of alkoxide precursors followed by aging and drying under ambient atmospheres

These approaches all require the evolution of a sol, a dispersion of colloidal particles in a liquid, and a gel, an interconnected, rigid network with pores of submicrometer dimensions and polymeric chains whose average length is greater than a micrometer. The specific definitions of colloids, gels, and the ligands involved in the steps of the process are complex and often specific to the type of chemistries being attempted[64,157]. With appropriate protocols, these coatings have been used in conjunction with optical fibre evanescent wave sensors. A

† [52,69,252,265,396]

porous cladding can be created, allowing an indicator or indicator-labelled reactive chemical to be held close to the surface of the fibre. The sol-gel film can be dip-coated onto the fibre†. Some limitations of current techniques include leaching of the trapped chemical, dissolution of the structures in some chemical environments, and cracking of the structure[157,235,236,265].

7.1.4 Other

Other methods of depositing thin films to surfaces have been attempted, based on materials varying from polyurethane to epoxy to photoresist. Films have been developed from molecules with particular affinities to certain surfaces (e.g., penicillinase[89,186,]). The lack of reproducibility of films as well as the need for adaptation to many different chemical reactions has limited the application of such methods.

7.2 Expected behaviour of thin films deposited on optical fibres

The configuration of molecular layers of the films deposited onto optical fibres is absolutely critical to their performance. Non-uniform layers interfere drastically with the efficiency of evanescent field interaction, as the index of refraction of most solutions used for organic material is nearly that of water. The molecular constituents of the films must either be induced to have a uniform orientation, or chosen to have such a characteristic inherently. For multimode fibres, a fairly stringent requirement for the depths of such films is established, but this is primarily to simplify the calculations of the optical field (from LP theory to ray approximation). It was found, as will be discussed in Chapter 8, that as long as the layers were optically smooth on the same order of magnitude of the wavelength, the film acted as the expected guide for the optical energy. In general, however, the films are treated as very thin films that do not contribute significantly to the effective refractive index of the waveguide, and can all but be neglected save for the presence of the fluorescent or absorbing sources, and are often treated as sources imbedded in the cladding. This assumption leads to a simple estimation for the fluorescence capture efficiency based on the analysis of Chapter 6, where

† [69,138,235,236,246,319]

the integral is re-evaluated from the surface to a small distance away from the surface $\rho + \delta\rho$. The efficiency is then twice what what we had before, or:

$$\eta = 2\frac{\log_e V}{V^4}\frac{(NA)^2}{n_1^2} \qquad (1)$$

V, the normalised wave number, is given by $\frac{2\pi a}{\lambda}$ NA; and NA, the numerical aperture of the taper, is given by $(n_1^2 - n_2^2)^{1/2}$.

In order to examine the behaviour of thin fluorescent films on the surface of the tapered single mode fibre, a very simple (chemical) system was chosen, as the point of the experiment was to examine the light-guiding properties of the immobilised layer rather than invent new chemical procedures for attaching functional groups to optical waveguides. Because of its unique affinity to glass, penicillinase[76,89,184] was chosen as the immobilised layer for the tapered optical fibre sensor.

7.3 Demonstration of the tapered fibre: an immobilised-indicator based penicillin sensor

The main goal for this experiment was to immobilise fluorescently-labeled penicillinase around the tapered single-mode fibre and measure penicillin levels based on quenching of fluorescence by release of penicilloic acid. This would serve to demonstrate immobilisation of fluorescent indicators on tapered fibre surface gives results similar to those of bulk solution; that is, the coated tapers are as least as sensitive. Although the experiment itself is relatively simple in conception, the chemical requirements for such a system are not trivial, and the use of enzymes required careful handling in order for the chemical activity of the species to be constant.

7.3.1 Preparation of the biochemical element of the sensor

First, the penicillinase had to be labelled with the fluorescent marker (fluorescein isothiocyanate, FITC). This required that the penicillinase be dissolved from its delivered dry

state and then desalted into an appropriate medium for binding. The recommended solution from the supplier (Sigma) was an alkaline phosphate buffer. The buffer salts from the original shipped penicillinase were removed by running the protein through a Sephadex column, which served to separate molecules of different weight. An ELISA-based analysis to locate the highest protein concentration from the eluate was performed, and the protein samples amassed, using the standard curve shown in Figure 2. Next, an appropriate amount of FITC

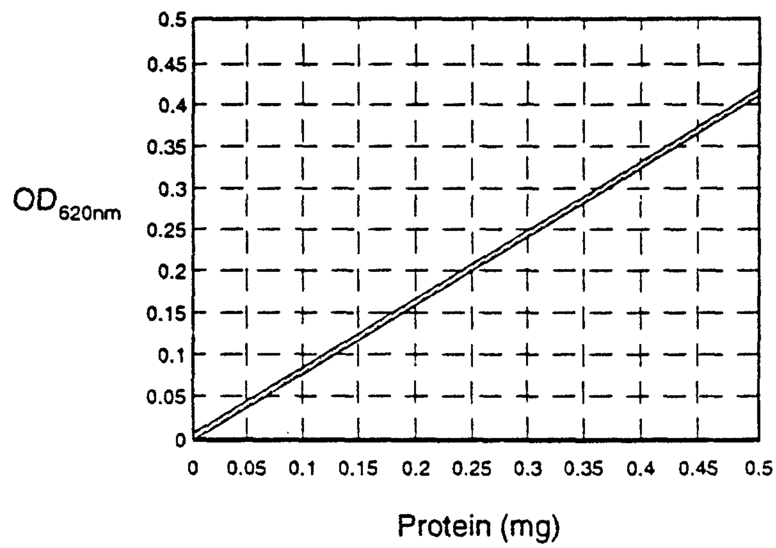

Figure 7.2 *Bio Rad Bovine serum albumin standard curve: used to relate ELISA read-out values to level of protein in the sample cell*

in the same alkaline buffer was added to the penicillinase samples. The system was allowed to react, and then the unbound FITC was separated from the labelled penicillinase by running the solution through another Sephadex column. Again, the protein-rich samples were combined; this was simplified once the penicillinase had been labelled by the FITC, as the labelled protein was visually different than the unbound FITC (dark yellow versus orange).

Next, the ability of the fluorophore to fluoresce and the penicillinase to react with penicillin had to be confirmed prior to immobilisation on the fibre surface. The labelled penicillinase had been switched to a slightly acidic phosphate buffer at the same time as the unbound FITC had been removed. Sigma recommended this buffer as more appropriate for maximum activity of the penicillinase. The fluorescence of varying concentration levels of unbound FITC was measured on a fluorimeter, and a simple concentration versus fluorescence level standard graph was developed (Figure 3). The bound FITC was then measured in dilutions

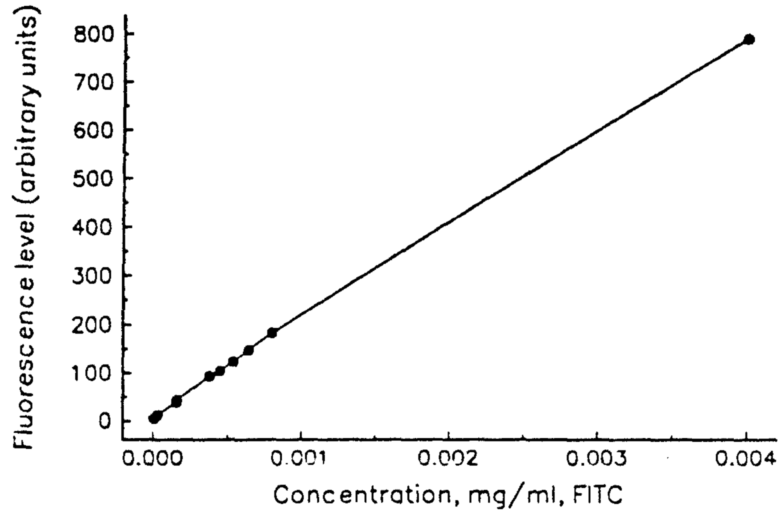

Figure 7.3 *Standard curve for fluorescence level of FITC solutions. The filled circles represent different FITC-labelled penicillinase dilutions and are compared to the standard. The bound FITC retains its fluorescent nature.*

to determine its effective concentration. The FITC-labelled penicillinase displayed an adequate fluorescence signal to be measurable on the fluorimeter.

The activity of labelled penicillinase had to be compared to the activity of unlabelled penicillinase against standard solutions of penicillin (for this experiment, Penicillin-G or benzylpenicillin). An indicator reagent (blue-black starch solution) that changed colour dramatically was used in conjunction with the ELISA-based system. A group of reaction controls were prepared and the indicator solution added. If the penicillinase reacted with penicillin, penicilloic acid would be released, which turned from blue-black to clear in the presence of the acid. The completeness of this change, and the speed of the reaction was assessed by examining the transmission through the solution. The labelled penicillinase did display the required level of activity, as shown in Figure 4. Details of the chemical procedure can be found in Appendix III.

Now that all the necessary chemical components had been developed, they had to be combined with the sensitive element of the sensor system: the tapered fibre. The immobilisation

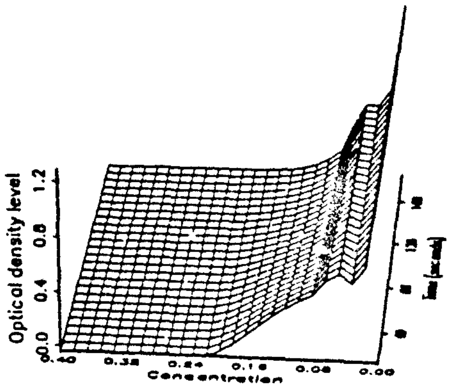

Figure 7.4 *As FITC-labelled penicillinase interacts with standard solutions of penicillin and releases H^+, a blue-black starch indicator turns clear, and the the measured OD increases dramatically.*

procedure was simple: the labelled penicillinase was allowed to react with tapered fibre in its mount overnight (at 4° C), as penicillinase will preferentially adsorb to glass[89,186].

7.3.2 Preparation of the optical element of the sensor

A taper was prepared and mounted in the dye cell. In addition, a coupler of known power-splitting ratio (i.e., 95:5) was constructed in order to monitor input power. The experimental setup, similar to the absorption measurements, is illustrated in Figure 5. The

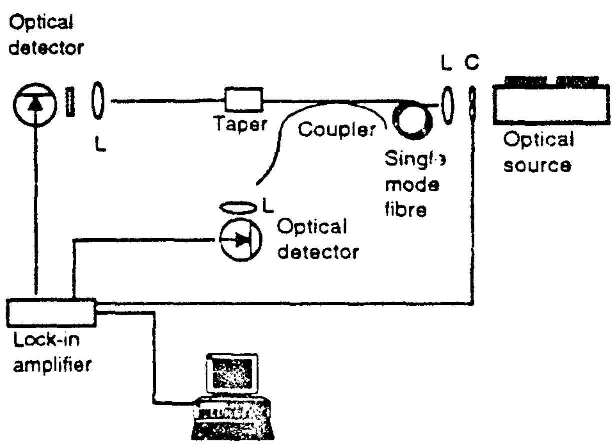

Figure 7.5 *Experimental set-up to measure fluorescence decrease as a function of penicillin concentration. C= optical chopper, L = lens. Taper with immobilised FITC-labelled penicillinase mounted in dye cell; samples are injected with a syringe.*

optimal setting for the monochromator was determined by taking an initial fluorescence spectrum, with the peak level found at 522 nm, ± 2 nm. The fluorescence spectrum for FITC-labelled penicillinase on a tapered single mode fibre is shown in Figure 6.

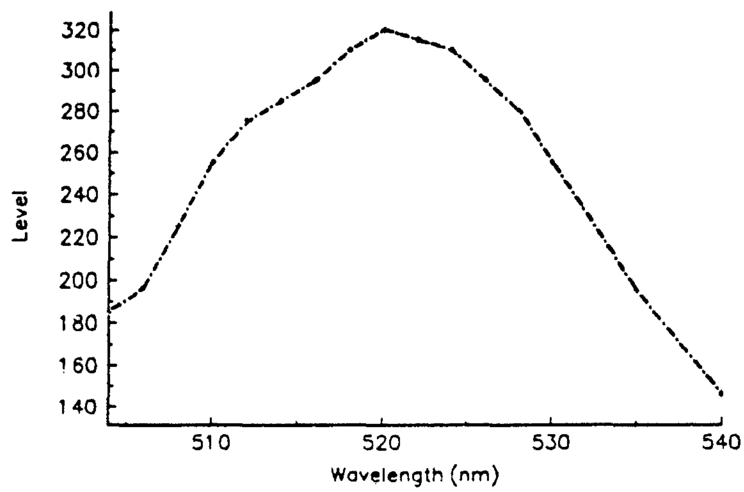

Figure 7.6 *Fluorescent spectrum of FITC-labelled penicillinase*

7.3.3 Testing the penicillin sensor

The penicillinase-coated taper was exposed to concentration levels of penicillin from 6 μM to 0.4 mM, and the fluorescence level was monitored continuously. The quenching of the FITC fluorescence as penicilloic acid was released could be seen by eye, especially at the highest concentration levels of penicillin. The rate of fluorescence decrease for each concentration level was calculated at 5 second intervals and compared. After each exposure, buffer solution was circulated through the dye cell mount to remove the penicillin. The fluorescence level was monitored and the process of rinsing continued until the fluorescence level recovered to its original level. It was expected that only an initial 'fast' rate could be used to separate the different concentrations as enzyme binding in a static environment [325,411,30,19] undergoes initial diffusion (Fick's law), and subsequently dissociation, electrostatic repulsion, steric deformation, and re-association events that may cause an oscillation in the received fluorescence signal independent of the reaction that is

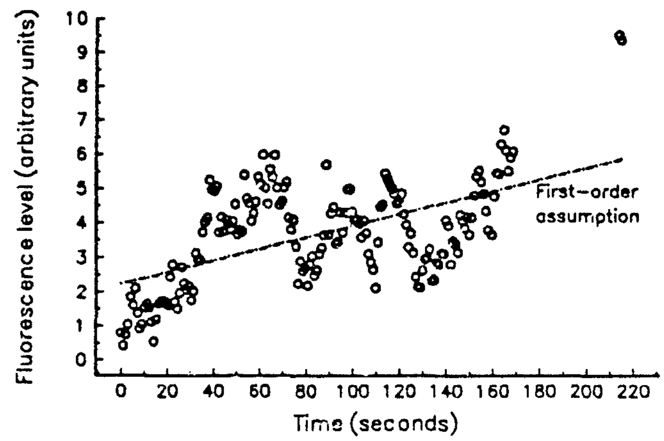

Figure 7.7 *Fluorescence uptake for fibre taper; protein-protein interaction on surface.*

being monitored. Figure 7 illustrates fluorescence uptake in a protein-binding event with such multiple processes.

Sampling times of less then 60 seconds were used to discriminate the initial concentration of the penicillin sample; Fick's law would apply in at least the first 40 seconds, as shown in Figure 8. A concentration curve versus level of fluorescence decrease could be developed for

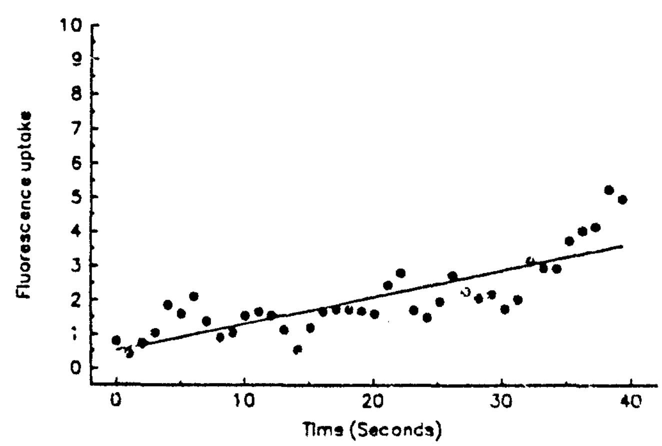

Figure 7.8 *Fluorescence uptake for fibre taper in the first 40 seconds of interaction, using the first order approximation (Fick's law).*

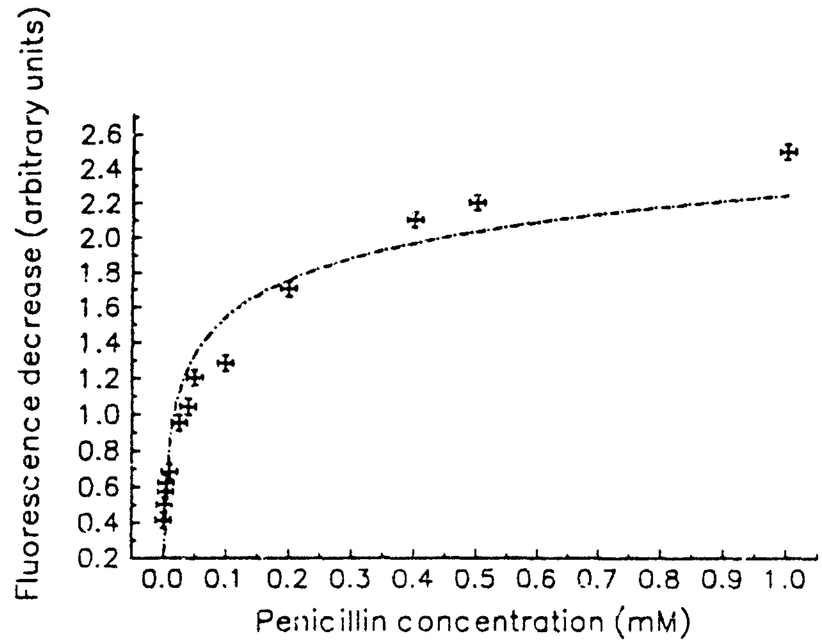

Figure 7.9 *Concentration of initial penicillin sample determined by the rate of decrease of fluorescence of FITC-labelled immobilised penicillinase after a 30 second sample exposure time.*

a fixed time interval. Thirty seconds was found to be best, and a calibration curve for penicillin concentration is shown in Figure 9.

As seen in Figure 7, it would be expected that other phenomena would interfere with the simple calibration curves being developed at arbitrary times. For example, if calibration curves for other time intervals are combined on one graph, the rate of fluorescence decrease does not continue monotonically. If the curves in Figure 10 are examined, it can be seen that there is crossover between the different fluorescent decreases measured after different times. The first explicit curve is chosen to represent the initial interaction (Fick's law) of the unknown penicillin sample and the immobilised FITC-labelled penicillinase.

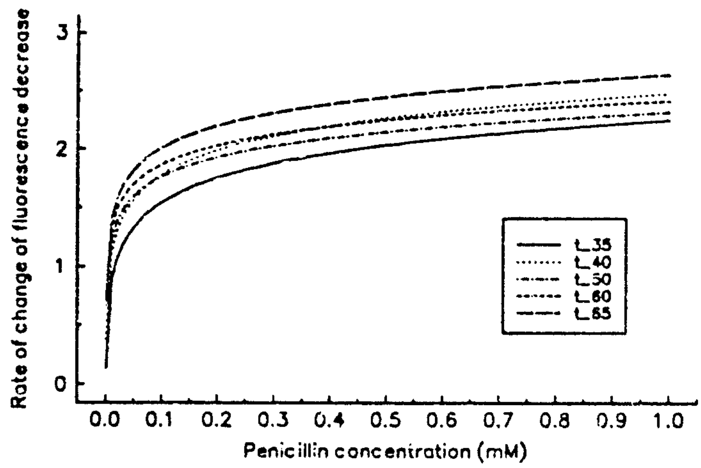

Figure 7.10 *Concentration versus reaction level (t=35, 40, 50, 60, 65 sec) FITC-labelled immobilized penicillinase: note that curves do not increase monotonically.*

7.4 Limitations of the current system

The limit of detection of the FITC-labelled penicillinase coated tapered fibre sensor is of the order of ppb. Although it is comparable to, and in some cases better than, the current penicillin sensors reported in the literature[†], the sensor as it stands has not been adequately tested against cross-reacting species or the varying types of penicillin. Although individual concentration levels of penicillin give reproducible results, the system is not likely to be useful to discriminate unknown samples. It did, however, demonstrate that if indicators were bound in the interaction region of the taper (at the taper waist), sensitive measurements could be made. The fluorescence levels captured were adequate to discriminate one sample concentration level from another.

† [132,161,193,194,210,248,262,437,65,75,249,274,275,278,399,443]

7.5 Conclusions

A more severe limitation of the penicillinase coated tapered fibre is its linear configuration. There is some difficulty in coating the taper in its current mount without contaminating the mount surface, and easily exposing the taper to samples. A new geometry for the tapered fibre and mounting arrangement was necessary, as will be described in Chapter 8. The penicillinase-coated single mode tapered fibre did demonstrate very effectively the capability of the device to use capture fluorescent power from immobilised indicators to determine analyte concentration. A more generic method for attaching recognition or selective elements to the optical fibre is also needed, as will be discussed in Chapter 9. Given some optimisation, in both configuration and immobilisation technique, it was expected that a very sensitive sensor for biological and chemical material could be developed.

Chapter 8

Optimising sensor configuration

Summary

Adiabatically tapered single mode fibre evanescent field devices have been demonstrated as a better alternative for fluorescent capture devices then those sensors based on multimode fibres, as well as suitable candidates for optical fibre evanescent absorption transducers. Despite this inherent capability, configuring the tapered fibre as a device suitable for biochemical sensing remains in general a problem. As is discussed in this chapter, a more desirable configuration for the tapered fibre had to be established. A lossless macrobend (180^0) was introduced in the tapered region of the single mode fibre. The tapered fibre loop was tested in conjunction with a silanisation process for indicator immobilisation. The expected fluorescent capture level is predicted, and compared to experimental results. It is found that when a suitable coating thickness is applied to the region near and including the taper waist of the fibre loop, a novel waveguide structure with potentially very high fluorescent capture is developed.

8.0 Optical fibre macrobends

In general, bends can be introduced to optical fibres as long as the radius of curvature is greater than the limit imposed by stress on the fibre (outer surface tension and inner surface compression) as defined below[137]:

$$R_b > \frac{b}{0.002} \qquad (1)$$

where b is the radius of the fibre taper at the bend and R_b is the radius of curvature.

For example, with a tapered fibre radius of 0.5 µm, the bend radius should be greater than 250 µm (0.25mm) in order to maintain a bend without stress losses or fracture. Typically, bend radii of 0.5 to 1.0 mm could be used without excess loss or breakage. The total

transmission loss of the tapered fibre loop was 0.1 dB or less; the introduction of the bend did not significantly add to the total loss through the tapered fibre.

Other researchers have used such macrobends with multimode sensors to induce losses[378]. A stripped (etched or melted with a CO_2 laser) multimode fibre is used as a refractometer, with the bend introduced to enhance the loss when the sensor was placed in contact with a medium of differing refractive index (in this case, the presence of water). Pressure, strain and magnetic sensors based on a biconically tapered (asymmetric) single-mode fibre with a bend radius of 62 mm have been constructed[78, 345]. These structures are too large to be used with type of sample volume expected for biochemical systems.

8.1 Applying the macrobend to the single mode tapered fibre

Structures that have approximately the same scale as desirable for the fibre loop sensor have been developed[79, 95, 261]. Some of these were made to radii of curvatures that were even smaller than the stress considerations would allow, and did not exhibit any breakage. Some preliminary theoretical work has been done to examine the actual effect of curvature changes along the taper, rather than simply applying the stress formula for untapered fibres. The Love slowness criterion introduced in Chapter 4 was applied to define a critical value for the radius of curvature with the distance along the curved taper axis. A proposed function for this relation was defined by Birks et al[48], which is not as easy to apply as the first formula. An example of the improvement in reduction of scale is given by the authors, who were able to bend a 15 µm diameter tapered fibre about a 0.75 mm bend radius with negligible loss. The fibre stress formula would predict a much larger radius, 3.75 mm, as a limit, so the revised approach is certainly attractive. The authors further suggested a thinner taper could be bent in almost any manner without loss.

In this work, the initial tapered fibres with macrobends were bent entirely by hand, and it was necessary to be conservative in the size of macrobend constructed. Further, an inability to measure the final taper waist diameter achieved in each case of tapering until after the taper loop was mounted required that a worst case assumption be made (in terms of thickness of waist diameter). Taking these various limitations into account, a fibre mount was constructed

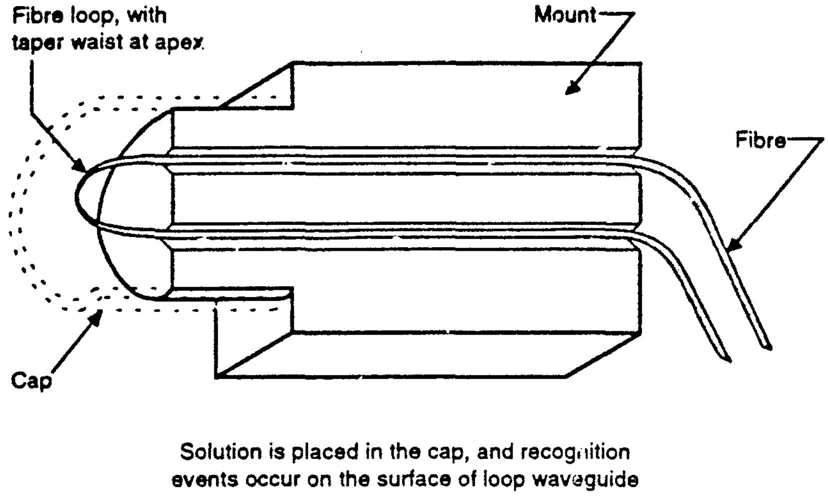

Figure 8.1 *Support for initial version of tapered single mode fibre loop sensor, cut away view. The upper half of the mount is placed over the bottom half with the fibre fixed in place; a cap can be placed over the complete mount to protect the taper loop or to allow chemical interactions to take place.*

to accommodate a radius of curvature of 1.0 mm as depicted in Figure 1. Loops of this bend radius were made repeatedly without significant transmission loss (0.1 dB or less). Subsequently, macrobends with a radius of 0.5 mm were made without difficulty.

Now that a much simpler configuration, with suitably low loss, had been devised, practical application of coatings to make the system specific to the desired chemistry was possible. Silanisation with an appropriate organofunctional silane could be used to introduce appropriate functional groups onto the silica fibre surface, without contaminating the mount. The tapered fibre loop could interact simply with the samples.

8.2 Use of the tapered single mode fibre loop in an immunoassay

The use of optical fibres with immobilised recognition elements for immunoassay sensors is well known[219]. In general, the fibre sensor will not be affected by fluorescence from molecules spaced away from the waveguide (i.e., background interference). This method not only allows the presence or absence of the fluorescent indicator to be detected but also enables quantitative measurements to be made. The biochemical materials bound to the waveguide

surface exhibit fluorescence in response to a change in the amount of analyte present (either quenching, the introduction of a fluorescent label, or a two-step fluorescent label assay).

To examine the tapered fibre loop in a fluorescent-based immunoassay, either fluorophores or recognition elements used with secondary fluorophore reactants were silanised directly to the fibre surface. If the fluorescence occured in the entire region surrounding the silanised tapered fibre, then the fluorescent collection efficiency would be given by Equation 2,

$$\eta = \frac{\log_e V}{V^4} \frac{(NA)^2}{n_1^2} \tag{2}$$

The tapered silanised fibre loop used for this analysis had a numerical aperture of 0.59 in the taper waist region where the external refractive index was 1.32, cladding refractive index was 1.458, taper radius ρ was 0.5 microns, and the wavelength of the expected fluorescence was 0.526 microns. Using this equation, the fluorescence capture efficiency was anticipated to be 0.13%. This assumed that the refractive index of the molecular layer of fluorescein isothiocyanate (FITC) and silane (and other proteins for appropriate linking) immediately adjacent to the fibre was negligible. However, even if a near-monolayer coating was applied, some effect was likely to be seen. In practise, a monolayer was not found, as illustrated in the scanning electron microscope photograph in Figure 2.

The coating here is approximately 160 nm in depth, which implies that for the tapers used in this immunoassay study, a coating about 1/3 as thick as the waveguide itself surrounds it. The fluorescent molecules appear to act as a thin surface layer radiating around the waveguide in dimensions significant to it. In order to take this into account, the fluorescence capture efficiency must again be evaluated from the surface to a small distance away, i.e., ρ to ρ + δ ρ to arrive at the appropriate efficiency, which is the same as used in the penicillinase experiment,

$$\eta = \frac{2 \log_e V}{V^4} \frac{(NA)^2}{n_1^2} \cdot \tag{1}$$

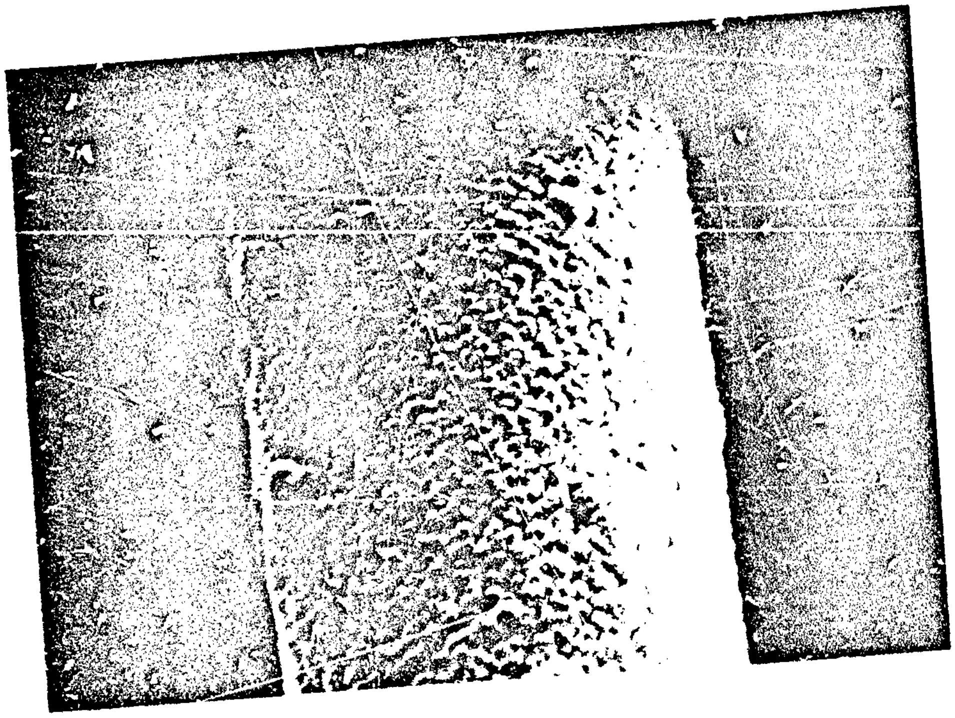

Figure 8.2 *Surface of a fibre with CTP_3-BSA attached to the silanised fibre at 2 micron resolution. NB: this section of the fibre is not at the taper waist.*

Thus the expected fluorescence capture rate would now be 0.27 % (including rounding). It is important to realise that there is a fundamental limitation in comparing theoretically derived fluorescent capture levels and experimentally measured ones. In an experimental set-up, typically the actual orientation and absorption cross-section of individual molecules are not known, nor is the quantum efficiency of the fluorophore. Experimental efficiency is based on the ratio of total collected fluorescent power (collecting energy at wavelengths above the pump wavelength having performed suitable spectroscopic analysis) to input power (measured via a suitable coupler). The pump power must be assumed to be completely absorbed, or the residual amount measured and subtracted from the denominator. Nonetheless, the theoretical capture levels should be upper limits of possible sensitivity of the system, and these are used as a figure of merit. The experimental study performed on the immobilised material on the tapered loop sensor was developed in order to verify that the theoretical level predicted by this second model adequately represented the effective

waveguide system of tapered fibre plus protein layer. This required investigation of a number of simple model systems.

8.2.1 Model systems based on silanisation and the avidin-biotin interaction

One of the most useful interactions in immunochemistry involves the specific binding of the water-soluble vitamin biotin to the egg white protein avidin†. Avidin is a tetramer containing four identical subunits of molecular weight 15,000. Each subunit contains a high affinity binding site for biotin with an extremely low dissociation constant. The binding is undisturbed by extremes of pH, buffer salts, or even chaotropic agents, such as guanidine hydrochloride (up to 3 M). The strength of the avidin-biotin interaction, the strongest known noncovalent biological recognition between protein and ligand, has provided researchers with a unique tool for use in immunoassays and protein isolation.

The avidin-biotin system is particularly well-suited for use as a sandwich or bridging system, in association with antibody-antigen interactions. The biotin molecule can easily be activated and coupled to either antigens or antibodies, usually with complete retention of activity. Subsequently, avidin can be conjugated with fluorochromes and used as a high affinity secondary reagent to greatly increase the sensitivity of an assay, or to make it optically detectable. The model systems used to initially examine the protein-tapered fibre loop waveguide system were very simplistic: first, FITC alone was bound to a silanised tapered fibre loop, then FITC-labelled avidin directly to the loop, and then FITC-labelled avidin was allowed to react with a tapered fibre loop with biotin silanised to it. Lastly, a more complex system was examined with FITC-labelled synthetic peptide CTP_3 bound to a carrier protein BSA (CTP_3 and its significance as an epitope for cholera toxin will be discussed in Chapter 9) attached to the silanised fibre as a preliminary measure for an antigen-antibody immunoassay.

† [140, 141, 142, 143, 187, 251, 260, 409]

8.2.1.1 Chemical preparation of the tapered fibre loop

Various methods of attaching these fluorophores to the optical fibre surface were explored. The silanes used for the chemical binding were specific to the functional groups present. In all cases, the solutions used were placed in a cap that fitted over the end of the tapered loop. In the case of FITC alone and NHS (N-hydroxysuccinimide ester of) -biotin an amino-functional silane was used. This required that the tapered fibre loop be activated with 3-aminopropyltriethoxysilane at 50° C for one hour. The fibre loop was rinsed thoroughly, and then 1 mg/ml FITC in 100 mM sodium phosphate buffer pH 8.3 or an equivalent amount of NHS-biotin was incubated in a cap at room temperature (taken to be 25° C) for an hour. The fibre loop was rinsed extensively with buffer to remove any unbound material and stored with buffer solution. For either FITC-avidin or FITC-labelled synthetic CTP_3-BSA, 3-glycidoxypropyltrimethylsilane was reacted with the tapered fibre loop for one hour at room temperature. Vicinal diols were formed after hydrolysis of the oxide function by using 11.6 mM HCl at 90° C for one hour. Aldehyde groups were then formed by oxidation by 0.1M $NaIO_4$ dissolved in 10% (volume to volume) acetic acid placed in a cap and reacted for another hour at room temperature. Lastly, either FITC-avidin or FITC-labelled synthetic CTP_3-BSA were reacted with the tapered fibre loop for an hour, and then the loop was rinsed exhaustively with buffer solution (the same as used in the amino-functional silane protocol) and stored with a cap filled with the same buffer. A pictorial representation of these functional groups, as they attach to the silica fibre surface, is shown in Figure 3.

8.2.1.2 Fluorescent measurements

The 488 nm line of a water-cooled argon-ion laser (Coherent Innova 90-5), passed through an optical chopper, was used to excite the fluorophore. The fluorescent light from the excited bound fluorophores was coupled into the guided mode of the taper. The input wavelength was removed with a high pass wavelength filter (OD 515 nm) which allowed wavelengths at or above 515 nm to pass through it; this completely blocked out (50 dB loss or more) the excitation wavelength. The filtered light, emissions from the captured fluorescence, was then

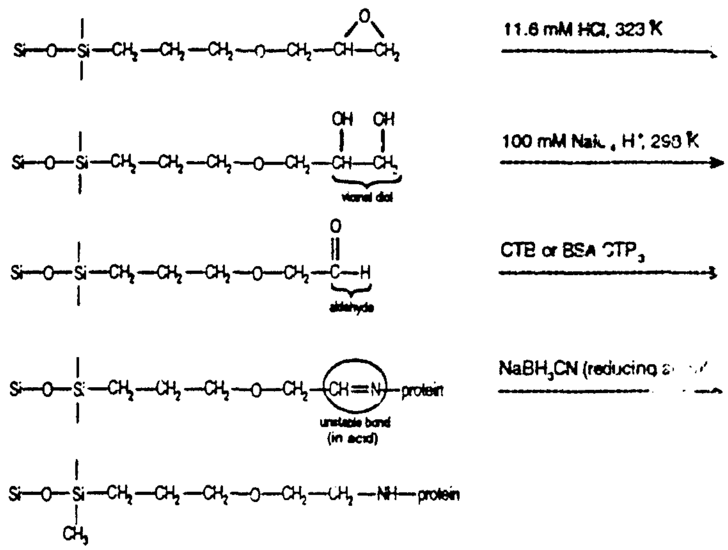

Figure 8.3 *Modification of terminal group of silane, attached to silica fibre surface, to bind protein*

detected by a large area photo diode. Voltage levels (converted from the current output of the photodiode) were recorded with a lock-in detector linked to the optical chopper. The lock-in detector was linked to a personal computer via an analogue to digital data acquisition card. Initial measurements of the excitation wavelength through the OD 515 nm filter were made and found to give statistically negligible readings. The photo diode alone, without any illumination source other than ambient light (the photo diode was mounted with a pin hole cover suitable for insertion of an optical fibre), gave extremely low readings, which were used in conjunction with the filter readings to give a noise level for comparison to the fluorescent readings. Fortunately, all the fluorescent emissions were found to be at least three orders of magnitude higher than the baseline noise level. The optical launch of the fibre did not need to be disturbed while the cap was filled with sample solutions, nor while the loop was being rinsed. A baseline fluorescence reading of a fibre loop in contact with 1 mg/ml FITC in solution (not bound to the fibre surface) was made as well.

The fluorescence levels captured from FITC attached directly to the silanised tapered fibre were in line with what was predicted by theory, as was the fluorescence measured for the FITC in solution. All the other model systems, however, exhibited fluorescence levels significantly higher than expected. This is shown in Table 1.

System	Power measured (mW)	Percentage of input power (%)
Predicted (theoretical) level	0.00892	0.268
FITC	0.0071	0.197
FITC in solution	0.0006	0.016
FITC-Avidin	0.096	2.67
Biotin-FITC-Avidin	0.091	2.53
FITC-CTP3-BSA	0.12	3.33

Table 8.1 *Fluorescence levels of various fluorescent or fluorescently-labelled proteins in contact with the tapered fibre. Input power was 3.8 mW at 488 nm.*

There are several ways to attempt to explain this result. A simple solution would be to note that the theoretical treatment of the fluorescing molecules on the surface of the optical waveguide assumes an equal density of fluorophores for all cases. This is certainly not the case since the number of FITC molecules that could bind to the fibre depends on the number of potentially accessible lysine groups (the biotin binding site of avidin may be sterically hindered when certain groups[48] are present near the lysine). In both the FITC-avidin and biotin-FITC-avidin systems, up to 10 FITC molecules could bind per avidin (though in practise only 6-7 are normally bound); for the FITC-BSA-CTP$_3$[164] system more than 40 FITC molecules may be bound (though only 24-28 would be expected). If this is taken into account simply by multiplying the fluorescent effect by the number of FITC possible per protein molecule, then the levels described by Table 2 are anticipated.

System	Maximum expected level	Level expected in practice (i.e., 7 out of 10 FITC molecules), %	Measured level, %
FITC	0.268	0.268	0.197
FITC-Avidin	2.68	1.88	2.67
FITC-Biotin-Avidin	2.68	1.88	2.53
FITC-CTP3-BSA	10.72	7.5	3.33

Table 8.2 *Fluorescent levels with simplistic fluorophore quantification.*

Although this seems to address the situation, it is not a very satisfactory explanation when the physical aspects of the protein are taken into account. Avidin is simply huge compared to FITC alone (molecular weights of ≈ 60,000 and 400, respectively). It is extremely unlikely that the fluorophore density in the volume surrounding the taper is distributed in such a multiplicatively-simplistic manner. These molecules will not occupy the same volume, and certainly not while on a surface[348]. It is more likely that another explanation is more plausible. When these tapered fibre loops were first considered for use in immunoassays, it was assumed that a monolayer or insignificantly thin layer (from the viewpoint of the wavelength of light utilised) would be attached. Although this appears to be true for silane alone (see Figure 4) or FITC in conjunction with silane (borne out by Table 2), it certainly is not true for protein coats. A number of methods were used to assess the surface yield (i.e., amount bound per surface area) as well as the thickness of the attached layer.

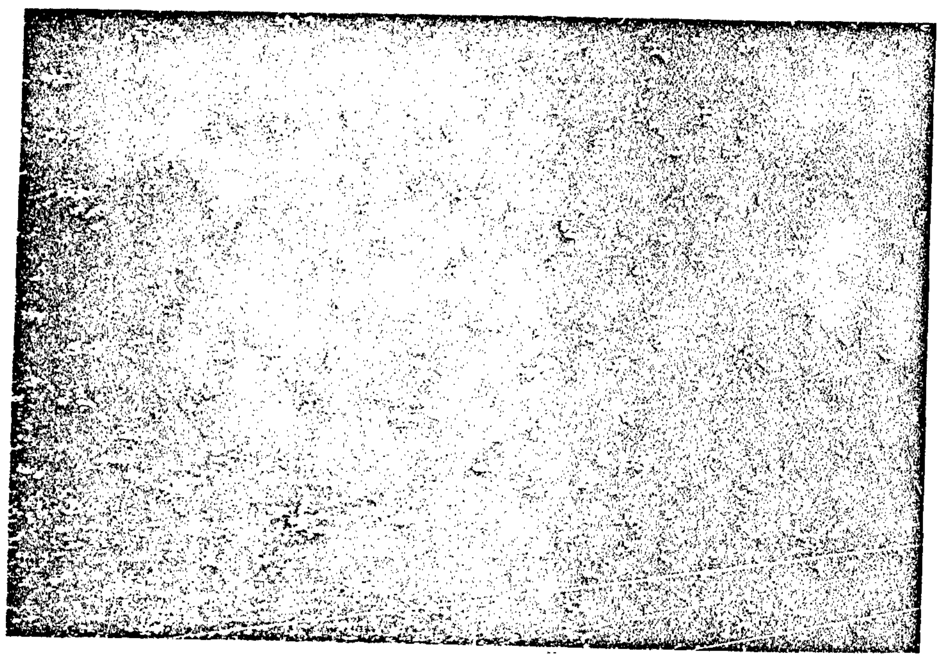

Figure 8.4 *Surface of tapered fibre loop with only silane (3-aminopropyltriethoxy-silane) at 2 micron resolution*

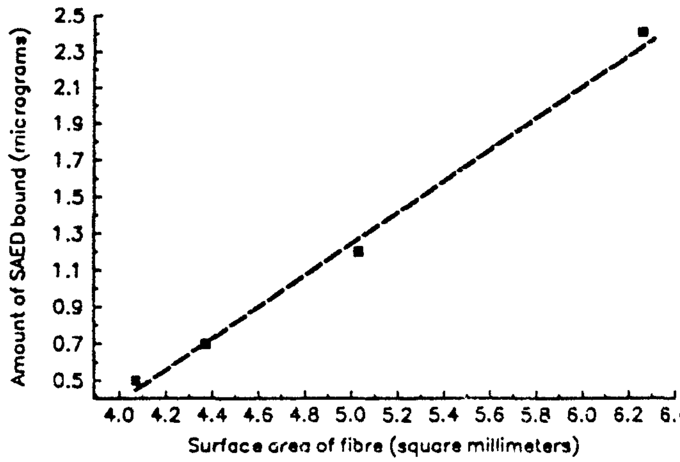

Figure 8.5 *Yield of SAED molecules covalently bound through a silanisation process to the surface of the fibre.*

8.2.2 Surface yield determination

Two chemical methods of determining surface yield were attempted. First, a fluorescent technique based on SAED (sulfosuccinimidyl 2-(7-azido-4-methyl coumarin-3-acetomido) ethyl-1,3'-dithiopropionate) and its interaction with TCEP·HCl (tris(2-carboxyethyl) phosphine) was tried. Next, these results were compared to radio-isotope protein yields derived from gamma counts.

SAED can be bound, using the 3-glycidoxypropyltrimethylsilane protocol, to fibres with a measured surface area. This molecule has a double sulphide bond that can be cleaved with a reducing molecule, TCEP. The part that is removed is the mobile fluorescent moiety. The fluorescence of these detached fluorophores could be measured on a fluorescence spectrometer and compared to reference concentrations. The resulting yield is calculated to be approximately 0.6 to 5.6 molecules /$Å^2$ or 40-125 pg/mm^2. This is shown in Figure 5. This calculation pre-supposes a surface area, rather than a volume. It is likely, if the upper range of the calculation is used, that the layer is at least 5 molecules thick. Another method was needed for comparison.

A radioassay was performed based on the gamma counts from sodium ^{125}I. Fibres of known surface area were prepared and bound through the amino-functional silane assay (Appendix III) to a commercially purified peptide (Arginine-Lysine-Aspartic Acid-Valine-Tyrosine peptide). The sodium ^{125}I should bind to the tyrosine in a 1:1 manner, thus allowing a good approximation of the number of protein molecules actually binding to the silanised fibre. Gamma counts of solutions with known concentrations of sodium ^{125}I were compared to those received for the radioactive fibres, yielding approximately 0.01 molecules/$Å^2$ and 125ng/mm^2, which was about 10-15 times more than expected for a surface area[273]. The peptide was attached to the fibre with an amino-silane, which typically does give rise to thicker (heavier) protein layers[109, 372]. This confirmed the notion that the protein layer was many molecules, possibly up to 10, thick.

Lastly, scanning electron microscopy of the fibre surfaces was used to assess thicknesses of various protein layers. Rough measurement of the thickness of the layer was possible from photos such as shown in Figure 6, which shows a thickness up to approximately 250 nm. The

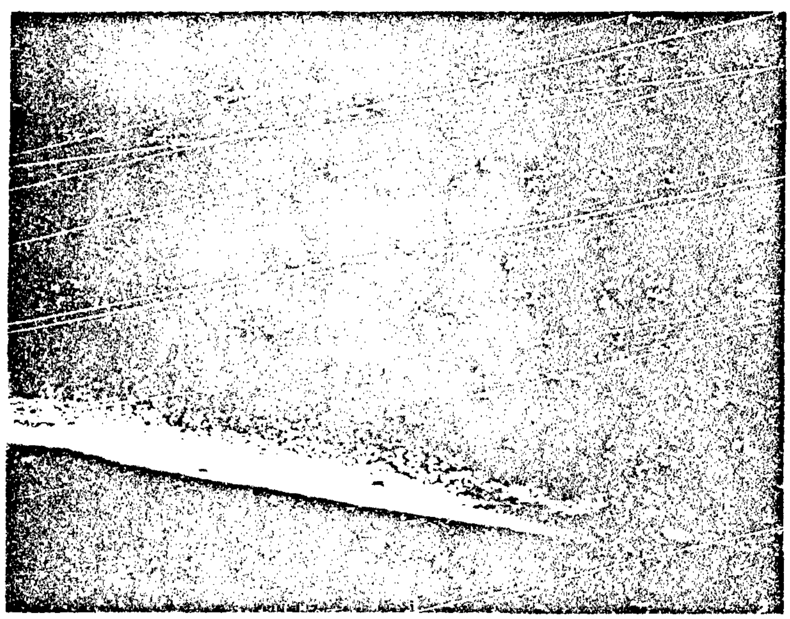

Figure 8.6 *Surface of a fibre with CTP_3-BSA attached to silanised surface, at 200 nm resolution.*

surface layer must indeed occupy a volume, as opposed to a two-dimensional surface area. As shown in Figure 7, the protein coatings were smooth from the standpoint of the optical

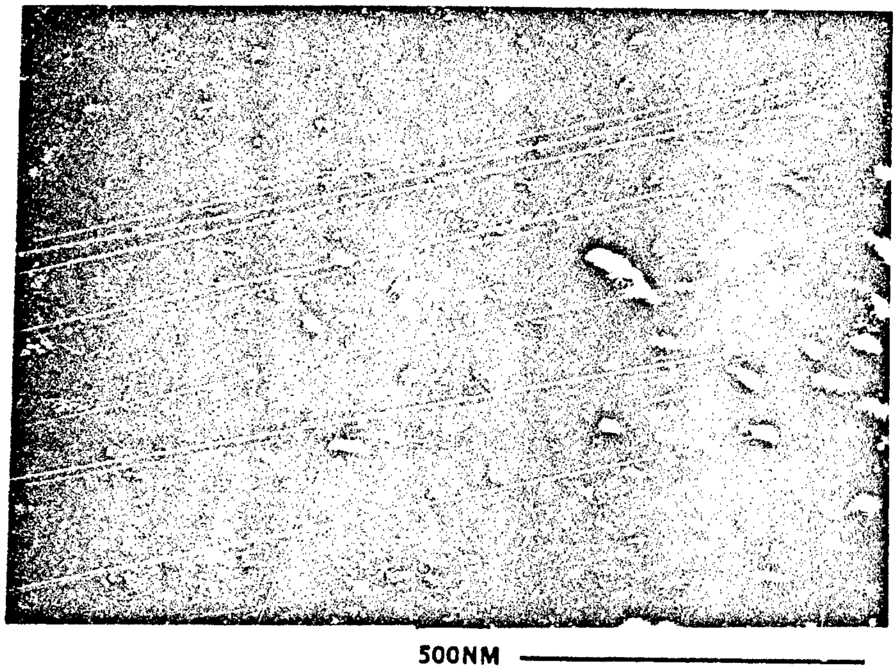

Figure 8.7 *500nm resolution of fibre with CTP_3-BSA attached to silanised surface. Protein coat appears to be optically smooth.*

wavelength (500 nm). This information, in conjunction with estimates for the index of refraction of the protein layer, were used to develop a model for the behaviour of the fluorescent light in the protein-tapered fibre waveguides.

8.3 Novel waveguide concept

Since careful definition of the protein conformation and binding behaviour was not possible, it is perhaps better to look at the optical field in conjunction with what information is available about the nature of the waveguide. The surface examination methods seemed to be consistent with one another in establishing that a multi-layer of protein built up around the optical fibre that remained accessible to the sample, and that was optically smooth. If this is the case, then

the protein coat could be acting as an effective waveguide in and of itself, and depending on the actual thickness and index of refraction of the material, the fluorescence generated in this protein waveguide may couple into the mode of the tapered fibre. Using the computer program described in Chapter 3 to analyse the modal field evolution through the tapered region near the taper waist, a four layer problem was evaluated, with the refractive index profile as shown in Figure 8. The thickness of the protein coating (silane, protein, fluorescent label) is approximated at 0.15 μm consistent with estimates from SEM photographs, and an estimated

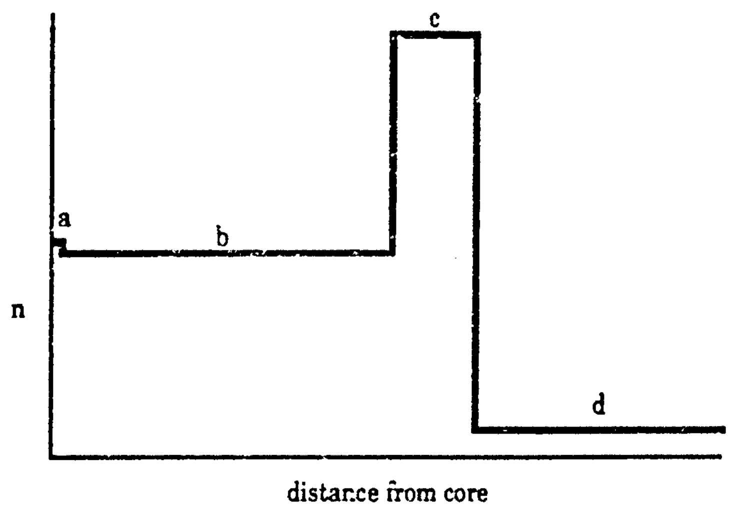

Figure 8.8 *Refractive index profile used in the computer model to analyse optical field propagation for the taper waist region. Letter **a** is the core dimension; **b** represents the extent of the cladding; **c** is representative of the protein coating extent; and **d** is the buffer extent (which, as far as the model is concerned, extends to infinity).*

index of refraction of 1.6 is used for the external protein coating[19, 199, 260].

As the evanescent field of the tapered fibre mode interacts with material silanised on its surface, the attached fluorophores generate fluorescence which is actually carried along in its own mode. The energy of the waveguide is now in both the fibre as well as the external protein layer. The interaction between the evanescent field of the tapered fibre loop fibre mode (core-guided) and the fluorescent mode of the protein layer (protein ring) occurs mainly at the taper waist. Figure 9 shows a possible evolution of light through the taper from the viewpoint of the total mode of the waveguide system (i.e., the combination of of the protein

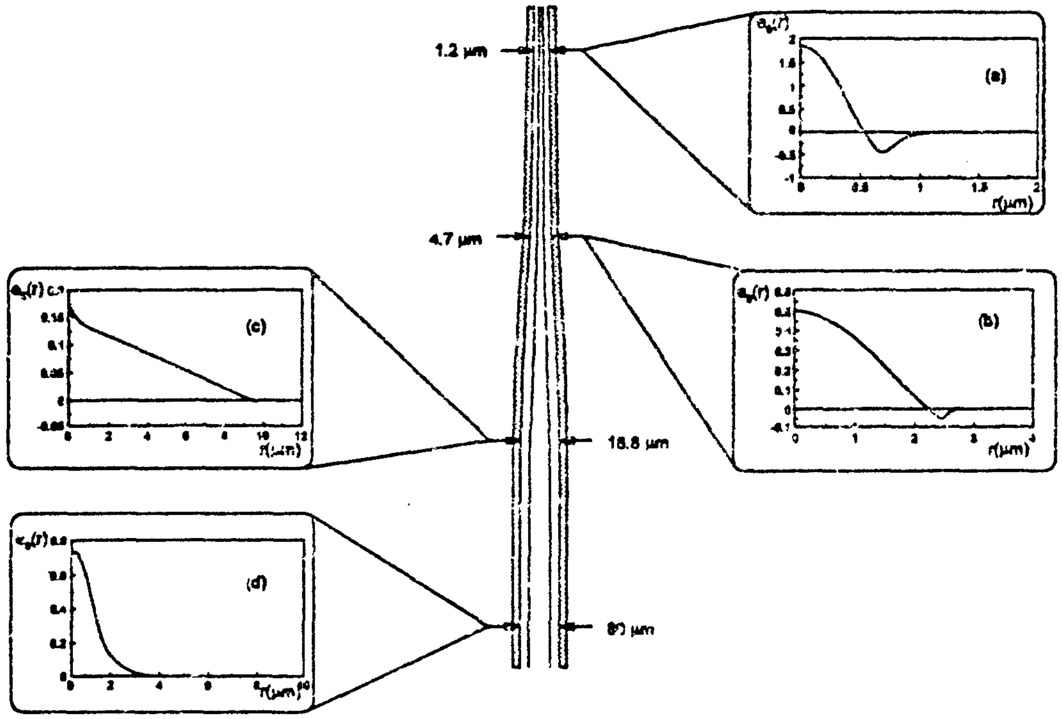

Figure 8.9 *Possible evolution of light through the taper*

ring and core-guided modes). At the taper waist (Figure 9a), a significant portion of the guided optical field is found in the fluorescent layer. As the mode travels along the taper it sees a fibre core of gradually increasing diameter, and the mode adiabatically evolves into a core guided mode when the fibre returns to its full diameter (Figure 9d). Figures 9b and 9c show the field at two intermediate points along the fibre.

The mode supported by the total waveguide structure depends critically on the thickness of the protein layer. If the protein layer is 150 nm thick, as assumed here, the mode shown in Figure 9 evolves: this is a second order mode, not the fundamental mode. The fundamental mode would be light guided as a ring shaped mode by the fluorescent layer, which is seen at thinner layers. The propagation constant of the fundamental mode does not intersect the β of any other modes, and so the evolution of this mode can occur adiabatically without coupling. The fluorescence capture efficiency initially increases as the protein layer decreases to about

100 nm, where the modal propagation constant crosses that of the ring type mode, which will allow modal coupling of power at some point along the taper - an additional, non-adiabatic

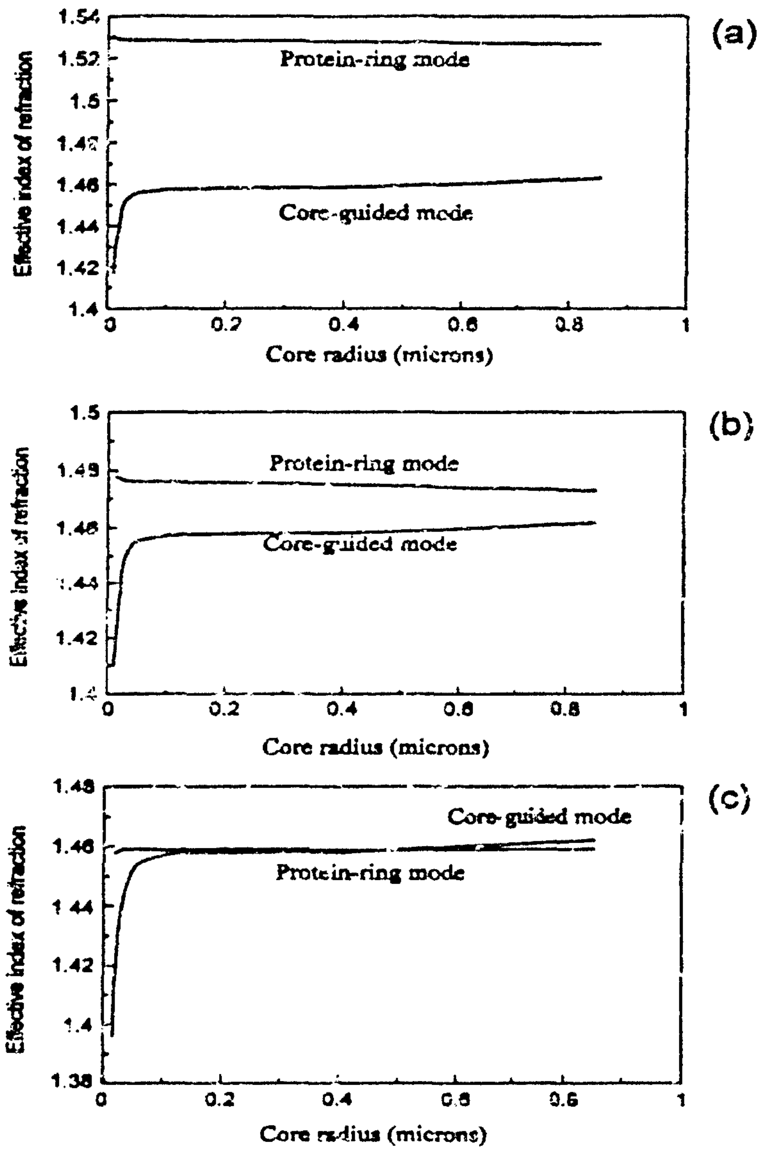

Figure 8.10 *Effect of the thickness of the protein coat on the propagation constants, βs, (curves on graphs) of the fibre and fluorescent modes. When the coating is 0.3 μm (a), the two βs are far away; when the coating is cut to 0.15 μm (b), the two βs move closer. When the coating is reduced still further to 0.10 μm (c), the two βs for the two modes actually intersect.*

transfer of energy, as shown in Figure 10. Reducing the coating thickness still further once again allows the modes to evolve adiabatically, without interaction.

An interesting point to note is that the cladding mode and the fibre mode never interact, even

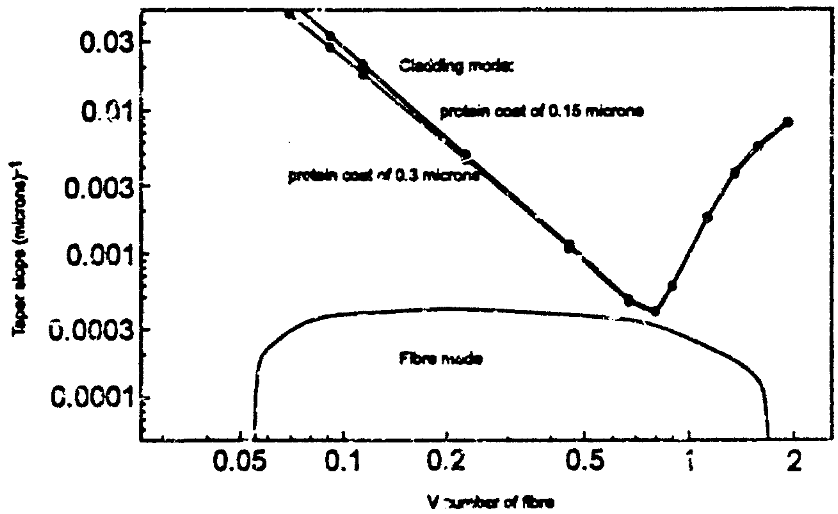

Figure 8.11 *Inverse taper slope as a function of V number of fibre: lower curve is for the fibre mode(i.e., measured on an actual taper); upper curves are for the cladding mode at two coating thicknesses - 0.3 microns and 0.15 microns. Reducing the coating thickness only moves the two sets of propagation constants further away.*

as the external coating thickness changes, as seen in Figure 11. It is only the protein ring mode that interacts with the core-guided fibre mode.

8.4 Conclusions

Although the exact experimental parameters were not known, this effective waveguide model describes a method in which the observed levels of fluorescent capture could occur. In fact, the external refractive index of the external buffer solution serves to enhance this effect, as seen in Figure 12. It must also be pointed out that non-adiabatic power transfer could have occured, and not been noted as non-adiabatic behaviour, as the input power was measured to the taper (via a fused fibre coupler) and the fluorescent power measured at the output end. Confirmation of low splice and transmission loss through the coupler-loop optical circuit is performed prior to the fluorescent sandwich assay. Further, the exact dimensions of the taper

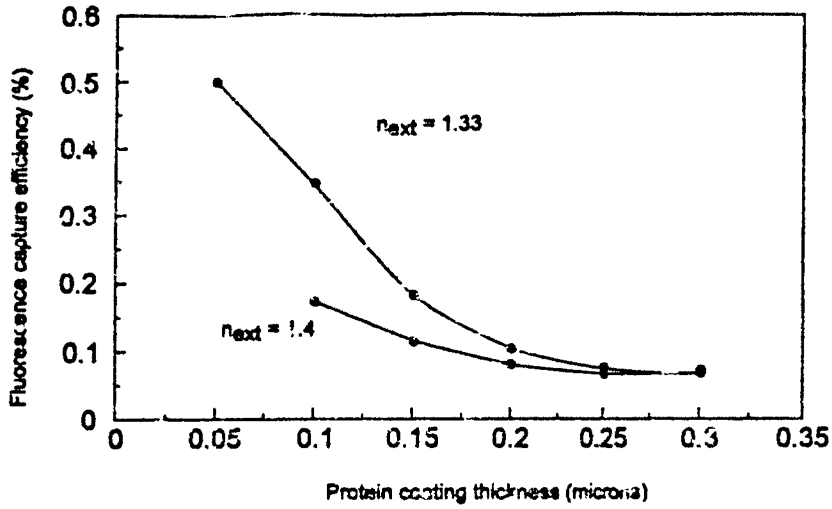

Figure 8.12 *Fluorescence capture efficiency as a function of protein coating thickness, given a fixed index of refraction for the protein layer. The external index of refraction is varied, as shown on the two curves. Note that this is theoretical fluorescence capture efficiency, based on the total fluorescent energy generated.*

waist and the protein coat are not known individually, as the SEM process is destructive to the sensor. Thus real values cannot be used in the computer model. Repeatedly making tapers of (statistically) known slope and waist diameter should be a focus for future work. Assessing the index of refraction of the protein coat could be done on a behavioural basis, if the dimensions of the entire waveguide system are known, and additional measurements to confirm adiabatic behaviour (or not) are made. Also, the behaviour of proteins as a portion of an immunoassay do not behave identically as those proteins pre-labelled with a maximum number of fluorophores, as used in the experiments in this chapter. The measurements made here do, however, demonstrate the ability of the coated tapered single mode fibre loop to capture far more fluorescence than is possible with a multimode system, even without adjustment of the external refractive index. Tapered fibre loop devices with low transmission loss, as expected, could be repeatedly made. The use of silanisation to apply selective elements was demonstrated, and a more complete sensor for a specific analyte could be devised. A further assay was performed to model the tapered fibre loop's capabilities in a more realistic antibody/antigen assay, examining "more interesting" chemistries, as is described in Chapter 9.

Chapter 9

Realistic chemistries applied to the tapered single mode optical fibre loop

Summary

As discussed in Chapter 7, the immobilisation of penicillinase onto an optical fibre is not very interesting from a practical chemistry viewpoint, nor were the model analytes of Chapter 8. In this chapter, the use of silanisation procedures in conjunction with more generic recognition elements are discussed, as is the behaviour of the tapered single mode fibre loop as a "true" sensor. A more complete immunoassay than the model systems of Chapter 8 is carried out, and the sensitivity of the device discussed.

9.0 Selective elements for optical fibre immunosensors

Antibody-antigen pairs, as well as enzyme-substrate ones, are suitable recognition elements for immunosensors. Both of these sets of proteins can almost uniquely respond to their respective other half, and if suitably chosen or labelled, can release optical information. The immobilisation of a protein to a silica-type waveguide can be accomplished covalently through the use of silanisation processes. Once immobilised, these recognition elements may be re-used, with obvious economic advantages.

9.1 Reusable probes

Typically, it is desirable that a sensor system be reusable in some manner. In the case of the penicillin sensor, this was relatively simple to regenerate as the penicillin did not bind sufficiently tenaciously to the recognition element, and repeated rinsing with buffers could restore the tapered fibre to its original configuration. In the case of antibody-antigen reactions, this regeneration is not necessarily as simple. Two techniques were explored: the replacement of the recognition element silanised to the fibre was investigated, as was the regeneration of

a reactive antigen (to allow repeated interaction) similarly attached to the waveguide. These two approaches gave some measure of the capability of the fibre loop system as a reusable sensor.

9.1.1 Replacement recognition entity investigation

The ability to completely replace the recognition element on the loop sensor was investigated first. The fibre loop is silica, made from the York Technology single mode fibre. The tapered fibre loop was silanised with 3-mercaptopropyltrimethoxysilane for one hour at 70° C. Next a dithio was added to the silanised fibre loop with Ellman's reagent (5,5′-dithio-bis-(2-nitrobenzoic acid)), shown in Figure 1. This allows the formation of a

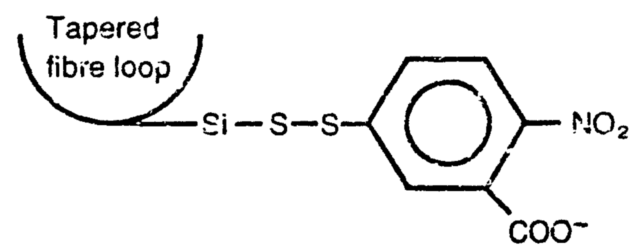

Figure 9.1 *Bound Ellman's reagent 5,5′-Dithio-bis-(2-nitrobenzoic acid); figure is not to scale.*

mercaptosilane-TNB (2-nitro-5-thiobenzoic acid) conjugate. Once the binding of Ellman's reagent had been confirmed through the use of a cysteine-standard (cysteine is used here as a protein standard for the ELISA control as was BSA in the penicillinase experiment) ELISA-based process, the conjugated di-sulphide group was carboxylated with mercaptopropionic acid, releasing 2-nitrio-5-thiobenzoic acid, which could be monitored using the cysteine standard. The protein of interest (enzyme, antigen, antibody) could then be added to the treated loop through the use of N-hydroxysuccinimide and N,N′-dicyclohexylcarbodiimide[illegible], and finally the protein itself. A disulfhydryl could be reformed with treatment by mercaptopropionic acid, and subsequent amination would allow another protein to be attached to the fibre.

This chemically-treated tapered fibre loop system was tested with the addition of FITC-labelled avidin. Once the fluorinated protein was bound to the loop, the fibre was

illuminated with the 488 nm line of an argon-ion laser (Coherent Innova 90-5). Fluorescent light was collected at the far end of the fibre through an OD-515 filter, which served to remove the pump beam, combined with a large area photo diode. The loop was treated with the mercapropropionic acid to release the protein, and the fluorescent power was monitored and seen to go to zero. Another solution of FITC-avidin was added after the fibre had been treated with N-hydroxysuccinimide and N, N'-dicyclohexylcarbodiimide, and the fluorescent power recovered to similar levels when compared to the signal from the intially-treated fibre loop. The ability to change the recognition element "on the go" for tests of multiple analytes is attractive, but the chemistry used was time-consuming and involved reagents that must be handled in a laboratory environment. Potentially, a better option would be to have multiple loops present if multiple analyte testing is desired.

9.1.2 Reusable probe with attached antigen

In this immunoassay, the presence of cholera toxin (CT) antibodies were sensed to test the ability of the recognition element to regenerate its responsiveness. An appropriate detection element, either the B subunit of cholera toxin or CTP_3, a well-established epitope for the toxin, were linked to a silanised tapered fibre loop. A two-step process was investigated using samples from blood drawn from volunteers who had expressed symptoms of cholera. If cholera toxin antibodies were in solution, they would bind to the antigen on the silanised fibre loop. The loop was then exposed to a labelling solution, containing fluorophores which would in turn bind to the antibodies on the loop if any were present. The regeneration of the system was tested by repeated use of the same concentration level (or titer) of a given blood sample in conjunction with a chaotropic solution, 0.1M glycine hydrochloride at pH 2.4, exposed to the silanised loop-antibody-fluorescent label system for 1 minute. This limit was chosen after varying exposure times to the glycine and sample solutions, as shown in Figures 2 and 3. The original fluorescent signal measured at the first incidence of testing was found repeatedly (using the same dilution level several times), verifying the viability of this simple regeneration technique.

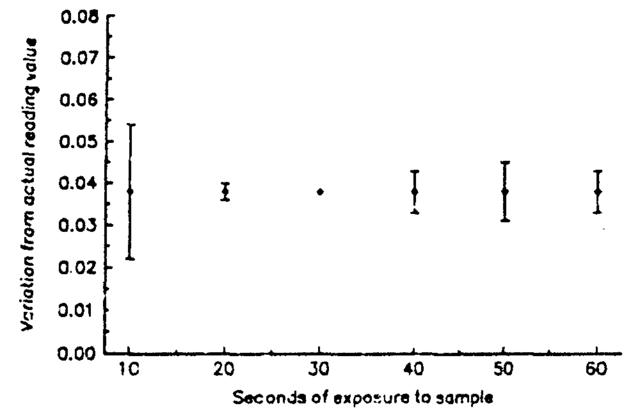

Figure 9.2 *Restoration of expected reading after varying the time of exposure to the sample at a fixed exposure time (1 minute) to the regeneration buffer.*

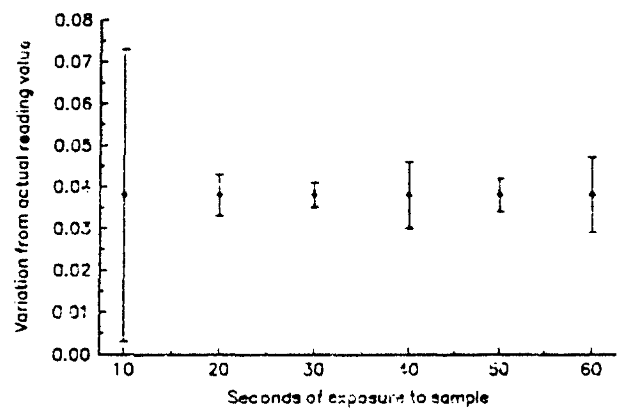

Figure 9.3 *Variation of signal received upon variation of sample exposure time, at a fixed exposure time (30 seconds) to the regeneration buffer.*

9.2 Complete assay of cholera toxin antibodies

The tapered portion of the optical fibre is initially treated with a suitable binding agent, in this case 3-glycidoxypropyltrimethoxysilane, following the protocol laid out in Appendix III. This may be achieved, as shown in Figure 4, by filling the cap with the silane, placing it over the fibre loop, and incubating it for an hour at 50° C. The silanised optical fibre is then treated in the same manner as described in the application of the model analytes of Chapter 8. The

end result is a tapered fibre loop with a recognition element for cholera toxin antibodies bound to its surface. The loop with either bound CTB or CTB subunit derived synthetic peptide (CTP_3) antigens is then placed in the solution potentially containing CT antibodies. Finally, the optical fibre having the bound antigen and antibodies is exposed to a solution of fluorescently labelled anti-IgG and -IgA which will bind to the antibodies, if present. The presence of fluorescence then indicates the presence of the cholera antibody, and the wavelength (526 nm for FITC-IgG, 575 nm for TRITC-IgA) determines which immunoglobulin was present.

9.2.1 Background of the samples used for the immunoassay

This assay examines the sensitivity of the tapered fibre loop sensor to the presence of anti-CT IgG or IgA antibodies to sera samples obtained from human volunteer studies exposing them to live, fully virulent pathogenic *Vibrio cholerae 01*. The samples were obtained from Dr M. M. Levine of the Center for Vaccine Development at the University of Maryland School of Medicine and prepared for use with the tapered optical fibre loops by Dr R. S. Marks of the Institute of Biotechnology at the University of Cambridge. Purified CTP_3 samples were prepared by Dr R. S. Marks while at the Weizmann Institute of Science, Rehovot, Israel. All the measurements with the fibres were accomplished in the Engineering Department of the University of Cambridge. The sera used as a basis of the diluted titers (Appendix III) were obtained from human volunteers before (pre-serum) and 28 days after (post-serum) oral challenge with fully enteropathogenic *Vibrio cholerae 01* Classical strain Inaba 569B. All sera used were from those volunteers who had shown both diarrhea and positive stool cultures for *Vibrio cholerae 01*. Total reactivity to cholera toxin was determined by standard ELISA processes[315]. All other reagents used were purchased from Pierce & Warriner.

Cholera toxin B subunit-derived synthetic peptide (CTP_3) is a well-described epitope[376] for cholera toxin. An epitope simulates the toxin antigen without carrying the pathogenic activity. Cholera was selected as a suitable basis for a realistic immunoassay†.

---

† [43,116,170,171,250,289,332,152,165,374,6,376]

9.2.1.2 Fluorescent measurements and regeneration of antigen activity

A water-cooled argon-ion laser (Coherent Innova 90-5) was used as the excitation source for both fluorophores; the 488 nm line was used to excite the FITC-labelled IgG and the 514 nm line was used to excite the TRITC-labelled IgA. The labelled immunoglobulins were applied simultaneously. The 514 nm line did not excite the FITC nor did the 488 nm line excite the TRITC. The reading for the FITC-generated fluorescence was taken using an OD-515 nm filter, which filtered out the pump power but allowed the fluorescence (maxima at 526 nm) to pass through. The argon-ion laser was then tuned to the 514 nm line (a matter of seconds) and the fluorescence for the TRITC-generated fluorescence (maxima at 575 nm) was recorded using an OD-550 filter. The OD-550 filter served to filter out the source wavelength (514.5 nm). Measurements of input power for 488 nm and 514 nm were taken as well. An optical chopper in conjunction with a lock-in detector was used to record voltage levels from the large area photo diode. The signals were passed via an analogue to digital card in a personal computer. Sera samples diluted by a factor of 1:50 to 1:26,214,400 (Appendix III) were tested for four patients. Non-specific binding of antibodies or other proteins rather than the cholera toxin B antibodies was minimal; pre-disease onset samples from the same four patients were tested as well (Appendix III) and had no significant fluorescent signal other than at the 1:50

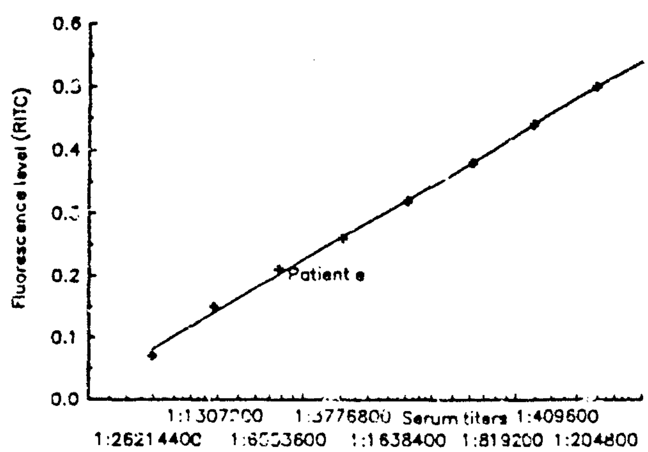

Figure 9.4 *Fluorescent level of TRITC-labelled IgA as a result of exposure to different dilution levels of sera sample.*

dilution. This noise level, as well as photo diode noise and total system noise, were used as a baseline for detection. Signals that could not be recorded 5 times above the noise level were rejected. The minimum detectable dilution for IgA was a titer of 1:26,2144,400, as shown in Figure 4, and 1:13,107,200 for IgG (and converted to an effective mass), as shown in Figure 5. IgG was purified through a selective column that extracted only IgG from the original sera sample; comparing the amount of IgG from a given volume of sera allowed a calculation of the mass of antibody.

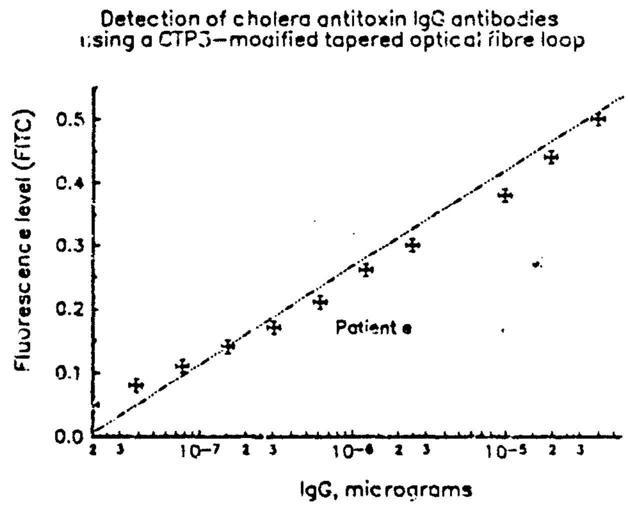

Figure 9.5 *Fluorescent signal from FITC-labelled IgG versus amount of IgG present in various dilutions (serial) of sera sample. 1:50 sample from 1 ml: 20µl of serum in 980 µl of buffer.*

The fluorescent levels seen in this immunoassay are also higher than what can be predicted using the $\rho + \delta\rho$ estimates, further confirming that the coating of the taper loop acts as an effective waveguide, as discussed in Chapter 8. The fluorescent level portrayed on the graphs represents percent capture of pump power: i.e., 0.5 represents 0.5%, or 20 microwatts of fluorescent light received at the end of the fibre taper for 4 mW input of pump light at the beginning of the fibre. Note at low concentrations some non-specific binding of the fluorophore may occur.

9.2 Conclusions

The immunoassay investigated was not complete in the sense that it did not include cross-reactivity controls†, as would be optimal. The use of the synthetic peptide helped to reduce the non-specific binding in the system, as the peptide is designed to react only with specific portions of the anti-CT antibodies. However, the overall good levels of sensitivity are comparable to (and even better than) current optical systems[299,273]. More in-depth investigations should focus on developing the means to make repeatable tapers in both waist thickness and overall taper length, as well as the ability to apply layers of known and repeatable thickness. This would allow suitable statistical analysis.

The fluorescent capture levels seen in the cholera toxin immunoassay confirm the novel waveguide structure, as discussed in Chapter 8. Since the immunoassay performed here used more realistic assay components than those of Chapter 8, the potential of the tapered single mode loop to perform as a useful element of a sensor system is confirmed. Further, the attractiveness of the tapered fibre loop is enhanced by the ability to re-use the system through a relatively simple process of chemical treatment. The tapered fibre loop can potentially be exploited in other areas of chemical and biological sensing, as is discussed in Chapter 10.

† [83,180,435,226,376]

Chapter 10

Conclusions and proposals for future work

Summary

This chapter discusses future work that could be carried out to refine the characteristics of the tapered fibre loop. A number of straight-forward follow-on experiments are proposed. The overall results of this research, as presented in this dissertation, are summarised.

10.0 Future work

The studies performed in the course of this research have demonstrated the concept of a novel waveguide system adapted for use in biological and chemical sensing applications. The various experiments discussed in this thesis established a proof of principle. In order for the limits of performance of the taper single mode loop fibre sensor to be well-defined, much more work must be done to statistically establish the requirements for the selective coating (refractive index and thickness), the uniformity of layer, the required taper length, waist diameter and radius of curvature. This sensor then can be applied towards other areas of interesting research with a well-defined understanding of its expected behaviour.

10.1 Luminescent Techniques

A physical system emitting luminescence is losing energy and some form of energy must be supplied from elsewhere. Most kinds of luminescence are defined according to the source from which this energy is derived. Energy from a chemical reaction may excite chemiluminescence, and chemiluminescence reactions taking place in living organisms give rise to bioluminescence[illegible]. Bioluminescent reactions are generally catalysed by specific enzymes of 'luciferases'. Considerable interest in applying luminescent techniques to optical

fibres has been seen as this would eliminate the (potentially) costly light source from the sensor system. However, the problem of detecting the luminescence remains. Because of the unpredictability of the light source, signal to noise ratios are likely to be lower than those generated by fluorescent systems. No optical chopper at the source can be used to influence the behaviour of received light. An optical coupler could be used in conjunction with the system in order to give a background "dark" reading to compare to the signal at a specific wavelength, integrated over time. There are a number of chemical systems currently reported in the literature that have been, or could be, used in conjunction with optical fibres†. Many of these systems rely upon the use of a membrane to attach the chemical elements to the optical fibre tip. This would not be required in the case of a tapered optical fibre, and depending on the system being used, a relatively simple optical detection device could be used (photodiode in conjunction with a selective wavelength filter). Application of the luminescent material in layers of controllable thickness and uniformity would have to be tried before the efficacy of such a system could be determined.

10.2 Surface plasmon resonance (SPR)

Another method of examining chemical behaviour could rely on the application of a thin metallic film to the tapered fibre. Surface plasmon waves, as discussed in Chapter 2, have traditionally been used in conjunction with evanescent waves of optical systems. The use of optical fibre would eliminate the requirement of coupling the light in and out of a prism, as typically used in SPR applications[4,347]. Further, the use of a thin (500 Å) film of silver provides a surface for chemical deposition with well-known characteristics, simplifying the chemical requirement for a tapered single mode fibre sensor. Work by other researchers [175] has utilised multimode fibre, with its inherent complexities of density of modes propagating and the behaviour of each one. The change of diameter along the taper to and from the waist serves to change the effective index of refraction, n_{eff} and this can be used in Equation 1 below to phase match with the plasma mode.

---

† [1,23,122,126,127,128,206,207,244,82,94,160,188,209,224,286]

$$n_{eff} = \frac{n_2 K}{\sqrt{K^2 - n_2^2}} \qquad (1)$$

n_2 is the external index to the fibre/metal surface, usually 1.32 in biochemical assays. K is the imaginary part of the metal's refractive index.

As in the effective waveguide system described in Chapter 7, the two modes at some point along the taper can couple energy from one to the other. It should be possible to measure changes in external refractive index as shifts in the output SPR wavelength spectrum with a silver (or gold)-coated tapered fibre loop.

10.3 Visible wavelength semiconductor laser as light sources

Another potential area for improvement of this fibre loop is to apply a different sort of laser source. Systems such as water-cooled argon-ion laser are very stable, very efficient, and typically very large and expensive. Recent developments in blue semiconductor lasers, particularly those expected to be available soon from Coherent, will allow a much less expensive and bulky laser system to be coupled directly into the input end of the tapered single mode fibre loop sensor. Further, modulating the semiconductor laser and providing that modulation as a reference signal is a simple matter. The experimental work performed throughout this research relied upon on low input power levels, with much of the tapered fibre work performed with input powers below 4 mW. Several sources currently available can provide this level of power. Remaining in the visible spectrum allows the use of common fluorescent labels such as fluorescein and rhodamine derivatives. Numerous fluorescent-based assays and protocols currently exist and can be readily applied to the tapered fibre system. The inherent sensitivity of the fibre sensor would provide benefit as a diagnostic tool. With the influx of blue (and other visible) wavelength semiconductor lasers into the marketplace, the cost of such components will drop from prohibitively high levels (as have other laser components done in the past).

10.4 Conclusion

This dissertation has presented the development of a new optical fibre biochemical sensor based on a tapered single mode optical fibre loop. This sensor's characteristics have been demonstrated to be orders of magnitude better than those of existing, multimode evanescent field fibre devices. Initially, the ability of the tapered fibre itself to perform evanescent absorption as well as fluorescent capture were demonstrated. Next, the robustness of the tapered single mode fibre in a macrobend (loop) was confirmed, and its ability to perform as a waveguide re-established. The looped configuration led to the discovery of a new effective waveguide system that allows for extremely efficient fluorescent energy capture and thereby great sensitivity in fluorescent assays. Tapered fibre loop sensors can therefore be used in many biochemical assays, and in novel sensing arrangements to gain information about the chemical constituents of samples.

Appendix I

Summary of Chemical and Biological Sensors

This appendix attempts to summarise most of the information available in the recent literature on chemical and biological sensing systems. The articles presented here are arranged by analyte, and each entry has the details of the experiment described in the article. Many of the papers discuss optical fibre sensor systems, though other techniques are represented. The method of detecting the analyte (character) is described in terms of extrinsic (for example, the waveguide merely carries photons rather than electrons) or intrinsic (an evanescent reaction or other inherent character of the sensitive element is used), as well as the means of detection (property): luminescence, fluorescence, absorption, reflection, or other technique. The state of the analyte is reported as gas, liquid, solid, or any other important attribute (i.e., blood).

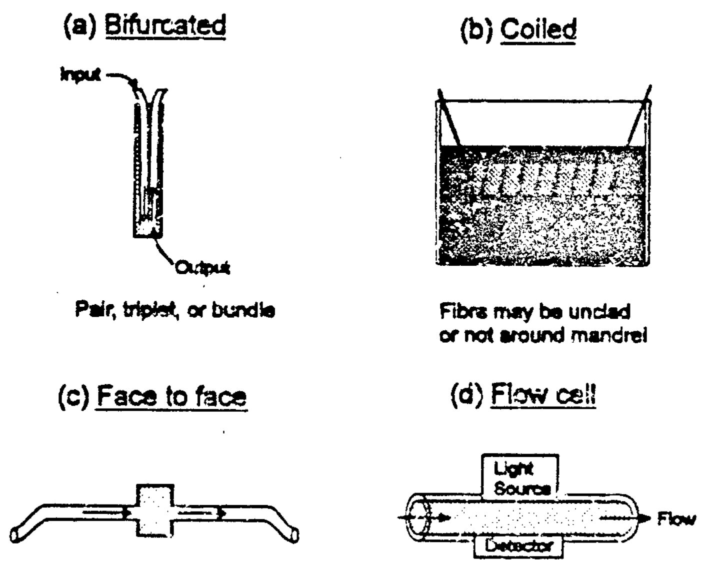

Figure I-1 *Sensing arrangements used in the chemical/biochemical systems reviewed in Table 1*

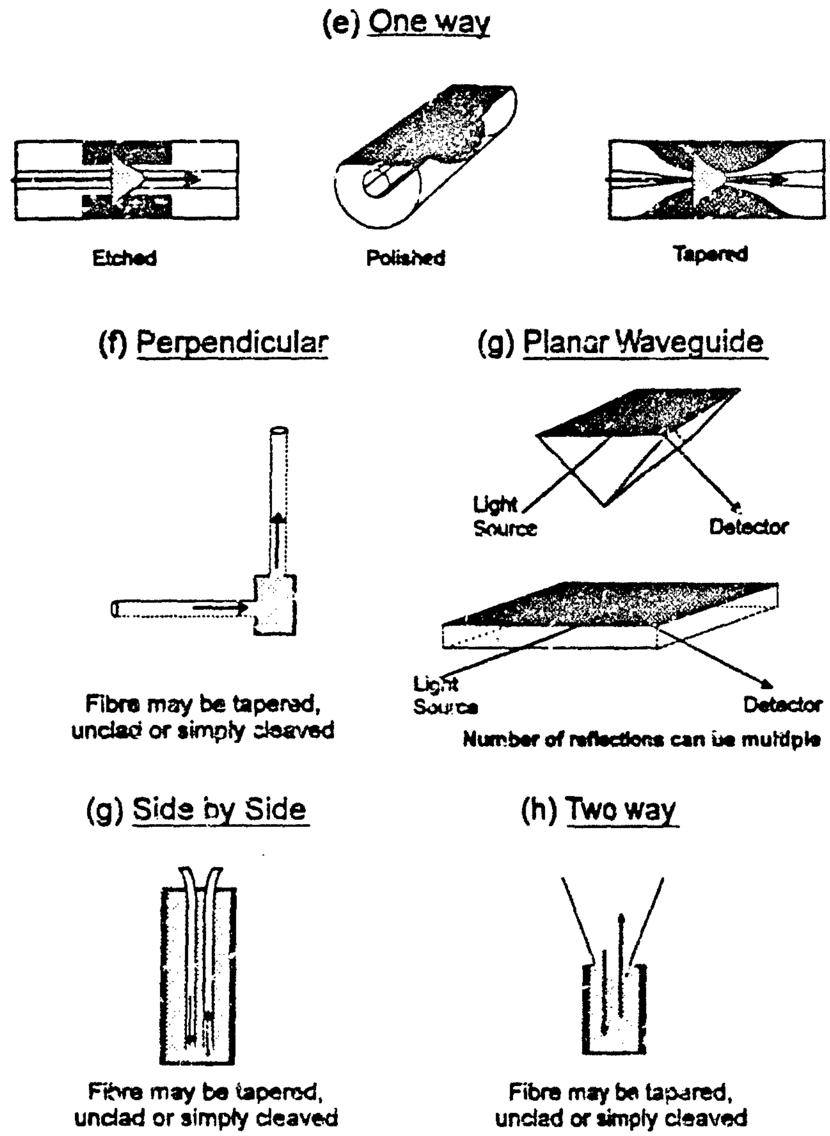

Figure I-1 *Sensing arrangements used in the chemical/biochemical systems reviewed in Table 1*

The methodology of selectively interacting is noted: reagent and means of immobilisation. The access to the sensitive element of the sensor system is described - membrane (if needed), as is the optical fibre and its arrangement (bifurcated, face to face, side by side, coiled, perpendicular, two way one way - other technologies are noted in this category). Lastly, the details of the optical source and detector element (including type, response time and levels achievable) are presented.

Analyte [Reference]	Character / Property / Sample	Reagent / Immobilization / Support	Membrane / Optical Fibre / Arrangement	Light Source / λ-Input / λ-Analysis	Detector / Dynamic Range / Response Time
ATP, NADH [127]	extrinsic/ reversible	Bacterial luciferase	Polyamide	Luminescence	PMT (?)
	bioluminescence	Covalent	Silica (?)	-	Limit of 0.25 to 5 pmol
	Aqueous	Polyamide membrane	Bifurcated	490 nm	-
Al^{3+} [329]	extrinsic/ reversible	Morin	None	Tungsten halogen white light source	PMT
	fluorescence	Adsorption	Silica	420 nm	1×10^{-6} to 1×10^{-4} M
	Aqueous	Cellulose	Bifurcated	488 nm	1 to 2 minutes
Alkaline phosphotase (model analyte) [121]	extrinsic/ irreversible	4-methylumbelliferyl phosphotase	Nylon	Tungsten halogen white light source	PMT
	fluorescence	Solution	Silica	355 nm	Limit of 3.6×10^{-6} M
	Aqueous	Sample well	Bifurcated	420 nm	5 to 20 seconds
Ammonia [18]	intrinsic/ reversible	p-nitrophenol and NH_4Cl (aq)	PTFE	Tungsten halogen white light source	PMT
	absorption	Solution	Plastic	-	2×10^{-5} to 4×10^{-4} M
	Aqueous	None	Bifurcated	404.7 nm	2-4 minutes
Antibodies [42]	intrinsic/ irreversible	FITC/TRITC/Texas Red	None	Laser (?)	PD
	fluorescence	Covalent	Plastic	442 nm (?)	Limit of 100 pM
	Aqueous	None	Two-way (tapered)	As appropriate	-
Antibodies (Clostridium botulinum Toxin A) [256]	extrinsic/ reversible	Rhodamine	None	Argon-ion laser	PD
	fluorescence	Covalent	Plastic	514.5 nm	Limit of 5 ng/ml
	Aqueous	None	Two-way (tapered)	550 nm	1 minute
Antibodies (Clostridium botulinum) [262]	extrinsic/ reversible	TRITC + antibotulinum antibodies	None	Argon-ion laser	PD
	fluorescence	Covalent	Fused silica	514.5 nm (?)	30 pM
	Aqueous	None	Two way (tapered)	550 nm (?)	Less than 1 minute
Antibodies (Cocaine) [196]	extrinsic/ reversible	Fluorescein+benzoyl ecgonine	None	Argon-ion laser	PD
	fluorescence	Covalent	None	514.5 nm	Limit of 5 ppb (5 ng/ml)
	Aqueous	Glass beads	Flow cell	540 nm (?)	1 minute

Analyte [Reference]	Character / Property / Sample	Reagent / Immobilization / Support	Membrane / Optical Fibre / Arrangement	Light Source / λ-Input / λ-Analysis	Detector / Dynamic Range / Response Time
Antibodies (Cocaine) [283]	extrinsic/ reversible	Fluorescein + benzoylecgonine	None	White light source	PMT
	fluorescence	Adsorbed	None	490 nm	Limit of 5 ng/ml
	Aqueous	Sepharose	None	520 nm	Rapid (approximately 12 seconds)
Antibodies (IgG) [41]	extrinsic/ irreversible	Carboxyfluorescein	None	Laser (?)	PD
	fluorescence	Covalent	Plastic	442 nm	Limit of 0.5 x 10^{-6} g/ml (3nM)
	Aqueous	None	Two-way (tapered)	530 nm	Fast
Antibodies (IgG) [134]	extrinsic/ irreversible	TRITC (Tetramethyl rhodamine isothiocyanate)	None	Argon-ion laser	PD
	fluorescence	Covalent	Plastic	514.5 nm	Limit of 66 pM or 3.3 ng
	Aqueous	None	Two-way (tapered)	572 nm	Minutes
Antibodies (IgG) [301]	extrinsic/ reversible	Eu 2-naphthoyltrifluoracetonate	None	Excimer laser	PMT
	fluorescence	Covalent	Silica (?)	308 nm	Limit of 10^{-12} M (0.1 µg/ml)
	Aqueous	None	One way	613 nm	Rapid
Antibodies (TNT) [176]	intrinsic/ reversible	Texas Red; Cy5	None	White light source	Fluorimeter
	fluorescence	Adsorption	None	583 nm	Limit of 10 ppb (5 ng/ml)
	Aqueous	Glass beads	None	607 nm	Less than 2 minutes
Antibodies (cocaine) [318]	intrinsic/ reversible	Benzoyl ecgonine + fluorescein	None	White light source	Fluorimeter
	fluorescence	Covalent	None	-	Limit of ng (pM)
	Aqueous	Sepharose beads	Flow cell	-	Less than 1 minute
Antibodies (dinitrophenol) [197]	extrinsic/ reversible	Fluorescein + Mab 51	None	White light source	Fluorimeter
	fluorescence	Covalent	None	490 nm	-
	Aqueous	None	Flow cell	520 nm	-
Antibodies (haptens) [40]	extrinsic/ irreversible	FITC	None	He-Cd laser	PMT
	fluorescence	Covalent	Silica	325 nm	Limit 25 mM to 250 mM
	Aqueous	None	Bifurcated	420 nm	5 minutes

Analyte [Reference]	Character	Reagent	Membrane	Light Source	Detector
	Property	Immobilization	Optical Fibre	λ-Input	Dynamic Range
	Sample	Support	Arrangement	λ-Analysis	Response Time
Antibodies (human chorionic gonadotrophin) [364]	intrinsic/ reversible	anti-hCG IgG + QFITC(quinolizino substituted FITC)	None	He-Ne laser	PMT
	fluorescence	Covalent	None	543.5 nm	0.83 nM
	Aqueous	Indium phosphate	Planar Waveguide	600 nm	Approximately 5 minutes
Antibodies (human serum albumin) [67]	extrinsic/ reversible	Pyridine	None	He-Cd laser	PMT
	fluorescence	Covalent	Quartz	325 nm	0.1 to 10 mg/ml
	Aqueous	None	Bifurcated	420 nm	20 to 30 minutes
Antibodies (human serum albumin) [111]	extrinsic/ irreversible	Rhodamine B isothiocyanate	None	HeNe laser	PMT
	fluorescence	Covalent	Silica (?)	543.5 nm	10^{-9} to 10^{-7} M
	Aqueous	None	Two-way (unclad)	[illegible]79 nm	8 minutes
Antibodies (phenytoin) [21]	extrinsic/ reversible	Texas Red	Dialysis	Argon-ion laser	PMT
	fluorescence	Covalent	Silica	514.5 nm	1 to 20 x 10^{-6} M
	Aqueous	Cellulose	Two-way	577 nm	20 minutes
Antibodies (pseudexin) [133]	extrinsic/ irreversible	Rhodamine	None	Argon-ion laser	PD
	fluorescence	Covalent	Plastic	514.5 nm	Limit of 10 ng/ml
	Aqueous	None	Two-way (tapered)	550 nm	2 minutes
Antibodies (synthetic peptide to represent) [77]	intrinsic/ irreversible	Tryptophan	None	Xenon white light source	PMT
	fluorescence	Covalent	Plastic	350 nm	-
	Aqueous	None	Polished one-way	550 nm	Rapid
Antigen (pseudexin) [7]	intrinsic/ reversible	TRITC (tetramethyl rhodamine isothiocyanate)	None	Argon-ion laser	PD
	fluorescence	Covalent	Silica	514.5 nm	165 pM to 33 nM
	Aqueous	None	Two-way	550 nm	Minutes
Antigen (pseudexin) [10]	intrinsic/ reversible	TRITC (tetramethyl rhodamine isothiocyanate)	None	Argon-ion laser	PD
	fluorescence	Covalent	Silica	514.5 nm	25 to 700 ng/ml
	Aqueous	None	Two-way	550 nm	Minutes
Be^{2+} [326]	extrinsic/ reversible	Morin	None	Tungsten halogen white light source	PMT
	fluorescence	Adsorption	Silica	420 nm	Limit of 10^{-6} M (9 ppb)
	Aqueous	Cellulose	Bifurcated	520 nm	1 to 2 minutes

Analyte [Reference]	Character	Reagent	Membrane	Light Source	Detector
	Property	Immobilization	Optical Fibre	λ-Input	Dynamic Range
	Sample	Support	Arrangement	λ-Analysis	Response Time
Bile acid [184]	extrinsic/ reversible	3-alpha-hydroxy steroid dehydrogenase; NADH (secondary fluorescent label)	None	Tungsten or Xenon halogen white light source	PMT
	fluorescence	Covalent	Silica	-	2 to 200 x 10^{-6} M
	Aqueous	None	Two-way	-	10 seconds
Bilirubin [92]	extrinsic/ reversible	Bilirubin	None	Argon-ion laser	PMT
	absorption	None	Quartz	457.8 nm	10 to 30 ppm (0.1 to 1.4 x 10^{-4} M)
	Aqueous	None	Two-way	457.8 nm	-
Bilirubin [127]	extrinsic/ reversible	Bilirubin	None	LED	PD
	absorption	None	Plastic	480, 860 nm	-
	In vivo	None	Trifurcated	480, 860 nm	-
CO_2 [103]	extrinsic/ reversible	Bromothymol blue; phenol red	Gas permeable	Tungsten halogen white light source	PD
	absorption	Solution	Silica; fused silica	430, 620, 750 nm	300 to 550 µatm
	Aqueous	Capillary tube	Side by side	430, 620, 750 nm	11 to 26 minutes
CO_2 [267]	extrinsic/ irreversible	Fluorescein + acrylamide; Fluorescein + 2-hydroxyethy methacrylate (HEMA); HPTS + acrylamide	Copolymer (semipermeable)	Argon-ion laser	PMT
	fluorescence	Adsorbed	Silica	488 nm	3.5 to 99 % CO_2
	Aqueous	Polymer matrix (p[illegible] method)	Two way	530 nm	30 seconds
Ca^{++} [20]	extrinsic/ irreversible	Crown ether	TEFLON	White light source (?)	?
	reflectance	Adsorption	Plastic	-	5 to 50 mM
	Aqueous	Styrene divinylbenzene	?	557 nm	10 minutes
Ca^{++} [334]	extrinsic/ reversible	Rhodamine B + lipid membrane	None	Xenon white light source	PMT
	fluorescence	Adsorption	Silica (?)	540 nm	0.1 to 10 mM
	Aqueous	Lipid membrane	Bifurcated	620 nm	Rapid
Ca^{++}/Mg^{++} [54]	extrinsic/ reversible	Crown ether 5	PTFE	Tungsten halogen white light source	PMT
	fluorescence	Covalent	Silica	358 nm	0.1 to 5 mM
	Aqueous	None	Bifurcated	420 nm	Less than 1 minute

Analyte [Reference]	Character / Property / Sample	Reagent / Immobilization / Support	Membrane / Optical Fibre / Arrangement	Light Source / λ Input / λ Analysis	Detector / Dynamic Range / Response Time
Chlorine [302]	intrinsic/ reversible	Lutetium biphthalocyanine	None	White light source	PD (avalanche)
	absorption	Adsorption	None	650, 950 nm	-
	Aqueous	Indium-tin-oxide surface	Planar waveguide	680, 950 nm	-
Chloroorganics [254]	extrinsic/ reversible	Pyridin	Aqueous impervious	White light source	PD
	fluorescence	Adsorption	Silica (?)	None	-
	Aqueous	None	Two way	600 nm	Nearly instantaneous
Co^{++}, Cr^{3+}, Fe^{2+}, Fe^{3+}, Ni^{2+}, NH_4^+ [68]	extrinsic/ reversible	Rhodamine 6G	None	Xenon white light source	PMT
	fluorescence	Entrapment	Silica	500 nm	Limit of 1×10^{-6} M
	Aqueous	Nafion film	Side by side	550 nm	Less than 1 minute
Electrolytes [220]	extrinsic/ reversible	Near-IR spectrum	None	White light source	Spectrometer
	reflectance	None	Plastic	-	Rapid
	Aqueous	None	Face to face	-	Varied per analyte
Enzymes [325]	intrinsic/ reversible	ABTS [diammonium 2, 2'-aziro-bis (3-ethylbenzo thiazolin)-6-sulphanate]	None	White light source	PMT (?)
	absorption	Covalent	None	578 nm	Limit of 8×10^{-6} M
	Aqueous	Controlled-pore glass	None	578 nm	Rapid
FITC (model analyte) [150]	intrinsic/ irreversible	FITC	None	Quartz halogen white light source	PD
	fluorescence	Adsorption	Silica (?)	485 nm	-
	Aqueous	None	One way	530 nm	-
Fluoride [272]	extrinsic/ reversible	Alizarin Fluorine Blue	None	Quartz halogen white light source	PMT
	absorption	Adsorption	Plastic	660 nm	0.16 to 0.96 mM
	Aqueous	Styrene divinylbenzene	Bifurcated	660nm	12 minutes
Fructose (model analyte) [369]	intrinsic/ reversible	Silver film	None	Tungsten halogen white light source	CCD array
	surface plasmon resonance	Evaporated	Plastic	400-900 nm	4.5×10^{-4} to 7.5×10^{-5} index of refraction units
	Aqueous	None	One way	400-900 nm	Rapid

Analyte [Reference]	Character	Reagent	Membrane	Light Source	Detector
	Property	Immobilization	Optical Fibre	λ-input	Dynamic Range
	Sample	Support	Arrangement	λ-Analysis	Response Time
Gasoline [71]	intrinsic/ reversible	None	None	LED	PD
	absorption	None	Plastic	-	-
	Liquid	None	One way	-	Rapid
Glucose [1]	extrinsic/ reversible	Bis-(2, 4, 6-trichlorophenyl) oxalate; perylene; glucose oxidase	Immunodyne	Luminescence	-
	chemiluminescence	Covalent	Silica	-	3×10^{-2} to 6×10^{-7} M
	Aqueous	Nylon	Perpendicular	-	4 to 10 seconds
Glucose [241]	extrinsic/ reversible	Fluorescein and dextran	None	Xenon white light source	PMT
	fluorescence	Solution (competing ligand)	Silica	490 nm	50 to 400 mg % glucose
	Aqueous, blood	None	Two-way	515 nm	5 to 7 minutes
Glucose [247]	extrinsic/ reversible	FITC + dextran	None	White light source	PMT
	fluorescence	Solution (competing ligand)	Silica (?)	470 nm	0.5 to 5.0 µg/ml
	Aqueous	None	Two-way	520 nm	5 minutes
Glutamine [82]	intrinsic/ reversible	Glutaminase and glutamate oxidase and luminol	None	Luminescence	PMT
	chemiluminescence	Adsorption	Silica	-	1 to 100 x 10^{-6} M
	Aqueous	Styrene divinylbenzene	Bundle	-	2 minutes
H_2O (model analyte) [337]	intrinsic/ reversible	Silver halide	None	Diode laser	Pyroelectric detector
	absorption	Doping	Polycrystalline	1.56 to 1.82 microns	-
	Aqueous	None	One way	1.56 to 1.82 microns	Rapid
H_2O (model analyte) [338]	intrinsic/ reversible	Silver halide	None	Diode laser	Pyroelectric detector
	absorption	Doping	Polycrystalline	1.56 to 1.82 microns	-
	Aqueous	None	One way	1.56 to 1.82 microns	Rapid
H_2O_2 [166]	extrinsic/ reversible	Peroxidase	Immunodyne	Luminescence	PMT (?)
	chemiluminescence	Covalent	Plastic (?)	-	0.3 x 10^{-6} to 100 x 10^{-6} M; limit of 0.05 x 10^{-6} M
	Aqueous	Glutaraldehyde	Bundle	-	30 seconds

Analyte [Reference]	Character Property Sample	Reagent Immobilization Support	Membrane Optical Fibre Arrangement	Light Source λ-Input λ-Analysis	Detector Dynamic Range Response Time
H_2O_2, ATP, NAD(P)H [94]	extrinsic/ reversible	Peroxidase, firefly luciferase, bienzyme system of marine bacteria	Immunodyne	Luminescence	PMT
	chemiluminescence bioluminescence	Adsorption	Silica (?)	As appropriate	2×10^{-8} to 1.6×10^{-6} M; 2.8×10^{-10} to 1.6×10^{-6} M; 1×10^{-9} to 3×10^{-6} M
	Aqueous	Immunodyne membrane	Bundle	As appropriate	1 minute
H_2S [243]	extrinsic/ irreversible	N, N-dimethyl-p-phenylenediamine (forms methylene blue)	None	Tungsten halogen white light source	PMT
	absorption	Adsorbed	Plastic	690 nm	0.1 to 0.7 mol/l (63 ppm limit)
	Aqueous	Cationic exchange resin	Bundle	690 nm	1 minute
H_2S [275]	extrinsic/ irreversible	Lead acetate	None	Quartz halogen white light source	PMT
	absorption	Adsorption	Plastic	580 nm	Limit of ppb (Volume to volume)
	Gaseous	Cellulose (paper)	Bifurcated	580 nm	10 seconds
HCN [33]	extrinsic/ irreversible	Pyridine, pyrimidinetrione	None	Tungsten halogen white light source	PD
	absorption	Adsorption (?)	Plastic	604, 540 nm	1 to 10 µl/l
	Gaseous	Styrene divinylbenzene	Bifurcated	604, 540 nm	1 minute
HCN [169]	extrinsic/ irreversible	4-picoline, chloramine T	None	LED	PD
	absorption	Adsorption	Silica (?)	560, 635 nm	Limit of 10×10^{-6} (v/v)
	Air	Styrene divinylbenzene	Bifurcated (?)	560, 635 nm	1 minute
HCl, NH_3 [199]	extrinsic/ reversible	Cresol Red + cryptocyanine; coumarin 540A + cresol violet + rhodamine 6G	None	N_2-pumped dye laser	PMT
	fluorescence	Adsorption	Plastic	540 nm (?)	1.8×10^{-4} mol/l; 5.6×10^{-3} mol/l
	Gaseous	?	Two-way	650 nm (?)	1 second

Analyte [Reference]	Character / Property / Sample	Reagent / Immobilization / Support	Membrane / Optical Fibre / Arrangement	Light Source / λ-Input / λ-Analysis	Detector / Dynamic Range / Response Time
Hemoglobin [253]	extrinsic/ reversible	Hemoglobin	None	Tungsten halogen white light source	Diode array
	absorption	Solution	Silica (?)	Spectra	-
	Blood	None	Two way	Spectra	30 seconds
Humidity [330]	extrinsic/ reversible	Crystal Violet + Malachite green	None	Deuterium white light source	Photodetector
	absorption	Adsorption	Quartz	400-800 nm	0-50% RH
	Gaseous	Nafion	Two way	400-800 nm	30 seconds
IgG [29]	extrinsic/ reversible	Fluorescein/Texas Red/HPTS	None	Xenon white light source	PMT (?)
	fluorescence	Adsorption	Silica	480, 570, 450 nm	500 $\times 10^{-6}$ g/ml
	Aqueous	Polymer	Two-way	520, 610, 515 nm	Slow (diffusion-limited)
Iodine [202]	intrinsic/ reversible	Polymer jacket (fibre)	None	Argon-ion laser	Diode array
	fluorescence	None	Fused silica	488 nm	Limit of 30 mTorr
	Vapour, aqueous	None	One way	605 nm	12 seconds
Ions (Al^{3+}, Cd^{2+}, ...) [329]	extrinsic/ reversible	Calcein (2', 7' -{[bis(carboxymethyl) amino] methyl}-fluorescein) or fluorexon	None	Tungsten halogen white light source	PMT
	fluorescence	Adsorbed	Silica	490 nm	-
	Aqueous	Cellulose	Bifurcated	520 nm	Rapid
K^+ [8]	extrinsic/ reversible	Crown ether	PTFE	Tungsten halogen white light source	PMT
	reflectance	Adsorption	Plastic	-	10^{-1} to 10^{-3} M
	Aqueous	Styrene divinylbenzene	Bifurcated	557 nm	5-7 minutes
K^+ [154]	extrinsic/ reversible	Nile blue and valinomycin	PVC/plastic	Tungsten halogen white light source	PMT (?)
	fluorescence	Adsorption	Silica (?)	550 nm	5 x 10^{-6} to 100 x 10^{-3} M
	Aqueous	PVC/plasticizer mixture	Bifurcated (?)	630 nm	1 minute
Liquid droplets [164]	intrinsic/ reversible	Leaky rays	None	LED or semiconductor laser	-
	absorption	None	Silica (?)	850 nm	-
	Liquid	None	Face to face (tapered or unclad)	850 nm	-

Analyte [Reference]	Character	Reagent	Membrane	Light Source	Detector
	Property	Immobilization	Optical Fibre	λ-Input	Dynamic Range
	Sample	Support	Arrangement	λ-Analysis	Response Time
Mercury [128]	extrinsic/ reversible	Mer	None	Luminescence	PMT (?)
	bioluminescence	Covalent	Silica (?)	-	-
	-	None	Bifurcated (?)	-	-
Methane [98]	intrinsic/ reversible	None	None	LED	Fabry-Perot resonato
	absorption	None	Silica	1.66 microns	Limit of 1000 ppm
	Gaseous	None	D-fibre, one way	1.66 microns	Rapid
Methane [263]	intrinsic/ reversible	Spectra	None	Semiconductor laser (?)	PD (?)
	absorption	None	Silica	1.66 microns	-
	Gaseous	None	D-shaped (polished or preform)	1.66 microns	Rapid
NADH [16]	extrinsic/ reversible	Luciferase	Gas permeable	Luminescence	PMT
	chemiluminescence	Covalent	Silica	-	40 to 190 x 10^{-6} M
	Aqueous	None	Bifurcated	550 nm	30 seconds
NADH [127]	extrinsic/ reversible	Luciferase/oxidoreductase	Polyamide	Luminescence	PMT (?)
	bioluminescence	Adsorption/covalent	Plastic (?)	-	Limit of 10 pmol (to 1 nmol)
	Aqueous	Collagen film or poly (vinyl alcohol); polyamide membrane	Bundle	490 nm	-
NH_3 [73]	intrinsic/ reversible	Bromothymol blue	None	Quartz halogen white light source	PMT
	reflectance	Adsorption	Plastic	550 nm	1.5 x 10^{-3} to 60 x 10^{-3} mol/l
	Gaseous	Hydrophilic polymer matrix	Two-way	550 nm	20 seconds
NH_3 [129]	Reversible	Oxazine perchlorate	None	LED	Phototransistor
	absorption	Spray coated	None	560 nm	Limit of 60 ppm
	Gaseous	Capillary tube	-	560 nm	Minutes
NH_3 [344]	intrinsic/ reversible	Bromocresol purple	None	Tungsten halogen white light source	PD
	absorption	Solution	Alkali borosilic	580 nm	Limit of 700 ppb
	Gaseous	Porous cladding of fibre	One way	580 nm	8 to 9 minutes

Analyte [Reference]	Character	Reagent	Membrane	Light Source	Detector
	Property	Immobilization	Optical Fibre	λ-Input	Dynamic Range
	Sample	Support	Arrangement	λ-Analysis	Response Time
NH_3, HCl [268]	intrinsic/ reversible	Thymol blue	None	Halogen white light source	Solar-cell detector
	absorption	Doped	Plastic	Spectrum	Limit of 10 ppm
	Gaseous	None	One way	Spectrum	Few minutes
NH_4^+ [311]	extrinsic/ reversible	Bromophenol blue	Gas-permeable	LED	PD
	absorption	Adsorption	Plastic	595, 660 nm	Limit of 3×10^{-6} M
	Aqueous	Gas-permeable (Teflon) membrane	Bundle	595, 660 nm	1 to 10 minutes
NH4+ [313]	extrinsic/ reversible	Chlorophenol red, bromothymol blue	gas permeable membrane	Quartz halogen white light source	PMT
	absorption	Solution	Plastic	578, 618 nm	10 to 300 $\times 10^{-5}$ M
	Aqueous	None	Bifurcated bundle	578, 618 nm	6 to 15 minutes
NO2, HCl, Cl_2 [59]	intrinsic/ reversible	Tetrphenylporphine (TPP)	None	White light souce (?)	PMT
	fluorescence	Langmuir Bldogett	Silica	440 nm	1 to 10 ppm
	Gaseous	None	None	652 nm	1 minute
NO_x [128]	extrinsic/ reversible	Aquocyancobinamide	Gas-permeable PTFE	Tungsten halogen white light source	PMT
	absorption	Solution	Silica	355, 550 nm	Limit of 5×10^{-6} M
	Gaseous	Sample well	Bifurcated	355, 550 nm	Minutes
Na^{++} [336]	extrinsic/ reversible	Rhodamine B + lipid membrane	None	Xenon white light source	PMT
	fluorescence	Adsorption	Silica (?)	540 nm	10 to 100 mM
	Aqueous	Lipid membrane	Bifurcated	620 nm	Rapid
NaOH, Cl^- [36]	extrinsic/ reversible	Bromothymol blue	Cation exchanger	White light source (?)	PMT
	absorption	Solution	Silica (?)	550 nm	4 to 50% (w/w); 10 ppm Cl^-
	Aqueous	None	Trifurcated	550 nm	25-105 seconds
Nile blue sulfate (model analyte) [266]	intrinsic/ reversible	Nile Blue sulfate salt (Nilblausulfat)	None	White light source (?)	PD (?)
	absorption	Solution	Silica	-	Limit of 0.06 g/ml
	Aqueous	None	One way, polished	-	Rapid
Nitric acid [74]	extrinsic/ reversible	Quinoxaline/quinolines	None	Xenon white light source	Diode array
	fluorescence	Covalent	Plastic	394, 420 nm	0.1 to 2 M; 2 to 10 M
	Gaseous	None	Two-way	530 nm	1 minute

Analyte [Reference]	Character / Property / Sample	Reagent / Immobilization / Support	Membrane / Optical Fibre / Arrangement	Light Source / λ-Input / λ-Analysis	Detector / Dynamic Range / Response Time
Nonpolar solvents [104]	intrinsic/ reversible	Oxazine 4 perchlorate	Polymer cladding	Tungsten halogen white light source or LED	PMT
	absorption	Solution	Plastic	500-650 nm	2×10^{-6} to 1×10^{-4} M
	Solution	Sample cell	Coiled	500-650 nm	-
Organic fluids [291]	intrinsic/ reversible	Rhodamine 6G	None	Argon-ion laser	PD
	absorption	Solution	Fused silica	514.5 nm	Limit of 10^{-3} cm-1
	Aqueous	None	One way (unclad, coiled)	514, 5 nm	Rapid
Oxygen [25]	intrinsic/ reversible	Tris (4-5-diphenyl-1, 10-phenanthroline) Ru^{++}	None	Nitrogen laser	Fluorimeter
	chemiluminescence	Entrapment	None	337 nm	0 to 160 torr
	Gaseous	Silicone films	None	610 nm	15 seconds
Oxygen [26]	extrinsic/ reversible	$Co(His)_2$	Hydrophobic	Tungsten halogen white light source	Spectrophotometer
	absorption	Capillary tube	Silica	Visible	Limit of 0.01 ppm
	Gaseous	Flow cell	Bifurcated	408, 440, 720 nm	2 minutes
Oxygen [122]	-	1, 1', 3, 3'-tetraethyl-2, 2'-bi(imidazolidium)	Teflon	Luminescence	PMT
	chemiluminescence	None	-	-	Limit of 1 ppm
	Gaseous	Sample chamber	Gas cell	-	20-24 seconds
Oxygen [178]	extrinsic/ reversible	Blood cells	None	White light source	PD
	absorption	Solution	Silica	640, 805 nm (?)	-
	In vivo	None	Side by side	640, 805 nm (?)	Rapid
Oxygen [211]	extrinsic/ reversible	Coumarin 1202	PTFE	Xenon white light source	Fluorimeter
	fluorescence	Adsorption	Plastic	-	0 to 10 %
	Gaseous	Styrene divinylbenzene	Bifurcated	-	40 seconds
Oxygen [215]	intrinsic/ reversible	9, 10-diphenyl anthracene	None	Xenon white light source	PMT
	fluorescence	Core-doped	Plastic	405 nm	-
	Gaseous	None	One way, unclad	560 nm	-

Analyte [Reference]	Character	Reagent	Membrane	Light Source	Detector
	Property	Immobilization	Optical Fibre	λ-Input	Dynamic Range
	Sample	Support	Arrangement	λ-Analysis	Response Time
Oxygen [214]	intrinsic/ reversible	9,10-diphenyl anthracene	None	Xenon white light source	PMT
	fluorescence	Core-doped	Fused silica	390 nm	Limit of 0.01 atm
	Gaseous	None	One way, coiled	430 nm	Seconds
Oxygen [309]	extrinsic/ reversible	Perylene dibutyrate	Hydrophobic, polypropylene	Deuterium lamp	PMT
	fluorescence	Adsorption	Plastic	420 nm	5 to 15 % O_2
	Blood, aqueous	Organic polymer	Side by side	500 nm	30 seconds
Oxygen [344]	extrinsic/ reversible	Pyrene + perylene	Flow cell	Xenon white light source	PMT
	fluorescence	Adsorbed	Plastic (?)	320 nm	0 to 100% Oxygen (v/v)
	Gaseous	Silicone prepolymer	Bifurcated	476 nm	1 to 2 seconds
Penicillin [76]	intrinsic/ reversible	Procion Blue MX-G	None	Quartz halogen white light source	PD
	absorption	Covalent	Silica	633 nm	0.4 to 4 mM
	Aqueous	None	One-way (polished)	633 nm	15 seconds
Penicillin [132]	-	Penicillinase	None	None	Electrode
	H^+ ions	Covalent	None	-	5×10^{-3} to 2.5×10^{-5} M
	Aqueous	Flow cell	None	-	1 to 3 minutes
Penicillin [161]	extrinsic/ reversible	Penicillinase + FITC	None	White light source (?)	Diode array
	fluorescence	Covalent	Silica (?)	490 nm (?)	1 to 10 mM
	Aqueous	Dextran	Bifurcated	520 nm (?)	1 minute
Penicillin [194]	extrinsic/ reversible	Fluoresceinamine + penicillinase	None	Tungsten halogen white light source	PMT
	fluorescence	Entrapment	Silica	490 nm (?)	0.00025 to 0.01 M
	Aqueous	Polyacrylamide membrane	Two-way	520 nm (?)	40 to 60 seconds
Penicillin [249]	-	Penicillinase	None	None	None
	H^+ release	Covalent	None	None	2 to 12 mM
	Aqueous, broth, milk	Glutaraldehyde	Electrode	None	10 seconds
Penicillin [277]	-	Penicillinase	None	None	None
	H^+ release	Covalent	None	None	Limit of 5 mM
	Aqueous, broth	None	Electrode	None	10 seconds

Analyte [Reference]	Character	Reagent	Membrane	Light Source	Detector
	Property	Immobilization	Optical Fibre	λ-Input	Dynamic Range
	Sample	Support	Arrangement	λ-Analysis	Response Time
Penicillin [443]	-	Polypyrrole + penicillinase	None	None	None
	H^+ ions	Adsorption	None	None	Limit of 4 mM
	Aqueous	Glutaraldehyde	ISFET	None	1 minute
Penicillin; glucose [193]	extrinsic/ reversible	Fluorescein +penicillinase/glucose oxidase	None	Tungsten halogen white light source	PMT
	fluorescence	Entrapment	Silica	490 nm (?)	0.1 to 100 mM
	Aqueous	Polyacrylamide membrane	Two-way	520 nm (?)	40 to 60 seconds; 5 to 12 minutes
Polar solvents (dioxan, ethanol...) [306]	extrinsic/ reversible	Thermal printer paper reagent	None	Tungsten halogen white light source	PMT
	absorption	Physical	Plastic	580 nm	Limits of 10 ppm to 600 ppm (depending on analyte)
	Gaseous	None	Bifurcated	580 nm	30 seconds
Polyethylamine (model analyte) [86]	extrinsic/ reversible	dextran+FITC; polyethyleneimine + fluorescein, RITC, Texas Red	Dialysis	Tungsten halogen white light source	PMT
	fluorescence	Solution	Silica (?)	493 nm	3.0 mM to 1.0 M
	Aqueous	None	Bifurcated	520, 620 nm	5 minutes
Polynuclear aromatic hydrocarbons [247]	extrinsic/ reversible	Benzo(a)pyrene	None	N_2-laser	PD array
	fluorescence	Solution	Quartz (or plastic)	337 nm	Limit of 0.01 µg/l
	Aqueous	None	Side by side	385 nm	Rapid
Propane [322]	intrinsic/ reversible	Fluoride	Teflon cladding	Tungsten halogen white light source	Photoconductive detector
	absorption	Doping	Silica	3.36 microns	Low to 100 % propane
	Gaseous	None	One way	3.36 microns	2 minutes (down to 45 seconds)
SF_6 [198]	intrinsic/ reversible	2,5-bis[5-tert-butyl-2-benzoxyazolyl] thiophene (BBOT)	None	Xenon white light source	Optical power meter
	fluorescence	Doping	Plastic	429 nm	-
	Gaseous	None	One-way	520 nm	Rapid
SO_2 [347]	extrinsic/ reversible	Pyrene + perylene	Flow cell	Xenon white light source	PMT
	fluorescence	Adsorbed	Plastic (?)	333 nm	0 to 100% SO_2 (v/v)
	Gaseous	Silicone prepolymer	Bifurcated	470 nm	1 to 2 seconds

Analyte [Reference]	Character	Reagent	Membrane	Light Source	Detector
	Property	Immobilization	Optical Fibre	λ-Input	Dynamic Range
	Sample	Support	Arrangement	λ-Analysis	Response Time
Solids: salicylic acid, acetyl salicylic acid [24]	extrinsic/ reversible	None	None	Xenon white light source	Fluorimeter
	fluorescence	None	Fused-silica	305 - 505 nm	0.3 to 200 ng
	Solid	Iron or filter paper	Bifurcated	As appropriate	Rapid
Solvents [183]	extrinsic/ reversible	2, 5-bis-[3-(5-sulfo-2, 3-dihydro-1H-indol-7-yl)-2-propenylidene]-cyclopene	Mylar	Tungsten halogen white light source	Fluorimeter
	fluorescence	Adsorbed	None	500 nm	80 to 100 % ethanol
	Solution	Cellulose	Flow cell	620 nm	15 seconds
Stearic acid (model analyte) [149]	intrinsic/ irreversible	Stearic acid	None	Nitrogen laser	PMT
	fluorescence	Covalent	Silica	377 nm	-
	Aqueous	None	One-way	485 nm	1 minute
Temperature [15]	intrinsic/ reversible	Neodymium	None	LED	PD
	absorption	Doped in core	Silica	850 nm (peak)	+5 to -40 °C
	Air	None	Two-way	830 nm, 860 nm	Minutes
Temperature [37]	intrinsic/ reversible	Aluminium-coating	None	LED	PD (?)
	reflectance	Sputtering	Silica (?)	850 nm (peak)	20 - 400 °C
	Air	None	Trifurcated	850 nm	Fast
Temperature [38]	intrinsic/ reversible	Heavy-metal, fluoride	None	Argon-ion laser or semiconductor	PD
	fluorescence	Doping	Silica	488, 972 nm	25 to 150 °C
	Air	None	Bifurcated	520 nm (?)	Rapid
Temperature [124]	intrinsic/ reversible	None	None	Semiconductor laser	PD (?)
	absorption	None	Silica	816 nm	5 to 80 °C
	Air	None	Interferometer	816 nm	2-8 seconds
Temperature [139]	intrinsic/ reversible	Neodymium	None	LED	PD
	fluorescence	Doping	Silica	810 nm (peak)	15 to 130 °C
	Air	None	One way	1.05 microns	Rapid
Temperature [384]	intrinsic/ reversible	Nd^{3+}, Pr^{3+}, Sm^{3+}, Yb^{3+}	None	White light source	PD
	absorption	Doping	Silica	600 to 1100 nm	0 to 100 °C; ± 1 °C
	Air	None	One way	600 to 1100 nm	Rapid

Analyte [Reference]	Character	Reagent	Membrane	Light Source	Detector
	Property	Immobilization	Optical Fibre	λ-Input	Dynamic Range
	Sample	Support	Arrangement	λ-Analysis	Response Time
Temperature [369]	intrinsic/ reversible	Mineral oil	None	LED	PD?
	absorption	Solution	Plastic	850 nm	0 to 100 °C ± 1°C
	Air	Glass tube	One way (de-clad)	850 nm	Rapid
Temperature, strain [118]	intrinsic/ reversible	None	None	HeNe laser (?)	PD
	absorption	None	Silica	633 nm	-
	Air	None	Bow-tie or elliptical core, one-way	633 nm	-
Terbutyn (pesticide) [44]	extrinsic/ reversible	FITC	None	Xenon white light source	PMT
	fluorescence	Covalent	Silica	480 nm	0.5 to 2.5 x 10^{-6} g/ml
	Aqueous	None	Two-way	520 nm	10 minutes
Toluene, xylene, etc [87]	extrinsic/ reversible	UV spectrum	None	N_2-pumped dye laser; Nd:YAG laser	PMT
	fluorescence	None	Fused silica	266 nm	Limit of ppb
	Aqueous	None	Bifurcated	as appropriate	Rapid
Toluene, xylene, etc [86]	extrinsic/ reversible	UV spectrum	None	Nd:YAG laser	PMT
	fluorescence	None	Fused silica	266 nm	Limit of ppb
	Aqueous	None	Bifurcated	as appropriate	Rapid
Toluene, xylene, gasoline [78]	intrinsic/ reversible	Aluminium coating	None	LEDs and white light source	-
	reflectance	Vacuum-deposited	Plastic	-	2%
	Gaseous	None	Side by side	-	Minutes
Trichloroethylene, chloroform [13]	extrinsic/ reversible	Pyridine	Porous TEFLON	Tungsten halogen white light source	PD
	absorption	Solution	Silica (?)	-	10 to 500 ppm TCE
	Gaseous	None	Side by side	540 nm, 640 nm	30 minutes
Urea [255]	-	Ammonium ion	Dried glutaraldehyde + BSA	None	None
	H+ ions	Adsorption	None	None	10^{-2} to 10^{-4} M
	Aqueous	Glutaraldehyde	ISFET	None	Rapid

Analyte [Reference]	Character	Reagent	Membrane	Light Source	Detector
	Property	Immobilization	Optical Fibre	λ-Input	Dynamic Range
	Sample	Support	Arrangement	λ-Analysis	Response Time
Urea [3,14]	extrinsic/ reversible	Urease + 2', 7'-bis (carboxyethyl)-5 and 6)-carboxyfluorescein + 5 (and 6)-carboxyfluorescein	None	Tungsten halogen white light source	PMT
	fluorescence	Adsorbed	Silica	490 nm	13 to 85 x 10^{-6} M
	Aqueous	Teflon membrane (glutaraldehyde)	Bifurcated bundle	520 nm	1 to 7 minutes
p-nitrophenoxide [17]	extrinsic/ reversible	alkaline phosphotase	Nylon mesh	Quartz halogen white light source	PMT
	absorption	Covalent	Silica	?	1 to 2 x 10^{-5} M
	Aqueous	Nylon mesh	Bifurcated	?	?
pH [3]	extrinsic/ reversible	Acroyloyl-fluorescein	None	White light source	PMT
	fluorescence	Covalent	Silica	430, 485 nm	4.5 to 8.0 pH: ± 0.3 pH units
	Broth (fermentation)	HEMA (poly hydroxy ethyl methacrylate)	Two-way	530 nm	seconds
pH [5]	extrinsic/ reversible	Bromothymol blue	PTFE	Tungsten halogen white light source	PMT
	reflectance	Adsorption	Plastic	-	7 to 9 pH
	Aqueous	Styrene divinylbenzene	Bifurcated	580 nm	5 minutes
pH [22]	extrinsic/ reversible	Bromothymol blue, phenol red, chlorophenol red, phenol red, alizarin	None	LED	PD (?)
	fluorescence	Adsorption	Silica (?)	443, 570 nm	6.6 to 9.7 pH units
	Aqueous	Styrene divinylbenzene	Two-way	Varied	Rapid
pH [24]	extrinsic/ reversible	Various	None	LEDs	PMT
	fluorescence absorption	Covalent	Silica	Various	5 to 10 pH units
	Aqueous	None	Trifurcated	Various	10 minutes
pH [25]	intrinsic/ reversible	Fluorescein	None	Laser (Argon-ion ?)	PMT (?)
	fluorescence	Covalent	Silica	480 nm	Limit of 0.008 pH units
	Aqueous	None	Two-way	520 nm	Less than 9 seconds

Analyte [Reference]	Character / Property / Sample	Reagent / Immobilization / Support	Membrane / Optical Fibre / Arrangement	Light Source / λ-Input / λ-Analysis	Detector / Dynamic Range / Response Time
pH [32]	extrinsic/ reversible	Phenol Red	None	LED	PD
	absorption	Adsorption	Silica	565 nm	7 to 9 pH units, ± 0.05 pH units
	Aqueous	None	Two-way	565 nm	Fast
pH [52]	extrinsic/ reversible	3, 4, 5, 6 tetra bromophenolsulphon phthalein, ...	None	LED	PD
	absorption	Covalent	Plastic	580, 850 nm	±0.05 pH units
	Aqueous	Styrene divinylbenzene	10 fibre bundle	580, 850 nm	Rapid
pH [60]	extrinsic/ reversible	Thymol blue, neutral red, methyl red, ...	None	Quartz halogen white light source	PD
	absorption reflectance	Covalent	Silica	As appropriate	5.5 to 8.5 pH units
	Aqueous	None	Two-way	555, 600, 535 nm,	Minutes
pH [61]	extrinsic/ reversible	Thymol blue, Bromophenol blue	None	Quartz halogen white light source	PMT/PD
	absorption	Adsorption	Plastic	-	0.8 to 3.2, 10-13 pH units; 3.2 to 7 pH units
	Aqueous	Styrene divinylbenzene	Side by side	555, 600 nm	1 minute
pH [106]	intrinsic/ reversible	Bromocresol purple, bromocresol green	None	Xenon white light source	PD
	absorption	Sol-gel	Silica + sodium	610 nm	3.8 to 5.4; 5.2 to 6.8 pH units
	Aqueous	None	End to end	610 nm	5 seconds
pH [123]	extrinsic/ reversible	FITC	-	Argon-ion laser	PMT (out); PD (in)
	fluorescence	Covalent	Fused silica	488 nm	3 to 7 pH units
	Aqueous	Silica bead	Two-way	520 nm (?)	20-35 seconds
pH [134]	intrinsic/ reversible	FITC	None	White light source	PMT
	fluorescence	Sol-gel	Plastic (?)	488 nm	5 to 9 pH units
	Aqueous	None	Bundle	524 nm (?)	-
pH [148]	extrinsic/ reversible	Bromothymol Blue	None	LED	PD
	fluorescence	Solution	Plastic (?)	-	5 to 10 pH units
	Aqueous	None	Bundle	-	Rapid

Analyte [Reference]	Character	Reagent	Membrane	Light Source	Detector
	Property	Immobilization	Optical Fibre	λ-Input	Dynamic Range
	Sample	Support	Arrangement	λ-Analysis	Response Time
pH [172]	extrinsic/ reversible	Congo Red	None	LED	Photometer
	absorption	Adsorbed	Plastic	565, 635 nm	0.0 to 4.2 pH units
	Aqueous	Cellulose	Side by side	565, 635 nm	Seconds
pH [174]	extrinsic/ reversible	Eosin, phenol red	None	Argon-ion laser	PMT
	fluorescence	Covalent	Silica	488 nm	Limit of 0.01 pH units; range from 4.49 to 8.6
	Aqueous	None	Side by side	546 nm	4 seconds
pH [183]	extrinsic/ reversible	Bromothymol blue	PTFE	Tungsten halogen white light source	PMT
	absorption	Adsorbed	Plastic	593 nm	8.0 to 10.5 pH units
	Aqueous	Styrene divinylbenzene	Bundle	593 nm	5 minutes
pH [234]	extrinsic/ irreversible	8-hydroxypyrene-1, 3, 6 trisulphonic acid (HPTS); HPTS + sulforhodamine 640	Parafilm	Xenon white light source	PMT
	fluorescence	Entrapment	Silica	405, 450; 488	5.5 to 8.0 pH units
	Aqueous	Ethylene-vinyl acetate	Two-way	515; 530, 610	Rapid
pH [236]	intrinsic/ reversible	Fluorescein	None	Argon-ion laser	PMT
	fluorescence	Entrapment	Plastic	488 nm	3.5 to 6.5 pH units
	Aqueous	Sol-gel	Two-way	530 nm	5 seconds
pH [257]	extrinsic/ reversible	Phenol red	Cuprophan	White light source	PMT (?)
	absorption	Entrapment	Silica (?)	433, 558 nm	6 to 9 pH units
	Aqueous	Styrene divinylbenzene	Two way	433, 558 nm	-
pH [244]	extrinsic/ reversible	Fluoresceinamine	None	Argon-ion laser	PMT
	fluorescence	Adsorbed	Silica	488 nm	4.0 to 8.0 pH units
	Aqueous	Acrylamide copolymer	Two way	530 nm	9 seconds
pH [251]	extrinsic/ reversible	1-hydroxypyrene-3, 6, 8-trisulphonate (HPTS); 7-hydroxycoumarin-3-carboxylic acid (HCC)	None	Xenon white light source	PMT
	fluorescence	Adsorption	Quartz	410; 465 nm	6.4 to 7.7 pH units; ±0.01 pH units
	Aqueous	Glass	Bifurcated	455; 520 nm	1 minute

Analyte [Reference]	Character	Reagent	Membrane	Light Source	Detector
	Property	Immobilization	Optical Fibre	λ-Input	Dynamic Range
	Sample	Support	Arrangement	λ-Analysis	Response Time
pH [299]	extrinsic/ reversible	Phenol red	Hydrophilic gel (microspheres, polyacryl	Tungsten halogen white light source	PD
	absorption	Adsorption	Plastic	560, 600 nm	7.0 to 7.4 ± 0.01 pH units
	Aqueous	Cellulose	Two way	560, 600 nm	Approximately 40 seconds
pH [306]	extrinsic/ reversible	FITC, eosin	None	Tungsten halogen white light source	PMT (?)
	fluorescence	Adsorbed	Plastic	495; 520 nm	0 to 7 pH units
	Aqueous	Cellulose	Bifurcated	530; 550 nm	20 seconds
pH [307]	intrinsic/ reversible	Rhodamine 6G, hydroxy pyrenetrisulphonic trisodium salt (HPTS)	None	Argon-ion laser	PMT
	reflectance	Solution	Silica	514.5 nm	-
	Aqueous	None	Two way (polished)	As appropriate	-
pH [319]	extrinsic/ reversible	Bromothymol blue	None	He-Ne laser	PMT
	absorption	Covalent	Plastic	632.8 nm	4 to 11 pH units
	Aqueous	None	Side by side (twisted)	632. 8 nm	Rapid
pH [327]	extrinsic/ reversible	Fluoresceinamine	None	Tungsten halogen white light source	PMT
	fluorescence	Adsorbed	Silica	480 nm	3 to 6 pH units
	Aqueous	Cellulose	Two-way	520 nm	15 to 30 seconds

Appendix II

Glossary

Acid — In general, an acid is a hydrogen-containing species which dissociates in solution in water to produce one or more hydrogen ions. Even more broadly speaking, an acid can be any compound which can furnish a proton or can attach itself to an unshared pair of electrons. For example, liquid ammonia is a nonaqueous system with an acid-base reaction where ammonia has the unshared pair of electrons (functioning as a base) and ammonium ions are readily formed (acid).

Acid-base indicator — a substance, either a weak acid or base, which has a different colour in acid or base solution. The colour change is due to a marked difference in colour between the undissociated and ionic forms.

Active site — portion of the coenzyme that does the catalytic work

Adsorption, physical — The surface of a solid or liquid is a seat of free energy. The process of adsorption in which foreign atoms or molecules become attached to the surface lowers the free energy of the surface. Many adsorption processes are not chemically specific and are readily reversible. The forces of attraction between the adsorbate and adsorbent are weak and similar in nature to those responsible for the cohesion of molecules in the liquid state, Van der Waals' forces. Physical adsorption often involves the formation of multiple layers at the adsorbent surface, weakly bound.

Affinity — the strength of binding between a given antibody and a single antigenic determinant or monovalent hapten. This depends on the area of contact, closeness of fit, and the nature of intermolecular forces involved.

Aldehyde — A group at a terminal end of an organic molecule with the following structure:

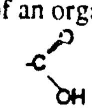

Aliquot — An exact volume of solution.

Amphoteric (or amphiprotic) — Able to function both as an acid (produce protons) and as a base (react with protons).

Analyte — Substance under analysis.

Anion — Negatively charged chemical species (ions); an atom which has gained one or more electrons or a negatively charged group of atoms.

Antibodies — Protein molecules present in the serum which are formed in the body in response to the presence of foreign substances called antigens. For each antigen there is a specific antibody. The effect is to agglutinate or precipitate the antigens. The antibody-antigen mechanism is the basis of the immune response.

Antigens — Macromolecular proteins which, when injected into the blood of an animal, stimulate the production of antibodies (neutralising proteins) - bacteria, viruses (living or not) foodstuffs, pollen, proteins, some polysaccharides, or nucleic acids.

Aqueous — Dissolved in water.

Aromatic ring — Carbon ring in which the carbon atoms are arranged in loops, with double and single bonds alternating: frequently depicted as a regular hexagon. Aromatic refers to the fact that several compounds of this type are fragrant (for example, naphthalene).

Aryl hydrogen — Hydrogen directly bonded to an aromatic ring.

Avidin — MW approximately 68000. A protein tetramer (four identical subunits) found in albumin (egg white); each of its four portions can bind, non-covalently, with one biotin in what is considered to be one of Nature's most tenacious bonds.

Avidity — a measure of the stability of the antibody-antigen complex formed when multivalent antigen and homologous antiserum are mixed. This depends not only on the affinity of the individual determinant-combining site bonds but also on the number of satisfied valencies of the antigens and

	antibodies (i.e., two antigens bound to two antibodies is more stable than two antigens bound to one antibody).
Base	A substance with a tendency to gain protons. For ionised solvents which do not contain protons a base is a substance which reacts with the acid of that system to produce a salt and the solvent. (see acid for comparison)
Beer's law	The proportion of radiation adsorbed depends on the thickness of the adsorbing layer, and on the molecular concentration of the absorbing substance in the layer.
Biotin	One of the vitamin-B factors. Biotin is present in yeast, egg yolk, liver and other tissues. Egg white contains a specific protein, avidin, that combines with biotin and effectively prevents its action. The avidin-biotin bond is the strongest known non-covalent chemical bond.
Bridging system	a system that connects two compounds in chain (i.e., enzyme-metal ion-substrate; the metal ion acts as the bridging system)
Buffer solutions	solutions that contain both acid and base and can respond to the addition of either, in an attempt to maintain a constant pH.
Carboxyl group	the chemical group COOH.
Cation	Positively charged chemical species (ions). The positive charge comes from the loss of one or more electrons or positively charged group of atoms.
Chaotropic agent	a substance that enhances the partitioning of nonpolar molecules from a nonaqueous (bound) to an aqueous phase (in solution) as a result of the disruptive effect that the substance has on the structure of water: such agents are used to solubilise bound proteins.
Chemiluminescence	The emission of light during a chemical reaction. The light emitted by the firefly or glow-worm, as well as luminous combustion, are examples of this very common phenomenon.
Chemiadsorption	The adsorption of a substance at a surface involving the formation of chemical bonds between the adsorbate, the

species undergoing adsorption, and the adsorbent, the surface at which adsorption is occurring.

Coenzyme	cofactor based on organic species.
Cofactor	nonprotein group in an enzyme. This group allows the characteristic catalytic activity to take place. (The apoenzyme is the whole protein portion.) A cofactor can be organic (coenzyme) or a metal ion (metal-ion activator).
Concentration	The amount of substance in a given volume of solution.
Conjugated	process of covalently binding two or more species of molecule to form a hybrid molecule (conjugate), i.e., a dye conjugated directly to a protein (as in fluorescein-conjugated penicillinase).
Covalent bond	The linkage of two atoms by the sharing of two electrons, one contributed by each of the atoms.
Debye-Huckel theory	The activity coefficient of an electrolyte depends markedly upon concentration.
Deprotonation	subtraction of the hydrogen ion.
Dimer	a compound composed of two specified atoms or molecules.
Dipole moment	In a heteronuclear diatomic molecule, because of the difference in electronegativities of the two atoms, one atom acquires a small positive charge and the other a small negative charge. The molecule is then said to have a dipole moment whose magnitude is the product of the charge and the distance between the charges. With polyatomic molecules the net dipole moment is the vector sum of the dipole moments of the individual bonds within the molecule.
Dissocation	The process whereby a molecule is split into smaller fragments, atoms, free radicals or ions. The extent of dissociation is measured by the dissociation constant, K.
Dithio	two consecutive sulphur atoms: -S-S
Dosage level (dose)	the amount delivered over time to a specific area or volume.

Ellman's reagent	5,5'-dithiobis(2-nitrobenzoic acid); a reagent for the determination of sulph-hydryl groups in proteins
ELISA	Enzyme-linked immunosorbent assay. Usually has a protein-based standard that is compared to an unknown protein sample. The standard may be one of many well-described systems, such as bovine serum albumin or cysteine. The assay can be combined with an indicator dye, a clear (optically) microtiter plate (with many wells), and an optical density reader of some sort.
Enteropathogenic	pathogenic for the intestine (i.e., live cholera toxin, which acts on the intestinal mucosa).
Enzyme	Proteins which catalyse reactions with a high degree of specificity and efficiency. Enzymes are present in all living organisms and are responsible for catalysing most of the reactions which take place in a cell. One outstanding feature of enzymes is that many of them are highly specific. Urease is an enzyme which approaches absolute efficiency.
Erichrome Black T	A useful complexometric reagent for Ca^{2+} and Mg^{2+} (used for determining water hardness). It has three acid sites, two of which are involved in colour changes.
Fermentation	any of a wide range of processes carried out by microorganisms, regardless of the type of metabolism conducted.
Fluoresccin	an indicator dye: in alkaline solution it shows intense green fluorescence.
Fluorescence	The process of energy emission following absorption of electromagenetic radiation. Part of the energy thus absorbed is re-emitted as radiation of longer wavelength.
Glacial acetic acid	Pure acetic acid (17.4 M).
Hardness of water	The property conferred on water by the presence of alkaline earth salts which prevent formation of a lather with soaps. Often mainly a measure of calcium and magnesium concentration: calcium and magnesium hydrogen carbonates are temporary, calcium and magnesium salts are more permanent.

Homologous derived from or associated with the same species as that being referred to (i.e., antibody elicited by a given antigen).

Hydrolysis splitting of a bond with water (e.g.,a hydroxyl ion becomes attached to a metal ion).

Hydroxyl the univalent radical or group, OH.

Indicator any of various substances that indicate a presence, absence or concentration of a substance by means of a characteristic change (usually colour).

In vivo processes carried out in the living organism.

Ionic a substance that is electrically charged by the local loss of one or more electrons (see polar).

Isothiocyanates derivatives of the type R-NCS.

Labile complex A complex which participates in very fast reactions, particularly ligand exchange reactions, generally within the time of mixing.

Luciferins Substances responsible for bioluminescence.

Mercapton An organic compound with following structure:

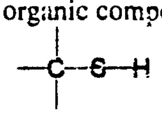

Methylene blue Basic Blue 4. An important dyestuff of considerable value as a staining agent in bacteriological work and microscopy.

Miscibility The degree to which two liquids combine to form one liquid phase. If, for example, toluene and benzene are combined, the mixture appears as one liquid phase: the two liquids are considered completely miscible. Immiscible liquids form completely separable liquid phases. Partially miscible liquids are between the two extremes: some dissolution is possible, but beyond this point immiscible layers are again formed.

Moiety one of two parts (usually describing a molecule).

Nicotinamide adenide dinucleotide (NAD) — an extremely important and widespread coenzyme, which functions as a hydrogen transfer agent; the reduced form of the coenzyme is often represented as NADH.

Organic compound — chemical compound formed from carbon.

Organochloride — an organic compound that contains one or more chlorines.

Organofunctional — carbon-based groups which participate in compound-forming macro-molecular reactions (i.e., linking polymers).

Phenol — any of a class of organic compounds whose molecules contain one or more hydroxyl groups bound directly to a carbon atom in an aromatic ring.

Photochemistry — the investigation of biochemical reactions brought about by the action of light. Only light which is absorbed by the system will produce chemical effects. Absorption of the light is a quantum process. The primary step in a photochemical reaction is therefore the absorption of a quantum of light energy by a particular atom, molecule or ion which is thereby raised to an excited state containing an excess quantum of energy equal to $h\ v$ (where h is Planck's constant and v is the frequency of light absorbed). Only electronic excitation can bring about chemical reaction; energy in or above the far infra red is ineffective. An excited molecule may return to its ground state within about 10^{-9} seconds while emitting its absorbed energy as fluorescence; in this case no photochemical reaction is produced. The quantum yield, i.e. the number of molecules which are caused to react for a single quantum of light absorbed, is only exceptionally equal to exactly unity.

pK — K represents the dissociaton rate of a given substance; i.e., acetic acid molecules and acetate ions: $\frac{[H^+][C_2H_3O_2^-]}{[HC_2H_3O_2^-]} = K = pH = pK - \log \frac{[HC_2H_3O_2]}{[C_2H_3O_2^-]}$ It is this last term that can cause the pH reading to be inaccurate if the concentration of an ion other than hydroxyl is measured.

Polar — (a molecule) having an uneven distribution of electrons and thus a permanent dipole moment.

Proteins	The proteins are the chief nitrogenous constituents of living organisms. They contain about 50% carbon, about 25% oxygen, about 15% nitrogen, about 7% hydrogen, and some sulphur. They give certain colour reactions which are caused by the presence of specific amino acids in the molecule. There are many different protein classes (which are not mutually exclusive). Proteins in general may contain more than one peptide chain. The three-dimensional arrangement of peptides is very important in determining the properties of the protein. Proteins typically have large molecular weights, ranging from 5000 to 6 000 000.
Reagent	any substance used in a chemical reaction to detect or measure other substances.
Sandwich assay	an indirect immunofluorescence technique: the antigen being sought is placed in contact with a surface of immobilised antibodies; the system is reacted and then unbound antigen is rinsed. Another solution of fluorescently labelied antibody is added, which will only bind if the antigen is present. The antigen is 'sandwiched' between labelled and unlabelled antibody.
Schiff's base	a base or reagent that attaches to (and often colours) aldehyde-containing compounds.
Sephadex	A gel produced by cross-linking dextran fractions with epichlorhydrin and marketed in bead form. Various types are available differing in pore size and other characteristic: if the matrix is a minor component, fractionalisation of high molecular weight substances occurs; if denser gels are used, then the low-molecular weight compounds are separated.
Silanisation/silylation	Silanising involves converting a silanol group SiH_3-OH to a less polar silyl ether, SiH_3-OR; silylation involves introducing a trimethylsilyl group, Si $(CH_3)_3$ into an organic compound.
Sol-gel	a chemical process in which a single or multi-component solution undergoes gelation (colloid of a more solid form) to form a coherent rigid network of the oxides present.
Solution	The qualitative characteristics of a solution are homogeneity, and the absence of any tendency for the

dissolved substance to settle out again. A solution is better defined as a homogeneous mixture of substances which is separable into its components by altering the state of one of them and whose properties vary continuously with the proportions of the components between certain limits. The amount of a substance dissolved in a given amount of another substance is described as the concentration of the solution, and may be expressed in grams per liter, or as mole fraction (i.e., molarity). A solution containing only a small proportion of the dissolved substance is termed dilute; one containing a high proportion is called concentrated.

Solvent — a substance capable of dissolving another substance. This is the substance that makes up the bulk of the solution. The substance dissolved in the solvent is termed the solute.

Spectrophotometer — An instrument that measures the relation between absorption of electromagnetic radiation and frequency (or wavelength) of that radiation.

Substrate — the compound whose reaction an enzyme catalyses (i.e., peptidase is a general enzyme for some reaction of a peptide).

Thymol blue — Thymolsulphonphthalein. One of the sulphonphthalein group of indicators, which two useful pH ranges.

Titration — the process of determining the concentration of a substance in solution by adding to it a standard reagent of known concentration in carefully measured amounts until a reaction of definite and known proportion is completed and then calculating the unknown concentration.

Titer — In blood analysis, a titration procedure is used to determine the strength of an antibody. Doubling dilutions (i.e. 1:50, 1:100, 1:200, and so on) are made in a suitable medium (viral transport medium, alkaline buffer, etc.) in a series of tubes. The appropriate antigen is added. and the reactions are read though agglutination, ELISA, or other means and scored for the degree of positivity. The actual titer (concentration) of the antibody is given by the dilution at which some degree of agglutination (or determining reaction), however weak, can still be seen (extracted from the noise level

Town gas	the general name for manufactured gas with a specific calorific value, typically used as a gaseous fuel. In many parts of the world natural gas is used, which has in general more than 50% hydrogen, 10-30% methane, as well as CO, higher hydrocarbons, CO_2 and N_2.
Van der Waals forces (and equation)	Weak forces of inter- and intra-molecular attraction (and repulsion). If these are considered in the equation of state for gases (pressure, volume, and temperature considerations), the volume occupied by the molecules and the attractive forces between the molecules are accounted for. Van der Waal' forces are stronger in liquids than in gases. The equation of state, for gases, is

$$\left(P + \frac{a}{V^2}\right)(V - b) = RT \qquad (2)$$

a = attractive forces between molecules

b = effective volume in one mole of gas

R = universal gas constant

Vicinal diol	vicinal refers to two substituents on adjacent carbon atoms (neighbouring positions of radicals, i.e., 1, 2, 3 positions of benzene ring; diol indicates hydroxyl (-OH) groups.
Viscosity	A liquid's resistance to change of form; a type of internal friction.
Volatile	evaporating rapidly; e.g. some volatile, poisonous substances that form vapours, such as chloral, chloroform, ether, etc.
Xanthene dye	any various brilliant fluorescent yellow to pink to bluish red dyes characterised by the heterocyclic compound $C_{13}H_{10}O$.

Appendix III

Details of chemical protocols

A. Initial penicillinase preparation

1. 10 mg dry penicillinase [Type 1: from Bacillus cereus; Sigma Chemical Company, product number P 0389] is dissolved in 1.5 ml nanopure water (stirred in vortex mixer) and then desalted with 0.2 M sodium phosphate buffer pH=8.2 (discard eluate). The 0.2 M phosphate buffer is prepared by mixing thoroughly 48 mls 0.2M Na_2HPO_4 and 2 mls 0.2M NaH_2PO_4 [360].

(Sigma recommends the optimal binding pH range for FITC (fluorescein isothiocyanate) onto penicillinase as 8.5 <pH < 9.0 [171,400].)

Penicillinase is sold in units (defined as the amount it takes to interact with 1 micromole of penicillin); 25000 units equates to approximately 10 mg of benzylpenicillinase [assay not performed by Sigma]. Benzylpenicillin (or Penicillin-G) is produced naturally.

2. A two-way adjustable valve burette dropper is added to the bottom [thereby allowing control of flow of sample] of a disposable Sephadex G-25M column (PD-10 from Pharmacia)

Remove cap of column

Discard excess liquid [be sure to leave enough fluid to keep bed moist and undisturbed]

Secure in burette holder

Cut off bottom tip of column

Equilibrate column with 0.2 M sodium phosphate buffer pH=8.2 and discard the eluate

3. Add penicillinase eluent (2.5 ml) and collect the eluate in 0.5 ml increments in labeled Eppendorf tubes. Once the penicillinase solution has entered the column, 3.5 mls 0.2M phosphate buffer pH=8.2 is added.

4. Store collected samples in refrigerator at 4° C.

B. Eluate total protein quantification

1. Prepare 15 standard serial dilutions of two of BSA (bovine serum albumin), starting at 2.5 mg/ml, to which a corresponding optical density can be determined. See Figure 1. 160µl of each standard solution is placed in triplicate in a 96-well microtiter plate

2. For evaluation of the unknown protein, place 160µl of 0.2 M phosphate buffer pH=8.2 in three wells (control), 150µl of 0.2 M phosphate buffer pH=8.2 in 15 sets of triplicates with 10 µl of eluted samples, and lastly 160µl of 0.2 M phosphate buffer in last three wells of the microtiter plate (control). Add 40µl of Bio-Rad protein assay dye reagent concentrate to all wells.

3. The Bio-Rad Protein assay is based on the observation that the absorption maximum for an acidic solution of Coomassie Brilliant Blue G-250 shifts from 465nm to 595nm when binding to protein occurs. A maximum signal appears where the maximum amount of protein is found. By using a grid such as the 96 well microtiter plate, the levels determined through the assay can be correlated to original sample vials, and thereby the highest levels of protein pinpointed.

4. The painstakingly filled microtiter plate should be read at 595nm for the Bio-Rad Protein assay, but the Titertex Multiscan has 620nm as the closest available wavelength. (It is also wise to avoid being near the excitation wavelength of the fluorescent label)

Turn machine on (switch on right side)

Enter date: DDMMYY

Enter mode: 1 (for absorption at 1 line)

Enter filter: 7 (for 620nm line)

Next comes a query regarding the location of a cell for'blanking' (baselining); simply press 'Enter'

The machine will display 'In"

Place an EMPTY microtiter plate in the tray of the machine

Press 'Step"

The machine will pull the tray in and read it.

It will prompt you with 'Blank'.

Press 'Blank'.

Wait: the machine will then prompt you with 'Blank OK'.

Press 'Stop'.

The empty tray ejects; replace it very carefully with your painstakingly filled sample tray.

Press 'Start'.

The machine will pull the tray in and read it; the machine will at last output the readings in columnar fashion on its ticker tape.

Press 'Stop': your sample tray ejects.

Remove ticker tape; turn off machine; average values for triplicate readings. Ignore obviously spurious results caused no doubt by less than painstaking effort.

C. Covalent binding of FITC to penicillinase

1. 0.7788 mg FITC (Isomer 1, Sigma Chemical Co, F 7250) is added to 1.5 mls of 0.2M phosphate buffer pH=8.2, combined with pooled protein samples and then mixed thoroughly. The MW (approximate) of penicillinase is 50,000. We have 10 mg of it or 1.2×10^{17} molecules. We expect at least 4-5 FITC molecules to bind to each penicillinase: this reaction is not expected to be completely efficient (so as a wag, we double this requirement) and thus want 10 FITC molecules per that of penicillinase. This means we want 1.2×10^{18} molecules of FITC. The MW of FITC is 389.4, which translates finally into 0.7788mg of material.

2. Let the FITC/penicillinase solution react at 4°C overnight.

D. Separation of unbound FITC

1. A sodium phosphate buffer pH=5.9 is prepared by thoroughly mixing 61.5 mls 0.2M Na_2HPO_4 and 438.5 mls 0.2M NaH_2PO_4.

2. Equilibrate the gel bed with 25 mls of 0.2 M phosphate buffer pH 5.9 , discarding the eluate.

3. Run penicillinase/FITC sample through the Sephadex G-25M column. The higher molecular weight (and larger) penicillinase/FITC will come out first from the column. We switch to the pH=6.0 phosphate buffer because this is now the regime at which we expect maximum activity from the penicillinase[1,44]; the binding has already been accomplished. The actual pH of our buffer, measured on a pH meter, turned out to be 5.9.

4. Collect penicillinase/FITC in 0.5 ml samples in labeled Eppendorf tubes. Colour change of FITC in bound vs. unbound state indicates visually where the bound FITC is; further the molecular weight difference and the size difference allow a great separation between the two samples, making the samples very separable as they pass through the column.

5. Store samples of FITC/penicillinase at 4° C.

E. Quantification of conjugated FITC fluorescence activity

1. 0.1 mg/ml standard FITC in 0.2M phosphate buffer pH=5.9 and six further standards by fivefold dilutions are prepared. Add 3 mls of each FITC/buffer solution to fluorimeter cuvettes (Hughes and Hughes, Ltd) (solutions are 0.1, 0.02, 0.004, 0.0008, 0.00016, 0.000032, 0.0000064 mg/ml).

2. Select penicillinase/FITC solutions with visually obvious high level of FITC; add 100 µl of sample to cuvette and then 2.9 ml of 0.2M phosphate buffer pH=5.9.

3. Measure fluorescence level of each cuvette (samples and standards). Standards detrmine a curve for comparison; the samples subsequently taken should fall on (or near) the curve.

<u>Procedure to use fluorimeter for FITC:</u>

Input excitation wavelength of 494 nm; Sigma's estimate

Input emission wavelength of 518 nm; Sigma's estimate

Open lid to sample area (front of machine) - only open sample bay when left-hand-side button is illuminated); put sample in holder farthest away from you

Press left-hand-side button

Wait until reading stabilises (a few seconds)

Write down result

Press left-hand-side button again

Replace cuvette with next one to be measured

Once all the cuvettes have been analysed, plot known concentrations (standards) vs. recorded fluorescence level. Valid levels should range from above 25 to below 999.9

Once graph has been accomplished, use the (hopefully) straight line to extrapolate unknown concentrations of the bound FITC

F. Iodometric assay of FITC-bound penicillinase

1. Prepare 1.2 mg/ml standard of penicillinase by adding 0.6 mg of dry penicillinase (1000 units) to 500 µl of 0.2 M pH=5.9 phosphate buffer and mixing vigourously. These controls serve as the basis to determine concentration of unknown proteins; can double-check original protein standard curve performed on BSA.

2. Prepare a blue/black reagent for iodometric assay of penicillinase: 80 ml of 0.2% (w/v) starch solution (0.2 g hydrolysed potato starch in 100 mls of 0.2M phosphate buffer pH 5.9 in a stirring flask) is mixed with .55 mls (if less than 80 mls remains of the starch solution, use less) iodine/potassium iodide solution (2.03g of iodine (0.08M), 53.12 g of potassium iodine (3.2M) with 100 mls deionised water).

3. Stir the starch while boiling gently - cover the solution lightly to minimise loss of liquid - the solution is done when it is translucent and starch does not fall out after removal from heat (could take upwards of an hour). Cool to room temperature and filter. This blue-black reagent will turn clear in the presence of penicilloic acid, which is released when penicillin-G and penicillinase react[290,297] . Thus as transmission through a cell is measured, a given level of penicillinase activity can also be measured.

4. Prepare standard solutions of Penicillin G to verify activity of penicillinase:

Concentration	Penicillin G amount	Phosphate buffer pH=5.9 amount
0.4mM	7.128 mg	50 mls
0.2mM	10 mls 0.4mM	10 mls
0.1mM	4 mls 0.4mM	12 mls
0.08mM	8 mls 0.4mM	8 mls
0.04mM	1 ml 0.4mM	9 mls
0.02mM	1 ml 0.4mM	19 mls

5. Prepare two 96-well microtiter plates, as illustrated in Figure 4, for transmission analysis in accordance with the below tables. This allows us to verify that the penicillinase/penicillin G/starch-iodide reaction is transpiring as expected. Use 620nm again as that is sufficiently far away from the excitation wavelength of FITC.

Notes for all tables of microtiter plates:

PB: 0.2M pH=6.0 phosphate buffer
PG: Penicillin-G
PG-1: 0.4mM standard solution of Penicillin-G
PG-2: 0.2mM standard solution of Penicillin-G
PG-3: 0.1mM standard solution of Penicillin-G
PG-4: 0.08mM standard solution of Penicillin-G
PG-5: 0.04mM standard solution of Penicillin-G
PG-6: 0.02mM standard solution of Penicillin-G
St/I: starch/iodine solution (blue-black reagent)
Pase: penicillinase standard (1.2 mg/ml)
Pase-1: penicillinase sample 1
Pase-2: penicillinase sample 2
Pase-3: penicillinase sample 3
Pase-4: penicillinase sample 4
Pase-5: penicillinase sample 5
Y: solution included in standard amount (see notes for each table) **-:** solution absent

Each well in the microtiter plate will have 190µl:

If Pase is to be added, then add 40 µl of PB and 10 µl of appropriate Pase

If 1 solution in addition to Pase appears, add 140 µl of it

If 2 solutions in addition to Pase appear, add 70 µl of each.

If two solutions appear (not Pase), then add 95 µl of each.

If one solution appears (not Pase), then add 190 µl.

Each column in the table refers to a triplet set of wells in the 96-well microtiter plate.

Notes for Plate 1: Preset machine PRIOR to addition of penicillinase

Add penicillinase LAST

Take three measurements, as quickly as machine will let you, and note the time intervals

Annotate the output paper of the microtiter reader appropriately

Plate 2: Each Penicillinase sample is read independently: the 10 µl aliquots are added to the two rows of the microtiter plate, and read by the Titertek machine.

Plate 1:

	1	2	3	4	5	6	7	8	9	10	11	12
PB	Y	-	-	-	-	-	-	-	Y	-	-	-
PG	-	PG-1	PG-2	PG-3	PG-4	PG-5	PG-6	-	-	PG-1	PG-2	PG-3
St/I	-	-	-	-	-	-	-	Y	-	Y	Y	Y
Pase	-	-	-	-	-	-	-	-	-	-	-	-

	13	14	15	16	17	18	19	20	21	22	23	24
PB	-	-	-	Y	-	-	-	-	-	-	-	Y
PC	PG-4	PG-5	PG-6	-	PG-1	PG-2	PG-3	PG-4	PG-5	PG-6	-	-
St/I	Y	Y	Y	Y	Y	Y	Y	Y	Y	Y	Y	-
Pase	-	-	-	-	Pase	Pase	Pase	Pase	Pase	Pase	Pase	Pase

Plate 2:

	1	2	3	4	5	6	7	8	9	10	11	12
PB	Y	-	-	-	-	-	-	-	Y	-	-	-
PG	-	-	PG-1	PG-2	PG-3	PG-4	PG-5	PG-6	-	-	PG-1	PG-2
St/I	-	Y	Y	Y	Y	Y	Y	Y	-	Y	Y	Y
Pase	Pase1	Pase1	Pase1	Pase1	Pase1	Pase1	Pase1	Pase1	Pase2	Pase2	Pase2	Pase2

	13	14	15	16	17	18	19	20	21	22	23	24
PB	-	-	-	-	Y	-	-	-	-	-	-	-
PG	PG-3	PG-4	PG-5	PG-6	-	-	PG-1	PG-2	PG-3	PG-4	PG-5	PG-6
St/I	Y	Y	Y	Y	-	Y	Y	Y	Y	Y	Y	Y
Pase	Pase2	Pase2	Pase2	Pase2	Pase3	Pase3	Pase3	Pase3	Pase3	Pase3	Pase3	Pase3

	25	26	27	28	29	30	31	32
PB	Y	-	-	-	-	-	-	-
PG	-	-	PG-1	PG-2	PG-3	PG-4	PG-5	PG-6
St/I	-	Y	Y	Y	Y	Y	Y	Y
Pase	Pase4	Pase4	Pase4	Pase4	Pase4	Pase4	Pase4	Pase4

Plate 3: Can be the bottom of Plate 1 after it has been read.

	25	26	27	28	29	30	31	32
PB	Y	-	-	-	-	-	-	-
PG	-	-	PG-1	PG-2	PG-3	PG-4	PG-5	PG-6
St/I	-	Y	Y	Y	Y	Y	Y	Y
Pase	Pase5	Pase5	Pase5	Pase5	Pase5	Pase5	Pase5	Pase5

Preparation of Cholera Toxin B (or CTP_3) tapered fibre loop

1. Add Cholera Toxin b antigen 100mg in 1 ml in 0.1M sodium phosphate buffer at pH 7.2 to aldehyde loop for one hour, at room temperature.

2. Rinse loop with buffer.

3. Add excess glycine and 0.1M sodium phosphate buffer at pH=8.0 for one hour at room temperature

4. Rinse loop with nanopure water .

5.Add cyanoborohydride. 50 mg/ml, in 0.1M sodium phosphate buffer at pH=8.0 for one hour at room temperature

6.Rinse loop in nanopure water.

7. Add sample: pre or post, of serum fluid at appropriate titer; the diluter is 0.1M sodium phosphate buffer at pH 7.2; titers are (v/v). Start with pre fluids (sera) the lowest titer is the first one to be sampled. **The sample must be incubated at 20 minutes exactly.**

8. Prepare human pre and post cholera infection sera in 1:50, 100, 200, 400, 800, 1600, 3200, 6400, 12800, 25600 titers:

1:50 - 40 ml sera, 19600 ml of 0.1M sodium phosphate buffer at pH 7.2 (this is 2 ml of fluid)

1:100 - take 1 ml of 1:50 titer, add 1 ml of 0.1M sodium phosphate buffer at pH 7.2

1:200 - take 1 ml of 1:100 titer, and add 1 ml of 0.1M sodium phosphate buffer at pH 7.2

1:400 - take 1 ml of 1:200 titer, and add 1 ml of 0.1M sodium phosphate buffer at pH 7.2

1:800 - take 1 ml of 1:400 titer, and add 1 ml of 0.1M sodium phosphate buffer at pH 7.2

1:1600 - take 1 ml of 1:800 titer, and add 1 ml of 0.1M sodium phosphate buffer at pH 7.2

1:3200 - take 1 ml of 1:1600 titer, and add 1 ml of 0.1M sodium phosphate buffer at pH 7.2

1:6400 - take 1 ml of 1:3200 titer, and add 1 ml of 0.1M sodium phosphate buffer at pH 7.2

1:12800 - take 1 ml of 1:6400 titer, add 1 ml of 0.1M sodium phosphate buffer at pH 7.2

1:25600 - take 1 ml of 1:12800 titer; add 1 ml of 0.1M sodium phosphate buffer at pH 7.2

8.Rinse loop with 0.1M sodium phosphate at pH=8.0 buffer

9.Add anti-IgA with Rhodamine isothiocyanate label (0.5 ml); anti-IgG with FITC label (0.5 ml). **Incubate for 20 minutes exactly.**

10. When not in use, all solutions must be at 4° C. Samples of serum (in liquid state) will only last for a few days.

Radiosurface assay: iodination of peptides silanised to fibres

1. Dissolve Arg-Lys-Asp-Val-Tyr Acetate salt in nanopure water at room temperature.

2. Use amino-silane to prepare fibre; expose each fibre (10 trial fibres) to peptide; incubate for 1 hour at room temperature.

3. Rinse exhaustively with nanopure water.

4. Place in empty reaction vial.

5. Prepare 10 unsilanised (no peptide) fibres in reactive vials.

6. In the radioactive materials room (basement, Institute of Biotechnology), prepare Iodo-beads (Pierce 28665): wash with 0.05M disodium hydrogen phosphate buffer at pH 7.4 (2 beads).

7. Add 2 beads to 10μl ^{125}I solution (IMS 30, Amersham) in reaction vial. Let stand 5minutes at room temperature.

8. Use 100 μl of ^{125}I solution for each reaction vial with fibre; let reaction proceed for 15 minutes.

9. Put all the tubes: buffer (no radioactive material), fibres with peptide (and radioactive material), fibres with no peptide (exposed to radioactive material) in Iso-Data tray for ICN gamma counter.

10. Repeat counts three times; take average; correlate counts to other reaction vials with known concentrations of ^{125}I solution.

References

1. Abdel-Latif, M.S., G.G. Guilbault, 'Fiber-optic sensor for the determination of glucose using micellar enhanced chemiluminescence of the peroxyoxalate reaction', *Analytical Chemistry*, 1988, **60**, pp. 175-84.

2. 'Handbook of mathematical functions' ed. Milton Abramowitz and Irene A. Stegun, Dover Publications, New York, U.S., 1972,

3. Agayn, V.I., D.R. Walt, 'Fiber-optic sensor for continuous monitoring of fermentation pH', *Bio/Technology*, 1993, **11**, pp. 726-9.

4. Al-Bader, S.J., M. Imtaar, 'Optical fiber hybrid-surface plasmon polaritons', *Journal of the Optical Society of America B*, 1993, **10, No 1**, pp. 83-88.

5. Alabbas, S.H., D.C. Ashworth, R. Narayanaswamy, 'Design and characterisation parameters of an optical fibre pH sensor' In Chemical, Biochemical and Environmental Applications of Fibers: Proceedings of the conference in Boston Massachusetts, 8-9 September, The International Society for Optical Engineers, Washington, U.S., 1988, **990**.

6. Albert, M.J., M. Ansaruzzaman, P.K. Bardhan, A.S. Faruque, S.M. Faruque, M.S. Islam, D. Mahalanabis, R.B. Sack, M.A. Salam, A.K. Siddique, M.D. Yunus, K. Zaman, 'Large epidemic of cholera-like disease in Bangladesh caused by Vibrio cholerae O139 synonym Bengal', *The Lancet*, 1993, **342**, pp. 387-90.

7. Albery, W.J., D.H. Craston, 'Amperometric enzyme electrodes: theory and experiment' in *Biosensors: Fundamentals and Applications*, ed. Anthony P.F. Turner, Isao Karube and George S Wilson, Oxford University Press, Oxford, U.K., 1987, pp. 180-210.

8. Alder, J.F., D.C. Ashworth, R. Narayanaswamy, R.E. Moss, I.O. Sutherland, 'An optical potassium ion sensor', *Analyst*, 1987, **112**, pp. 1191-2.

9. Anderson, G.P., J.P. Golden, F.S. Ligler, 'Fiber-optic based biosensor: fluorescence signal acquisition from step-etched fibers', *Unpublished work*.

10. Anderson, G.P., L.C. Shriver-Lake, J.P. Golden, F.S. Ligler, 'Fiber optic-based biosensor: signal enhancement in a production model' In Fiber Optic Medical and Fluorescent Sensors and Applications: Proceedings of the Symposium in Los Angeles, California, 23-24 January, The International Society for Optical Engineers, Washington, U.S., 1992, **1648**, pp. 39-43.

11. Anderson, G.D., J.P. Golden, F.S. Ligler, 'A fiber optic biosensor: combination tapered fibers - improved signal acquisition', *Biosensors and Bioelectronics*, 1993, **8**, pp. 249-56.

12. Andrade, J.D., D.E. Vanwagenen, D.E. Gregonis, K. Newby, J. Lin, 'Remote fiber-optic biosensors based on evanescent-excited fluoro-immunoassay: concept and progress', IEEE Transactions on Electron Devices, 1985, **ED-32, No 7**, pp. 1175-9.

13. Angel, S.M., K. Langry, J. Roe, B.W. Colston, Jr, P.F. Daley, F.P. Milanovich, 'Preliminary field demonstration of a fibre-optic TCE sensor' In Chemical, Biochemical and Environmental Fiber Sensors II: Proceedings of the Symposium in San Jose California, 19-21 September The International Society for Optical Engineers, Washington, U.S., 1990, **1368**, pp. 98-103.

14. Ankiewicz, A. , G. Peng, 'Generalized Gaussian approximation for single-mode fibers', *Journal of Lightwave Technology*, 1992, **10**, pp. 22-7.

15. Appleyard, A.P., P.L. Scrivener, P.D. Maton, 'Intrinsic optical fiber temperature sensor based on the differential absorption technique', *Review of Scientific Instrumentation*, 1990, **6**, No **10**, pp. 2650-4.

16. Arnold, M.A., 'Fiber optic biosensing probes for biomedically important compounds' In Optical Fibers in Medicine III. Proceedings of the Symposium in Los Angeles, California, 13-16 January, International Society for Optical Engineers, Washington, U.S., 1988, **906**, pp. 128-33.

17. Arnold, M.A., 'Enzyme-based fiber optic sensor', *Analytical Chemistry*, 1985, **57**, pp. 565-6.

18. Arnold, M.A., T.J. Ostler, 'Fiber-optic ammonia gas sensing probe', *Analytical Chemistry*, 1986, **58**, pp. 1137-40.

19. Arwin, H. , 'Optical pproperties of thin layers of bovine serum albumin, γ-globulin, and hemoglobin', *Applied Spectroscopy*, 1986, **40, No 3**, pp. 313-8.

20. Ashworth, D.C., H.P. Huang, R. Narayanaswamy, 'An optical calcium ion sensor', *Analytica Chimica Acta*, 1988, **213**, pp. 251-7.

21. Astles, J.R., W.G. Miller, 'Reversible fiber-optic immunosensor measurements', *Sensors and Actuators B*, 1993, **11**, pp. 73-8.

22. Bacci, M. , F. Baldini, A.M. Scheggi, 'Chemical studies on acid-base indicators for the development of an extrinsic optical fiber pH sensor' In Chemical, Biochemical, and Environmental Applications of Fibers: Proceedings of the Symposium in Boston Massachusetts, 8-9 September, International Society for Optical Engineers, Washington, U.S., 1988, **990**, pp. 84-7.

23. Bacon, J.R., J.N. Demas, 'Determination of oxygen concentrations by luminescence quenching of a polymer-immobilized transition-metal complex', *Analytical Chemistry*, 1987, **59, No 23**, pp. 2780-5.

24. Balaei, S. , J.J. Aaron, 'Solid-surface fluorescence analysis using a fibre-optic sensor', *Analytica Chimica Acta*, 1991, **255**, pp. 305-9.

25. Baldini, F. , S. Bracci, 'Optical-fibre sensors by silylation techniques', *Sensors and Actuators B*, 1993, **11**, pp. 353-60.

26. Baldini, F. , M. Bacci, F. Cosi, A. DelBianco, 'Absorption-based optical-fibre oxygen sensor', *Sensors and Actuators B*, 1992, **7**, pp. 752-7.

27. Baldini, F. , 'Recent progress in fibre optic pH sensing' In Chemical, Biochemical and Environmental Fiber Sensors II: Proceedings of the Symposium in San Jose, California, September 19-21, International Society for Optical Engineers, Washington, U.S., 1990, **1368**, pp. 184-90.

28. Baldini, F. , M. Bacci, S. Bracci, 'Analysis of acid-base indicators covalently bound on glass supports' In Chemical, Biochemical and Environemntal Fiber Sensors II (1990): Proceedings of the Symposium in San Jose, California, September 19-21, International Society for Optical Engineers, Washington, U.S., 1990, **1368**, pp. 210-7.

29. Barnard, S.M., D.R. Walt, 'Optical immunosensors using controlled-release polymers' in *Biosensors and chemical sensors: Optimizing performance through polymeric materials*, American Chemical Society, Washington D.C., U.S., 1992,

30. Bartlett, P.N., 'The use of electrochemical methods in the study of modified electrodes' in *Biosensors: Fundamentals and applications*, ed. Anthony P.F. Turner, Isao Karube, and George S. Wilson, Oxford University Press, Oxford, U.K., 1987, pp. 211-46.

31. Belovolov, M.I., E.M. Dianov, A.V. Kuznetsov, A.M. Prokhorov, 'Single-mode fiber-optic directional couplers', *Fiber and Integrated Optics*, 1987, **6, No 4**, pp. 239-53.

32. Benaim, N. , K.T. Grattan, A.W. Palmer, 'Simple fibre optic pH sensor for use in liquid titrations', *Analyst*, 1986, **111**, pp. 1095-7.

33. Bentley, A.E., J.F. Alder, 'Optical fibre sensor for detection of hydrogen cyanide in air: Part 1. Reagent characterization and impregnated bead detector performance', *Analytica Chimica Acta*, 1989, **222**, pp. 63-73.

34. Berlman, I.B., '*Handbook of fluorescence Spectra of Aromatic Compounds: second edition*', Academic Press, England, U.K., 1971, pp. 410-1.

35. Berman, R.J., L.W. Burgess, 'Flow optrodes for chemical analysis' In Chemical, Biochemical and Environmental Fiber Sensors II (1990): Proceedings of the Symposium in San Jose, California, September 19-21, International Society for Optical Engineers, Washington, U.S., 1990, **1368**, pp. 25-35.

36. Berthold III, J.W., 'Industrial applications of fiber optic sensors' in *Fiber optic sensors: An introduction for engineers and scientists*, ed. Eric Udd, Wiley and Sons, Inc, Ltd, London, U.K., 1991, pp. 409-37.

37. Berthold III, J.W., S.E. Reed. R.G. Sarkis, 'Simple, repeatable, fiber-optic intensity sensor for temperature measurement' In Fiber Optic and Laser Sensors VII (1989): Proceedings of the Symposium in Boston, Massachusetts, International Society for Optical Engineers, Washington, U.S., 1989, **1169**, pp. 512-520.

38. Berthou, H. , C.K. Jorgensen, 'Optical-fiber temperature sensor based on upconversion-excited fluorescence', *Optics Letters*, 1990, **15, No 19**, pp. 1100-2.

39. Beswick, R.B., C.W. Pitt, 'Optical detection of toxic gases using fluorescent porphyrin Langmuir-Blodgett films', *Journal of Colloid and Interface Science*, 1988, **124, No 1**, pp. 146-55.

40. Betts, T.A., G.C. Calena, J. Huang, K.S. Litwiler, J. Zhang, J. Zagrobelny, F.A. Bright, 'Fiber-optic-based immunosensors for haptens', *Analytica Chimica Acta*, 1991. **246**, pp. 55-63.

41. Bhatia, S.K., L.C. Shriver-Lake, K.J. Prior, J.H. Georger, J.M. Calvert, R. Bredehorst, F.S. Ligler, 'Use of thiol-terminal silanes and heterobifunctional crosslinkers for immobilization of antibodies on silica surfaces', *Analytical Chemistry*, 1989, **178**, pp. 408-13.

42. Bhatia, S.K., R.B. Thompson, L.C. Shriver-Lake, M. Levine, F.S. Ligler, 'Fiber optic-based immunosensors: A progress report' In Fluorescence Detection III (1989): Proceedings of the Symposium in Boston, Massachusetts, 16-18 January, International Society for Optical Engineers, Washington, U.S., 1989, **1054**, pp. 184-190.

43. Bhattacharya, M.K., S.K. Bhattacharya, S. Garg, P.K. Saha, D. Dutta, G.B. Nair, B.C. Deb, K.P. Das, 'Outbreak of *vibrio cholerae* non-01 in India and Bangladesh', *The Lancet*, 1993, **341**, pp. 1346-7.

44. Bier, F.F., W. Stockholm, M. Bocher, U. Bilitewski, R.D. Schmidt, 'Use of a fibre optic immunosensor for the detection of pesticides', *Sensors and Actuators B*, 1992, **7**, pp. 509-12.

45. 'Bile sensor goes home with the patient', *Opto and Laser Europe*, 1993, p. 13.

46. Bilodeau, F. , K.O. Hill, D.C. Johnson, S. Faucher, 'Compact, low-loss, fused biconical taper coupler: overcoupled operation and antisymmetric super mode cutoff', *Optics Letters*, 1987, **12, No 8**, pp. 634-6.

47. Birks, J.B., 'Organic Molecular Photophysics: Volume 2' John Wiley and Sons, London, U.K., 1975, pp. 153-5.

48. Birks, T.A., K.P. Oakley, C.D. Hussey, 'Adiabaticity of miniature loops in tapered single-mode fibre', *Electronics Letters*, 1992, **28, No 22**, pp. 2034-5.

49. Birks, T.A., Y.W. Li, 'The shape of fiber tapers', *Journal of Lightwave Technology*, 1992, **10, No 4**, pp. 432-8.

50. Birks, T.A., 'Twist-induced tuning in tapered fibre couplers', *Applied Optics*, 1989, **28, No 19**, pp. 4226-33.

51. Birks, T.A., C.D. Hussey, 'Control of power-splitting ratio in asymmetric fused-tapered single-mode fiber couplers', *Optics Letters*, 1988, **13, No 8**, pp. 681-3.

52. Biswas, P.K., D. Kundu, D. Ganguli, 'A sol-gel-derived antireflective coating on optical glass for near-infrared applications', *Journal of Material Science Letters*, 1989, **8**, pp. 1436-7.

53. Black, R.J., S. Lacroix, F. Gonthier, J.D. Love, 'Tapered single-mode fibres and devices. Part 2: Experimental and theoretical quantification', *IEE Proceedings-J*, 1991, **138, No 5**, pp. 355-64.

54. Black, R.J., J. Bures, J. Lapierre, 'Finite-cladding fibres: HE12 and local-mode coupling evolution', *unpublished work*, 1989.

55. Blackburn, G.F., 'Chemically sensitive field effect transistors' in *Biosensors: Fundamentals and applications*, ed. Anthony P.F. Turner, Isao Karube, and George S. Wilson, Oxford University Press, Oxford, U.K., 1987, pp. 481-530.

56. Blair, T.L., T. Cynkowski, L.G. Bachas, 'Fluorocarbon-based immobilization of a fluoroionophore for preparation of a fiber optic sensor', *Analytical Chemistry*, 1993, **65, No 7**, pp. 945-7.

57. Blodgett, K.B., 'Use of interference to extinguish reflection of light from glass', *Physical Review*, 1939, **55**, pp. 391-404.

58. Bluestein, B.I., I.M. Walczak, S. Chen, 'Fiber optic evanescent wave immunosensor for medical diagnostics', *Trends in Biotechnology*, 1990, **8**, pp. 161-8.

59. Boisde, G. , F. Blanc, X. Machuron-Mandard, 'pH measurements with dyes co-immobilized on optodes: principles and associated instrumentation', *International Journal of Optoelectronics*, 1991, **6, No 5**, pp. 407-23.

60. Boisde, G. , B. Biatry, B. Magny, B. Dureault, F. Blanc, 'Comparison between two dye-immobilization techniques on optodes for the pH-measurement by absorption

and reflectance' In Chemical, Biochemical and Environmental Sensors: Proceedings of the Symposium in Los Angeles, California, 6-7 September, International Society for Optical Engineers, Washington, U.S., 1989, **1172**, pp. 239-250.

61. Boisde, G. , F. Blanc, J. Perez, 'Chemical measurements with optical fibers for process control', *Talanta*, 1988, **35, No 2**, pp. 75-82.

62. Bolthauser, T. , H. Baltes, 'Capacitive humidity sensors in SACMOS technology with moisture absorbing photosensitive polyimide', *Sensors and Actuators A*, 1988, **25-27**, pp. 509-12.

63. Borman, S. , 'Biosensors: Potentiometric and amperometric', *Analytical Chemistry*, 1987, **59, No 18**, pp. 1901A-8A.

64. Boucouvalas, A.C., G. Georgiou, 'Tapering of single mode optical fibres', *IEE Proceedings*, 1986, **133 Part J**, pp. 385-90.

65. Brand, U. , T. Scheper, K. Schugerl, 'Penicillin G sensor based on penicillin amidase coupled to a field effect transistor', *Analytica Chimica Acta*, 1989, **226**, pp. 87-97.

66. Bricheno, T. , A. Fielding, 'Stable low-loss single-mode couplers', *Electronics Letters*, 1984, **20**, pp. 230-2.

67. Bright, F.V., T.A. Betts, K.S. Litwiler, 'Regenerable fiber-optic-based immunosensor', *Analytical Chemistry*, 1990, **62**, pp. 1065-9.

68. Bright, F.V., G.G. Poirier, G.M. Hieftjie, 'A new ion sensor based on fiber optics', *Talanta*, 1988, **35, No 2**, pp. 113-8.

69. Brinker, C.J., G.W. Scherer, 'Sol-gel science: the physics and chemistry of sol-gel processing,' Academic Press, Ltd, London, U.K., 1990.

70. Brophy, T.J., P.M. Shankar, L.C. Bobb, 'Formation and measurement of tapers in optical fibers', *Review of Scientific Instrumentation*, 1992, **64 No 9**, pp. 2650-4.

71. Brossia, C.E., S.C. Wu, 'Low-cost in-soil organic contaminant sensor' In Chemical, Biochemical and Environmental Fiber Sensors II: Proceedings of the symposium in San Jose, California, 19-21 September, International Society for Optical Engineers, Washington, U.S., 1990, **1368**, pp. 115-20.

72. Burns, W.K., M. Abebe, C.A. Villarruel, 'Parabolic model for shape of fiber taper', *Applied Optics*, 1985, **24, No 17**, pp. 2753-5.

73. Caglar, P. , R. Narayanaswamy, 'Ammonia-sensitive fibre-optic probe utilising an immobilised spectrophotometric indicator', *Analyst*, 1987, **112**, pp. 1285-8.

74. Carey, W.P., B.S. Jorgensen, 'Optical sensors for high acidities based on fluorescent polymers', *Applied Spectroscopy*, 1991, **45, No 5**, pp. 834-8.

75. Carlsen, M. , L.H. Christensen, J. Nielsen, 'Flow-injection analysis for the measurement of penicillin V in fermented media', *Analytica Chimica Acta*, 1993, **274**, pp. 117-23.

76. Carlyon, E.E., C.R. Lowe, D. Reid, I. Bennion, 'A single mode fibre-optic evanescent wave biosensor', *Biosensors and Bioelectronics*, 1992, **7**, pp. 141-6.

77. Carome, E.F., G.A. Coghlan, C.N. Sukenik, J.E. Zull, 'Fiberoptic evanescent wave sensing of antigen-antibody binding', *Sensors and Actuators B*, 1993, **13-14**, pp. 732-3.

78. Carome, E.F., G. Fischer, V. Kubulins, 'Fiber-optic sensor system for hydrocarbon vapors', *Sensors and Actuators B*, 1993, **13-14**, pp. 305-8.

79. Caspar, C. , E. Bachus, 'Fibre-optic micro-ring-resonator with 2mm diameter', *Electronics Letters*, 1989, **25, No 22**, pp. 1506-8.

80. Cass, A.E., 'Biosensors: a practical approach' Oxford University Press, Oxford, U.K., 1989, pp. 233-63.

81. Cassidy, D.T., D.C. Johnson, K.O. Hill, 'Wavelength-dependent transmission of monomode optical fiber tapers', *Applied Optics*, 1985, **24, No 7**, pp. 945-50.

82. Cattaneo, M.V., J.H. Luong, 'Monitoring glutamine in animal cell cultures using a chemiluminescence fiber optic biosensor', *Biotechnology and Bioengineering*, 1993, **41**, pp. 659-65.

83. Chart, H. , B. Rowe, 'Antibody cross-reactions with lipopolysaccharide from E coli O157 after cholera vaccination', *The Lancet*, 1993, **341**, p. 1282.

84. 'Chemical fibre sensors go home with the patient', *Opto and Laser Europe*, 1993, pp. 23-24.

85. Christensen, D. , S. Dyer, J. Kimmel, J. Herron, 'Evanescent coupling in a waveguide fluoro-immunosensor' In Fiber Optic Medical and Fluorescent Sensors and Applications: Proceedings of the Symposium in Los Angeles, California, 23-24 January, International Society for Optical Engineers, Washington, U.S., 1992, 1648, pp. 223-6.

86. Christian, L.M., W.R. Seitz, 'An optical ionic-strength sensor based on polyelectrolyte association and fluorescent energy transfer', *Talanta*, 1988, **35, No 2**, pp. 119-22.

87. Chudyk, W.A., M.M. Carabba, J.E. Kenny, 'Remote detection of groundwater contaminants using far-ultraviolet laser-induced fluorescence', *Analytical Chemistry*, 1985, **57**, **No 7**, pp. 1237-42.

88. Chudyk, W. , K. Pohlig, 'Dynamic range limits in field determination of fluorescence using fiber optic sensors' In Chemical, Biochemical and Environmental Fiber Sensors II: Proceedings of the symposium in San Jose, California, 19-21 September, International Society for Optical Engineers, Washington, U.S., 1990, **1368**, pp. 105-14.

89. Citri, N. , 'Two antigenically different states of active penicillinase', *Biochimica et Biophysica Acta*, 1958, **27**, pp. 277-81.

90. Claremont, D.J., J.C. Pickup, 'In vivo chemical sensors and biosensors in clinical medicine' in *Biosensors: Fundamentals and applications*, ed. Anthony P.F. Turner, Isao Karube, and George S. Wilson, Oxford University Press, Oxford, U.K., 1987, pp. 356-76.

91. Claudon, P. , M. Donner, J.F. Stoltz, 'Potential interest of optical fibres as immunosensors: study of different antigen coupling methods', *Journal of Materials Science: Materials in Medicine*, 1991, **2**, pp. 197-201.

92. Coleman, J.T., J.F. Eastham, M.J. Sepaniak, 'Fiber optic based sensor for bioanalytical absorbance measurements', *Analytical Chemistry*, 1984, **56**, pp. 2246-9.

93. Colin, T.B., K.H. Yang, W.C. Stwalley, 'The effect of mode distribution on evanescent field intensity: applications in optical fiber sensors', *Applied Spectroscopy*, 1991, **45, No 8**, pp. 1291-5.

94. Coulet, P.R., L.J. Blum, S.M. Gautier, 'Luminescence-based fibre optic probes', *Sensors and Actuators B*, 1993, **11**, pp. 57-61.

95 Cryan, C.V., C.D. Hussey, 'Bending of fused polished couplers', *Electronics Letters*, 1992, **28, No 27**, pp. 2104-6.

96. Cryan, C.V., C.D. Hussey, 'Fused polished singlemode fibre couplers', *Electronics Letters*, 1991, **28, No 2**, pp. 204-5.

97. Culshaw, B. , 'Optical systems and sensors for measurement and control', *Journal of Physics E: Scientific Instrumentation*, 1983, **16**, pp. 978-86.

98. Culshaw, B. , F. Muhammad, G. Stewart, S. Murray, D. Pinchbeck, J. Norris, S. Cassidy, M. Wilkinson, D. Williams, I. Crisp, R. Van Ewyk, A. McGhee, 'Evanescent wave methane detection using optical fibres', *Electronics Letters*, 1992, **19**, pp. 2232-4.

99. Culshaw, B. , 'Fiber optic sensor networks' In Fiber Optic Sensors: Engineering and Applications: Proceedings of the Symposium in The Hague, the Netherlands, 14-5 March, International Society for Optical Engineers, Washington, U.S., 1991, **1511**, pp. 168-78.

100. Das, A.K., A.K. Mandal, 'Measurement sensitivity of liquid droplet parameters using optical fibers' In Fiber optic and Laser Sensors VII: Proceedings of the Symposium in Boston, Massachusetts, International Society for Optical Engineers, Washington, U.S., 1989, **1169**, pp. 586-95.

101. Debe, M.K., 'Optical probes of organic thin films: photons-in and photons-out', *Progress in Surface Science*, 1987, **24, No 1-4**, pp. 1-282.

102. deGraeve, J.S., N. Andrien, P. Valdiquie, G. Fichant, 'Evaluation of the "Cobas-Bio" centrifugal microanalyzer', *Clinical Chemistry*, 1981, **27, No 2**, pp. 337-8.

103. DeGrandpre, M.D., 'Measurement of seawater pCO2 using a renewable-reagent fiber-optic sensor with colorimetric detection', *Analytical Chemistry*, 1993, **65, No 4**, pp. 331-7.

104. DeGrandpre, M.D., L.W. Burgess, 'All-fiber spectroscopic probe based on an evanescent wave sensing mechanism' In Chemical, Biochemical, and Environmental Applications of Fibers: Proceedings of the Symposium in Boston, Massachusetts, 8-9 September, International Society for Optical Engineers, Washington, U.S., 1988, **990**, pp. 170-4.

105. DeGrandpre, M.D., L.W. Burgess, 'Long path fiber-optic sensor for evanescent field absorbance measurements', *Analytical Chemistry*, 1988, **60**, pp. 2582-6.

106. Ding, J.Y., M.R. Shahriari, G.H. Sigel, Jr, 'Fibre optic pH sensors prepared by sol-gel immobilisation technique', *Electronics Letters*, 1991, **27**, pp. 1560-2.

107. Drexhage, K.H., 'Structure and Properties of Laser Dyes' in *Topics in Applied Physics: Volume 1. Dye Lasers*, ed. Fritz P. Schafer, Springer-Verlag, London, U.K., 1990, pp. 155-200.

108. 'Dye Laser Principles with Applications' ed. F. J. Duarte and Lloyd W Hillman, Academic Press, London, U.K., 1990, pp. 435-47.

109. Duschl, C. , E.A. Hall, 'Adsorption and complex formation of immunoglobulins on silicon wafers, studied by interference-enhanced reflectometry', *Journal of Colloid and Interface Science*, 1991, **144, No 2**, pp. 368-80.

110. Edmonds, T.D., N.J. Flatters, C.F. Jones, J.N. Miller, 'Determination of pH with acid-base indicators: implications for optical fibre probes', *Talanta*, 1988, **35, No 2**, pp. 103-7.

111. Eenink, R.G., H.E. deBruijn, R.P. Kooyman, J. Greve, 'Fibre-fluorescence immunosensor based on evanescent wave detection', *Analytica Chimica Acta*, 1990, **238**, pp. 317-21.

112. Egalon, C.O., R.S. Rogowski, 'Efficiency of core light injection from sources in the cladding: bulk distribution', *Optical Engineering*, 1992, **31, No 4**, pp. 846-51.

113. Egalon, C.O., R.S. Rogowski, 'Theoretical model for a thin cylindrical film optical fiber fluorosensor', *Optical Engineering*, 1992, **31, No 2**, pp. 237-44.

114. Egalon, C.O., R.S. Rogowski, A.C. Tai, 'Excitation efficiency of an optical fiber core source' In Structures, Sensing and Control: Proceedings of the Symposium in Orlando, Florida, 2-3 April, International Society for Optical Engineers, Washington, U.S., 1991, **1485**, pp. 9-16.

115. Egalon, C.O., R.S. Rogowski, 'Model of a thin film optical fiber fluorosensor' Chemical, Biochemical and Environmental Fiber Sensors II: Proceedings on the Symposium in San Jose, California, 19-21 September, International Society for Optical Engineers, Washington, U.S., 1990, **1368**, pp. 134-49.

116. Evans. I. , 'Cholera on the rocks', *The Lancet*, 1993, **341**, p. 300.

117. Falcai, R. , F. Baldini, P. Bechi, F. Cosi, 'In vivo entero-gastric reflux detection by optical fibres', *International Journal of Optoelectronics*, 1991, **6, No 5**, pp. 443-50.

118. Farahi, F. , D.A. Jackson, 'Temperature and strain sensing using monomode optical fiber' In Fiber Optic Sensors: Engineering and Applications: Proceedings of the Symposium in The Hague, the Netherlands, 14-5 March, International Society for Optical Engineers, Washington, U.S., 1991, **1511**, pp. 234-43.

119. Fiol, C. , S. Alexandre, N. Delpire, J.M. Valleton, E. Paris, 'Molecular resolution images of enzyme-containing Langmuir-Blodgett films', *Thin Solid Films*, 1992, **215**, pp. 88-93.

120. Freeman, M.K., L.G. Bachas, 'Fiber optic sensor for NO_x', *Analytica Chimica Acta*, 1992, **256**, pp. 269-75.

121. Freeman, M.K., L.G. Bachas, 'Fiber-optic biosensor with fluorescence detection based on immobilized alkaline phosphatase', *Biosensors and Bioelectronics*, 1992, **7**, pp. 49-55.

122. Freeman, T.N., W.R. Seitz, 'Oxygen probe based on tetrakis(alkylamino)ethylene chemiluminescence', *Analytical Chemistry*, 1981, **53, No 1**, pp. 98-102.

123. Fuh, M.S., L.W. Burgess, T. Hirshfeld, G.D. Christian, 'Single fibre optic fluorescence pH probe', *Analyst*, 1987, **112**, pp. 1159-63.

124. Gahler, C. , S. Friedrich, R.O. Miles, H. Melchior, 'Fiber optic temperature sensor using sampled homodyne detection', *Applied Optics*, 1991, **30, No 21**, pp. 2938-40.

125. Garside, B.K., T.K. Lim, J.P. Marton, 'Ray trajectories in optical fiber tapered sections', *Applied Optics*, 1978, **17, No 22**, pp. 3670-4.

126. Gautier, S.M., L.J. Blum, P.R. Coulet, 'Fibre-optic sensor with co-immobilised bacterial bioluminescence enzymes', *Biosensors*, 1989, **4**, pp. 181-94.

127. Gautier, S.M., L.J. Blum, P.R. Coulet, 'Bioluminescence-based fibre-optic sensor with entrapped co-reactant: an apporach for designing a self-contained biosensor', *Analytica Chimica Acta*, 1991, **243**, pp. 149-56.

128. Geiselhart, L. , M. Osgood, D.J. Holmes, 'Construction and evaluation of a self-luminescent biosensor', *Annals of the New York Academy of Science*, 1991, pp. 53-60

129. Giuliani, J.F., H. Wohltjen, N.L. Jarvis, 'Reversible optical waveguide sensor for ammonia vapors', *Optics Letters*, 1983, **8, No 1**, pp. 54-6.

130. Glass, T.R., S. Lackie, T. Hirschfeld, 'Effect of numerical aperture on signal level in cylindrical waveguide evanescent fluorescence', *Applied Optics*, 1987, **2, No 11**, pp. 2181-2.

131. Gloge, D. , 'Weakly guiding fibers', *Applied Optics*, 1971, **10, No 10**, pp. 2252-8.

132. Gnanasekaran, R. , H.A. Mottola, 'Flow injection determination of penicillins, using immobilized penicillinase in a single bead string reactor', *Analytical Chemistry*, 1985, **57**, pp. 1005-9.

133. Golden, J. , L.C. Shriver-Lake, G.P. Anderson, R.B. Thompson, F.S. Ligler, 'Fluorometer and tapered fiber optic probes for sensing in the evanescent wave', *Optical Engineering*, 1992, **31, No 7**, pp. 1458-62.

134. Golden, J.P., G.P. Anderson, S.Y. Rabbany, F.S. Ligler, 'An evanescent wave biosensor: fluorescent signal acquisition from tapered fiber optic probes', *unpublished work.*

135. Gollnick, K. , T. Franken, M.F. Fouda, H.R. Paur, S. Held, 'Merbromin (mercurochrome) and other xanthene dyes: quantum yields of triplet sensitizer generation and singlet oxygen formation of alcoholic solutions', *Journal of Photochemistry and Photobiology: B*, 1992, **12**, pp. 57-81.

136. Gopel, 'Sensors: A Comprehensive Survey Volume 3: Chemical and Biochemicals Part II' ed. W. Gopel, T.A. Jones, M. Kleitz, I. Lundstrom, and T. Seiyama, VCH, Cambridge, U.K., 1992,

137. Gowar, J. , in *Optical Communication Systems*, Prentice-Hall International, Inc., London, U.K., 1984,

138. Grattan, K.T., G.E. Badini, A.W. Palmer, A.C. Tseung, 'Use of sol-gel techniques for fibre-optic sensor applications', *Sensors and Actuators A*, 1991, **25-27**, pp. 483-7.

139. Grattan, K.T., A.W. Palmer, 'Infrared fluorescence "decay-time" temperature sensor', *Review of Scientific Instrumentation*, 1985, **56, No 9**, pp. 1784-7.

140. Green, N.M., 'Spectrophotometric determination of avidin and biotin', *Methods of Immunology*, pp. 418-24.

141. Green, N.M., 'Avidin: 1. The use of [^{14}C] biotin for kinetic studies and for assay', *Biochemistry Journal*, 1963, **89**, pp. 585-9.

142. Green, N.M., 'Avidin: 3: The nature of the biotin-binding site', *Biochemistry Journal*, 1963, **89**, pp 599-609.

143. Green, N.M., 'Avidin: 4: Stability at extremes of pH and dissociation into sub-units by guanidine', *Biochemistry Journal*, 1963, **89**, pp. 609-620.

144. Griffith, O.H., W.A. Houle, K.F. Kongslie, W.W. Sukow, 'Photoelectron microscopy and photoelectron quantum yields on the fluorescent dyes fluorescein and rhodamine', *Ultramicroscopy*, 1984, **12**, pp. 299-308.

145. Griffiths, D. , G. Hall, 'Biosensors - what real progress is being made?', *Trends in Biotechnology*, 1993. **11**, pp. 122-130.

146. Grynkiewicz G. , M. Poenie, R.Y. Tsien, 'A new generation of $Ca^{[2+]}$ indicators with greatly improved fluorescence properties', *The Journal of Biological Chemistry*, 1985, **260**, pp. 3440-50.

147. Guthrie, A.J., R. Narayanaswmay, D.A. Russell, 'Application of Kubelka-Munk diffuse reflectance theory to optical fibres sensors', *Analyst*, 1988, **113**, pp. 457-61.

148. Guthrie, A.J., R. Narayanaswamy, N.A. Welti, 'Solid-state instrumentation for use with optical-fibre chemical-sensors', *Talanta*, 1988, **35, No 2**, pp. 157-9.

149. Hale, Z.M., F.P. Payne, 'Fluorescent sensors based on tapered single mode optical fibres', *Sensors and Actuators*, 1994, **17**, pp. 233-40.

150. Halfan, H. , R. Abuknesha, M. Rand-Weaver, R.G. Price, D. Robinson, 'Aminomethyl coumarin acetic acid: a new fluorescent labelling agent for proteins', *Histochemical Journal*, 1986, **18**, pp. 497-9.

151. Hall, E.A., 'Overview of biosensors' in *Biosensors and Chemical Sensors: Optimizing Performance through Polymeric Materials*, ed. Peter G Edelman and Joseph Wang, American Chemical Society, Washington D.C., U.S., 1992, pp. 1-14.

152. Hall, R.H., F.M. Khambaty, M. Kothary, S.P. Keasler, 'Non-01 vibrio cholerae', *The Lancet*, 1993, **342**, p. 430.

153. Harrick, N.J., G.I. Loeb. 'Multiple internal reflection fluorescence spectrometry', *Analytical Chemistry*, 1973, **45, No 4**, pp. 687-91.

154. He, H. , O.S. Wolfbeis, 'Fluorescence based optrodes for alkali ions based on the use of ion carriers and lipophilic acid/base indicators' Chemical, Biochemical and Environmental Fiber Sensors II: Proceedings of the Symposium in San Jose, California, 19-21 September, International Society for Optical Engineers, Washington, U.S., 1990, **1368**, pp. 165-74.

155. Heideman, R.G., R.P. Kooyman, J. Greve, B.S. Altenburg, 'Simple interferometer for evanescent field refractive index sensing as a feasibility study for an immunosensor', *Applied Optics*, 1992, **30, No 12**, pp. 1474-9.

156. Hellen, E.H., D. Axelrod, 'Fluorescence emission at dielectric and metal-film interfaces', *Journal of Optical Society of America B*, 1987, **4, No 3**, pp. 337-50.

157. Hench, L.L., J.K. West, 'The sol-gel process', *Chemical Review*, 1990, **90**, pp. 33-72.

158. Herskowitz, G.J., M. Mezhoudi, 'Automated fiber optic moisture sensor system' Chemical, Biochemical and Environmental Fiber Sensors II: Proceedings of the Symposium in, International Society for Optical Engineers, Washington, U.S., 1990, **1368**, pp. 55-60.

159. Hill, K.O., R.I. MacDonald, A. Natanabe, 'Evanescent-wave amplification in asymmetric slab waveguides', *Journal of the Optical Society of America*, 1974, **64, No 3**, pp. 263-73.

160. Hlavay, J. , G. Guilbault, 'A fiber-optic biosensor for determination of hydrogen peroxide: effect of the membrane type on the immobilization of POD enzyme', *Acta Chimica Hungarica - Models in Chemistry*, 1993, **30, No 1**, pp. 83-93.

161. Hobel, W. , A. Papperger, J. Polster, 'Penicillinase optodes: substrate determinations using batch, continuous flow and flow injection analysis operation conditions', *Biosensors and Bioelectronics*, 1992, **7**, pp. 549-57.

162. Hui, H.K., S. Divers, T. Lumsden, T. Wallner, S. Weir, 'An accurate, low-cost, easily manufacturable oxygen sensor' In Chemical, Biochemical and Environmental Sensors: Proceedings of the Symposium in Los Angeles, California, 6-7 September, International Society for Optical Engineers, Washington, U.S., 1989, **1172**, pp. 233-8.

163. Hussey, C.D., J.D. Minelly, 'Optical fibre polishing with a motor-driven polishing wheel', *Electronics Letters*, 1988, **24, No 13**, pp. 805-7.

164. Ippen, E.P., C.V. Shank, 'Evanescent-field-pumped dye laser', *Applied Physics Letters*, 1972, **21, No 7**, pp. 301-2.

165. Islam, M.S., M.K. Hasan, M.A. Miah, F. Qadri, M. Yunus, R.B. Sack, M.J. Albert, 'Isolation of vibrio cholerae 0139 Bengal from water in Bangladesh', *The Lancet*, 1993, **342**, p. 430.

166. Jacob, C.O., M. Sela, R. Arnon, 'Antibodies against synthetic peptides of the B subunit of cholera toxin: cross-reaction and neutralization of the toxin', *Proceedings of the Academy of Science (USA)*, 1983, **80**, pp. 7611-5.

167. Janata, J. , 'Principles of Chemical Sensing' Plenum Press, New York, U.S., 1989,

168. Janata, J. , 'Do optical sensors really measure pH?', *Analytical Chemistry*, 1987, **59**, pp. 1351-6.

169. Jawad, S.M., J.F. Alder, 'Optical fibre sensor for detection of hydrogen cyanide in air Part 2: Theory and design of an automatic detection system', *Analytica Chimica Acta*, 1991, **246**, pp. 259-66.

170. Jesudason, M.V., T.J. John, 'Major shift in prevalence of non-01 and El Tor *vibrio cholerae*', *The Lancet*, 1993, **341**, pp. 1090-1.

171. Johnson, P. , P.B. Garland, 'Fluorescent triplet probes for measuring the rotational diffusion of membrane proteins', *Biochemical Journal*, 1982, **203**, pp. 313-21.

172. Jones, T.P., S.J. Coldiron, W.J. Deninger, M.D. Porter, 'A field-deployable dual-wavelength fiber-optic pH sensor instrument based on solid-state and electrical components', *Applied Spectroscopy*, 1991, **45, No 8**, pp. 1271-7.

173. Jones, T.J., M.D. Porter, 'Optical pH sensor based on the chemical modification of a porous polymer film', *Analytical Chemistry*, 1988, **60, No 5**, pp. 404-6.

174. Jordan, D.M., D.R. Walt, F.P. Milanovich, 'Physiological pH fiber-optic chemical sensor based on energy transfer', *Analytical Chemistry*, 1987, **59, No 3**, pp. 437-9.

175. Jorgenson, R.C., S.S. Yee, 'A fiber-optic chemical sensor based on surface plasmon resonance', *Sensors and Actuators B*, 1993, **12**, pp. 213-220.

176. Judd, L.L., A.W. Kusterbeck, P.T. Charles, F.S. Ligler, J.P. Whelan, 'The flow immunosensor used to detect the small molecular weight molecule TNT', *unpublished work*.

177. Kang, J.J., A. Tarsenfalvi, E. Fujimoto, Z. Shahrokh, S.B. Shohat, 'Specific labeling of the foot protein moiety of the triad with a novel fluorescent probe: application to the studies of conformational changes of the foot protein', *Biophysical Journal*, 1991, **59**, p. 249a.

178. Kapany, N.S., N. Silbertrust, 'Fibre optics spectrophotometer for in vivo oximetry', *Nature*, 1964, **254**, pp. 138-42.

179. Karube, I. , 'Microbiosensors based on silicon fabrication technology' in *Biosensors: Fundamentals and Applications*, ed. Anthony P.F. Turner, Isao Karube and George S. Wilson, Oxford University Press, Oxford, U.K., 1987, pp. 471-80.

180. Keasler, S.P., R.H. Hall, 'Detecting and biotyping *vibrio cholerae* 01 with multiplex polymerase chain reaction', *The Lancet*, 1993, **341**, p. 1661.

181. Kenny, R.P., T.A. Birks, K.P. Oakley, 'Control of optical fibre taper shape', *Electronics Letters*, 1991, **27**, No **18**, pp. 1654-6.

182. Kessler, M.A., J.G. Gailer, O.S. Wolfbeis, 'Optical sensor for on-line determination of solvent mixtures based on a fluorescent solvent polarity probe', *Sensors and Actuators B*, 1991, **3**, pp. 267-72.

183. Kirkbright, G.F., R. Narayanaswamy, N.A. Welti, 'Fibre-optic pH probe based on the use of an immobilised colorimetric indicator', *Analyst*, 1984, **109**, pp. 1025-8.

184. Klainer, S.M., J.M. Harris, 'The use of fiber optic chemical sensors (FOCS) in medical applications: enzyme-based systems' , International Society for Optical Engineers, Washington, U.S., 1988, pp. 139-147.

185. Kobayashi, Y. , H. Sasaki, S. Muto, S. Yamazaki, Y. Kurokawa, 'Preparation of a transparent alumina film doped with fluorescence dye and its energy transfer laser emission', *Thin Solid Films*, 1991, **200**, pp. 321-7.

186. Kogut, M. , M.R. Pollock, E.J. Tridgell, 'Purification of penicillin-induced penicillinase of Bacillus cereus NRRL 569: A comparison of its properties with those of a similarly purified penicillinase produced spontaneously by a constitutive mutant strain', *Biochimica et Biophysica Acta*, 1956, **62**, pp. 391-401.

187. Korenman, S.G., B.W. O'Malley, 'Newer methods of avidin assay', *Methods of Enzymology*, pp. 427-30.

188. Kricka, L.J., 'Chemiluminescence and bioluminescence', *Analytical Chemistry*, 1993, **65**, No **12**, pp. 460-2R.

189. Krull, U.J., R.S. Brown, R.F. DeBong, B.D. Hougham, 'Towards a fluorescent chemoreceptive lipid membrane-based optode', *Talanta*, 1988, **35**, No **2**, pp. 129-37.

190. Krull, U.J., R.S. Brown, B.D. Hougham, I.H. Brock, 'Selective interactions of Concavalin A at lipid membranes on the surface of an optical fibre', *Talanta*, 1990, **37, No 8**, pp. 801-7.

191. Kuan, S.S., G.G. Guilbart, 'Ion-selective electrodes and biosensors based on ISEs' in *Biosensors: Fundamentals and Applications*, ed. Anthony P.F. Turner, Isao Karube, and George S. Wilson, Oxford University Press, Oxford, U.K., 1987, pp. 135-52.

192. Kuffer, H. , P. Degiampietro, 'Automated determination of calcium by a new photometric method', *Clinical Chemistry*, 1975, **21, No 7**, p. 961.

193. Kulp, T.J., I. Camins, S.M. Angel, 'Enzyme-based fiber optic sensors' In Optical Fibers in Medicine III: Proceedings of the Symposium in Los Angeles, California, 13-6 January, International Society for Optical Engineers, Washington, U.S., 1988, **906**, pp. 134-8.

194. Kulp, T.J., I. Camins, S.M. Angel, C. Munkholm, D.R. Walt, 'Polymer immobilized enzyme optrodes for the detection of penicillin', *Analytical Chemistry*, 1987, **59**, pp. 2849-53.

195. Kurosawa, K. , T. Sawa, H. Sawada, A. Tanaka, N. Wakatsuki, 'Diagnostic techniques for electrical power equipment using fluorescent fiber' In Chemical, Biochemical and Environmental Fiber Sensors II: Proceedings of the Symposium in San Jose, California, 19-21 September., International Society for Optical Engineers, Washington, U.S., 1990, **1368**, pp. 150-6.

196. Kusterbeck, A.W., F.S. Ligler, 'Detection of small molecules with a flow immunosensor', *unpublished work*.

197. Kusterbeck, A.W., G.A. Wemhoff, F.S. Ligler, 'Antibody-based biosensor for continuous monitoring' in *Biosensor Technology: Fundamentals and Applications*, ed. Richard P Buck, William E Hatfield, Mirtha Umana and Edmond F Bowden, Marcel Dekker, Inc, New York, U.S., 1990, pp. 345-9.

198. Kvasnik, F. , A.D. McGrath, 'Distributed chemical sensing utilising evanescent wave interactions' In Chemical, Biochemical and Environmental Sensors: Proceedings of the Symposium in Los Angeles, California, 6-7 September, International Society for Optical Engineers, Washington, U.S., 1989, **1172**, pp. 75-82.

199. Lacroix, S. , F. Gonthier, R.J. Black, J. Bunes, 'Taperded-fiber interferometric wavelength response: the achromatic fringe', *Optics Letters*, 1988, **13, No 5**, pp. 395-7.

200. Lacroix, S. , R. Bourbonnais, F. Gonthier, J. Bunes, 'Tapered monomode optical fibers: understanding large power transfer', *Applied Optics*, 1986, **25, No 23**, pp. 4421-5.

201. Lakowicz, J.R., H. Szmacinski, K.W. Berndt, 'Fluorescence lifetime-based sensing of blood gases and cations' In Fiber Optic Medical and Fluorescent Sensors and Applications: Proceedings of the Symposium in Los Angeles, California, 23-24 January, International Society for Optical Engineers, WA, U.S., 1992, **1648**, pp. 150-163.

202. Lal, S. , M.C. Yapport, 'Development, characterization, and application of a double-waveguide evanescent sensor', *Applied Spectroscopy*, 1991, **45, No 10**, pp. 1607-12.

203. Lambeck, P.V., 'Chemo-optical micro-sensing systems' In Fiber Optic Sensors: Engineering and Applications: Proceedings of the Symposium in The Hague, The Netherlands, 14-15 March, International Society for Optical Engineers, WA, U.S., 1991, **1511**, pp. 100-13.

204. Lambeck, P.V., 'Integrated opto-chemical sensors', *Sensors and Actuators*, 1992, **8**, pp. 103-116.

205. Lee, E. , R.E. Bennen, J.B. Fenn, R.K. Chang, 'Augular distribution of fluorescence from liquids and monodispersed spheres by evanescent wave excitation', *Applied Optics*, 1979, **18, No 6**, pp. 862-8.

206. Lee, E.D., T.C. Werner, W.R. Seitz, 'Luminescence ratio indicators for oxygen', *Analytical Chemistry*, 1987, pp. 279-83.

207. Leiner, M.J., 'Luminescence chemical sensors for biomedical applications: scope and limitations', *Analytica Chimica Acta*, 1991, **255**, pp. 209-22.

208. Lew, A. , C. Depeursinge, F. Cocket, H. Berthou, O. Parriaux, 'Single-mode fiber evanescent wave spectroscopy' In OFS '84 2nd International Conference in Optical Fiber Sensors: Proceedings of the Symposium in Stuttgart, 5-7 September, VDE-Verlag GmbH, 1984, **514**, pp. 71-4.

209. Lewis, S.W., D. Price, P.J. Worsfold, 'Flow injection assays of chemiluminescence and bioluminescence detection - a review', *Journal of Bioluminescence and Chemiluminescence*, 1993, **8**, pp. 183-99.

210. Li, Y. , M. Chen, F. Ruan, W. Ng, 'Characteristics and readout correlation of flow-injection analysis for penicillin', *Analytica Chimica Acta*, 1992, **269**, pp. 34-40.

211. Li, P.Y., R. Narayanaswamy, 'Oxygen-sensitive optical fibre transducer', *Analyst*, 1989, **114**, pp. 1191-5.

212. Lieberman, R.A., 'Recent progress in intrinsic fiber-optic chemical sensing II', *Sensors and Actuators B*, 1993, pp. 43-55.

213. Lieberman, R.A., 'Recent progress in intrinsic fiber optic chemical sensing' In Chemical, Biochemical, and Environmental Fiber Sensors II (Vol 1368): Proceedings of the Symposium in San Jose, California, 19-21 September, International Society for Optical Engineers, Washington, U.S., 1990, **1368**, pp. 15-24.

214. Lieberman, R.A , L.L. Blyler, L.G. Cohen, 'A distributed fiber optic sensor based on cladding fluorescence', *Journal of Lightwave Technology*, 1990, **8, No 2**, pp. 212-20.

215. Lieberman, R.A., K.G. Brown, 'Intrinsic fiber optic chemical sensor based on two-stage fluorescent coupling' In Chemical, Biochemical, and Environmental Applications of Fibers in Boston, Massachusetts, 8-9 September, International Society for Optical Engineers, Washington, U.S., 1988, **990**, pp. 104-110.

216. Liedtke, R.J., G. Kroon, 'Automated calmagite complexometric measurement of magnesium in serum, with sequential addition of EDTA to eliminate endogenous interference', *Clinical Chemistry*, 1984, **30**, pp. 1801-4.

217. Liedtke, R.T., G. Kroon, J.D. Batjer, 'Centrifugal analysis with automated sequential reagent addition: measurement of serum calcium', *Clinical Chemistry*, 1981, **27, No 12**, pp. 2025-8.

218. Ligler, F.S., A.W. Kusterbeck, R.A. Ogert, G.A. Wemhoff, 'Drug detection using the flow immunosensor in biosensor design and application, ACS Symposium Series No 511' in *Biosensor Design and Application: ACS Symposium Series*, ed. Paul R Mathewson and John W Finley, American Chemical Society, U.S., 1992, pp. 73-80.

219. Ligler [Eigler], F.S., J. Georger, S.K. Bharia, J. Calvert, L.C. Shriver-Lake, R. Bredehorst, 'Immobilization of active agents on substrates with a silane and heterobifunctional crosslinking agent', *United States Patent*, U.S., 1991, **5077210**.

220. Lin, J. , C.W. Brown, 'Near-IR fiber-optic probe for electrolytes in aqueous solution', *Analytical Chemistry*, 1993, **65, No 3**, pp. 287-92.

221. Lin, J. , J. Herron, J.D. Andrade, M. Brizgys, 'CHaracterization of immobilized antibodies on silica surfaces', *IEEE Transactions on Biomedical Engineers*, 1988, **35, No 6**, pp. 466-71.

222. Lindstrom, F. , H. Diehl, 'Indicator for the titration of calcium plus magnesium with (Ethylenedinitrilo)tetraacetate', *Analytical Chemistry*, 1960, **32**, pp. 1123-7.

223. Lippitsch, M.E., J. Posterhofer, M.J. Leiner, O.S. Wolfbeis, 'Fibre-optic oxygen sensor with the fluorescence decay time as the information carrier', *Analytica Chimica Acta*, 1988, **205**, pp. 1-5.

224. Lippitsch, M.E., S. Drexler, 'Luminescence decay-time-based optical sensors: principles and problems', *Sensors and Actuators B*, 1993, **11**, pp. 97-101.

225. Lipson, D. , K.D. McLeaster, B. Cohn, R.E. Fischer, 'Drilled optical fiber sensors: A novel single fiber sensor' In Chemical, Biochemical and Environmental Fiber Sensors II: Proceedings of the Symposium in San Jose, California, 19-21 September, International Society for Optical Engineers, Washington, U.S., 1990, **1368**, pp. 36-43.

226. Losonsky, G.A., C.O. Tacket, S.S. Wasserman, J.B. Kaper, M.M. Levine, 'Secondary Vibrio Cholerae-specific cellular antibody responses following wild-type homologous challenge in people vaccinated with CVD 103-HgR live oral cholera vaccine: changes with time and lack of correlation with protection', *Infection and Immunity*, 1993, **61, No 2**, pp. 729-33.

227. Love, W.F., L.J. Button, 'Optical characteristics of fibre optic evanescent wave sensors' In Chemical, Biochemical and Environmental Applications of Fibers: Proceedings of the Symposium in Boston, Massachusetts, 8-9 September, International Society for Optical Engineers, Washington, U.S., 1988, **990**, pp. 175-80.

228. Love, J.D., 'Application of a low-loss criterion to optical waveguides and devices', *IEE Proceedings Part J*, 1989, **136, No 4**, pp. 225-8.

229. Love, J.D., 'Spot size, adiabaticity and diffraction in tapered fibres', *Electronics Letters*, 1986, **23, No 19**, pp. 993-4.

230. Lowe, C.R., 'Biosensors', *Trends in Biotechnology*, 1984, **2, No 3**, pp. 59-65.

231. Lukosz, W. , 'Light emission by magnetic and electric dipoles close to a plane dielectric surface: III. Radiation patterns of dipoles with arbitrary orientation', *Journal of the Optical Society of America*, 1979, **69, No 11**, pp. 1495-1503.

232. Lukosz, W. , K. Tiefenthaler, 'Sensitivity of integrated optical grating and prism couplers as (bio)chemical sensors', *Sensors and Actuators*, 1988, **15**, pp. 273-84.

233. Lundstrom, I. , B. Ivarsson, U. Jonsson, H. Elwing, 'Protein adsorption and interaction at solid surfaces' in *Polymer Surfaces and Interfaces*, ed. W J Feast and H S Munro, John Wiley and Sons, London, U.K., 1987, pp. 201-230.

234. Luo, S. , D.R. Walt, 'Fiber-optic sensors based on reagent delivery with controlled-release polymers', *Analytical Chemistry*, 1989, **61**, pp. 174-7.

235. MacCraith, B.D., 'Enhanced evanescent wave sensors based on sol-gel-derived porous glass coatings', *Sensors and Actuators B*, 1993, **11**, pp. 29-34.

236. MacCraith, B.D., V. Ruddy, C. Potter, B. O'Kelly, J.F. McGilp, 'Optical waveguide sensor using evanescent wave excitation of fluorescent dye in sol-gel glass', *Electronics Letters*, 1991, **27, No 14**, pp. 1247-8.

237. MacKenzie, H.S., 'Evanescent-field devices for non-linear optical applications' in *A dissertation submitted for Doctor of Philosophy at the Engineering Department*, University of Cambridge, Cambridge, U.K., 1990,

238. MacKenzie, H.S., F.P. Payne, 'Evanescent field amplification in a tapered single-mode optical fibre', *Electronics Letters*, 1990, **26**. pp. 130-2.

239. MacKenzie, H.S., F.P. Payne, 'Saturable absorption in a tapered single-mode optical fibre', *Electronics Letters*, 1990, **26, No 21**, pp. 1744-5.

240. Manning, B. , T. Maley, 'Immunosensors in medical diagnostics - major hurdles to commercial success', *Biosensors and Bioelectronics*, 1992, **7**, pp. 391-5.

241. Mansouri, S. , J.S. Schultz, 'A miniature optical glucose sensor based on affinity binding', *Bio/Technology*, 1984, **2**, pp. 885-90.

242. Marcuse, D. , 'Launching light into fiber cores from sources located in the cladding', *Journal of Lightwave Technology*, 1988, **6, No 8**, pp. 1273-9.

243. Martinez, A. , M.C. Moreno, C. Camara, 'Sulfide determination by N,N, dimethyl-p-phenylenediamine immobilization in cationic exchange resin using an optical fiber system', *Analytical Chemistry*, 1986, **58, No 8**, pp. 1877-81.

244. McCapra, F. , 'Potential applications of bioluminescence and chemiluminescence in biosensors' in *Biosensors: Fundamentals and Applications*, ed. Anthony P.F. Turner, Isao Karube, and George S. Wilson, Oxford University Press, Oxford, U.K., 1987, pp. 617-37.

245. McCurley, M.F., W.R. Seitz, 'Swelling of a polymer membrane for use in a glucose biosensor' , American Chemical Society, Washington D.C., U.S., 1992,

246. McGilp, J. , B. O'Kelly, B. MacCraith, V. Ruddy, 'A waveguide sensor' , *Patent Cooperation Treaty Patent Application*, U.K., 1992,

247. Meadows, D. , J.S. Schultz, 'Fiber-optic biosensors based on fluorescence energy transfer', *Talanta*, 1988, **35, No 2**. pp. 145-50.

248. Meier, H. , C. Tran-Minh, 'Determination of penicillin-V in standard solution and in fermentation broth by flow-injection analysis using fast-responding glass electrodes in different detection cells', *Analytica Chimica Acta*, 1992, **264**, pp. 13-22.

249. Meier, H. , S. Kumaran, A.M. Danna, C. Tran-Minh, 'Rapid measurement of penicllin contained in complex media using enzyme-loaded glass electrodes', *Analytica Chimica Acta*, 1991, **249**. pp. 405-11.

250. Mekalonos, J.J., 'Production and purification of cholera toxin', *Methods in Enzymology: Microbial Toxins: Tools in Enzymology*, 1988, **165**, pp. 169-75.

251. Melamed, M.D., N.M. Green, 'Avidin: 2. Purification and composition', *Biochemistry Journal*, 1963, **89**, pp. 591-9.

252. 'Antireflective coating, insulating and sodium barrier layers for liquid crystal displays', *Liquicoat Technical Notes*, Merck, Frankfurt, Germany, 1985.

253. Milano, M.J., K. Kim, 'Diode array spectrometer for the simultaneous determination of hemoglobins in whole blood', *Analytical Chemistry*, 1977, **49**, No **4**, pp. 555-9.

254. Milanovich, F.P., 'Detecting chloroorganics in groundwater: fiber-optic-based sensors permit in situ analysis', *Environmental Science and Technology*, 1986, **20**, No **5**, pp. 441-2.

255. Miyahara, Y. , K. Tsukada, H. Miyagi, W. Simon, 'Urea sensor based on an ammonia-ion-sensitive field-effect transistor', *Sensors and Actuators B*, 1991, **3**, pp. 287-93.

256. Mizutani, S. , T. Ohtake, 'Recent sensor technology in Japan', *Sensors and Actuators*, 1986, pp. 35-44.

257. Monici, M. , R.B.G. Bonifort, D. DeRossi, A. Nannini, 'Fibre-optic pH sensor for seawater monitoring' In Fiber Optic Sensors II: Proceedings of the Symposium in The Hague, The Netherlands, 31 March - 3 April, International Society for Optical Engineers, Washington, U.S., 1987, **798**, pp. 294-300.

258. Moore, E.D., P.L. Becker, K.E. Fogarty, D.A. Williams, F.S. Fay, 'Ca[2+] imaging in single living cells: theoretical and practical issues', *Cell Calcium*, 1990, **11**, pp. 157-79.

259. Mort, W.E., K. Seiler, B. Rusterholz, W. Simon, 'Design of a calcium-selective optode membrane based on neutral ionophores', *Analytical Chemistry*, 1990, **62**, No **7**, pp. 738-42.

260. Morgan, H. , D.M. Taylor, C. D'Silva, 'Surface plasmon resonance studies of chemisorbed biotin-stretavidin multilayers', *Thin Solid Films*, 1992, **209**, pp. 122-6.

261. Mortimore, D.B., J.V. Wright, 'Low-loss joints between dissimilar fibres by tapering fusion splices', *Electronics Letters*, 1986, **22**, No **6**, pp. 318-9.

262. Mosbach, K. , *Methods in Enzymology: Immobilized Enzymes*, 1976, **44**, pp. 592-3.

263. Muhammad, F.A., G. Stewart, 'D-shaped optical fibre design for methane gas sensing', *Electronics Letters*, 1992, **28**, No **13**, pp. 1205-6.

264. Muhammad, F.A., G. Stewart, 'Polarised finite-difference analysis of D-fibre and application for chemical sensing', *International Journal of Optoelectronics*, 1992, **7**, No **6**, pp. 705-21.

265. Mukharjee, S.P., 'Sol-gel processes in glass science and technology', *Journal of Non-Crystalline Solids*, 1980, **42**, pp. 477-88.

266. Munkholm, C. , D.R. Walt, F.P. Milanovich, S.M. Klainer, 'Polymer modification of fiber optic chemical sensors as a method of enhancing fluorescence signal for pH measurement', *Analytical Chemistry*, 1986, **58**, pp. 1427-30.

267. Munkholm, C. , D.R. Walt, F.P. Milanovich, 'A fiber-optic sensor for CO_2 measurement', *Talanta*, 1988, **35**, No **2**, pp. 109-112.

268. Muto, S. , A. Ando, T. Ochiai, H. Ito, H. Sawada, A. Tanaka, 'Sample gas sensor using dye-doped plastic fibers', *Japanese Journal of Applied Physics*, 1989, **28**, No **1**, pp. 125-7.

269. Narayanaswamy, R. , 'Current developments in optical biochemical sensors', *Biosensors and Bioelectronics*, 1991, **6**, pp. 467-75.

270. Narayanaswamy, R. , F. Sevilla, III, 'Paper tape analyser for gases based on optical fibres', *Analyst*, 1988, **113**, pp. 661-3.

271. Narayanaswamy, R. , F. Sevilla, III, 'Flow cell studies with immobilised reagents for the development of an optical fibre sulphide sensor', *Analyst*, 1986, **111**, pp. 1085-8.

272. Narayanaswamy, R. , D.A. Russell, F. Sevilla, III, 'Optical-fibre sensing of fluoride ions in a flow stream', *Talanta*, 1988, **35**, No **2**, pp. 83-88.

273. Nellen, P.M., W. Lukosz, 'Model experiments with integrated optical input grating couplers as direct immunosensors', *Biosensors and Bioelectronics*, 1991, **6**, pp. 517-25.

274. Nestaas, E. , D.I. Wang, H. Suzuki, L.B. Evans, 'A new sensor, the "filtration probe," for quantitative characterization of the penicillin fermentation. II The monitor of mycelial growth', *Biotechnology and Bioengineering*, 1981, **XXIII**, pp. 2815-24.

275. Nestaas, E. , D.I. Wang, 'A new sensor - the "filtration probe" - for quantitative characterization of penicillin fermentation III An automatically operating probe', *Biotechnology and Bioengineering*, 1983, XXV, pp. 1981-7.

276. Neumann, E.G., *Single-mode fibers: Fundamentals*, Springer-Verlag, London, U.K., 1988,

277. 'Projects in fiber optics applications handbook: primer in fiber optics' Newport Corporation, California, U.S., 1993, pp. 3-77.

278. Nishizawa, M. , T. Matsue, I. Uchida, 'Penicillin sensor based on a microarray electrode coated with pH-responsive polypyrrole', *Analytical Chemistry*, 1992, **64**, pp. 2642-4.

279. Niwa, M. , T. Yamamoto, N. Atigashi, 'pH-responsive plastic optical fibres modified with polyion complexed multibilayers containing a poly(methacrylic acid) segment', *Journal of the Chemistry Society, Chemical Communications*, 1991, pp. 444-5.

280. Novick, R.P., 'Micro-iodometric assay for penicillinase', *Biochemistry Journal*, 1962, **83**, pp. 236-40.

281. Offenbacher, H. , O.S. Wolfbeis, E. Furlinger, 'Fluorescence optical sensors for continuous determination of near-neutral pH values', *Sensors and Actuators*, 1986, **9**, pp. 73-84.

282. Ogert, R.A., J.E. Brown, B.R. Singh, L.C. Shriver-Lake, F.S. Ligler, 'Detection of Clostridium botulinum Toxin A using a fiber optic-based biosensor', *Analytical Chemistry*, 1992, **205**, pp. 306-12.

283. Ogert, R.A., A.W. Kusterbeck, G.A. Wemhoft, R. Burke, F.S. Ligler, 'Detection of cocaine using the flow immunosensor', *Analytical Letters*, 1992, **25, No 1**, pp. 1999-2019.

284. Opitz, N. , D.W. Lubbers, 'Electrochromic dyes, enzyme reactions and hormono-protein interactions in fluorescence optic sensor (optode) technology', *Talanta*, 1988, **35, No 2**, pp. 123-7.

285. Orvedahl, D.S., W.F. Love, R.E. Slovacek, 'Theoretical considerations for evanescent wave immunosensors in biomedical applications' In Chemical, Biochemical and Environmental Fiber Sensors III: Proceedings of the Symposium in Boston, Massachusetts, 4-5 September, International Society for Optical Engineers, Washington, U.S., 1991, **1587**, pp. 187-98.

286. Owaku, K. , M. Guto, Y. Ikariyama, M. Aizawa, 'Optical immunosensing for IgG', *Sensors and Actuators B*, 1993, **13-14**, pp. 723-4.

287. Panne, U. , R. Niessner, 'A fiber-optical sensor for polynuclear aromatic hydrocarbons based on multidimensional fluorescence', *Sensors and Actuators B*, 1993, **13-14**, pp. 288-92.

288. Papkovsky, D.B., 'Luminescent porphyrins as probes for optical (bio)sensors', *Sensors and Actuators B*, 1993, **11**, pp. 293-300.

289. Parikh, I. , P. Cuatrecasas, 'Ganglioside-agarose and cholera toxin', *Methods in Enzymology: Affinity Techniques: Enzyme Purification: Part B*, 1974, **34**, pp. 610-9.

290. Parker, C.A., 'Photoluminescence of solutions: with applications to photochemistry and analytical chemistry' Elsevier Publishing Company, Ltd, London, U.K., 1968,

291. Paul, P.H., G. Kychakoff, 'Fiber-optic evanescent field absorption sensor', *Applied Physics Letters*, 1987, **51, No 1**, pp. 12-4.

292. Payne, F.P., C.D. Hussey, M.S. Yataki, 'Modelling fused single-mode-fibre couplers', *Electronics Letters*, 1985, **21, No 11**, pp. 461-2.

293. Payne, F.P., H.S. MacKenzie, 'Novel applications of monomode fibre tapers' In Fiber-Optic Metrology and Standards: Proceedings of the Symposium in the Hague, the Netherlands, 12-14 March, International Society for Optical Engineers, Washington, U.S., 1991, **1504**, pp. 165-75.

294. Payne, F.P., Z.M. Hale, 'Deviation from Beer's law in multimode optical fibre evanescent field sensors', *International Journal of Optoelectronics*, 1994, **8**,

295. Pendock, G.J., 'Optical fibre dye lasers' *A dissertation submitted for Doctor of Philosophy at the Engineering Department*, University of Cambridge, U.K., 1993.

296. Peng, G.D., J.D. Love, A. Ankiewicz, 'Optimum design of adiabatic weakly guiding nonlinear optical fibre tapers', *Optical and Quantum Electronics*, 1991, **23**, pp. 1179-88.

297. Perret, C.J., 'Iodometric assay of penicillinase', *Nature*, 1954, **174, No 4439**, pp. 1012-3.

298. Petersen, J.V., R.E. Dessy, 'Direct exchange of metal ions onto silica waveguides' In Chemical, Biochemical and Environmental Fiber Sensors II: Proceedings of the Symposium in San Jose, California, 19-21 September, International Society for Optical Engineers, Washington, U.S., 1990, **1368**, pp. 61-72.

299. Peterson, J.I., S.R. Goldstein, R.V. Fitzgerald, D.K. Buckhold, 'Fiber optic pH probe for physiological use', *Analytical Chemistry*, 1980, **52**, pp. 864-9.

300. Peterson, J.I., R.V. Fitzgerald, D.K. Buckhold, 'Fiber-optic probe for in vivo measurement of oxygen partial pressure', *Analytical Chemistry*, 1984, **56, No 1**, pp. 62-7.

301. Petrea, R.D., M.J. Sepaniak, T. Vo-Dinh, 'Fiber-optic time-resolved fluorimetry for immunoassays', *Talanta*, 1988, **35, No 2**, pp. 139-44.

302. Piraud, C. , E.K. Mwarania, J. Yao, K. O'Dwyer, D.J. Schiffrin, J.S. Wilkinson, 'Optochemical transduction on planar optical waveguides', *Journal of Lightwave Technology*, 1992, **10,** No **5**, pp. 693-9.

303. Piraud, C. , E. Mwarania, G. Wylangowski, J. Wilkinson, K. O'Dwyer, D.J. Schiffrin, 'Optoelectrochemical thin-film chlorine sensor employing evanescent fields on planar waveguides', *Analytical Chemistry*, 1992, **64**, pp. 651-5.

304. Place, J.F., R.M. Sutherland, C. Dahne, 'Opto-electronic immunosensors: a review of optical immunoassay at continuous surfaces', *Biosensors*, 1985, **1**, pp. 321-53.

305. Posch, H.E., M.J. Leiner, O.S. Wolfbeis, 'Towards a gastric pH-sensor: an optrode for the pH 0-7 range', *Fresenius Zeitschrift für Analytische Chemie*, 1989, **334**, pp. 162-5.

306. Posch, H.E., O.S. Wolfbeis, J. Pusterhofer, 'Optical and fibre-optics sensors for vapours of polar solvents', *Talanta*, 1988, **35, No 2**, pp. 89-94.

307. Poscio, P. , C. Depeursinge, G. Vorin, B. Sheja, O. Parriaux, 'Realization of a miniaturized optical sensor for biomedical applications', *Sensors and Actuators A*, 1990, **21-23**, pp. 1092-6.

308. Quoi, K.W., R.A. Lieberman, L.G. Cohen, D.S. Schenk, J.R. Simpson, 'Rare-earth doped optical fibers for temperature sensing', *Journal of Lightwave Technology*, 1992, **10, No 6**, pp. 847-52.

309. Rabbany, S.Y., A.W. Kusterbeck, R. Bredehorst, F.S. Ligler, 'Effect of antibody density on the kinetics and detection sensitivity of a flow immunosensor', *unpublished work.*

310. Rao, B.S., J.B. Puschett, K. Matyjaszewski, 'Preparation of pH sensors by covalent linkage of dye molecules to the surface of polystyrene optical fibers', *Journal of Applied Polymer Science*, 1991, **43**, pp. 925-8.

311. Reichert, J. , W. Sellien, H.I. Ache, 'Development of a fiber-optic sensor for the detection of ammonia in envrionmental waters', *Sensors and Actuators A*, 1991, **25-7**, pp. 481-2.

312. Reisfeld, R. , M. Eyal, R. Grishi, 'Spectroscopic behaviour of fluorescein and its di(mercury acetate) adduct in glasses', *Chemical Physics Letters*, 1987, **138, No 4**, pp. 377-83.

313. Rhines, T.D., M.A. Arnold, 'Simplex optimization of a fiber-optic ammonia sensor based on multiple indicators', *Analytical Chemistry*, 1988, **60, No 1**, pp. 76-81.

314. Rhines, T.D., M.A. Arnold, 'Fiber-optic biosensor for urea based on sensing of ammonia gas', *Analytica Chimica Acta*, 1989, **227**, pp. 387-96.

315. Richardson, K. , J.B. Kaper, M.M. Levine, 'Human immune response to Vibrio cholerae 01 whole cells and isolated outer membrane techniques', *Infection and Immunity*, 1989, **57**, pp. 495-501.

316. Robinson, G.A., 'Optical immunosensing systems - meeting the market needs', *Biosensors and Bioelectronics*, 1991, **6**, pp. 183-91.

317. Rogers, A.J., 'Distributed optical-fibre sensing' In Fiber-Optic Metrology and Standards: Proceedings of the Symposium in The Hague, The Netherlands, 12-4 March, International Society for Optical Engineers, Washington, U.S., 1991, **1504**, pp. 2-24.

318. Rogers, K.R., N.A. Anis, J.J. Valdes, M.E. Eldefrawi, 'Fiber-optic biosensors based on total internal-reflection fluorescence' ed. Paul R Mathewson and John W Finley, American Chemical Society, Washington D.C., U.S., 1992,

319. Romaniuk, R.S., R. Stepien, 'Glass-ceramic fiber optic sensors' In Chemical, Biochemical and Environmental Fiber Sensors II: Proceedings of the Symposium in San Jose, California, 19-21 September International Society for Optical Engineers, Washington, U.S., 1990, **1368**, pp. 73-84.

320. Ross, I.N., A. Mbanu, 'Optical monitoring of glucose concentration', *Optics and Laser Technology*, 1985, pp. 31-5.

321. Ruddy, V. , 'An effective attenuation coefficient for evanescent wave spectroscopy using multimode fiber', *Fiber and Integrated Optics*, 1990, **9**, pp. 142-50.

322. Ruddy, V. , S. McCabe, 'Detection of propane by IR-ATR in a Teflon-clad fluoride glass optical fiber', *Applied Spectroscopy*, 1990, **44, No 9**, pp. 1461-3.

323. Ruddy, V. , B.D. MacCraith, J.A. Murphy, 'Evanescent wave absorption spectroscopy using multimode fibers', *Journal of Applied Physics*, 1990, **67**, pp. 6070-4.

324. Ruddy, V. , B.D. MacCraith, J.A. Murphy, 'Spectroscopy of fluids using evanescent wave absorption on multimode fiber' In Chemical, Biochemical and Environmental Sensors: Proceedings of the Symposium in Los Angeles, California, 6-7 September, International Society for Optical Engineers, Washington, U.S., 1989, **1172**, pp. 83-92.

325. Ruzicka, J. , J. Flossdorf, 'Characterization of immobilized enzymes by flow-injection techniques with variable forward flow', *Analytica Chimica Acta*, 1985, **218**, pp. 291-301.

326. Saari, L.A., W.R. Seitz, 'Optical sensor for beryllium based on immobilised morin fluorescence', *Analyst*, 1984, **109**, pp. 655-7.

327. Saari, L.A., W.R. Seitz, 'pH sensor based on immobilised fluoresceinamine', *Analytical Chemistry*, 1982, **54**, pp. 821-3.

328. Saari, L.A., W.R. Seitz, 'Immobilized morin as fluorescence sensor for determination of aluminum^{3+}', *Analytical Chemistry*, 1985, **55, No 7**, pp. 667-70.

329. Saari, L.A., W.R. Seitz, 'Immobilized calcein for metal ion preconcentration', *Analytical Chemistry*, 1986, **56, No 4**, pp. 810-3.

330. Sadaoka, V. , M. Matsuguchi, Y. Sakai, 'Optical-fibre and quartz oscillator type gas sensors: Humidity detection by Nafion® film with crystal violet and related compounds', *Sensors and Actuators A*, 1991, **25-7**, pp. 489-92.

331. Santos, J.L., D.A. Jackson, 'Coherence sensing of time-addressed optical-fiber sensors illuminated by a multimode laser diode', *Applied Optics*, 1991, **30** No 34, pp. 5068-76.

332. Sarkar, B.L., S.P. De, B.K. Sircar, S. Garg, G.B. Nair, B.C. Deb, 'Polymyxin B sensitive strains of *vibrio cholerae* non-01 from recent epidemic in India', *The Lancet*, 1993, **341**, p. 1090.

333. Savory, J. , K.S. Margrey, J.R. Shipe, Jr, M.G. Savory, M.H. Margrey, T.E. Mifflin, M.R. Wills, J.C. Boyd, 'Stabilization of the calmagite reagent for automated measurement of magnesium in serum and urine', *Clinical Chemistry*, 1985, **31, No 3**, pp. 487-8.

334. Schaffar, B.P., O.S. Wolfbeis, 'A calcium-selective optrode based on fluorimetric measurement of membrane potential', *Analytica Chimica Acta*, 1989, **217**, pp. 1-9.

335. Schaffar, B.P., O.S. Wolfbeis, A. Leitner, 'Optical sensors Part 23. Effect of Langmuir-Blodgett layer composition on the response of ion-selective optrodes for potassium, based on fluorimetric measurement of membrane potential', *Analyst*, 1988, **113**, pp. 693-7.

336. Schaffar, B.P., O.S. Wolfbeis, 'A sodium-selective optr ,e', *Mikrochimica Acta*, 1989, **III**, pp. 109-16.

337. Schnitzer, I. , A. Katzir, U. Schiessl, W.J. Riedel, M. Tacke, 'Evanescent field IR spectroscopy using optical fibres and tunable diode lasers', *Materials Science and Engineering*, 1990, **B5**, pp. 333-7.

338. Schnitzer, I. , A. Katzir, U. Schiessl, W.J. Riedel, M. Tacke, 'Fiber-optic-based evanescent field chemical sensor using tunable diode lasers for the midinfrared spectral region', *Journal of Applied Physics*, 1989, **66, No 11**, pp. 5667-70.

339. Schultz, J.S., 'Design of fibre-optic biosensors based on bioreceptors' in *Biosensors: Fundamentals and Applications*, ed. Anthony P.F. Turner, Isao Karube, and George S. Wilson, Oxford University Press, Oxford, U.K, 1987, pp. 638-54.

340. Schultz, J.S., M. Meyerhoff, 'Status of monitoring in biotechnology', *Enzyme Microbiology Technology*, 1987, **9**, pp. 697-9.

341. Seitz, W., 'Chemical sensors based on fiber optics', *Analytical Chemistry*, 1984, **56, No 1**, pp. 16A-34A.

342. Seitz, W.R., 'Optical sensors based on immobilized reagents' in *Biosensors: Fundamentals and Applications*, ed. Anthony P.F. Turner, Isao Karube, and George S. Wilson, Oxford University Press, Oxford, U.K., 1987, pp. 599-616.

343. Sethi, R.S., 'Transducer aspects of biosensors', *GEC Journal of Research*, 1991, **9, No 2**, pp. 81-96.

344. Shahriari, M.R., Q. Zhou, G.H. Sigel, Jr, 'Porous optical fibers for high-sensitivty ammonia-vapor sensors', *Optics Letters*, 1988, **13, No 5**, pp. 407-9.

345. Shankar, P.M., L.C. Bobb, H.D. Krumboltz, 'Coupling of modes in bent biconically tapered single-mode fibers', *Journal of Lightwave Technology*, 1991, **9, No 7**, pp. 832-7.

346. Sharma, A. , O.S. Wolfbeis, 'Fiberoptic oxygen sensor based on fluorescence quenching and energy transfer', *Applied Spectroscopy*, 1988, **42, No 6**, pp. 1009-11.

347. Sharma, A. , O.S. Wolfbeis, 'Fiber optic fluorosensor for sulfur dioxide based on energy transfer and exciplex quenching' In Chemical, Biochemical and Environmental Applications of Fibers: Proceedings of the Symposium in Boston, Massachusetts, 8-9 September, International Society for Optical Engineers, Washington, U.S., 1988, **990**, pp. 116-20.

348. Shaw, D.J., 'Introduction to colloid and surface chemistry' Butterworths and Company, Publishers, Ltd, London, U.K., 1980,

349. Sheem, S.K., T.G. Giallorenzi, 'Single-mode fibre-optical power divider encapsulated etching technique', *Optics Letters*, 1979, **4**, pp. 29-31.

350. Shimanouchi, H. , T. Imai, S. Aoyagi, 'A simple, versatile automatic flow time measurement system for viscometers using optical fibre sensors', *Measurement Science Technology*, 1990, **1**, pp. 85-6.

351. Shriver-Lake, L.C., G.P. Anderson, J.P. Golden, F.S. Ligler, 'The effect of tapering the optical fiber on evanescent wave measurements', *Analytical Letters*, 1992, **25, No 7**, pp. 1183-99.

352. Shriver-Lake, L.C., R.A. Ogert, F.S. Ligler, 'A fiber-optic evanescent-wave immunosensor for large molecules'. *Sensors and Actuators B*, 1993, **11**, pp. 239-43.

353. Sloper, A.N., M.T. Flanagan, 'Scattering in planar surface waveguide immunosensors', *Sensors and Actuators B*, 1993, **11**, pp. 537-42.

354. Sloper, A.N., J.K. Deacon, M.T. Flanagan, 'A planar indium phosphate monomode waveguide evanescent wave immunosensor', *Sensors and Actuators B*, 1990, **1**, pp. 589-91.

355. Slovacek, R.E., S.C. Furlong, W.F. Love, 'Feasibility study of a plastic evaescent wave sensor', *Sensors and Actuators B*, 1993, **11**, pp. 307-11.

356. Smardzewski, R.R., 'Multi-element optical waveguide sensor: general concept and design', *Talanta*, 1988, **35, No 2**, pp. 95-101.

357. Snyder, A.W., W.R. Young, 'Modes of optical waveguides', *Journal of the Optical Society of America*, 1978, **68, No 3**, pp. 297-309.

358. Snyder, A.W., J.D. Love, *Optical Waveguide Theory*, Chapman and Hall, London, U.K., 1991, pp. 208-355.

359. Soares, E.A., T.M. Dantas, 'Bare fiber temperature sensor' In Fiber Optic and Laser Sensors VIII: Proceedings of the Symposium in San Jose, California, 17-19 September, International Society for Optical Engineers, Washington, U.S., 1990, **1367**, pp. 261-5.

360. Sorenson, *Methods in Enzymology*, 1955, **1**, p. 143.

361. Sorin, W.V., B.Y. Kim, H.J. Shaw, 'Highly selective evanescent modal filter for two-mode optical fibers', *Optics Letters*, 1986, **11, No 9**, pp. 581-3.

362. Sorin, W.V., K.P. Jackson, H.J. Shaw, 'Evanescent amplification in a single-mode optical fibre', *Electronics Letters*, 1983, **19, No 20**, pp. 820-2.

363. Speiser, S. , F.L. Chisena, 'Optical bistability in fluorescein dyes', *Applied Physics B*, 1988, **45**, pp. 137-44.

364. Speiser, S. , V.H. Houlding, J.T. Yardley, 'Nonlinear optical properties of organic dye dimer-monomer systems', *Applied Physics B*, 1988, **45**, pp. 237-43.

365. Starodub, N.F., P.Y. Arenkov, A.E. Rachkov, V.A. Berezin, 'Fiber optic immunosensors for detection of some drugs', *Sensors and Actuators B*, 1993, **13-14**, pp. 728-31.

366. Steffen, R.L., F.E. Lytle, 'Multipoint measurements in optically dense media by using two-photon excited fluorescence and a fiber-optic star coupler', *Analytica Chimica Acta*, 1988, **215**, pp. 203-10.

367. Steiner, G. , C.P. Renschen, 'Determination of the evanescent-field absorption using optics elements by means of totally reflected Gaussian beams', *Sensors and Actuators B*, 1993, **11**, pp. 515-20.

368. Stewart, G. , J. Norris, D.F. Clark, B. Culshaw, 'Evanescent-wave chemical sensors - a theoretical evaluation', *International Journal of Optoelectronics*, 1991, **6, No 3**, pp. 227-38.

369. Stewart, G. , J. Norris, D. Clark, M. Tribble, I. Andonovic, B. Culshaw, 'Chemical sensing by evanescent field absorption: the sensitivity of optical waveguides' In Chemical, Biochemical and Environmental Applications of Fibers: Proceedings of the Symposium in Boston, Massachusetts, 8-9 September, International Society for Optical Engineers, Washington, U.S., 1988, **990**, pp. 188-95.

370. Stewart, G. , D.F. Clark, B. Culshaw, I. Andovic, 'Referencing systems for evanescent wave sensors' In Fibre Optics '90: Proceedings of the Symposium in London, England, 24-6 April, International Society for Optical Engineers, Washington, U.S., 1990, **1314**, pp. 262-9.

371. Sutherland, R.M., C. Dahne, 'IRS devices for optical immunoassays' in *Biosensors: Fundamentals and Applications*, ed. Anthony P.F. Turner, Isao Karube, and George S. Wilson, Oxford University Press, Oxford, U.K., 1987, pp. 655-678.

372. Sutherland, R. , C. Dahne, J. Place, 'Preliminary results obtained with a no-label, homogeneous, optical immunoassay for human immunoglobulin G', *Analytical Letters*, 1984, **B1, No 17**, pp. 43-53.

373. Sutherland, R.M., C. Dahne, J.F. Place, A.S. Ringrose, 'Optical detection of antibody-antigen reactions at a glass-liquid interface', *Clinical Chemistry*, 1984, **30, No 9**, pp. 1533-8.

374. Swerdlow, D.L., A.A. Ries, '*Vibrio cholerae* non-01 - the eighth pandemic?', *The Lancet*, 1993, **342**, pp. 382-3.

375. Tabacco, M. , Q. Zhou, B. Nelson, 'Chemical sensors for environmental monitoring' In Chemical, Biochemical and Environmental Fiber Sensors III: Proceedings of the Symposium in Boston Massachusetts, 4-5 September, International Society for Optical Engineers, Washington, U.S., 1991, **1587**, pp. 271-7.

376. Tacket, C.O., G. Losonsky, J.P. Nataro, S.J. Cryz, R. Adelman, J.B. Kaper, M.M. Levine, 'Onset and duration of protective immunity in challenged volunteers after vaccination with live oral cholera vaccine CVD 103-HgR', *The Journal of Infectious Diseases*, 1992, **166**, pp. 837-41.

377. Tai, H. , H. Tanaka, T. Yoshino, 'Fiber-optic evanescent-wave methane-gas sensor using optical absorption for the 3.392 micron line of a He-Ne laser', *Optics Letters*, 1987, **12, No 6**, pp. 437-9.

378. Takeo, T. , H. Hattori, 'Application of a fiber optic refractometer for monitoring skin condition' In Chemical, Biochemical and Environmental Fiber Sensors III: Proceedings of the Symposium in Boston, Massachusetts, 4-5 September, International Society for Optical Engineers, Washington, U.S., 1991, **1587**, pp. 284-7.

379. Takeuchi, Y. , J. Noda, 'Novel fiber coupler tapering process using a microheater', *IEEE Photonics Technology Letters*, 1992, **4, No 5**, pp. 465-7.

380. Tam, H.Y., 'Simple fusion splicing technique for reducing splicing loss between standard singlemode fibres and erbium-doped fibres', *Electronics Letters*, 1991, **27, No 17**, pp. 1597-9.

381. Taylor, H.F., 'Application of guided-wave optics in signal processing and sensing', *Proceedings of the IEEE*, 1987, **75, No 11**, pp. 1524-35.

382. Taylor, J.A., E.A. Young, 'Multiplexed fluorescence detector for capillary electrophoesis using axial optical fiber illumination', *Analytical Chemistry*, 1993, **65, No 7**, pp. 956-60.

383. Thevenin, B.J., Z. Shahrokh, R.L. Willard, E.K. Fujimoto, N. Ikemoto, S.B. Shohet, 'A novel reagent for functionally-directed site-specific fluorescent labeling of proteins', *Biophysical Journal*, 1991, **59**, p. 358a.

384. Thompson, R.B., F.S. Ligler, 'Chemistry and technology of evanescent wave biosensors' in *Biosensors with fiberoptics*, ed. D L Wise and L B Wingard, Humana Press, Inc, New Jersey, U.S., 1991, pp. 111-38.

385. Thompson, R.B., C.A. Villarruel, 'Waveguide-binding sensor for use with assays', *US Patent*, 1991, **5061857**,

386. Thompson, R.B., E.R. Jones, 'Enzyme-based fiber optic zinc biosensor', *Analytical Chemistry*, 1993, **65, No 6**, pp. 730-4.

387. Thompson, R.B., J.R. Lakowicz, 'Fiber optic pH sensor based on phase fluorescence lifetimes', *Analytical Chemistry*, 1993, **65, No 7**, pp. 853-6.

388. Thompson, R.B., F.S. Ligler, 'Recent developments in fiber optic biosensors' In Microsensors and Catheter-based Imaging Technology: Proceedings of the Symposium in Los Angeles, California, 11-12 January, International Society for Optical Engineers, Washington, U.S., 1988, **904**, pp. 27-34.

389. Tomita, S. , H. Tachino, N. Kasahara, 'Water sensor with optical fiber', *Journal of Lightwave Technology*, 1990, **8, No 12**, pp. 1829-32.

390. Trettnak, W. , M.J. Leiner, O.S. Wolfbeis, 'Fibre-optic glucose sensor with a pH optrode as the transducer', *Biosensors*, 1988, **4**, pp. 15-26.

391. Trettnak, W. , M.J. Leiner, O.S. Wolfbeis, 'Optical sensors Part 34: Fibre optic glucose biosensor with an oxygen optrode as the transducer', *Analyst*, 1988, **113**, pp. 1519-23.

392. Trettnak, W. , O.S. Wolfbeis, 'A fully reversible fiber optic lactate biosensor based on the intrinsic fluorescence of lactate monooxygenase', *Fresenius Zeitschrift Analytische Chemie*, 1989, **334**, pp. 427-30.

393. Tromberg, B.J., J.F. Eastham, M.J. Sepaniak, 'Optical fiber fluoroprobes for biological measurements', *Applied Spectroscopy*, 1984, **38, No 1**, pp. 38-42.

394. Tromberg, B.J., M.J. Sepaniak, T. Vo-Dinh, G.D. Griffin, 'Fiber-optic chemical sensors for competitive binding fluoroimmunoassay', *Analytical Chemistry*, 1987, **59, No 8**, pp. 1226-30.

395. Tseng, S. , C. Chen, 'Side-polished fibres', *Applied Optics*, 1992, **31, No 18**, pp. 3438-47.

396. Ulrich, R. , H.P. Weber, 'Solution-deposited thin films as passive and active light guides', *Applied Optics*, 1972, **11, No 2**, pp. 428-34.

397. Urbano, E. , H. Offenbacher, O.S. Wolfbeis, 'Optical sensor for continuous determination of halides', *Analytical Chemistry*, 1984, **56**, pp. 427-9.

398. Vandevyver, M. , A. Barraud, 'Methods of characterization for Langmuir-Blodgett films', *Journal of Molecular Electronics*, 1988, **4**, pp. 207-22.

399. Ventura, S. , M. Silva, D. P'erez-Bendito, 'Stopped-flow chemiluminescence spectrometry to improve the determination of penicllins based on the luminol-iodine reaction', *Analytica CHimica Acta*, 1992, **266**, pp. 301-7.

400. Vera, J.C., C.I. Rivas, P.A. Cortes, J.O. Carcamo, J. Delgado, 'Purification, amino terminal analysis, and peptide mapping of proteins after in situ postelectrophoretic fluorescent labeling', *Analytical Biochemistry*, 1988, **174**, pp. 38-45.

401. Villarruel, C.A., D.D. Dominguez, A. Dandridge, 'Evanescent wave fiber optical chemical sensor' In Fiber Optic Sensors II: Proceedings of the Symposium in The Hague, the Netherlands, 31 March - 3 April, International Society for Optical Engineers, Washington, U.S., 1987, **798**, pp. 225-9.

402. Vo-Dinh, T. , B.J. Tromberg, G.D. Griffin, K.R. Ambrose, M.J. Sepaniak, E.M. Gardenhire, 'Antibody-based fiberoptics biosensor for the carcinogen benzo(a)pyrene', *Applied Spectroscopy*, 1987, **41, No 5**, pp. 735-8.

403. Vurek, G.G., P.J. Feustel, J.W. Seneringhaus, 'A fiber optic pCO_2 sensor', *Annals of Biomedical Engineering*, 1983, **11**, pp. 499-510.

404. Walczak, I.M., W.F. Love, R.E. Slovecek, 'A sensitive fiber optic immunoassay' In Optical Fibers in Medicine VI: Proceedings of the Symposium in Los Angeles, California, 23-5 January, International Society for Optical Engineers, Washington, U.S., 1991, **1420**, pp. 2-12.

405. Walczak, I.M., W.F. Love, T.A. Cook, R.E. Slovacek, 'The application of evanescent wave sensing to a high-sensitivity fluoroimmunoassay', *Biosensors and Bioelectronics*, 1991, **7**, pp. 39-48.

406. Walters, B.S., T.J. Nielsen, M.A. Arnold, 'Fiber-optic biosensor for ethanol based on an internal enzyme concept', *Talanta*, 1988, **35, No 2**, pp. 151-5.

407. Wangsa, J. , M.A. Arnaold, 'Fiber-optic biosensors based on the fluorometric detection of reduced nicotinamide adeninedinucleotide', *Analytical Chemistry*, 1988, **60, No 10**, pp. 1080-2.

408. Weetall, H.H., 'Covalent coupling methods for inorganic support materials', *Methods of Enzymology: Immobilized Enzymes*, 1976, **44**, pp. 134-48.

409. Wei, R. , 'Assay of avidin', *Methods of Enzymology: Avidin*, pp. 424-7.

410. Wemhoff, G.A., A.W. Kusterbeck, F.S. Ligler, 'Drug detection by using an antibody-based sensor: the flow immunosensor', *NRL Review*, 1991,

411. Wemhoff, G.A., S.Y. Rabbany, A.W. Kusterbeck, R.A. Ogert, R. Bredehorst, F.A. Ligler, 'Kinetics of antibody binding at solid-liquid interfaces in flow', *unpublished work.*

412. Williamson, M.L., D.H. Atha, D.J. Deeder, P.V. Sundaram, 'Anti-T2 monoclonal antibody immobilization on quartz fibers: stability and recognition of T2 mycotoxin', *Analytical Letters*, 1989, **22**, No **4**, pp. 803-16.

413. Wilson, G.S., 'Fundamentals of amperometric sensors' in *Biosensors: Fundamentals and Applications*, ed. Anthony P.F. Turner, Isao Karube, and George S. Wilson, Oxford University Press, Oxford, U.K., 1987, pp. 165-79.

414. Wingard Jr, L.B., J. Castner, 'Potentiometric biosensors based on redox electrodes' in *Biosensors:Fundamentals and Applications*, ed. Anthony P.F. Turner, Isao Karube, and George S. Wilson, Oxford University Press, Oxford, U.K., 1987, pp. 153-60.

415. Wolfbeis, O.S., 'Biomedical applications of fibre optic chemical sensors', *International Journal of Optoelectronics*, 1991, **6**, **No 5**, pp. 425-41.

416. Wolfbeis, O.S., 'Chemical sensors - survey and trends', *Fresenius' Zeitschrift fur Analytische Chemie*, 1990, **337**, pp. 522-7.

417. Wolfbeis, O.S., 'Feasibility of optically sensing two parameters simultaneously using one indicator' In Chemical, Biochemical and Environmental Fibre Sensors II: Proceedings of the Symposium in San Jose, California, 19-21 September, International Society for Optical Engineers, Washington, U.S., 1990, **1368**, pp. 218-22.

418. Wolfbeis, O.S., 'Fiber-optic probe for kinetic determination of enzyme activities', *Analytical Chemistry*, 1986, **58**, **No 13**, pp. 2874-6.

419. Wolfbeis, O.S., P. Hochmuth, 'A new method for the endpoint determination in argonmetry using halide-sensitive fluorescent indicators and fiber optical light guides', *Mikrochimica Acta*, 1984, **III**, pp. 129-48.

420. Wolfbeis, O.S., M.J. Leiner, H.E. Posch, 'A new sensing material for optical oxygen measurement, with the indicator embedded in an aqueous phase', *Mikrochimica Acta*, 1986, **III**, pp. 359-66.

421. Wolfbeis, O.S., H. Offenbacher, 'Fluorescence sensor for monitoring ionic strength and physiological pH values', *Sensors and Actuators*, 1986, **9**, pp. 85-91.

422. Wolfbeis, O.S., H. Offenbacher, H. Kroneis, H. Marsoner, 'A fast responding fluorescence sensor for oxygen (fluorimetric analysis IX)', *Mikrochimica Acta*, 1984, **I**, pp. 153-8.

423. Wolfbeis, O.S., H.E. Posch, 'Optical sensors Part 20. A fibre optic ethanol biosensor', *Fresenius Zeitschrift fur Analytische Chemie*, 1988, **332**, pp. 255-7.

424. Wolfbeis, O.S., H.E. Posch, H.W. Kroneis, 'Fiber optical fluorosensor for determination of halothane and/or oxygen', *Analytical Chemistry*, 1985, **57**, pp. 2556-61.

425. Wolfbeis, O.S., B.P. Schaffar, E. Kaschnitz, 'Optical fibre titrations Part 3. Construction and performance of a fluorimetric acid-base titrator with a blue LED as a light source', *Analyst*, 1990, **111**, pp. 1331-4.

426. Wolfbeis, O.S., A. Sharma, 'Fibre-optic fluorimetric for sulphur dioxide', *Analytica Chimica Acta*, 1988, **208**, pp. 53-8.

427. Wolfbeis, O.S., E. Urbano, 'A fluorimetric, heavy-metal-free method for the analysis of chlorine, bromine, and iodine in organic materials', *Fresenius Zeitschrift fur Analytische Chemie*, 1983, **314**, pp. 577-81.

428. Wolfbeis, O.S., E. Urbano, 'Fluorescence quenching method for determination of two or three components', *Analytical Chemistry*, 1983, **55, No 12**, pp. 1904-6.

429. Wolfbeis, O.S., L.J. Weis, M.J. Leiner, W.E. Ziegler, 'Fiber-optic fluorosensor for oxygen and carbon dioxide', *Analytical Chemistry*, 1988, **60**, pp 2028-30.

430. Wolthius, R. , D. McCrae, E. Saaski, J. Hartl, G. Mitchell, 'Development of a medical fiber-optic pH sensor based on optical absorption', *IEEE Transactions on biomedical engineering*, 1992, **39, No 5**, pp. 531-7.

431. Wolthius, R.A., D. McCrae, J.C. Hartl, E. Saaski, G.K. Mitchell, K. Garcin, R. Willard, 'Development of a medical fiber-optic oxygen sensor based on optical absorption change', *IEEE Transactions on biomedical engineering*, 1992, **39, No 2**, pp. 185-93.

432. Woods, B.A., J. Ruzicka, G.D. Christian, N.J. Rose, R.J. Charlson, 'Measurement of rainwater pH by optosensing: flow injection analysis', *Analyst*, 1988, **113**,

433. Wyatt, W.A., G.E. Poirier, F.V. Bright, G.M. Hieftje, 'Fluorescence spectra and lifetimes of several fluorophores immobilised on nonionic resins for use in fiber-optic sensors', *Analytical Chemistry*, 1987, **59, No 4**, pp. 572-6.

434. Xie, X. , A.A. Sulieman, G.G. Guilbault, 'A fluorescence-based fiber optic biosensor for the flow-injection analysis of penicillin', *Biotechnology and Bioengineering*, 1992, **39**, pp. 1147-50.

435. Yalow, R.S., S.A. Berson, 'Assay of plasma insulin in human subjects by immunological methods', *Nature*, 1959, **184, No 4699**, pp. 1648-9.

436. Yeh, Y. , C.E. Lee, R.A. Atkins, W.N. Gibler, H.F. Taylor, 'Fiber optic sensor for substrate temperature monitoring', *Journal of Vacuum Science Technology A*, 1990, **8, No 4**, pp. 3247-50.

437. Yerian, T.D., G.D. Christian, J. Ruzicka, 'Flow injection analysis as a diagnostic tool for development and testing of a penicillin sensor.', *Analytical Chemistry*, 1988, **60**, pp. 1250-6.

438. Yuan, P. , D.R. Walt, 'Calculation for fluorescence modulation by absorbing species and its application to measurements using optical fibers', *Analytical Chemistry*, 1987, **59**, pp. 2391-4.

439. Zhao, S. , W.M. Reichert, 'Protein adsorption using an evanescent chemical sensor with a fused optical fiber coupler', *Journal of Colloid and Interface Science*, 1990, **140, No 1**, pp. 294-7.

440. Zhao, S. , W.M. Reichert, 'Influence of biotin liquid surface density and accessibility on avidin binding to the tip of an optical fiber sensor', *Langmuir*, 1992, **8**, pp. 2785-91.

441. Zhao, S. , W.M. Reichert, 'Modeling of fluorescence emission from cyanine-dye impregnated Langmuir-Blodgett films deposited on the surface of an optical fiber', *Thin Solid Films*, 1991, **200**, pp. 363-73.

442. Zhao, Z. , T. Shen, H. Xu, 'The absorption and structure of fluorescein and its ethyl derivatives in various solutions', *Spectrochimica Acta A*, 1989, **45, No 11**, pp. 1113-6.

443. Zhong, L. , G. Li, 'Biosensor based on ISFET for penicllin determination', *Sensors and Actuators B*, 1993, **13-4**, pp. 570-1.

444. Zhou, Q. , G.H. Sigel, Jr, 'Porous polymer optical fiber for carbon monoxide detection' In Chemical, Biochemical and Environmental Sensors: Proceedings of the Symposium in Los Angeles, California, 6-7 September, International Society for Optical Engineers, Washington, U.S., 1989, **1172**, pp. 157-61.

445. Zhou, Q. , G.H. Sigel, Jr, 'Detection of carbon monoxide with a porous polymer optical fibre', *International Journal of Optoelectronics*, 1989, **4, No 5**, pp. 415-23.

446. Zhou, Y. , P.J. Laybourn, J.V. Magill, R.M. DeLaRue, 'An evanescent fluorescence biosensor using ion-exchanged buried waveguides and the enhancement of peak fluorescence', *Biosensors and Bioelectronics*, 1991, **6**, pp. 595-607.

447. Zhujun, Z. , W.R. Seitz, 'Optical sensor for oxygen based on immobilized hemoglobin', *Analytical Chemistry*, 1986, **58**, pp. 220-2.

448. Zur, A. , A. Katzir, 'Theory of fiber optic radiometry, emissivity of fibers, and ditributed thermal sensors', *Applied Optics*, 1991, **30**, No 6, pp. 660-673.